Faculteit Farmaceutische, Biomedische en Diergeneeskundige Wetenschappen
Departement Farmaceutische Wetenschappen
Medicinale Chemie

Fragment-based approaches to inhibitors of urokinase plasminogen activator (uPA)

Fragment-gebaseerde methoden voor de ontwikkeling van inhibitoren van urokinase plasminogeen activator (uPA)

Proefschrift voorgelegd tot het behalen van de graad
van doctor in de farmaceutische wetenschappen
aan de Universiteit Antwerpen te verdedigen door

Rafaela Gladysz

Promotoren: **Prof. dr. Pieter Van der Veken**
Prof. dr. Koen Augustyns

Antwerpen, 2016

Table of contents

List of abbreviations

3CR	three component reaction
AChE	acetylcholinesterase
AD	Alzheimer's disease
ADME	absorption, distribution, metabolism, and excretion
AIDS	acquired immune deficiency syndrome
AMC	7-amino-4-methylcoumarin
APN	aminopeptidase N
Atg4B	autophagy related 4B, cysteine peptidase, an enzyme that in humans is encoded by the ATG4B gene
BACE1	β-secretase 1; β-site amyloid precursor protein cleaving enzyme 1
BcII MBL	BcII metallo-β-lactamase
bFGF	basic fibroblast growth factor
BM	basement membrane
cAMP	cyclic adenosine monophosphate
CXCR4	CXC chemokine receptor 4
DCC	dicyclohexylcarbodiimide
DCC	dynamic combinatorial chemistry
DCLs	dynamic combinatorial libraries
DCM	dichloromethane
DFI	disease free interval
DFMP	difluoromethylphosphonate
DIPA	diisopropylamine
DMF	dimethylformamide
DNA	deoxyribonucleic acid
ECM	extracellular matrix
EDC	1-(3-dimethylaminopropyl)-3-ethylcarbodiimide
EGF	epidermal growth factor
EORTC	European Organization for Research and Treatment of Cancer
equiv	equivalent
ESI	electrospray ionization
FAK	focal adhesion kinase
FBDD	fragment-based drug discovery
FVIIa	factor VIIa
FXa	factor Xa
GABA	γ-aminobutyric acid
GAR TFase	phosphoribosylglycinamide formyltransferase
GBB	Groebke-Blackburn-Bienaymé reaction
HATU	1-[bis(dimethylamino)methylene]-1*H*-1,2,3-triazolo[4,5-*b*]pyridinium 3-oxid hexafluorophosphate
hCA II	human carbonic anhydrase
HD	Huntington's disease
HEPES	2-[4-(2-hydroxyethyl)piperazin-1-yl]ethanesulfonic acid
HER2	human epidermal growth factor receptor 2

HGF	hepatocyte growth factor
HIV	human immunodeficiency virus
HIV-RT	HIV reverse transcriptase
HOBt	hydroxybenzotriazole
hPK	human plasma kallikrein
HRMS	high resolution mass spectrometry
HTS	high-throughput screening
Htt	huntingtin gene
IC_{50}	inhibitor concentration that blocks 50% of enzyme activity
IDE	insulin-degrading enzyme
IGFs	insulin-like growth factors
IMCRs	isocyanide-based multicomponent reactions
IPISC	iterative peptide *in situ* click chemistry
ITC	isothermal titration calorimetry
KTGS	kinetic target-guided synthesis
LC/MS	liquid chromatography-mass spectrometry
LOE-1	level-of-evidence-1 studies
MBC	metastatic breast cancer
MCR	multicomponent reaction
MMPs	metalloproteases
MRM	multiple reaction monitoring
MS	mass spectrometry
MSAS	modified substrate activity screening
NMR	nuclear magnetic resonance
PAD	protein arginine deiminase
PAD3	protein arginine deiminase 3
PAI's	plasminogen activator inhibitors
PDB	protein data bank
PDE3	phosphodiesterase 3
PSA	prostate specific antigen
PTPs	tyrosine phosphatases
PyBrop	bromotripyrrolidinophosphonium hexafluorophosphate
QM/MM	quantum and molecular mechanics
RA	rheumatoid arthritis
RFUs	relative fluorescence units
RNA	ribonucleic acid
rt	room temperature
SAR	structure-activity relationship
SAS	substrate activity screening
SMCs	smooth muscle cells
SPR	surface plasmon resonance
STEP	striatal-enriched protein tyrosine phosphatase
suPAR	soluble form of urokinase plasminogen activator receptor
TBD	1,5,7-triazabicyclo[4.4.0]dec-5-ene
TBTU	*O*-(benzotriazol-1-yl)-*N,N,N',N'*-tetramethyluronium tetrafluoroborate

TEA	triethylamine
TFA	trifluoroacetic acid
TFFH	tetramethylfluoroformamidinium hexafluorophosphate
TGF-β	transforming growth factor-β
TGS	target-guided strategies
THF	tetrahydrofurane
tPA	tissue plasminogen activator
TS	transition state
uPA	urokinase plasminogen activator
uPAR	urokinase plasminogen activator receptor
VEGF	vascular endothelial growth factor

Chapter 1

Proteases as drug targets

1. Proteases as drug targets

1.1. General introduction

Proteases (also known as proteolytic enzymes, peptidases or proteinases) are an extremely large and diverse class of enzymes, occurring in all organisms. Based on bioinformatics analysis of human genomes approximately 600 proteases have been identified, accounting for around 2% of the gene content.[1,2] The role of these enzymes is to catalyze the breakdown of proteins by hydrolysis of peptide bonds (**Figure 1.1**). Based on the mechanism of catalysis, proteases fall into five classes: metalloproteases, aspartic, serine, cysteine and threonine proteases, with the remaining peptidases belonging to groups with an unknown or unclassified catalytic mechanism. Besides, proteases which detach amino acids from the N or C termini of the protein substrates are classified as exopeptidases (aminopeptidases and carboxypeptidases, respectively), and those which target the internal peptide bonds are known as endopeptidases.[3,4]

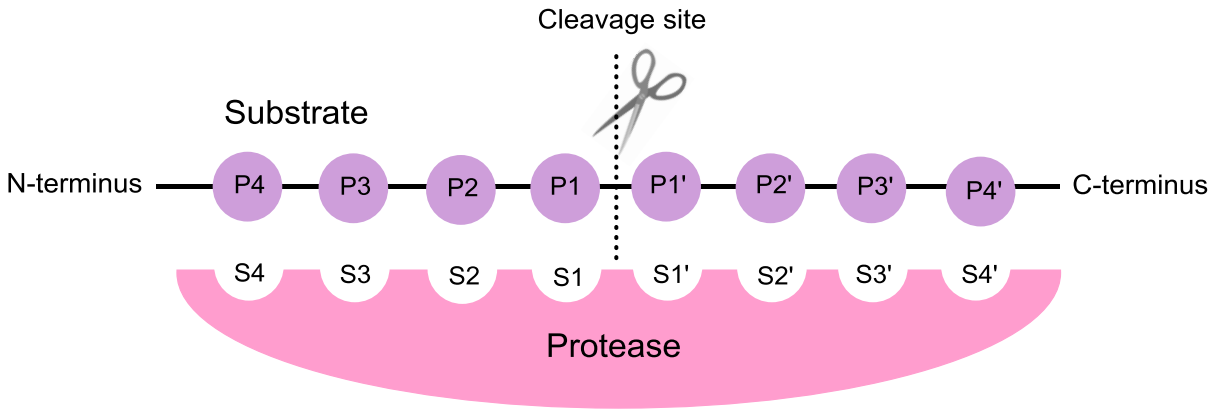

Figure 1.1. Schematic representation of a protein substrate binding to a protease (P – substrate residues, S – protease binding sites/pockets).

By their catalytic function, proteases are involved in controlling a large number of key physiological processes such as cell-cycle progression, cell proliferation and cell death, DNA replication, tissue remodeling, haemostasis (coagulation), wound healing, and immune response.[3] Inappropriate proteolysis is implicated in a broad range of diseases, proteases are therefore considered excellent targets for influencing such pathological processes *via* inhibitor-mediated blocking of protease activity.[5] Over the last decades, so-called "drugable" protease targets have been identified in nearly all fields of human pathology, including cancer, immune diseases, diabetes, cardiovascular disorders, and retroviral, bacterial and protozoal infections.[6] Subsequently, an impressive research effort has occurred in both pharmaceutical industry and academia aimed at programs for protease inhibitor development.[1,7] This has resulted in several compounds with "blockbuster" potential entering the

market during recent years. Currently, it is estimated that 5-10% of all pharmaceutical targets being pursued for drug development are proteases.[4]

1.2. Serine proteases

1.2.1. General aspects

Serine proteases are the largest group of proteases, and constitute over one-third of all known proteolytic enzymes.[9] These enzymes were named after the nucleophilic Ser residue, a part of Asp-His-Ser "charge relay" system, also known as "catalytic triad", which participates in the enzyme catalytic machinery.[10,11] Serine proteases are classified in a number of clans and families depending on the exact catalytic mechanism and common ancestry, and they adapt two basic structural folds: trypsin-like (also known as chymotrypsin-like) and subtilisin-like.[12,13] The most abundant in nature are trypsin-like peptidases belonging to family S1, clan PA.[9] The latter play an important role in many relevant physiological processes, such as digestion, immune responses, blood coagulation, fibrinolysis, and reproduction (**Table 1.1**).[10] Many among these processes, for instance, blood coagulation and immune response, involve cascades of sequential activation of inactive forms of serine proteases (zymogens).[1] Substrate specificity of serine proteases can be predicted by the topology of the substrate binding sites next to the catalytic triad, and is classified by the P1-S1 interaction.[7,10] Three major classes can be differentiated here: trypsin-like, chymotrypsin-like, and elastase-like. Trypsin-like substrate specific serine proteases are characterized by their preference for the positively charged residues like Arg or Lys side chains at the P1 position of the substrate. Chymotrypsin prefers large hydrophobic residues such as Phe, Tyr, Leu; and elastase small hydrophobic residues as Ala, Val at P1. Most proteases of clan PA are characterized by trypsin-like substrate specificity.[9]

Table 1.1. Examples of mammalian serine proteases of clan PA involved in a number of physiological processes.

Digestive proteases	Immune response	Blood coagulation	Fibrinolysis	Reproduction
- trypsin - chymotrypsin - pancreatic elastase	- tryptase - cathepsin G - neutrophil elastase - complement factors B, C, D	- coagulation factors VIIa, IXa, Xa, XIIa - thrombin	- urokinase (uPA) - tissue plasminogen activator (tPA) - plasmin - kallikrein	- acrosin - prostate specific antigen (PSA)

1.2.2. Catalytic mechanism

The catalytic mechanism of trypsin-like serine proteases involves a catalytic triad consisting of the active site residues Ser195, His57, and Asp102 (**Figure 1.2**).[9,10,14] The hydroxyl group of Ser195 acts as a nucleophile during the hydrolytic process, His57 serves as a general base/acid catalyst, and Asp102 is involved in positioning His57 in a proper orientation. Initially, the OH group of Ser195 attacks the carbonyl group of the substrate peptide bond (scissile bond) using His57 in function of a general base (step 1, **Figure 1.2**). As a result, a tetrahedral intermediate is being formed (step 2). The negatively charged oxyanion of the tetrahedral intermediate is stabilized through the backbone NH groups of Gly193 and Ser195 generating a positively charged pocket in the active site called the oxyanion hole.[10] In the next step, His57 in function of a general acid transfers a proton to the amine of the tetrahedral intermediate, which leads to collapse of the tetrahedral intermediate, formation of acyl-enzyme intermediate, and release of an amine product (step 3). Next, a water molecule attacks the acyl-enzyme complex (step 4) forming a new tetrahedral intermediate, which is stabilized by the oxyanion hole (step 5). Finally, due to the general acid catalysis by His57, the tetrahedral intermediate collapses generating the free acid product, as well as regenerating Ser195 (step 6).

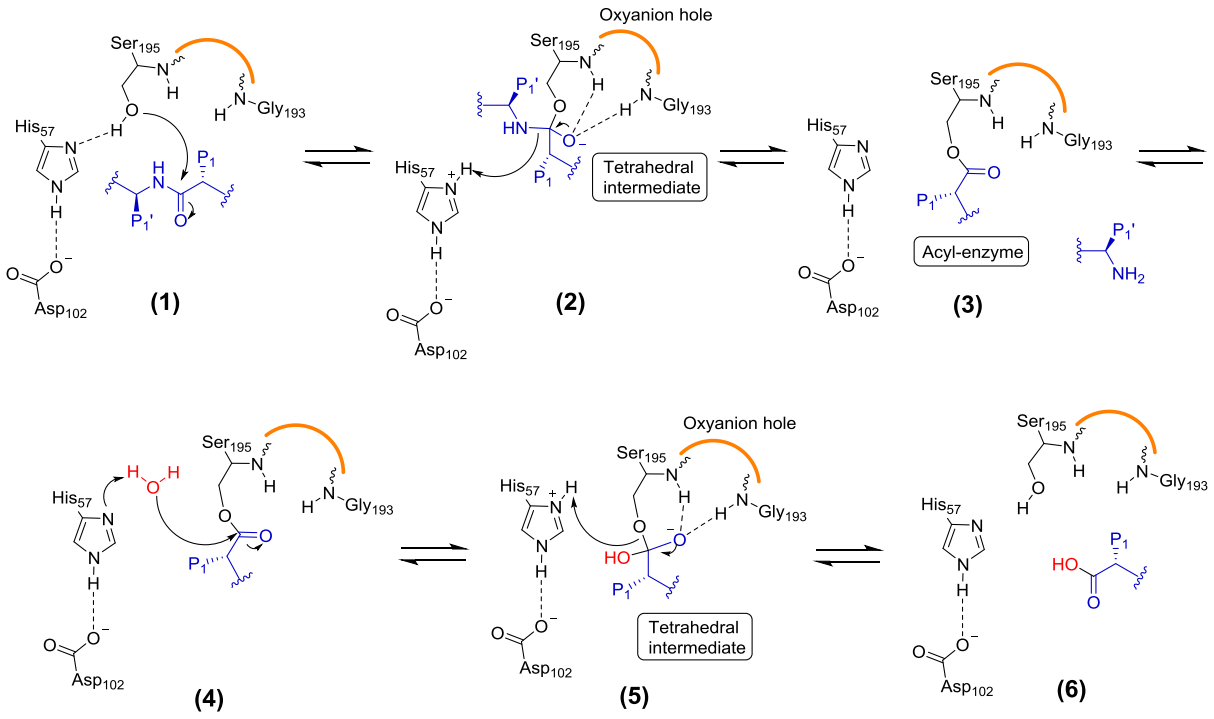

Figure 1.2. Outline of the catalytic mechanism of trypsin-like serine proteases.

1.2.3. Inhibitors of serine proteases

Due to the prominent role of serine proteases in many physiological processes they have become important targets in drug design. Several strategies have been used in serine protease inhibitor development, and among them (1) mimicking natural products (e.g. proteins, polysaccharides), (2) transforming enzyme substrates into inhibitors, (3) screening large and diverse compound libraries, followed by the "lead" optimization, and (4) preparing inhibitors equipped in a mechanism-based warhead (e.g. halomethyl ketones, phosphonates, nitriles).[15,16] Depending on the mechanism of inhibition, we can differentiate reversible and irreversible inhibitors of serine proteases. Reversible inhibitors attach to one of the enzyme forms during the reaction cycle in a reversible manner (e.g. *via* hydrogen bonding, hydrophobic interactions), while irreversible inhibitors bind covalently to the enzyme active site and irreversibly prevent the substrate from binding and being processed.[17] Many inhibitors mimic the transition state tetrahedral intermediate of the serine protease reaction; they are known as transition state analogues, for example, reversible boronic acid inhibitors or irreversible diaryl phosphonates.[14,16] Besides, several inhibitors work by the formation of stable acyl-enzyme intermediates, as, for instance, serpins, being natural inhibitors of serine proteases.[10]

Involvement of several academic and industrial groups in the development of serine protease inhibitors resulted in many potent drugs and clinical candidates for the treatment of disorders such as blood-clotting disorders, Alzheimer's disease, diabetes, obesity, hypertension, or bacterial and viral infections, including HIV/AIDS. Examples of drugs which entered the market more recently include sitagliptin (Merck), rivaroxaban (Bayer), dabigatran (Boehringer Ingelheim), telaprevir (Vertex Pharmaceuticals and Janssen Pharmaceutica), rivastigmine (Novartis), orlistat (Roche), aliskiren (Novartis), and darunavir (Tibotec and Janssen Pharmaceutica) (**Table 1.2**).[3,4,8,15,18]

Nonetheless, the field of serine protease inhibitor discovery still faces two important challenges: (1) obtaining inhibitors of better selectivity and specificity, and (2) improving the pharmacokinetic profile of derived inhibitors. Therefore, there is a need to develop novel approaches addressing these aspects in protease inhibitor design.

Table 1.2. Examples of serine protease inhibitors approved for clinical use.

Target enzyme	Drug name (trade name)	Drug structure	Disease
HCV-protease	telaprevir (Incivek®)	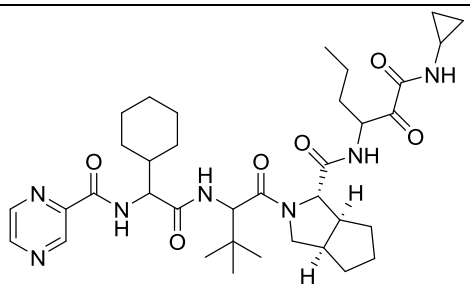	hepatitis C
factor Xa	rivaroxaban (Xarelto®)	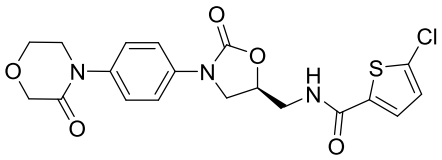	thromboembolism
thrombin	dabigatran (Pradaxa®)	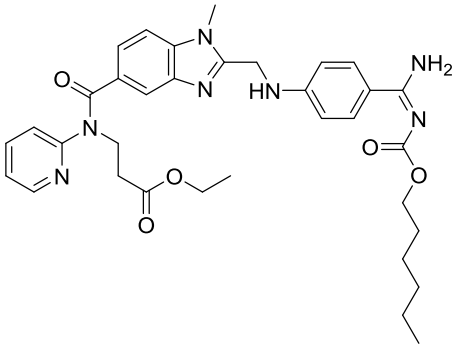	thromboembolism
pancreatic or gastric lipases	orlistat (Xenical®)	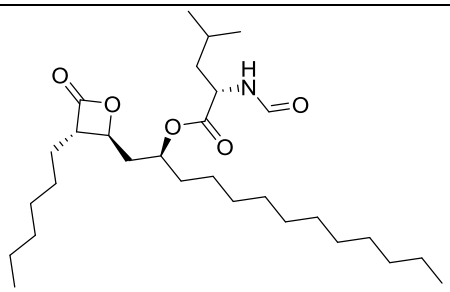	obesity
DPP IV (dipeptidyl peptidase-IV)	sitagliptin (Januvia®)	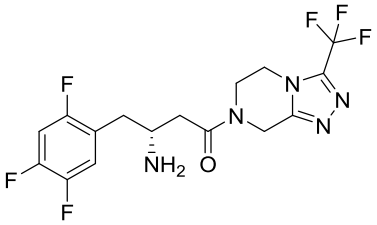	diabetes
AChE	rivastigmine (Exelon®)	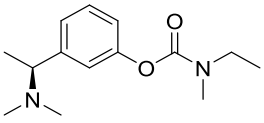	Alzheimer's disease and associated dementia

renin	aliskiren (Rasilez®)	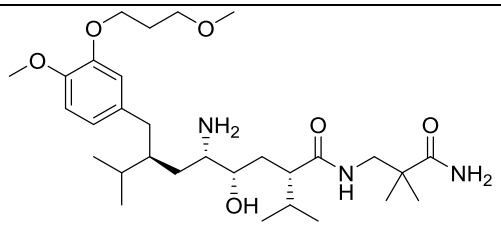	hypertension
HIV-protease	darunavir (Prezista®)	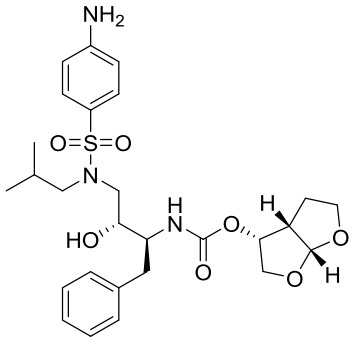	HIV infection

References

(1) Cudic, M.; Fields, G. B. Extracellular Proteases as Targets for Drug Development. *Curr Protein Pept Sci* **2009**, *10*, 297–307.

(2) Vizovišek, M.; Vidmar, R.; Fonović, M.; Turk, B. Current Trends and Challenges in Proteomic Identification of Protease Substrates. *Biochimie* **2015**, *122*, 77–87.

(3) Turk, B. Targeting Proteases: Successes, Failures and Future Prospects. *Nat. Rev. Drug Discov.* **2006**, *5*, 785–799.

(4) Drag, M.; Salvesen, G. S. Emerging Principles in Protease-Based Drug Discovery. *Nat. Rev. Drug Discov.* **2010**, *9*, 690–701.

(5) López-Otín, C.; Bond, J. S. Proteases: Multifunctional Enzymes in Life and Disease. *J. Biol. Chem.* **2008**, *283*, 30433–30437.

(6) Turk, B.; Turk, D.; Turk, V. Protease Signalling: The Cutting Edge. *EMBO J.* **2012**, *31*, 1630–1643.

(7) Abbenante, G.; Fairlie, D. P. Protease Inhibitors in the Clinic. *Med. Chem.* **2005**, *1*, 71–104.

(8) https://clinicaltrials.gov (accessed november 10, 2015).

(9) Di Cera, E. Serine Proteases. *IUBMB Life* **2009**, *61*, 510–515.

(10) Hedstrom, L. Serine Protease Mechanism and Specificity. *Chem. Rev.* **2002**, *102*, 4501–4523.

(11) Polgár, L. The Catalytic Triad of Serine Peptidases. *CMLS, Cell. Mol. Life Sci.* **2005**, *62*, 2161-2172.

(12) Madala, P. K.; Tyndall, J. D. A.; Nall, T.; Fairlie, D. P. Update 1 of: Proteases Universally Recognize Beta Strands in Their Active Sites. *Chem. Rev.* **2010**, *110*, PR1–PR31.

(13) https://merops.sanger.ac.uk/cgi-bin/clan_index?typ (accessed november 19, 2015).

(14) Walker, B.; Lynas, J. F. Strategies for the Inhibition of Serine Proteases. *CMLS, Cell. Mol. Life Sci.* **2001**, *58*, 596–624.

(15) Bachovchin, D. A.; Cravatt, B. F. The Pharmacological Landscape and Therapeutic Potential of Serine Hydrolases. *Nat. Rev. Drug Discov.* **2012**, *11*, 52–68.

(16) Powers, J. C.; Asgian, J. L.; Ekici, O. D.; James, K. E. Irreversible Inhibitors of Serine, Cysteine, and Threonine Proteases. *Chem. Rev.* **2002**, *102*, 4639–4750.

(17) Lambeir, A.-M. *Aspects of Enzyme Kinetics*; Antwerp, 2003.

(18) *U.S. Food and Drug Administration:* http://www.fda.gov (accessed november 20, 2015).

Chapter 2

Target protein: urokinase plasminogen activator (uPA)

2. Target protein: urokinase plasminogen activator (uPA)

This chapter will focus on the characterization of urokinase plasminogen activator (uPA), which was selected as target protein for the research performed during this PhD project.

2.1. Urokinase plasminogen activator system

2.1.1. Introduction

Urokinase plasminogen activator (uPA, urokinase) is a trypsin-like serine protease and a therapeutical target for many cancer types, including breast, ovarian, and pancreatic cancer.[1-3] It is part of an extracellular enzyme system overexpressed in metastasizing solid tumors, comprising the urokinase-type plasminogen activator (uPA), plasminogen activator inhibitors (PAI's), tissue-type plasminogen activator (tPA), and the uPA receptor (uPAR) (**Figure 2.1**).[1]

The uPAR is an important regulator of extracellular matrix (ECM) proteolysis, cell-ECM interactions, and cell signaling.[4] Binding of uPA to its receptor activates the enzyme and triggers a proteolytic cascade through which plasminogen is converted into plasmin. This in turn activates matrix metalloproteases (MMPs) leading to proteolytic degradation of the ECM components.[1,4] As a result, tumor cells degrade the surrounding tissue, invade into healthy tissue and migrate with the bloodstream to form metastasized tumors at distant organs. The uPA system also interacts with a number of relevant molecular-biological systems promoting tumor growth: it can activate growth factors and interacts with proteins involved in cell adhesion and signal transduction (vitronectin, integrins).[2,4]

2.1.2. Structure of uPA system components

Urokinase is a 411-amino acid residue (53 kDa) multidomain glycoprotein consisting of two α-helices and two anti-parallel β-strands.[1,3] It is synthesized as a one-chain zymogen (pro-uPA or single chain uPA) which is activated by the plasmin-mediated cleavage of the Lys158-Ile159 peptide bond. Also, cathepsin-B and -L, thermolysin, trypsin or kallikrein can activate pro-uPA.[2] As a result, the proteolytically active uPA consists of two chains: chain A with residues 1-158 and chain B with residues 159-411. These chains are linked together by a single disulfide bridge Cys148-Cys279.[5] The serine protease domain is located at the C-terminal end (chain B), while the N-terminal-fragment sequence (chain A) contains two domains: the growth factor and the kringle domain, and is responsible for binding to uPAR. Activated uPA converts plasminogen into its active form plasmin by cleavage of the Arg561-Val562 bond. Consequently, uPA and plasmin generate a positive feedback-type loop based on mutual activation.[1,5]

Another component of the uPA system, the urokinase plasminogen activator receptor (uPAR), is a 55-60 kDa cysteine-rich glycoprotein lacking a transmembrane domain. It consists of three homologous domains (D1, D2 and D3), and is attached to the cell membrane with a glycosylphosphatidylinositol (GPI) anchor.[3,4] uPAR can be released from the cell membrane by cleavage of the GPI anchor, which results in the soluble form of uPAR (suPAR).[2] Moreover, the uPA receptor is characterized by a high binding affinity for uPA, pro-uPA as well as several other proteins.

The activity of uPA is physiologically counteracted by its endogenous inhibitors belonging to the serpin family, PAI-1 and PAI-2. Of these two inhibitors, PAI-1 plays the most important role by inhibiting the active forms of uPA and tPA. PAI-1 rapidly binds to the uPA-uPAR adduct forming a covalent complex uPAR-uPA-PAI-1. This trimolecular complex is further processed in lysosomes. uPA and PAI-1 undergo degradation, while uPAR is partially recycled back to the cell membrane.[2,3]

Tissue-type plasminogen activator (tPA) on the other hand is a 527 amino acid (70 kDa) glycoprotein synthesized also in the form of inactive zymogen, which is activated through the plasmin-mediated hydrolysis of Arg275-Ile276 bond. In general, tPA has a similar role to uPA being its homologous protein. These two enzymes are known as two main endogenous plasminogen activators which work by hydrolyzing the Arg561-Val562 bond.[1] However, tPA's major function is related to intravascular thrombolysis, whereas uPA participates in pericellular proteolysis in the course of tissue remodeling, migration, and wound healing.[6,7]

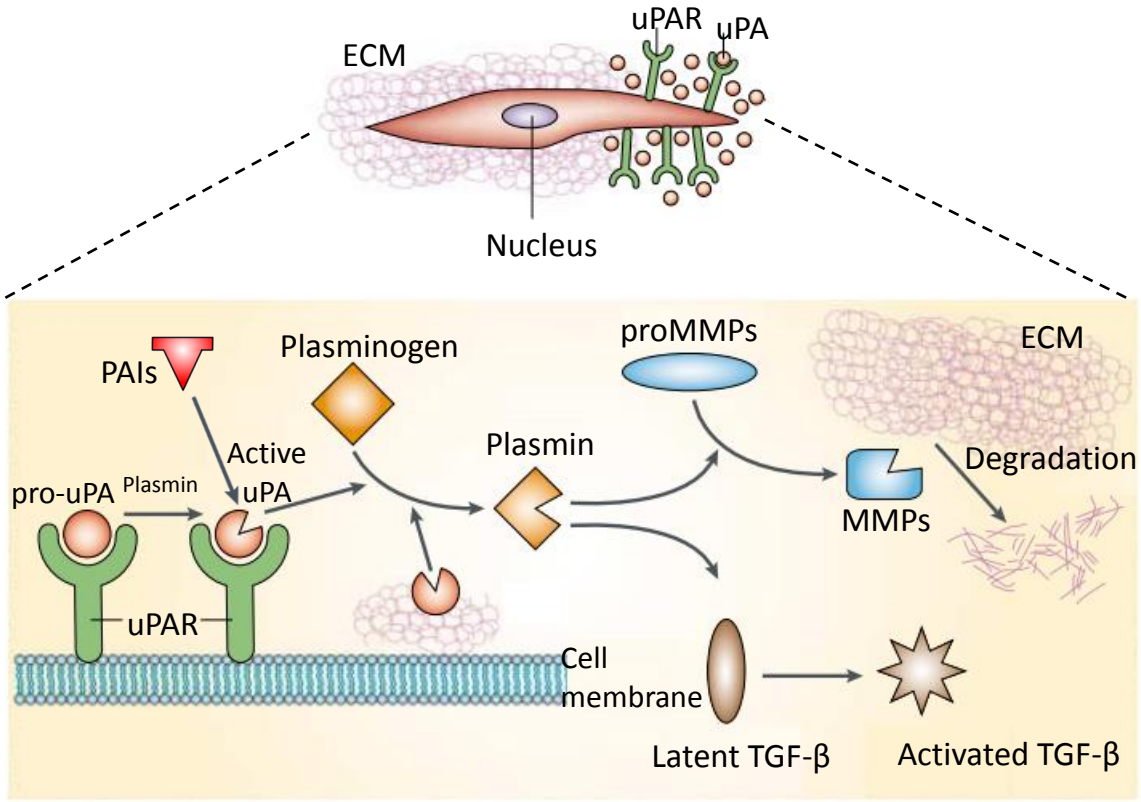

Figure 2.1. Schematic representation of the uPA system activity (adapted from Blasi et al.[4]). Binding of pro-uPA to its receptor (uPAR) activates the enzyme and triggers a proteolytic cascade through which plasminogen is converted into plasmin, which activates matrix metalloproteases (MMPs) leading to proteolytic degradation of the ECM (extracellular matrix) components. Outcome of these events are key processes during cancer, i.e., tissue degradation, tumor cell migration (metastasis), and primary tumor growth. Also activated plasmin converts zymogen pro-uPA into active uPA. Additionally, the uPA system interacts with a number of relevant molecular-biological systems promoting tumor growth, for e.g., by activating growth factors. The activity of uPA is physiologically counteracted by its endogenous inhibitors (PAIs).

2.1.3. Active site of uPA

Similar as in case of other enzymes belonging to the trypsin-like serine protease family, the active site of uPA consists of the catalytic triad involving Ser195, His57 and Asp102, and the oxyanion hole (**Figure 2.2**). The S1 pocket of uPA is deep, well-defined, and it has a negatively charged Asp189 at its bottom. This negative charge is responsible for the high affinity and specificity of uPA to positively charged residues, such as the Arg side chain located at the substrate's P1 position. Consequently, many reported inhibitors of uPA are characterized by the presence of highly basic functionalities, as for instance, guanidine, amidine, or their mimetics, forming a salt bridge with the carboxylate of Asp189, and therefore significantly contributing to the inhibitor's affinity and selectivity for the uPA

active site.[8] Additionally, studies on known uPA substrates showed that the enzyme has a preference for small hydrophobic residues at positions P2, P1', P2'.[5,9]

Except similarities there are also significant differences between urokinase and other trypsin-like serine proteases. First, the uPA's S2 and S4 subsites are smaller than in case of for e.g. thrombin or factor Xa (FXa). Secondly, next to the substrate-binding groove the active site of uPA is characterized by the presence of many other subsites. The latter can bind small molecule inhibitors, or can be explored during uPA inhibitor design to improve potency and selectivity. An example of such a subsite in proximity of the S1 pocket is the S1β site.[5,10] Besides, different trypsin-like serine proteases can vary at position 190. In case of uPA, trypsin, plasmin, and factor VIIa (FVIIa) position 190 is occupied by Ser, while tPA, thrombin or factor Xa (FXa) are characterized by the presence of Ala in position 190. Therefore, position 190 is a main determinant of the binding specificity of the S1 pocket.[11,12]

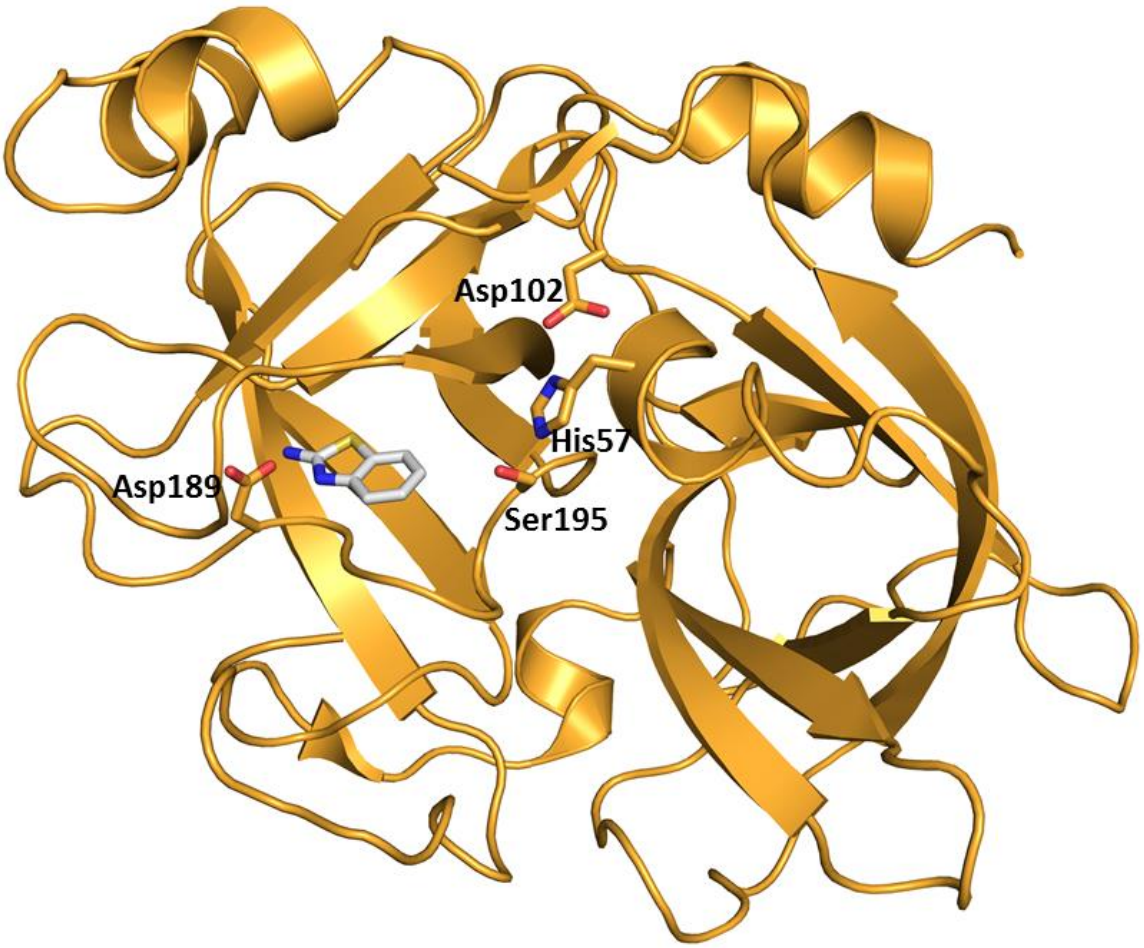

Figure 2.2. Model of the active site of uPA together with inhibitor (PDB code 3MHW)[13].

2.1.4. Role of the uPA system components in cancer

The uPA system components are involved in many physiological and pathological processes associated with ECM and BM (basement membrane) remodeling, like for instance tissue regeneration, wound healing, immune response, angiogenesis, tumor progression, and metastasis.[14] In case of cancer, the uPA system triggers a proteolytic cascade through which cancer cells degrade the surrounding tissue (ECM and BM) at the primary tumor site, subsequently invading the healthy tissues and blood vessels, in order to finally migrate and colonize target metastatic tissues.[15]

Through binding of pro-uPA to its receptor (uPAR) activation of uPA and plasmin takes place, which is regulated by two endogenous inhibitors of this system, PAI-1 and PAI-2. Plasmin can be regarded as a broad-spectrum peptidase due to its high potential to cleave numerous substrates. It can degrade different ECM and BM components, such as fibronectin, vitronectin, laminin, type IV collagen, proteoglycans, and fibrin. Additionally, plasmin can promote the ECM degradation by activating the latent forms of matrix metalloproteases (MMPs, e.g. MMP1-3, MMP9, MMP12, and MMP13) and pro-uPA. The activated MMPs are able to degrade different collagens, kallikrein-related peptidases, and other ECM proteins.[14,16] Subsequently, cleavage of the ECM proteins leads to release and activation of several growth factors, including basic fibroblast growth factor (bFGF), transforming growth factor-beta (TGF-β), hepatocyte growth factor (HGF), vascular endothelial growth factor (VEGF), epidermal growth factor (EGF), and insulin-like growth factors (IGFs). The ECM degradation and activation of growth factors associated with cancer cells promotes tumor cell proliferation, migration, invasion, angiogenesis, and metastasis (**Figure 2.3**).[14,17,18] Noteworthy, the effect of uPAR on tumor progression and metastasis can have not only proteolytic (uPAR in complex with uPA), but also nonproteolytic character. The nonproteolytic function of uPAR includes for instance interaction with proteins involved in cell adhesion and signal transduction (vitronectin and integrins), regulation of cAMP levels, and interaction with tyrosine kinases as well as with various serine/threonine kinases.[1] Besides, uPAR activates many intracellular signaling molecules, like for instance tyrosine kinase Src, the serine kinase Raf, and focal adhesion kinase (FAK), which promotes cell proliferation, adhesion, and metastasis.[3] Therefore, uPAR, both separately and bound to uPA, is regarded as a significant regulator of ECM proteolysis, cell-ECM interactions, and cell signaling.[4,19]

Interestingly, PAI-1 has a dual function in cancer progression. On one side, by inhibiting uPA activity it inhibits tumor invasion and metastasis, and on the other side it can promote tumor growth and angiogenesis.[1] Most probably, PAI-1 promotes angiogenesis by preventing ECM from excessive degradation, and in turn ECM creates a scaffold for endothelial cell migration and capillary formation.[17] Similar as uPAR, PAI-1 can also interact with vitronectin and its integrin, and it can compete with uPAR for binding to vitronectin. It is able to modify cell adhesion and to stimulate cell

proliferation.[1,3,14] Additionally, PAI-1 is believed to promote cancer progression by inhibiting apoptosis, hence increasing cancer cell survival.[17]

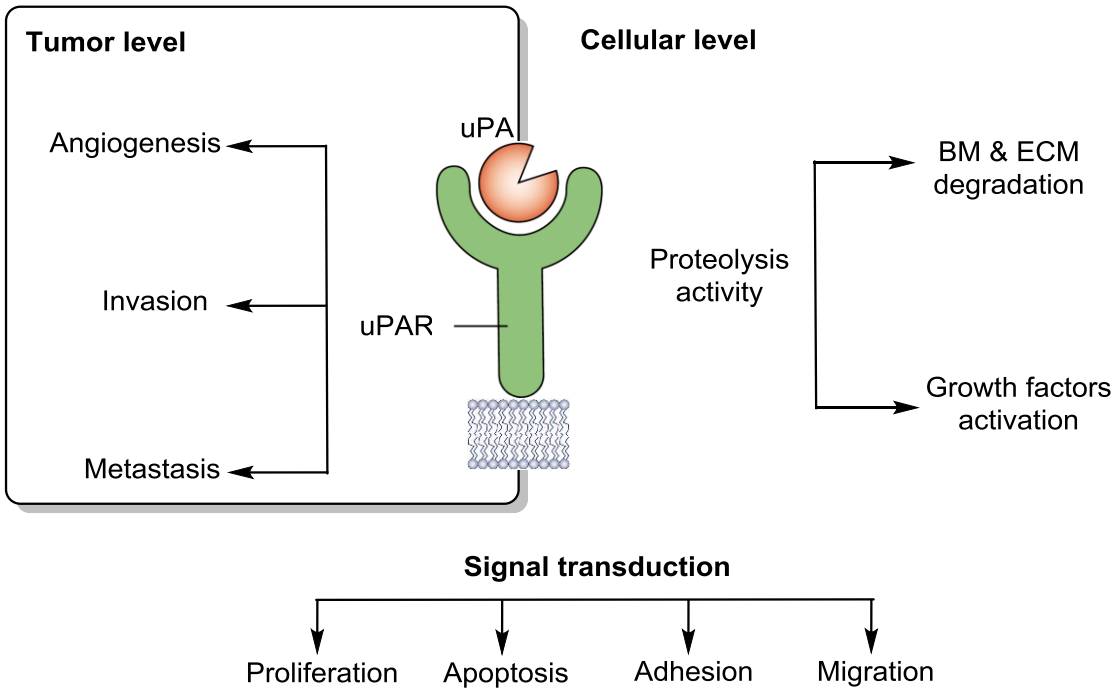

Figure 2.3. Role of the uPA system in cancer (adapted from Mekkawy et al.[2]).

2.1.5. uPA system components as biomarkers in cancer

Individual components of the uPA system are differently expressed in cancer tissues than in healthy tissues, they can therefore serve as prognostic and/or therapeutic anticancer targets.[20] The prognostic role of uPA was first proposed for breast cancer by Duffy et al. in 1988.[21] This study showed that high activity of uPA stimulates primary tumor growth and significantly reduces patients' disease free interval (DFI). Since then, overexpression of one or more uPA system components has been demonstrated to have a significant role in tumor growth and metastasis (**Table 2.1**). As a result, the uPA system components have become potential prognostic biomarkers in many cancer types, among which are breast, ovarian, endometrial, lung, cervical, esophageal, gastric, pancreatic, colorectal, prostate, bladder, kidney and thyroid cancer, as well as osteocarcoma, melanoma, and other cancer types.[14,16,20,22]

In general, high levels of uPA and uPAR have been associated with advanced metastatic cancer types.[1] Also normally low levels of suPAR, significantly increase in cancer patients.[2,23] Interestingly, PAI-1 is rather an unusual prognostic marker. By inhibiting the uPA activity, it could be expected only

to reduce tumor progression. However, at levels found in many cancer types PAI-1 was also demonstrated to stimulate tumor invasion and angiogenesis, it has therefore been associated with a poor prognosis. On the other hand, loss of the PAI-1, or blocking its activity by a specific PAI-1 inhibitor, was found to suppress angiogenesis and tumor progression.[18,24-26] In several cancer types, high levels of uPA and PAI-1 have been linked to unfavorable disease progression and shorter disease-free survival of cancer patients.[22] Currently, uPA and PAI-1 are among the best validated biomarkers for breast cancer, and have proven their clinical applicability in two independent level-of-evidence-1 (LOE-1) studies by the European Organization for Research and Treatment of Cancer (EORTC).[15,17,27]

Table 2.1. Correlation between expression of different uPA system components and their effect on tumor progression for selected cancer types.

Cancer type	**Component of the uPA system**	**Biological effect**	**Ref.**
Breast	uPA, PAI-1	metastasis and poor survival, advanced tumor, poor prognosis	Duffy et al.[17]
Pancreatic	uPA, uPAR	tumor growth and metastasis, rapid progression, poor survival	Bauer et al.[28], Gorantla et al.[29]
Gastric	uPA, uPAR	poor prognosis, increased angiogenesis	Zhang et al.[30]
Ovarian	uPA, PAI-1	invasion and metastasis	Cai et al.[31]
Prostate	uPA, uPAR	metastasis	Li et al.[32]
Melanoma	PAI-2	inhibition of apoptosis	Zhou et al.[33]

2.1.6. Role of uPA in other diseases

The uPA system represents a powerful mechanism of extracellular proteolysis, and it plays a crucial role in wound healing, a process which engages three partially overlapping phases: (1) blood clotting and inflammation, (2) new tissue formation, and (3) tissue remodeling.[34] Deregulation of expression of the uPA system components has been associated with pathogenesis of several diseases, as, for instance, chronic, nonhealing ulcers. Chronic dermal ulcers are a condition linked to excessive and uncontrolled proteolytic degradation leading to ulcer extension, loss of functional matrix molecules, as, for instance, fibronectin, and finally slowing down epithelialization and ulcer curing. Chronic ulcers are characterized by high levels of uPA localized diffusely throughout the ulcer periphery and

the lesion.[35] A study of Herouy and co-workers[36] provided direct evidence of increased expression of uPA and uPAR at the mRNA and protein levels in venous leg ulcers. Also, the soluble forms of uPAR (suPAR and its fragments) were found in the surroundings of venous ulcers. The latter can serve as indicators of venous ulcer healing tendency and are believed to play an important role in the wound healing process.[37]

Also the role of uPA in the development of rheumatoid arthritis was investigated. Rheumatoid arthritis (RA) is a chronic inflammatory joint disease distinguished by immune and inflammatory cell infiltration into the synovium and proliferation of synovial tissue, resulting in cartilage and bone destruction.[38] Urokinase was found to be a relevant regulator of fibrinolysis in the synovial fluid. It has a proinflammatory effect; increased activity of uPA and expression of uPAR were observed in joints of patients with RA.[39-41] Interestingly, it was demonstrated that intraarticular injection of uPA induces arthritis in mice, and that the developed joint inflammation is mediated by the serine protease activity of uPA, rather than its interaction with the uPAR.[40] However, the definitive role of uPA in the development of RA in humans is still under investigation.

A number of studies proved that the uPA system is implicated in the pathogenesis of atherosclerosis.[42,43] Atherosclerosis is a disease leading to thickening of the artery wall, as a consequence of (1) invasion and accumulation of monocyte-derived macrophage-foam cells loaded with cholesterol, and (2) proliferation of intimal smooth muscle cells (SMCs), resulting in the formation of atheromatous plaques. It was demonstrated that cells within advanced atherosclerotic plaques (e.g., endothelial cells, SMCs, macrophages) express high levels of uPA and uPAR. Besides, a strong relationship between uPA/uPAR expression in macrophages and atherosclerotic lesion development was observed.[42] Interestingly, transgenic mice with macrophage-targeted overexpression of uPA showed that overexpression of uPA in the aorta elevated the atherosclerosis level two-fold.[44] Involvement of the uPA system in increased atherogenicity makes it a potential therapeutic target against atherosclerosis. Nonetheless, the exact role of the uPA system in the atherosclerotic plaque development has to be further investigated.

2.1.7. Inhibitors of uPA

Although uPA is a valuable oncology target, clinical development of uPA inhibitors has been problematic. This is most probably related to the doubtful biopharmaceutical performance of compounds developed so far and their insufficient selectivity with respect to other, phylogenetically related trypsin-like proteases. Nonetheless, the field of urokinase inhibitor discovery still produces a significant number of relevant compounds, mostly small molecules with a competitive, reversible

inhibition profile. Wilex's amidine-based inhibitor WX-UK1 (**2.1a**, **Figure 2.4**) and its orally bioavailable prodrug WX-671 (**2.1b**, **Figure 2.4**) are currently the most advanced products. Interestingly, **2.1a** (K_i = 410 nM) and **2.1b** are the first inhibitors of uPA in oncology trials worldwide. The latter has successfully completed two clinical phase I trials, and recently showed favorable results in a randomized phase II trial in patients with locally advanced nonmetastatic pancreatic cancer as well as met its primary objective in a phase II trial in patients with HER2 receptor negative metastatic breast cancer (MBC).[15,45-48] In addition to compounds developed by Wilex (**2.1a-b**), a significant number of optimized inhibitors of urokinase has been reported, but these have only been investigated in preclinical studies. Pfizer reported 1-isoquinolinylguanidine UK-356,202 (**2.2**, K_i = 37 nM) and its sulfonamide derivative UK-371,804 (**2.3**, K_i = 10 nM) as potent and selective inhibitors of uPA.[35,49,50] These compounds were selected for preclinical evaluation for the treatment of chronic dermal ulcers, a condition characterized by high levels of uPA promoting uncontrolled matrix breakdown and inhibition of wound repair. As a result, compound **2.3** was demonstrated to inhibit exogenous uPA activity both in human chronic wound fluid *in vitro*, and in the porcine acute excisional wound model.[35] Besides, according to Barber et al., UK-356,202 was selected for human clinical trials, but apparently these plans have never been materialized for unknown reasons.[49] An amidine based, peptide-derived uPA inhibitor CJ-463 (**2.4**, K_i = 20 nM) was found to reduce the number of experimental lung metastases in a fibrosarcoma mouse model as well as primary tumor growth and metastasis formation in a murine lung carcinoma model.[51,52] A fragment-based approach by Astex led to the discovery of a mexiletine-derived, low basicity inhibitor of uPA (**2.5**, IC_{50} = 72 nM) with moderate selectivity against closely related proteases and high oral bioavailability.[53] Abbott Laboratories developed a series of naphthamidine inhibitors of uPA (compound **2.6** as a representative example; K_i = 263 nM) with improved pharmacokinetic properties, with good oral bioavailability and extended half-life in rats.[54] Zhu and co-workers reported the 4-oxazolidinone analogue UK122 (**2.7**) as a selective inhibitor of uPA with significant potency to inhibit the migratory and invasive capacity of pancreatic cancer cells.[55] Additionally, the oral potassium-sparing diuretic drug amiloride was found to be a selective, competitive inhibitor of uPA of moderate potency (compound **2.8**, K_i = 7 μM) and significant anti-tumor/metastasis effects *in vivo*.[56,57]

Other approaches have been focusing on the discovery of irreversible uPA ligands, antibodies or peptide-based molecules. Our group described a series of highly potent and selective, irreversible diaryl phosphonate inhibitors of uPA (**2.9a**, IC_{50} = 3.1 ± 0.5 nM, and **2.9b**, IC_{50} = 3.4 ± 0.4 nM) with significant antimetastatic activity in a rodent model of breast cancer.[58] Mazar and co-workers developed a novel therapeutic uPAR antibody ATN-658 demonstrating antitumor effects across a variety of tumor models, including inhibition of invasion, metastasis and proliferation as well as

induction of apoptosis.[59,60] Additionally, bicyclic peptide constructs were recently reported as highly potent uPA inhibitors.[61,62] Nonetheless, given all the preclinical evidence mentioned, it is remarkable that none of the compounds were developed clinically.

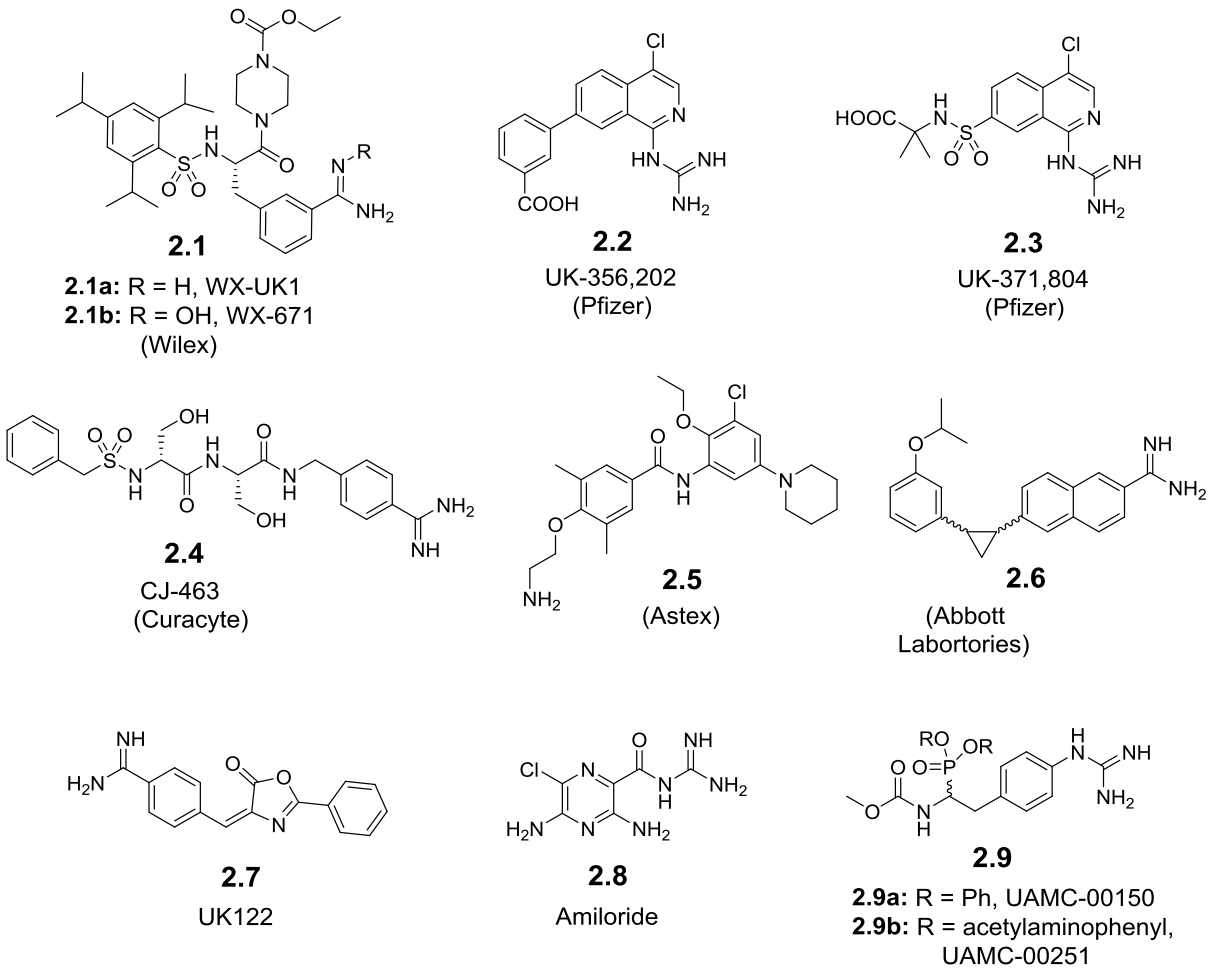

Figure 2.4. Reported inhibitors of uPA.

References

(1) Dass, K.; Ahmad, A.; Azmi, A. S.; Sarkar, S. H.; Sarkar, F. H. Evolving Role of uPA/uPAR System in Human Cancers. *Cancer Treat. Rev.* **2008**, *34*, 122–136.

(2) Mekkawy, A. H.; Pourgholami, M. H.; Morris, D. L. Involvement of Urokinase-Type Plasminogen Activator System in Cancer : An Overview. *Med. Res. Rev.* **2014**, *34*, 918–956.

(3) Tang, L.; Han, X. The Urokinase Plasminogen Activator System in Breast Cancer Invasion and Metastasis. *Biomed. Pharmacother.* **2013**, *67*, 179–182.

(4) Blasi, F.; Carmeliet, P. uPAR: A Versatile Signalling Orchestrator. *Nat. Rev. Mol. Cell Biol.* **2002**, *3*, 932–943.

(5) Spraggon, G.; Phillips, C.; Nowak, U. K.; Ponting, C. P.; Saunders, D.; Dobson, C. M.; Stuart, D. I.; Jones, E. Y. The Crystal Structure of the Catalytic Domain of Human Urokinase-Type Plasminogen Activator. *Structure* **1995**, *3*, 681–691.

(6) Thorsen, S. The Mechanism of Plasminogen Activation and the Variability of the Fibrin Effector during Tissue-Type Plasminogen Activator-Mediated Fibrinolysis. *Ann. N. Y. Acad. Sci.* **1992**, *667*, 52–63.

(7) Cesarman-Maus, G.; Hajjar, K. A. Molecular Mechanisms of Fibrinolysis. *Br. J. Haematol.* **2005**, *129*, 307–321.

(8) Sperl, S.; Jacob, U.; Arroyo de Prada, N.; Stürzebecher, J.; Wilhelm, O. G.; Bode, W.; Magdolen, V.; Huber, R.; Moroder, L. (4-Aminomethyl)Phenylguanidine Derivatives As Nonpeptidic Highly Selective Inhibitors of Human Urokinase. *Proc. Natl. Acad. Sci. U. S. A.* **2000**, *97*, 5113–5118.

(9) Zesławska, E.; Stürzebecher, J.; Oleksyn, B. J. Geometry of GPPE Binding to Picrate and to the Urokinase Type Plasminogen Activator. *Bioorg. Med. Chem. Lett.* **2007**, *17*, 6212–6215.

(10) Rockway, T. W.; Giranda, V. L. Inhibitors of the Proteolytic Activity of Urokinase Type Plasminogen Activator. *Curr. Pharm. Des.* **2003**, *9*, 1483–1498.

(11) Katz, B. A.; Sprengeler, P. A.; Luong, C.; Verner, E.; Elrod, K.; Kirtley, M.; Janc, J.; Spencer, J. R.; Breitenbucher, J. G.; Hui, H.; McGee, D.; Allen, D.; Martelli, A.; Mackman, R. L. Engineering Inhibitors Highly Selective for the S1 Sites of Ser190 Trypsin-like Serine Protease Drug Targets. *Chem. Biol.* **2001**, *8*, 1107–1121.

(12) Mackman, R. L.; Katz, B. A.; Breitenbucher, J. G.; Hui, H. C.; Verner, E.; Luong, C.; Liu, L.; Sprengeler, P. A. Exploiting Subsite S1 of Trypsin-like Serine Proteases for Selectivity: Potent and Selective Inhibitors of Urokinase-Type Plasminogen Activator. *J. Med. Chem.* **2001**, *44*, 3856–3871.

(13) Jiang, L.-G.; Yu, H.-Y.; Yuan, C.; Wang, J.-D.; Chen, L.-Q.; Meehan, E. J.; Huang, Z.-X.; Huang, M.-D. Crystal Structures of 2-Aminobenzothiazole-Based Inhibitors in Complexes with Urokinase-Type Plasminogen Activator. *Chin. J. Struct. Chem.* **2009**, *28*, 1427–1432.

(14) Ulisse, S.; Baldini, E.; Sorrenti, S.; D'Armiento, M. The Urokinase Plasminogen Activator System: A Target for Anti-Cancer Therapy. *Curr. Cancer Drug Targets* **2009**, *9*, 32–71.

(15) *Therapeutic Target Mesupron*; Wilex Ag: Munich; http://www.wilex.de/portfolio-English/mesupron/therapeutic-Target/ (accessed january 19, 2015).

(16) Schmitt, M.; Wilhelm, O. G.; Reuning, U.; Krüger, A.; Harbeck, N.; Lengyel, E.; Graeff, H.; Gänsbacher, B.; Kessler, H.; Bürgle, M.; Stürzebecher, J.; Sperl, S.; Magdolen, V. The Urokinase Plasminogen Activator System as a Novel Target for Tumour Therapy. *Fibrinolysis and Proteolysis* **2000**, *14*, 114–132.

(17) Duffy, M. J.; McGowan, P. M.; Harbeck, N.; Thomssen, C.; Schmitt, M. uPA and PAI-1 as

Biomarkers in Breast Cancer: Validated for Clinical Use in Level-of-Evidence-1 Studies. *Breast Cancer Res.* **2014**, *16*, 428.

(18) Andreasen, P. A.; Egelund, R.; Petersen, H. H. The Plasminogen Activation System in Tumor Growth, Invasion, and Metastasis. *CMLS, Cell. Mol. Life Sci.* **2000**, *57*, 25–40.

(19) Smith, H. W.; Marshall, C. J. Regulation of Cell Signalling by uPAR. *Nat. Rev. Mol. Cell Biol.* **2010**, *11*, 23–36.

(20) Duffy, M. J.; Duggan, C. The Urokinase Plasminogen Activator System: A Rich Source of Tumour Markers for the Individualised Management of Patients with Cancer. *Clin. Biochem.* **2004**, *37*, 541–548.

(21) Duffy, M. J.; O'Grady, P.; Devaney, D.; O'Siorain, L.; Fennelly, J. J.; Lijnen, H. J. Urokinase-Plasminogen Activator, a Marker for Aggressive Breast Carcinomas. Preliminary Report. *Cancer* **1988**, *62*, 531–533.

(22) Kwaan, H. C.; Mazar, A. P.; Mcmahon, B. J. The Apparent uPA / PAI-1 Paradox in Cancer : More than Meets the Eye. *Semin Thromb Hemost* **2013**, *39*, 382–391.

(23) Mekkawy, A. H.; Morris, D. L.; Pourgholami, M. H. Urokinase Plasminogen Activator System as a Potential Target for Cancer Therapy. *Futur. Oncol.* **2009**, 1487–1500.

(24) Bajou, K.; Noel, A.; Gerard, R. D.; Masson, V.; Brunner, N.; Holst-Hansen, C.; Skobe, M.; Fusenig, N. E.; Carmeliet, P.; Collen, D.; Foidart, J. M. Absence of Host Plasminogen Activator Inhibitor 1 Prevents Cancer Invasion and Vascularization. *Nat. Med.* **1998**, *4*, 923–928.

(25) Gutierrez, L. S.; Schulman, A.; Brito-Robinson, T.; Noria, F.; Ploplis, V. A.; Castellino, F. J. Tumor Development Is Retarded in Mice Lacking the Gene for Urokinase-Type Plasminogen Activator or Its Inhibitor, Plasminogen Activator Inhibitor-1. *Cancer Res.* **2000**, *60*, 5839–5847.

(26) Masuda, T.; Hattori, N.; Senoo, T.; Akita, S.; Ishikawa, N.; Fujitaka, K.; Haruta, Y.; Murai, H.; Kohno, N. SK-216, an Inhibitor of Plasminogen Activator Inhibitor-1, Limits Tumor Progression and Angiogenesis. *Mol. Cancer Ther.* **2013**, *12*, 2378–2388.

(27) Schmitt, M.; Harbeck, N.; Brünner, N.; Jänicke, F.; Meisner, C.; Mühlenweg, B.; Jansen, H.; Dorn, J.; Nitz, U.; Kantelhardt, E. J.; Thomssen, C. Cancer Therapy Trials Employing Level-of-Evidence-1 Disease Forecast Cancer Biomarkers uPA and Its Inhibitor PAI-1. *Expert Rev. Mol. Diagn.* **2011**, *11*, 617–634.

(28) Bauer, T. W.; Liu, W.; Fan, F.; Camp, E. R.; Yang, A.; Somcio, R. J.; Bucana, C. D.; Callahan, J.; Parry, G. C.; Evans, D. B.; Boyd, D. D.; Mazar, A. P.; Ellis, L. M. Targeting of Urokinase Plasminogen Activator Receptor in Human Pancreatic Carcinoma Cells Inhibits c-Met- and Insulin- like Growth Factor-I Receptor-Mediated Migration and Invasion and Orthotopic Tumor Growth in Mice. *Cancer Res.* **2005**, *65*, 7775–7781.

(29) Gorantla, B.; Asuthkar, S.; Rao, J. S.; Patel, J.; Gondi, C. S. Suppression of the uPAR-uPA System Retards Angiogenesis, Invasion, and in Vivo Tumor Development in Pancreatic Cancer Cells. *Mol. Cancer Res.* **2011**, *9*, 377–389.

(30) Zhang, L.; Zhao, Z. S.; Ru, G. Q.; Ma, J. Correlative Studies on uPA mRNA and uPAR mRNA Expression with Vascular Endothelial Growth Factor, Microvessel Density, Progression and Survival Time of Patients with Gastric Cancer. *World J. Gastroenterol.* **2006**, *12*, 3970–3976.

(31) Cai, Z.; Li, F. Y.; Liu, F. Y.; Feng, Y. L.; Hou, J. H.; Zhao, M. Q. Expression and Clinical Significance of uPA and PAI-1 in Epithelial Ovarian Cancer. *Ai Zheng.* **2007**, *26*, 312–317.

(32) Li, Y.; Cozzi, P. J. Targeting uPA/uPAR in Prostate Cancer. *Cancer Treat Rev.* **2007**, *33*, 521–527.

(33) Zhou, H. M.; Bolon, I.; Nichols, A.; Wohlwend, A.; Vassalli, J. D. Overexpression of Plasminogen

Activator Inhibitor Type 2 in Basal Keratinocytes Enhances Papilloma Formation in Transgenic Mice. *Cancer Res.* **2001**, *61*, 970–976.

(34) Schäfer, M.; Werner, S. Cancer as an Overhealing Wound: An Old Hypothesis Revisited. *Nat. Rev. Mol. Cell Biol.* **2008**, *9*, 628–638.

(35) Fish, P. V; Barber, C. G.; Brown, D. G.; Butt, R.; Collis, M. G.; Dickinson, R. P.; Henry, B. T.; Horne, V. a; Huggins, J. P.; King, E.; O'Gara, M.; McCleverty, D.; McIntosh, F.; Phillips, C.; Webster, R. Selective Urokinase-Type Plasminogen Activator Inhibitors. 4. 1-(7-Sulfonamido-isoquinolinyl)guanidines. *J. Med. Chem.* **2007**, *50*, 2341–2351.

(36) Herouy, Y.; Trefzer, D.; Hellstern, M. O.; Stark, G. B.; Vanscheidt, W.; Schöpf, E.; Norgauer, J. Plasminogen Activation in Venous Leg Ulcers. *Br. J. Dermatol.* **2000**, *143*, 930–936.

(37) Ahmad, A.; Saha, P.; Evans, C.; Thurison, T.; Hoyer-Hansen, G.; Patel, A.; Modarai, B.; Smith, A. The Soluble Urokinase Plasminogen Activator Receptor and Its Fragments in Venous Ulcers. *J. Vasc. Surg. Venous Lymphat. Disord.* **2014**, *3*, 190–197.

(38) Judex, M. O.; Mueller, B. M. Plasminogen Activation/Plasmin in Rheumatoid Arthritis. **2005**, *166*, 645–647.

(39) Busso, N.; So, A. Urokinase in Rheumatoid Arthritis: Causal or Coincidental? *Ann. Rheum. Dis.* **1997**, *56*, 705–706.

(40) Jin, T.; Tarkowski, A.; Carmeliet, P.; Bokarewa, M. Urokinase, a Constitutive Component of the Inflamed Synovial Fluid, Induces Arthritis. *Arthritis Res. Ther.* **2003**, *5*, R9–R17.

(41) Hamilton, J. A. Plasminogen Activator/Plasmin System in Arthritis and Inflammation: Friend or Foe? *Arthritis Rheum.* **2008**, *58*, 645–648.

(42) Fuhrman, B. The Urokinase System in the Pathogenesis of Atherosclerosis. *Atherosclerosis* **2012**, *222*, 8–14.

(43) Falkenberg, M.; Tom, C.; DeYoung, M. B.; Wen, S.; Linnemann, R.; Dichek, D. A. Increased Expression of Urokinase during Atherosclerotic Lesion Development Causes Arterial Constriction and Lumen Loss, and Accelerates Lesion Growth. *PNAS* **2002**, *99*, 10665–10670.

(44) Cozen, A. E.; Moriwaki, H.; Kremen, M.; DeYoung, M. B.; Dichek, H. L.; Slezicki, K. I.; Young, S. G.; Véniant, M.; Dichek, D. A. Macrophage-Targeted Overexpression of Urokinase Causes Accelerated Atherosclerosis, Coronary Artery Occlusions, and Premature Death. *Circulation* **2004**, *109*, 2129–2135.

(45) Abbenante, G.; Fairlie, D. P. Protease Inhibitors in the Clinic. *Med. Chem.* **2005**, *1*, 71–104.

(46) Heinemann, V.; Ebert, M. P.; Laubender, R. P.; Bevan, P.; Mala, C.; Boeck, S. Phase II Randomised Proof-of-Concept Study of the Urokinase Inhibitor Upamostat (WX-671) in Combination with Gemcitabine Compared with Gemcitabine Alone in Patients with Non-Resectable, Locally Advanced Pancreatic Cancer. *Br. J. Cancer* **2013**, *108*, 766–770.

(47) Meyer, J. E.; Brocks, C.; Graefe, H.; Mala, C.; Thäns, N.; Bürgle, M.; Rempel, A.; Rotter, N.; Wollenberg, B.; Lang, S. The Oral Serine Protease Inhibitor WX-671 - First Experience in Patients with Advanced Head and Neck Carcinoma. *Breast Care* **2008**, *3*, 20–24.

(48) Setyono-Han, B.; Sturzebecher, J.; Schmalix, W. A.; Muehlenweg, B.; Sieuwerts, A. M.; Timmermans, M.; Magdolen, V.; Schmitt, M.; Klijn, J. G. M.; Foekens, J. A. Suppression of Rat Breast Cancer Metastasis and Reduction of Primary Tumour Growth by the Small Synthetic Urokinase Inhibitor WX-UK1. *Thromb. Haemost.* **2005**, *93*, 779–786.

(49) Barber, C. G.; Dickinson, R. P.; Fish, P. V. Selective Urokinase-Type Plasminogen Activator (uPA) Inhibitors. Part 3: 1-Isoquinolinylguanidines. *Bioorg. Med. Chem. Lett.* **2004**, *14*, 3227–3230.

(50) Bayliss, M. A. J.; Venn, R. F.; Edgington, A. M.; Webster, R.; Walker, D. K. Determination of a Potent Urokinase-Type Plasminogen Activator, UK-356,202, in Plasma at pg/mL Levels Using Column-Switching HPLC and Fluorescence Detection. *J. Chromatogr. B* **2009**, *877*, 121–126.

(51) Schweinitz, A.; Steinmetzer, T.; Banke, I. J.; Arlt, M. J. E.; Stürzebecher, A.; Schuster, O.; Geissler, A.; Giersiefen, H.; Zeslawska, E.; Jacob, U.; Krüger, A.; Stürzebecher, J. Design of Novel and Selective Inhibitors of Urokinase-Type Plasminogen Activator with Improved Pharmacokinetic Properties for Use as Antimetastatic Agents. *J. Biol. Chem.* **2004**, *279*, 33613-33622.

(52) Henneke, I.; Greschus, S.; Savai, R.; Korfei, M.; Markart, P.; Mahavadi, P.; Schermuly, R. T.; Wygrecka, M.; Stürzebecher, J.; Seeger, W.; Günther, A.; Ruppert, C. Inhibition of Urokinase Activity Reduces Primary Tumor Growth and Metastasis Formation in a Murine Lung Carcinoma Model. *Am. J. Respir. Crit. Care Med.* **2010**, *181*, 611–619.

(53) Frederickson, M.; Callaghan, O.; Chessari, G.; Congreve, M.; Cowan, S. R.; Matthews, J. E.; McMenamin, R.; Smith, D.-M.; Vinković, M.; Wallis, N. G. Fragment-Based Discovery of Mexiletine Derivatives as Orally Bioavailable Inhibitors of Urokinase-Type Plasminogen Activator. *J. Med. Chem.* **2008**, *51*, 183–186.

(54) Bruncko, M.; McClellan, W. J.; Wendt, M. D.; Sauer, D. R.; Geyer, A.; Dalton, C. R.; Kaminski, M. A.; Weitzberg, M.; Gong, J.; Dellaria, J. F.; Mantei, R.; Zhao, X.; Nienaber, V. L.; Stewart, K.; Klinghofer, V.; Bouska, J.; Rockway, T. W.; Giranda, V. L. Naphthamidine Urokinase Plasminogen Activator Inhibitors with Improved Pharmacokinetic Properties. *Bioorg. Med. Chem. Lett.* **2005**, *15*, 93–98.

(55) Zhu, M.; Gokhale, V. M.; Szabo, L.; Munoz, R. M.; Baek, H.; Bashyam, S.; Hurley, L. H.; Von Hoff, D. D.; Han, H. Identification of a Novel Inhibitor of Urokinase-Type Plasminogen Activator. *Mol. Cancer Ther.* **2007**, *6*, 1348–1356.

(56) Matthews, H.; Ranson, M.; Kelso, M. J. Anti-Tumour/Metastasis Effects of the Potassium-Sparing Diuretic Amiloride: An Orally Active Anti-Cancer Drug Waiting for Its Call-of-Duty? *Int. J. Cancer* **2011**, *129*, 2051–2061.

(57) Ding, Y.; Zhang, H.; Zhou, Z.; Zhong, M.; Chen, Q.; Wang, X.; Zhu, Z. u-PA Inhibitor Amiloride Suppresses Peritoneal Metastasis in Gastric Cancer. *World J. Surg. Oncol.* **2012**, *10*, 270–277.

(58) Joossens, J.; Ali, O. M.; El-Sayed, I.; Surpateanu, G.; Van der Veken, P.; Lambeir, A.-M.; Setyono-Han, B.; Foekens, J. A.; Schneider, A.; Schmalix, W.; Haemers, A.; Augustyns, K. Small, Potent, and Selective Diaryl Phosphonate Inhibitors for Urokinase-Type Plasminogen Activator with In Vivo Antimetastatic Properties. *J. Med. Chem.* **2007**, *50*, 6638–6646.

(59) Parry, G.; Mazar, A. P. Urokinase-Type Plasminogen Activator Receptor Epitope, Monoclonal Antibodies Derived Therefrom and Methods of Use Thereof. **2012**, US Patent 8105602.

(60) Xu, X.; Cai, Y.; Wei, Y.; Donate, F.; Juarez, J.; Parry, G.; Chen, L.; Meehan, E. J.; Ahn, R. W.; Ugolkov, A.; Dubrovskyi, O.; O'Halloran, T. V.; Huang, M.; Mazar, A. P. Identification of a New Epitope in uPAR as a Target for the Cancer Therapeutic Monoclonal Antibody ATN-658, a Structural Homolog of the uPAR Binding Integrin CD11b (αM). *PLoS One* **2014**, *9*, e85349: 1–13.

(61) Chen, S.; Gfeller, D.; Buth, S. A.; Michielin, O.; Leiman, P. G.; Heinis, C. Improving Binding Affinity and Stability of Peptide Ligands by Substituting Glycines with D-Amino Acids. *ChemBioChem* **2013**, *14*, 1316–1322.

(62) Roodbeen, R.; Paaske, B.; Jiang, L.; Jensen, J. K.; Christensen, A.; Nielsen, J. T.; Huang, M.; Mulder, F. A. A.; Nielsen, N. C.; Andreasen, P. A.; Jensen, K. J. Bicyclic Peptide Inhibitor of Urokinase-Type Plasminogen Activator: Mode of Action. *ChemBioChem* **2013**, *14*, 2179–2188.

Chapter 3

Objectives of this work

3. Objectives of this work

The primary objective of this work was the application of the substrate activity screening (SAS) approach and its modified variant (MSAS) to the discovery of potent and selective inhibitors of urokinase plasminogen activator (uPA). The second complementary objective that emerged towards the end of this PhD research was the application of the "on-target" strategies to uPA inhibitor discovery.

3.1. Objective 1: Application of SAS and its modified variant (MSAS) to uPA inhibitor discovery

The substrate activity screening (SAS) was introduced a decade ago as an efficient fragment-based approach to inhibitor discovery.[1] Since then, it has been applied successfully to different families of enzymatically active drug targets including various serine and cysteine proteases, metallopeptidases, protein tyrosine phosphatases, protein tyrosine kinases, and protein arginine deiminase. A detailed discussion on different aspects and applications of the SAS method is given in Chapter 6.

In this PhD study we decided to apply SAS to the discovery of inhibitors of urokinase plasminogen activator, a therapeutical target and a validated biomarker for several cancer types.[2,3] Although uPA is a relevant oncological target, development of its inhibitors has been problematic in terms of current drug discovery approaches. By implementing SAS and related fragment-based strategies, this study differs fundamentally from the existing approaches; it therefore provides a new route to potent and selective inhibitors of urokinase.

3.1.1. SAS *versus* the MSAS experiment

The first goal of this PhD project was the synthesis of a SAS library of fluorogenic molecules as potential substrates for the target enzyme. It was important that the members of this library contained fragment-sized acyl residues selected either in a target-biased or non-target-biased manner, in order to explore a large part of the druglike chemical space. In the next step, the prepared SAS library had to be screened for substrates of uPA using a simple fluorescence-based assay. The main challenge during this step was devising an appropriate experimental protocol for the library screening. Our SAS experiments revealed a number of unreported limitations of this approach. In response we devised a modified methodology: "MSAS" (modified substrate activity screening), which circumvents the limitations of SAS and provides more coherent SAR data (*vide infra*, Chapter 4). The validation of the MSAS methodology was based on the preparation of scaffold-based inhibitors containing the identified fragments. In particular, in the case of protease targets, such scaffold-based compounds have the potential to bypass certain ADME related liabilities of classical, peptide-based protease inhibitors. Besides, several recently approved small-molecule

drugs share an overall comparable architecture consisting of a central rigid heterocyclic scaffold decorated with additional substituents, which contribute to the affinity for the drug target. Given the druglike architecture of imidazopyridine as well as the ease of its synthetic preparation *via* the Groebke-Blackburn-Bienaymé (GBB) reaction, this scaffold type was selected for the construction of uPA inhibitors.[4-8]

3.1.2. Potent and selective uPA inhibitors

The next goal of my PhD project was obtaining potent and selective imidazopyridine inhibitors of uPA. To reach this goal we proposed a general strategy consisting of two steps: (1) preparing a set of monosubstituted scaffolds for the selection of an optimal fragment with affinity for the uPA S1-pocket, and (2) further structural optimization by combining the optimal S1-substituent with additional affinity-conferring substituents on the imidazopyridine scaffold (**Scheme 3.1**). Noteworthy, the SAR for uPA inhibition around the imidazopyridine ring system extensively relied on the molecular modeling study to guide the compound optimization. Another relevant issue addressed here was the selectivity of the obtained uPA inhibitors with respect to the related trypsin-like serine proteases.[9] Insufficient selectivity is often responsible for the failure of uPA inhibitors during further stages of drug development.

Development and SAR of the imidazo[1,2-*a*]pyridine inhibitors of uPA will be the subject of Chapter 5 of this PhD thesis.

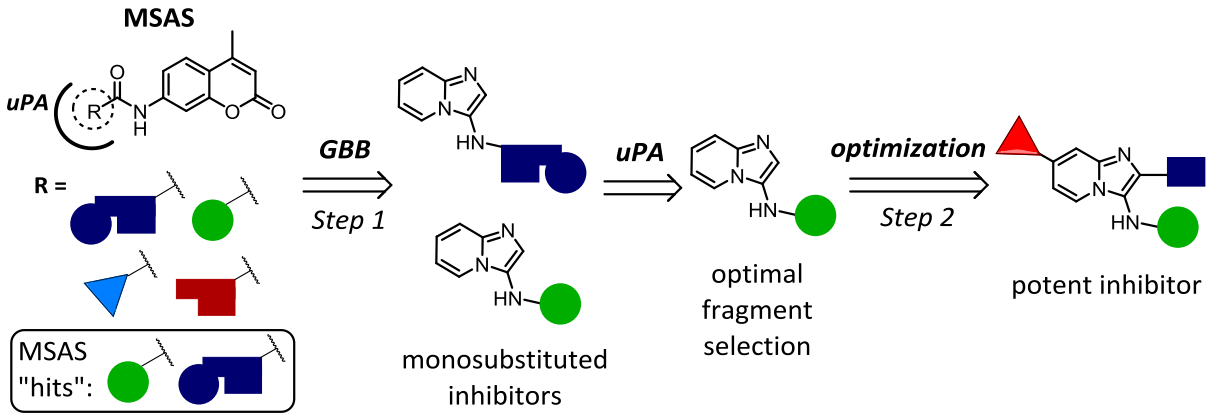

Scheme 3.1. The general strategy followed during preparation of imidazopyridine inhibitors of uPA.

3.2. Objective 2: "On-target" approaches to inhibitors of urokinase

The last goal of this PhD project was the application of "on-target" strategies to the discovery of uPA inhibitors. The developed methodology differs fundamentally from approaches existing in uPA drug discovery by the implementation of target-assisted selection and assembly strategies for inhibitor building blocks.

On-target approaches in drug discovery rely on direct assistance of the target enzyme active site, which functions as a physical template that selects useful drug fragments and assembles them into finalized molecules.[10] It allows combining the inhibitor synthesis and potency determination, along with other aspects of molecular drug design, into a single, time-efficient step. The reaction type to be studied in this part of my PhD research is the Groebke-Blackburn-Bienaymé reaction. This isocyanide-based three component reaction (3CR) belongs to the most widely used transformations in combinatorial drug discovery.[11-13] It delivers small molecules with a druglike architecture, consisting of a central, heterocyclic scaffold decorated with substituents. Given the intrinsic druglike architecture of such compounds, the on-target variants of the GBB reaction can be expected to have significant value for drug discovery. Additional impact of this study could come from the fact that to date, no examples of "on-target" 3CRs have been reported. As reference for the on-target work in this PhD thesis served the uPA inhibitors prepared beforehand (*vide supra*, Part 3.1.2).

"On-target" approaches to inhibitors of urokinase are the subject of Chapter 7 of this PhD thesis.

References

(1) Wood, W. J. L.; Patterson, A. W.; Tsuruoka, H.; Jain, R. K.; Ellman, J. A. Substrate Activity Screening: A Fragment-Based Method for the Rapid Identification of Nonpeptidic Protease Inhibitors. *J. Am. Chem. Soc.* **2005**, *127*, 15521–15527.

(2) Ulisse, S.; Baldini, E.; Sorrenti, S.; D'Armiento, M. The Urokinase Plasminogen Activator System: A Target for Anti-Cancer Therapy. *Curr. Cancer Drug Targets* **2009**, *9*, 32–71.

(3) Duffy, M. J.; McGowan, P. M.; Harbeck, N.; Thomssen, C.; Schmitt, M. uPA and PAI-1 as Biomarkers in Breast Cancer: Validated for Clinical Use in Level-of-Evidence-1 Studies. *Breast Cancer Res.* **2014**, *16*, 428: 1-10.

(4) Groebke, K.; Weber, L.; Mehlin, F. Synthesis of Imidazo[1,2-*a*] Annulated Pyridines, Pyrazines and Pyrimidines by a Novel Three Component Condensation. *Synlett* **1998**, 661–663.

(5) Brown, D. J., Evans, R. F., Cowden, W. B., Fenn, M. D. *Chemistry of Heterocyclic Compounds: The Pyrimidines*; Wiley, New York, 1994.

(6) Gladysz, R.; Cleenewerck, M.; Joossens, J.; Lambeir, A.-M.; Augustyns, K.; Van der Veken, P. Repositioning the Substrate Activity Screening (SAS) Approach as a Fragment-Based Method for Identification of Weak Binders. *ChemBioChem* **2014**, *15*, 2238–2247.

(7) Salunke, D. B., Yoo, E., Shukla, N. M., Balakrishna, R., Malladi, S. S., Serafin, K. J., Day, V. W., Wang, X., David, S. A. Structure–Activity Relationships in Human Toll-like Receptor 8-Active 2, 3-Diamino-furo[2,3-*c*]pyridines. *J. Med. Chem.* **2012**, *55*, 8137–8151.

(8) Ren, J.; Yang, M.; Liu, H.; Cao, D.; Chen, D.; Li, J.; Tang, L.; He, J.; Chen, Y.-L.; Geng, M.; Xiong, B.; Shen, J. Multi-Substituted 8-Aminoimidazo[1,2-*a*]pyrazines by Groebke–Blackburn–Bienaymé Reaction and Their Hsp90 Inhibitory Activity. *Org. Biomol. Chem.* **2015**, *13*, 1531-1535.

(9) Gladysz, R.; Adriaenssens, Y.; De Winter, H.; Joossens, J.; Lambeir, A.-M.; Augustyns, K.; Van der Veken, P. Discovery and SAR of Novel and Selective Inhibitors of Urokinase Plasminogen Activator (uPA) with an Imidazo[1,2-*a*]pyridine Scaffold. *J. Med. Chem.* **2015**, *58*, 9238–9257.

(10) Oueis, E.; Sabot, C.; Renard, P.-Y. New Insights into the Kinetic Target-Guided Synthesis of Protein Ligands. *Chem. Commun.* **2015**, *51*, 12158–12169.

(11) Devi, N.; Rawal, R. K.; Singh, V. Diversity-Oriented Synthesis of Fused-Imidazole Derivatives *via* Groebke–Blackburn–Bienayme Reaction: A Review. *Tetrahedron* **2015**, *71*, 183–232.

(12) Dömling, A.; Ugi, I. Multicomponent Reactions with Isocyanides. *Angew. Chem. Int. Ed. Engl.* **2000**, *39*, 3168–3210.

(13) Slobbe, P.; Ruijter, E.; Orru, R. V. A. Recent Applications of Multicomponent Reactions in Medicinal Chemistry. *MedChemComm* **2012**, *3*, 1189–1218.

Chapter 4

Modification of the substrate activity screening (SAS) approach as an efficient fragment-based method for the identification of weak binders

The content of this chapter is based on:

Gladysz, R.; Cleenewerck, M.; Joossens, J.; Lambeir, A.-M.; Augustyns, K.; Van der Veken, P. Repositioning the Substrate Activity Screening (SAS) Approach as a Fragment-Based Method for Identification of Weak Binders. *ChemBioChem* **2014**, *15*, 2238-2247.

4. Modification of the substrate activity screening (SAS) approach as an efficient fragment-based method for the identification of weak binders

4.1. Introduction

Over the last decade, fragment-based drug discovery (FBDD) has become a well-established methodology, delivering several high-quality leads, clinical candidates and at least one FDA-approved drug (vemurafenib).[1] FBDD has emerged as an efficient "hit"-identification and/or -optimization strategy, being an alternative to high-throughput screening (HTS) for "lead" discovery. FBDD approaches have in common that they construct "lead" molecules from smaller fragments, typically containing less than 12 heavy atoms and possessing relatively low individual affinities. Such fragments in general allow orthogonal optimization to meet predefined criteria for target affinity ("ligand-efficiency") and biopharmaceutical behavior, as proposed in, for example, the "rule of three" for fragments (molecular weight < 300, ClogP < 3, the number of hydrogen bond donors and acceptors each < 3 and the number of rotatable bonds < 3).[2] Another advantage of the approach is that the compound libraries used for fragment identification can be multiple orders of magnitude smaller in size than those required for HTS. This relates to the fact that drug-like diversity space can be much more efficiently probed with small fragments than with the typically larger molecules found in drug-like HTS libraries.[3-6] There are several recent reviews that extensively document these concepts with relevant examples from case studies.[7]

Nonetheless, FBDD still faces a number of fundamental challenges.[6] One of these relates to the need for better methodology to detect and to study weakly binding fragments. X-ray crystallography and protein NMR are among the most established techniques for this purpose.[8,9] However, their main drawback is the requirement for substantial amounts of highly purified target protein and specialized infrastructure that runs at high financial cost and with medium throughput capacity. Also other biophysical techniques have been applied to FBDD. These include, among others, surface plasmon resonance (SPR), ^{19}F NMR, thermal denaturation, mass spectrometry, thermal electrophoresis, and isothermal titration calorimetry.[10-17]

Specifically for enzyme targets, substrate activity screening (SAS) was proposed by Ellman and co-workers[18] as an attractive fragment-based approach to inhibitor discovery. Promising results with different classes of enzyme targets have been reported, mainly by the group of Ellman.[19-25] Notable examples include identification of nonpeptidic inhibitors for serine and cysteine proteases, receptor tyrosine kinases and the protein tyrosine phosphatases PtpA and PtpB of *Mycobacterium tuberculosis*.[18-20,26] The SAS approach, demonstrated for a protease target, consists of three steps. First of all, a library of small, fragment-sized molecules, each linked to a scissile fluorogenic amide

bond, is screened for substrates of a target protease (**Scheme 4.1, step 1**). Next, the identified substrates are optimized in a separate cycle (**Scheme 4.1, step 2**) and finally transformed into inhibitors by replacing the scissile amide bond with a warhead functionality (**Scheme 4.1, step 3**).[18] Diversity in the substrate library comes from druglike, fragment-sized groups that function as potential affinity-conferring recognition units for the target enzyme. These are linked to a functionality that can be processed by the target enzyme, thereby releasing a quantifiable reporter molecule. The main rationale of the SAS methodology is that the cleavage efficiencies (expressed as the k_{cat}/K_m ratio) for the individual library members are positively correlated with a fragment's affinity for the enzyme's transition state-stabilizing conformation and hence with its potential for inhibitor design. It is worth mentioning that this principle had already been recognized decades ago and has been applied extensively to discovery of substrate-derived enzyme inhibitors. SAS, however, does not rely on library molecules that are direct analogues of a target's natural substrates. In this way, it is not biased to deliver inhibitors with an overall biomolecule-derived architecture but has the unique potential to provide fragments with favorable, more druglike structures immediately.

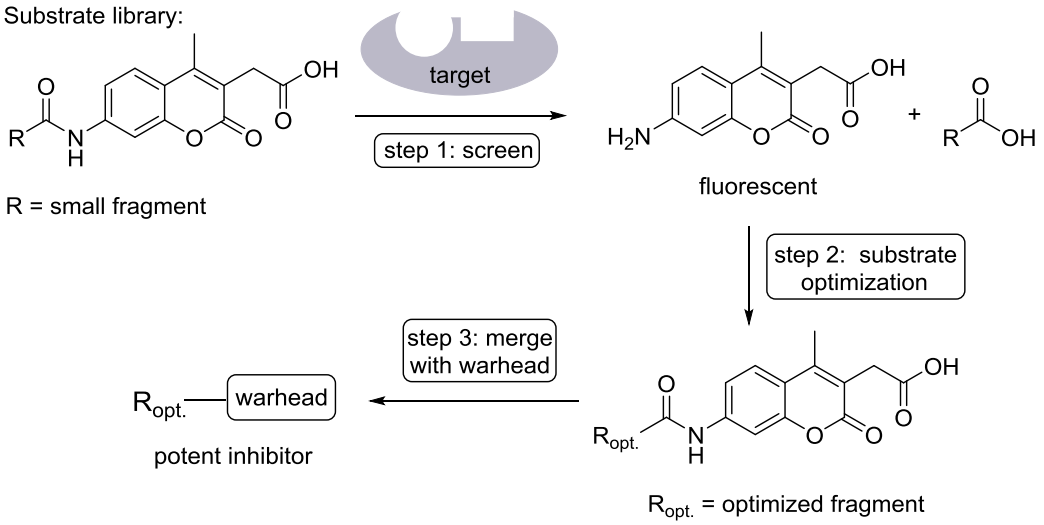

Scheme 4.1. The SAS approach, demonstrated for a protease target (adapted from Wood et al.[18]).

In practice, it is necessary to optimize fragments after the first stage. This is done by creating additional, directed chemical diversity around the best substrates identified. Optimized substrates are ultimately transformed into inhibitors by direct replacement of the enzyme-processed functionality in a substrate molecule with a mechanism-based warhead or pharmacophore.[18,27] Although only superficially examined for this purpose, SAS fragments could also be subjected to a standard FBDD-optimization strategy for obtaining small-molecule inhibitors that do not draw upon a warhead functionality to gain target affinity.

The goal of my PhD research was to apply the SAS approach to inhibitor discovery for urokinase plasminogen activator (uPA), a trypsin-like serine protease that is overexpressed in metastasizing solid tumors (*vide supra*, Chapter 2).[28-30] The enzyme is a valuable oncology target, but clinical development of its inhibitors has been problematic. This is most probably related to the doubtful biopharmaceutical performance of compounds developed so far and their insufficient selectivity with respect to other, phylogenetically related trypsin-like proteases. Nonetheless, the field of urokinase inhibitor discovery still enjoys highly interesting developments, such as with recent approaches based on bicyclic peptide constructs.[31,32]

Earlier, our group described selective, irreversible inhibitors of uPA with significant antimetastatic activity in a rodent model of breast cancer.[33] Discovering structurally novel uPA inhibitors therefore continues to raise interest in our group. During our exploration of SAS we encountered a number of limitations of the reported approach. This chapter describes a simple and effective alternative for SAS, which we have named "MSAS" (modified substrate activity screening). We demonstrate that screening the library for inhibitors of a target enzyme rather than for its substrates avoids false negatives: that is, fragments with high potential for inhibitor discovery that are not identified in a SAS assay. We also show that MSAS avoids false positives that can surface during a regular SAS assay, and runs with better cost and time efficiency. Furthermore, an FBDD strategy is reported to transform identified fragments into inhibitors that do not rely on a warhead functionality for target affinity. Additionally, we demonstrate with the aid of experimental data that the classical SAS step in which substrates are translated into inhibitors by addition of a warhead, although intrinsically highly valuable, does not *per se* lead to compounds of practical biopharmaceutical quality. Finally, our results show that adoption of the MSAS approach can not only circumvent limitations of the parent methodology, but can also offer additional potential for FBDD on enzyme targets.

4.2. SAS experiment for the library of *N*-acyl aminocoumarins

4.2.1. Library design

We started our investigations with the synthesis of a SAS library of 137 fluorogenic *N*-acyl-7-amino-4-methylcoumarin substrates (*N*-acyl AMCs). All the compounds in the library contained fragment-sized *N*-acyl residues (molecular weight < 150). Selection of around 90 of these residues was done in a non-target-biased manner, aiming to cover as much of druglike chemical space as possible: steric, electronic and electrostatic parameters were taken into account. In addition, several target-biased subsets were prepared, containing moieties of known uPA inhibitors and/or fragments that might reasonably be anticipated to bind to the active centers of trypsin-like enzymes. Inclusion of these

fragments as positive controls was considered most helpful for investigation of the intrinsic performance of SAS during fragment identification and the internal coherence of results obtained. Although highly interesting, potential issues of this type have not been investigated earlier. It is also worth mentioning that on the basis of the dimensions of fragments and SAS's reliance on enzymatic activity, processed substrates can reasonably be expected to be accommodated in the S1 region of the enzyme (i.e., the S1 pocket and the parts of the active center immediately surrounding it). This consideration was taken into account during the selection of the positive control set, containing mainly basic groups and S1-binding substituents of known uPA inhibitors.

4.2.2. Chemistry

A substantial part of the *N*-acyl AMCs library was prepared by a one-pot protocol, by starting from the individual acyl residues and 7-amino-4-methylcoumarin and using a mild acyl chlorinating agent, namely Ghosez's reagent (1-chloro-*N,N*,2-trimethyl-1-propenylamine) as the coupling mediator (**Scheme 4.2**).[34,35] Of a large series of mild coupling reagents evaluated, including DCC, EDC, TBTU, HATU, TFFH, PyBrop, Ghosez's reagent, only the latter was found capable of cleanly and efficiently promoting the reaction with the very weakly nucleophilic 7-amino-4-methylcoumarin. For several compounds, additional steps (protection, homologation, and functionalization) were necessary in order to obtain the desired derivatives (**Schemes 4.3, 4.4**). Structures of all the library members can be found in **Table 4.1** and their chemical characterization is given in the Experimental section (*vide infra*, **Table 4.5**).

Scheme 4.2. Synthesis of the library members using Ghosez's reagent.[a]

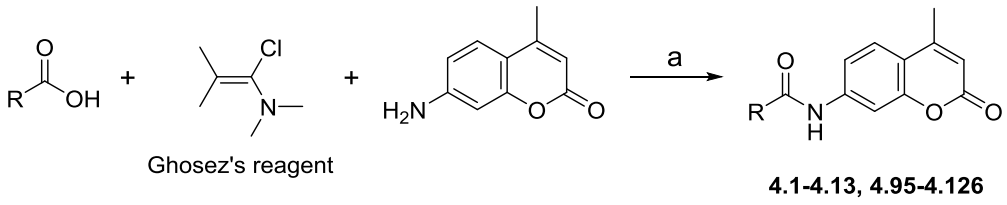

[a]Reagents and conditions: (a) TEA, DCM/THF, rt.

Scheme 4.3. Synthesis of the library members involving a bromoacetylated AMC intermediate step.[a]

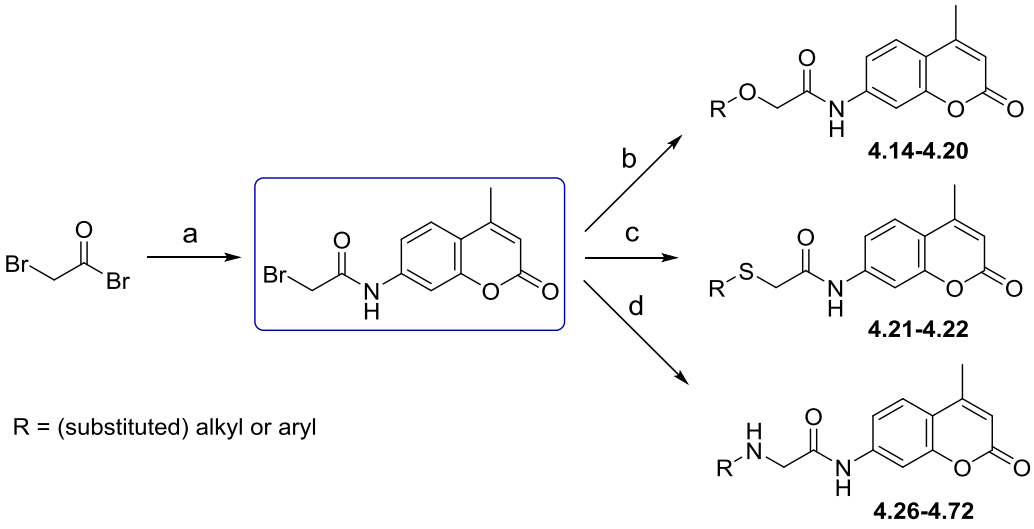

[a]Reagents and conditions: (a) 7-amino-4-methylcoumarin (AMC), TEA, DCM/THF, rt; (b) phenol derivative, K_2CO_3, DMF/toluene; (c) corresponding thiol derivative, K_2CO_3, DMF/toluene; (d) (i) corresponding amine, DMF; in case of compounds **4.31**, **4.42**, **4.49** (ii) TFA/DCM (1:1).

Scheme 4.4. Synthesis of AMCs with *N*-alkyl-amino-azaheteroaromatic or guanidine-containing *N*-acyl groups.[a]

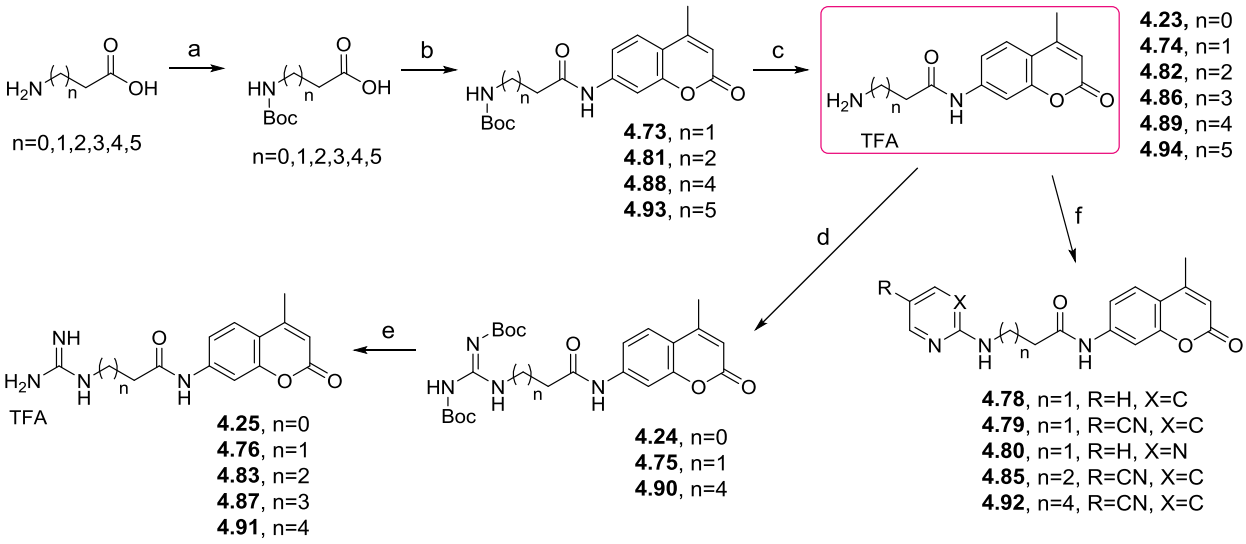

[a]Reagents and conditions: (a) Boc_2O, NaOH, 1,4-dioxane/water; (b) (i) AMC, Ghosez's reagent, TEA, DCM/THF, rt; (c) TFA/DCM (1:1), rt; (d) *N,N'*-di-Boc-1*H*-pyrazole-1-carboxamidine, TEA, DMF; (e) TFA/DCM (1:1), rt; (f) corresponding 2-chloroazine derivative, $KHCO_3$, DMF, reflux. Additionally, compounds **4.77** and **4.84** were obtained according to a standard nucleophilic substitution reaction (*vide infra*, Experimental section, General procedure C-II), whereas compounds **4.127-4.137** were synthesized following the synthetic procedure presented on **Scheme 4.4** (steps a-e) from different starting materials (*vide infra*, Experimental section).

Table 4.1. Members of the synthesized library of *N*-acyl aminocoumarins (*N*-acyl AMCs).[a]

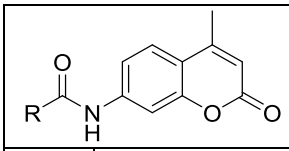

Cpd	R =	Cpd	R =	Cpd	R =
4.1	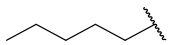	**4.14**	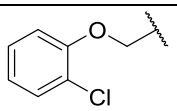	**4.27**	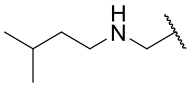
4.2	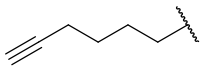	**4.15**	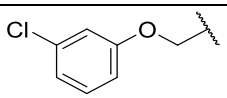	**4.28**	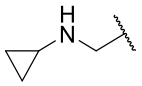
4.3	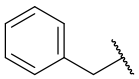	**4.16**	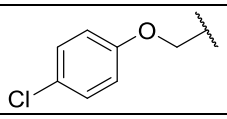	**4.29**	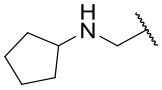
4.4	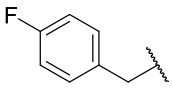	**4.17**	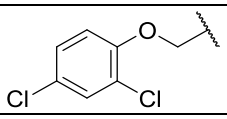	**4.30**	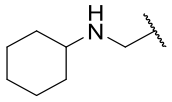
4.5	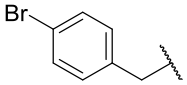	**4.18**	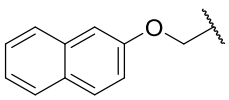	**4.31**	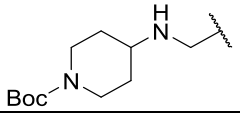
4.6	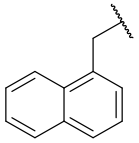	**4.19**	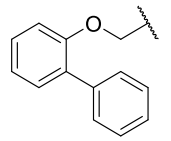	**4.32**	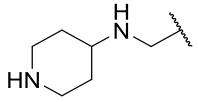
4.7	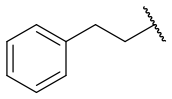	**4.20**	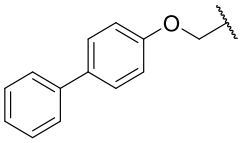	**4.33**	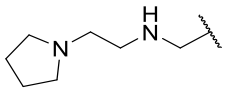
4.8	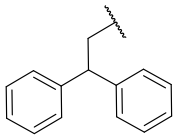	**4.21**	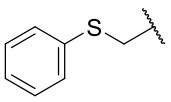	**4.34**	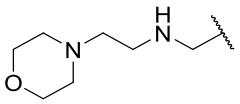
4.9	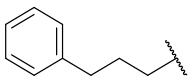	**4.22**	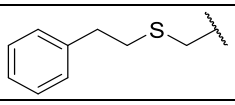	**4.35**	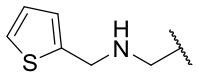
4.10	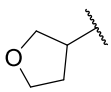	**4.23**	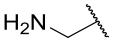	**4.36**	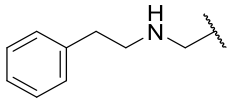
4.11	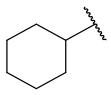	**4.24**	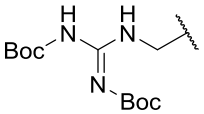	**4.37**	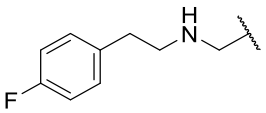
4.12	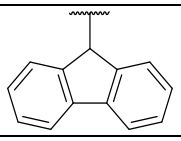	**4.25**	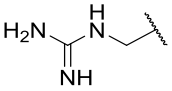	**4.38**	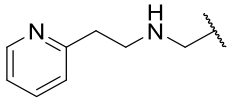
4.13	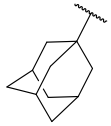	**4.26**	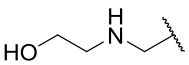	**4.39**	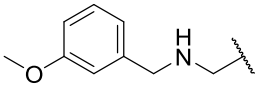

Cpd	R =	Cpd	R =	Cpd	R =
4.40	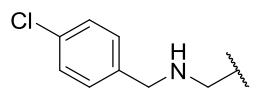	**4.53**	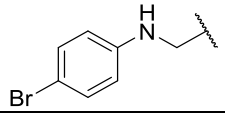	**4.66**	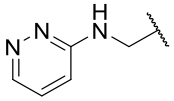
4.41	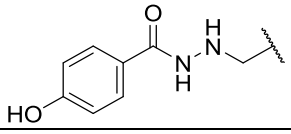	**4.54**	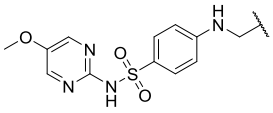	**4.67**	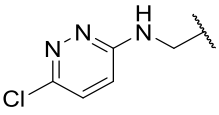
4.42	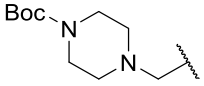	**4.55**	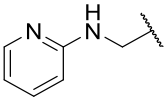	**4.68**	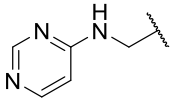
4.43	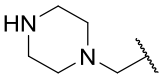	**4.56**	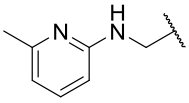	**4.69**	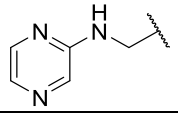
4.44	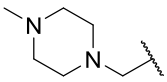	**4.57**	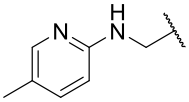	**4.70**	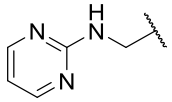
4.45	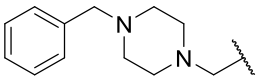	**4.58**	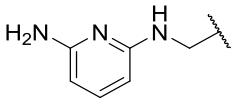	**4.71**	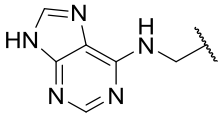
4.46	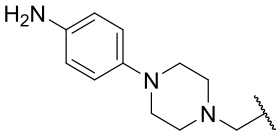	**4.59**	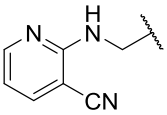	**4.72**	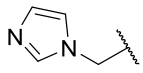
4.47	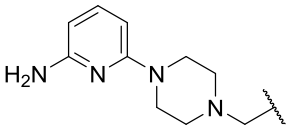	**4.60**	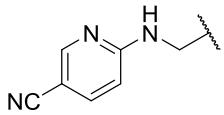	**4.73**	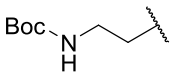
4.48	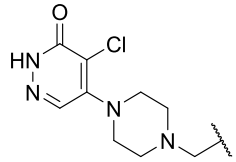	**4.61**	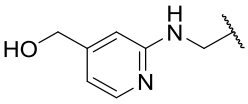	**4.74**	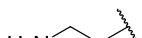
4.49	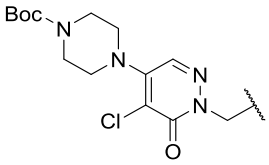	**4.62**	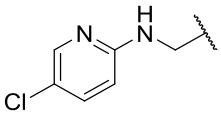	**4.75**	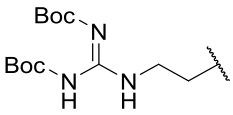
4.50	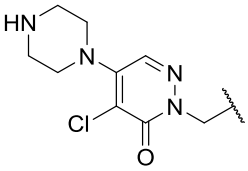	**4.63**	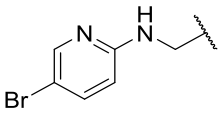	**4.76**	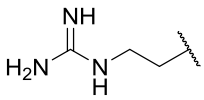
4.51	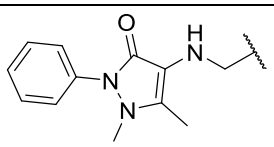	**4.64**	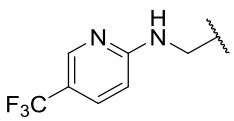	**4.77**	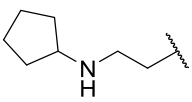
4.52	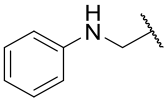	**4.65**	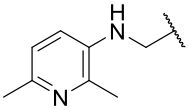	**4.78**	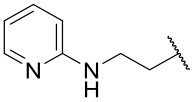

Cpd	R =	Cpd	R =	Cpd	R =
4.79	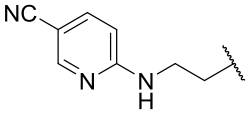	**4.93**	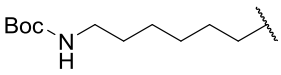	**4.107**	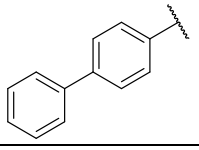
4.80	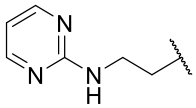	**4.94**	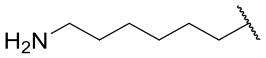	**4.108**	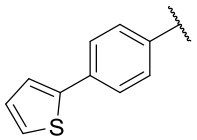
4.81	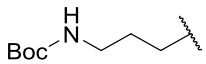	**4.95**	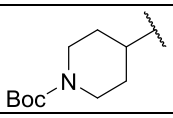	**4.109**	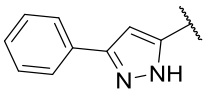
4.82	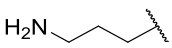	**4.96**	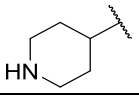	**4.110**	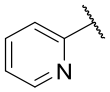
4.83	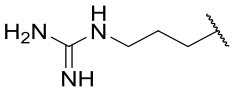	**4.97**	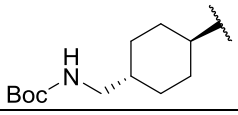	**4.111**	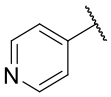
4.84	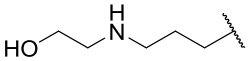	**4.98**	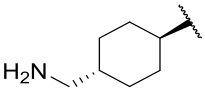	**4.112**	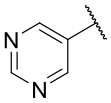
4.85	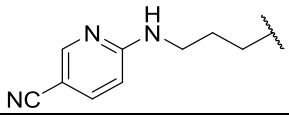	**4.99**	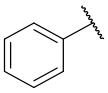	**4.113**	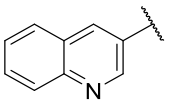
4.86	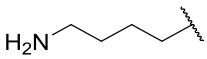	**4.100**	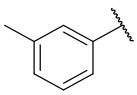	**4.114**	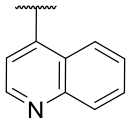
4.87	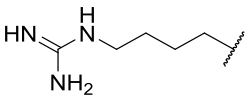	**4.101**	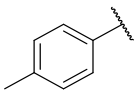	**4.115**	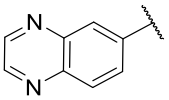
4.88	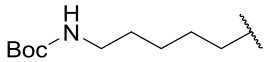	**4.102**	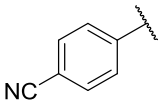	**4.116**	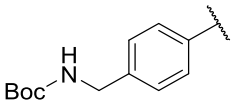
4.89	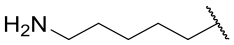	**4.103**	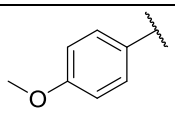	**4.117**	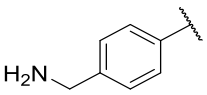
4.90	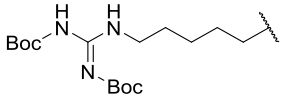	**4.104**	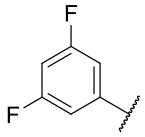	**4.118**	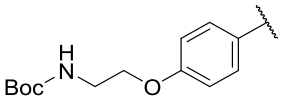
4.91	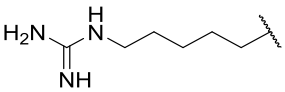	**4.105**	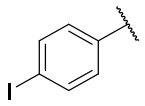	**4.119**	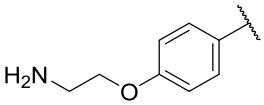
4.92	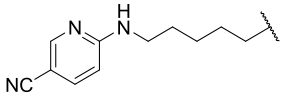	**4.106**		**4.120**	

Cpd	R =	Cpd	R =	Cpd	R =
4.121	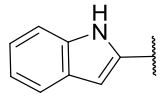	**4.127**	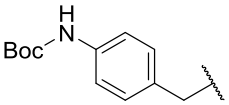	**4.133**	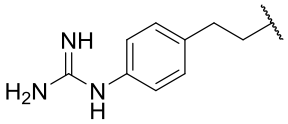
4.122	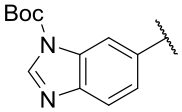	**4.128**	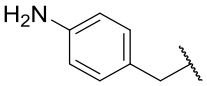	**4.134**	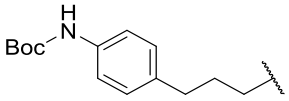
4.123	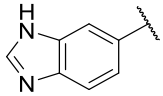	**4.129**	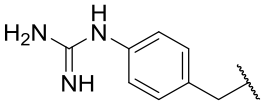	**4.135**	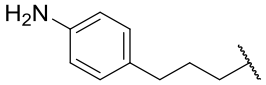
4.124	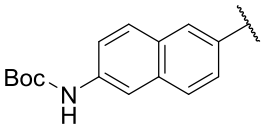	**4.130**	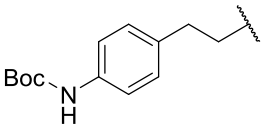	**4.136**	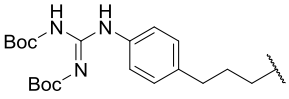
4.125	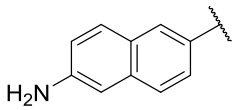	**4.131**	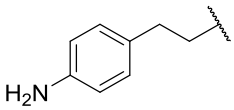	**4.137**	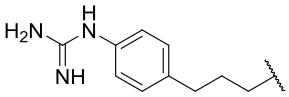
4.126	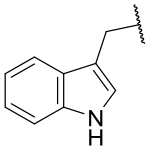	**4.132**	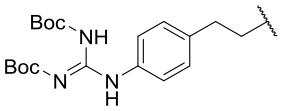		

[a]Synthesized according to **Schemes 4.2-4.4**. General procedures for the preparation of all the library members can be found in the Experimental section of this chapter (Part 4.7).

4.3. Results and discussion

4.3.1. Biochemical evaluation of the library of *N*-acyl AMCs during the SAS experiment

The prepared library of *N*-acyl AMCs was first screened for uPA substrates by a typical SAS protocol. All these experiments were conducted in duplicate in HEPES (2-[4-(2-hydroxyethyl)piperazin-1-yl]ethanesulfonic acid) buffer at pH 8.2, thus allowing near-maximum enzymatic activity to be combined with minimal aspecific hydrolysis of *N*-acyl AMCs. An initial screening of the library was performed with 200 nM of recombinant human uPA and the highest substrate concentration allowed by compound solubility. Although these concentrations varied for the individual library members, they were generally in the 100-500 µM range. We reasoned that the use of high substrate concentrations in the exploratory phase of the project would allow identification of all library members that are processed by uPA, even those characterized by low k_{cat} values.

Under the initial conditions, eleven *N*-acyl AMCs from the library were found to behave as substrates of uPA, albeit with large differences in cleavage rate. To allow reliable ranking of cleavage efficiencies, assays for these compounds were repeated at subsaturating substrate concentrations ([S] < K_m). To avoid the need to determine K_m values for all the obtained hits, we followed the

approach proposed by Ellman et al.[18] Here, only the K_m value of the optimal substrate in the series is determined. Subsequently, all initially obtained hits were investigated again at a concentration below the K_m value of the best substrate, with this serving as a reference relative to which cleavage efficiencies are reported. We considered the guanidinophenyl-based compound **4.133** (**Table 4.2**), displaying a K_m value of 120 µM, to be the best substrate. Subsequently, all initially obtained hits were rescreened at 100 µM concentration, and this reconfirmed guanidinophenyl derivative **4.133** as the most efficiently cleaved substrate in the series. The cleavage efficiencies of all eleven hits, relative to compound **4.133**, are summarized in **Table 4.2** ("substrate screening" columns).

Given uPA's substrate preferences and the intentional inclusion of a substantial number of basic compounds in the library, it is not surprising that most other identified hits contain a basic functionality, most likely accommodated in the acidic S1 pocket of uPA. Additionally, the distance between this basic functionality and the acyl-AMC group in each substrate roughly equals the corresponding distance between the guanidine group and the scissile amide bond in a typical P1(Arg)-containing peptide substrate of the enzyme. The lipophilic aryl derivatives **4.17** and **4.100** are the only non-basic hits in the series, with **4.17** being processed by uPA with similar efficiency to **4.133**. Notably, even a small deviation from a hit compound's structure was observed to cause a total loss of substrate properties. This is illustrated by the cleavage efficiency pattern within the series (1) **4.15-4.17**, (2) **4.129, 4.133, 4.137**, (3) **4.83**, **4.87**, and indicates that the robustness of SAS as a method to identify useful fragments for inhibitor discovery is not optimal. It is indeed highly conceivable that "unbiased" SAS libraries will overlook potentially interesting fragments if either (1) the linker distance between the fragment and the acyl-AMC functionality or (2) the fragment substitution pattern does not precisely fit the requirements for stabilization of the transition state of substrate conversion. In our opinion, these findings demonstrate that unmodified application of the SAS protocol can lead to loss of relevant information and hence "false negatives". In addition, predictive application of the obtained processing data by construction of structure-cleavage efficiency relationships (analogous to structure-activity relationships in traditional inhibitor discovery) seems compromised by the use of a readout system that is very sensitive to minute structural changes. Furthermore, we observed that the SAS protocol requires substantial amounts of target protein (~2.5 µg per well), together with long screening times. Both experimental parameters were used according to Ellman's reports and were found to be crucial for detection of slowly degraded library members. Also the critical importance of enzyme purity is worth highlighting. In a separate screening of our library with commercial uPA obtained from human urine, a series of additional hits characterized by very high turnover efficiencies was obtained. These compounds, however, were not cleaved to any extent by the recombinant enzyme (**Scheme 4.5**). During further

investigations of this apparent discrepancy between the two uPA preparations, we were able to show that the processing of those compounds could not be inhibited by addition of a nanomolar uPA inhibitor that has been reported earlier by our group (**UAMC-00122**).[33] Application of chromatographic and gel electrophoretic techniques were not helpful for identifying the catalyst responsible for cleavage in the human uPA preparation. Nonetheless, these results also indicate that the published SAS protocol is susceptible to possible occurrence of false positives, with the presence of other catalytically active species (e.g., other enzymes occurring as impurities) being responsible.

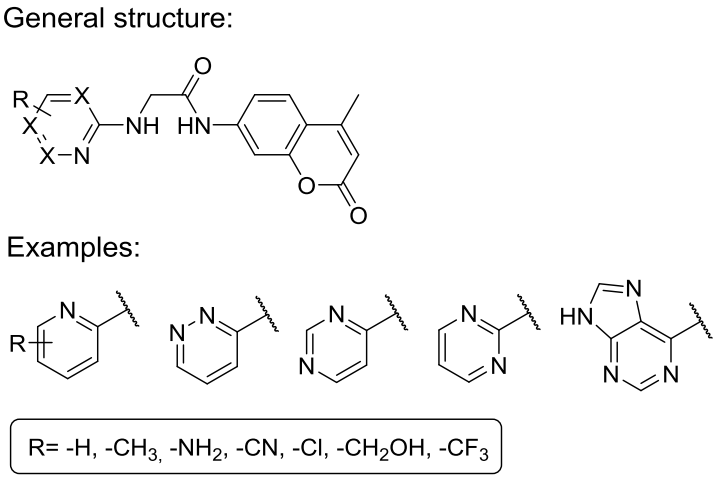

Scheme 4.5. Compounds that were processed by a commercial human uPA preparation obtained from urine, but not by recombinant human uPA.

4.3.2. Application of the MSAS protocol to screening the library of *N*-acyl AMCs

In response to the relevant and unreported limitations of SAS, we devised a modified and fundamentally different experimental setup for library evaluation: "MSAS" (modified substrate activity screening). In the proposed screening method the inhibitory properties of the library members are investigated, rather than their substrate properties. A protocol strongly related to the archetypical assay normally used for enzyme inhibitor evaluation was elaborated. Here, the library members' potential to inhibit degradation of a known, peptide-derived chromogenic substrate of the target is evaluated. We hypothesized that this strategy should be able to uncover all fragments with affinity for uPA, and not only those characterized by an ideal linker distance or an optimal substitution pattern. Additionally, selection of the efficiently processed chromogenic substrate pyro-Glu-Gly-Arg-pNA (K_m = 80 µM) for this assay allowed to lower tenfold the enzyme concentration relative to the SAS protocol.[36] The application of a single, kinetically well-characterized substrate also avoided the possibility of "false positive" results to occur and removed the need to verify whether the library members are processed by the actual target enzyme or by another catalytically active species present in the enzyme preparation.

Table 4.2. Hits obtained after screening of a 137-compound library of *N*-acyl AMCs.

Cpd	Structure 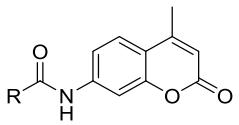 R =	Substrate screening	Inhibitor screening		Cpd	Structure 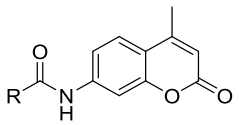 R =	Substrate screening	Inhibitor screening	
		cleavage efficiency [%][a]	conc [µM]	I [%][b]			cleavage efficiency [%][a]	conc [µM]	I [%][b]
4.1	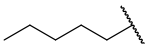	– [c]	100	27	**4.86**	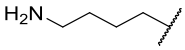	14	500	20
4.5	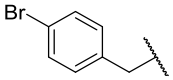	–	50	21	**4.87**	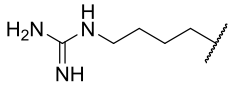	65	500	45
4.9	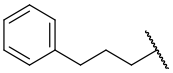	–	100	24	**4.89**	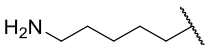	9	500	17
4.13	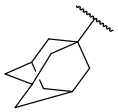	–	100	19	**4.98**	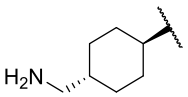	72.3	500	50
4.15	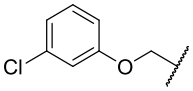	–	50	25.7	**4.100**	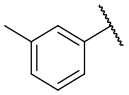	8.2	100	27
4.16	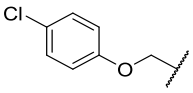	–	100	33.6	**4.101**	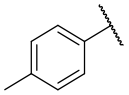	–	100	27.5
4.17	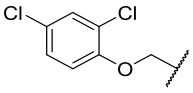	**98.7**	400	50	**4.105**	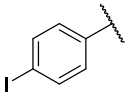	–	50	23
4.18	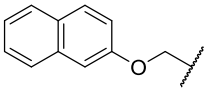	–	50	25	**4.106**	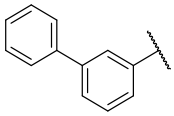	–	100	31
4.43	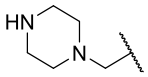	20.5	500	28	**4.109**	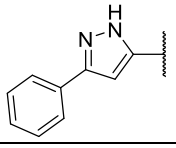	–	100	32.6
4.44	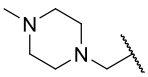	3.2	500	23	**4.117**	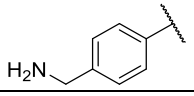	30	500	39
4.50	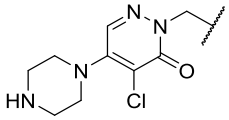	–	500	21.5	**4.119**	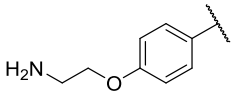	34.5	500	30.4
4.53	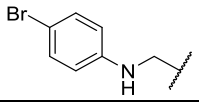	–	250	27.3	**4.129**	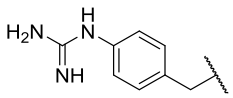	–	100	63.4
4.54	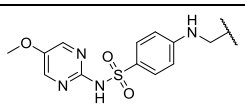	–	250	20.3	**4.133**	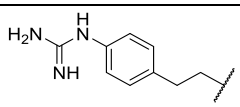	**100**	100	50
4.83	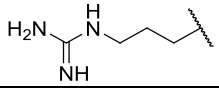	–	500	64.3	**4.137**	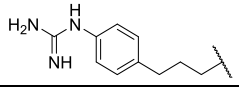	–	250	58

[a]Cleavage efficiency is defined as the cleavage rate of a compound relative to the "best" substrate in the library (compound **4.133**). [b]Inhibition (I) is defined as the % decrease in the processing rate of reference uPA substrate pyro-Glu-Gly-Arg-pNA. [c] "–" indicates that no uPA-mediated cleavage of the compound was observed.

In this experiment, with use of 20 nM uPA, the 137 library members were screened again at 50-500 µM, with concentrations depending upon compound solubility. The readout consisted of the evaluation of uPA-mediated *para*-nitroaniline release from the chromogenic substrate pyro-Glu-Gly-Arg-pNA, at 100 µM concentration. The results, expressed as percentage inhibition of pyro-Glu-Gly-Arg-pNA cleavage at a given compound concentration, are summarized in **Table 4.2** ("inhibitor screening" columns). In general, it deserves mentioning that the affinities displayed by the "hits" are well within the range that is generally reported for fragments (high micromolar). Furthermore, our alternative approach identifies all eleven "hits" initially revealed by the traditional SAS protocol. The relative affinities observed for these eleven compounds in the inhibition experiment (extrapolated from their inhibitory potencies) roughly reflect the cleavage efficiencies of the compounds.

Most interestingly, though, our modified screening procedure also discloses an additional 17 molecules that inhibit the release of *para*-nitroaniline. Inspection of the compounds with inhibitory properties immediately provides a more coherent image of structural classes that possess potential for uPA inhibitor discovery within the library. As an example, all guanidinophenyl (**4.129, 4.133, 4.137**) and guanidinoalkyl (**4.83**, **4.87**) homologues present in the library were identified as inhibitors, whereas SAS had only selected one of either class. Analogously, all chlorophenyl (**4.15-4.17**) and closely related lipophilic phenyl derivatives (**4.5** and **4.53, 4.18, 4.100-4.101** and **4.105-4.106**) that were present in the library turned up as potentially valuable constituents for new uPA inhibitors. Again, from the results of the SAS approach, one would conclude that **4.17** and **4.100** are two singletons of interest within the library, whereas they instead belong to a group of closely related structures that could all be valuable for uPA inhibitor design. Furthermore, our alternative method avoids false positives due to other catalytically active species present in the enzyme preparation. False positive results caused by compound-induced aggregation or denaturation of the enzyme were also not observed during the inhibitor screening.

These findings confirm that, to identify useful fragments in a given SAS library, it could be more efficient to evaluate the inhibitory properties of the library members rather than their substrate characteristics. More emphasis can in this way be placed on creating a structurally diverse library because the need for a number of homologues or close analogues around each structural feature is reduced. A point-by-point comparison of the two screening modes is given in **Table 4.3**.

Table 4.3. Comparison of SAS and inhibitor screening protocols.

Parameter	SAS	Inhibitor screening
Amount of enzyme per well	2.5 µg (400 IU)	0.25 µg (40 IU)
Screening time	6 h [a]	10 min
False positives	yes [b]	not observed
False negatives	yes [c]	not observed

[a]Long screening times can cause errors due to, for e.g., enzyme denaturation, autoproteolysis or buffer evaporation.[27] [b]Depending on enzyme purity, presence of additives/preservatives in the enzyme formulation. [c]Resulting in incomplete SAR data.

When using a library of AMC amides for fragment identification, one might nonetheless speculate on the possibility that the AMC moiety might interfere during the process of target binding. Although peptidyl-AMC amides have been used successfully for decades in inhibitor discovery, this is not completely inconceivable in, for example, hypothetical cases in which the AMC ring is not accommodated in the S1' region of the enzyme. Theoretically, such interference could consist either of (1) a net hampering effect on fragment binding (e.g., by steric hindrance) or, alternatively, (2) a net supportive effect (e.g., if the AMC ring were to contribute to affinity). We expect that interference of the first type would surface in the form of incoherent SAR data, involving "outliers" that unexpectedly do not show target affinity. The identification of all positive controls in our library and the near complete coverage of compounds that belong to inhibiting structural subgroups of the library do indicate that, in general, the AMC ring is not significantly hampering fragment binding. Similarly, the obtained results also do not suggest that the AMC ring contributes significantly to affinity, because most of the library members evaluated were devoid of measurable uPA affinity. Taking all these considerations into account, we expect the AMC portion of the library members not to interfere significantly with the inhibitory properties of the fragments. Equally illustrative of this is the fact that the isolated guanidinobenzene fragment **4.138** (*vide infra,* **Scheme 4.7**) has an affinity broadly comparable to those of AMC-linked fragments **4.129, 4.133,** and **4.137**. So far we have also not observed indications of interference in a number of other ongoing projects dealing with inhibitor design for caspases and autophagins during which the same library was screened for inhibiting fragments.

It also deserves mentioning that the highest affinities observed within the structural subgroups with inhibitory properties do not necessarily belong to the compounds that are also substrates. This is seen, for example, on comparing the slightly higher inhibitory potency of guanidinophenyl derivative **4.129** with that of homologue **4.133**, of which only the latter is processed as a substrate. We

therefore investigated whether apparently lower affinities of library members displaying substrate properties might be accounted for by their gradual consumption during the inhibition experiment. Quantification of cleavage during the course of an inhibition experiment was determined by monitoring the release of AMC. The process was, however, found to be too slow to interfere significantly with determination of inhibitory potency. This is read out after 10 min, typically during the linear phase of peptide substrate consumption (**Figure 4.1**). In hypothetical cases in which library members with exceptionally high k_{cat}/K_m values relative to the peptide substrate used might be present, however, such an effect could not be excluded. In addition, therefore, two control experiments were also carried out for each inhibitory library member to ascertain whether or not the identified inhibitor series could include noncompetitive, allosteric or irreversible compounds. Again, the SAS protocol would not allow identification of such fragments, although they could certainly be of interest to specific inhibitor discovery programs. For all compounds in **Table 4.2**, inhibition was found to decrease with increasing concentration of the chromogenic substrate, thus indicating competition for the enzyme's active site. The percentage inhibition increased with inhibitor concentration and did not change significantly with longer inhibitor preincubation times, as would be the case for slowly and irreversibly binding compounds.

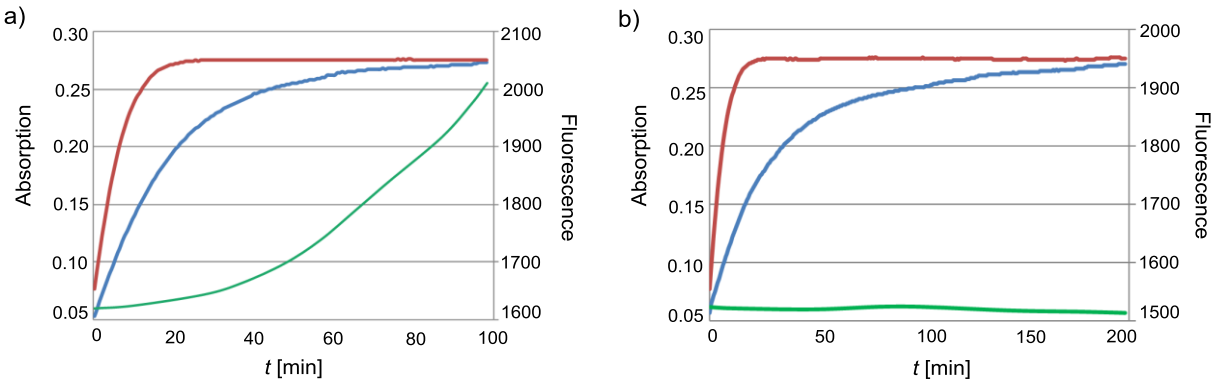

Figure 4.1. Inhibitory profiles of two selected structurally related MSAS hits: (a) Inhibitory profile of compound 4.133, a library member with substrate properties. At *t* = 10 min, consumption of 4.133 is minimal, and read-out of inhibitory potency is not significantly influenced. (b) Inhibitory profile of compound 4.137, a library member that is not a substrate. On the graph "—" relates to uPA+ pyro-Glu-Gly-Arg-pNA (control experiment), measuring release of pNA. "—" Relates to uPA+ pyro-Glu-Gly-Arg-pNA+ compound 4.133 or 4.137, measuring release of pNA. "—" Relates to uPA+ pyro-Glu-Gly-Arg-pNA + compound 4.133 or 4.137, measuring release of AMC.

On the basis of the obtained results, we devised the MSAS experimental protocol. The proposed strategy combines optimal efficiency and maximum extraction of useful structural information during screening of SAS libraries. Its key steps are represented in **Scheme 4.6**. In MSAS, the library is first screened for inhibitory fragments (**Scheme 4.6, step 1**). This experimental layer will provide SAR data for the interesting fragment types present within the library. As demonstrated, the hits obtained in the inhibition experiment will also include library members with substrate properties. Because step 1 runs with higher time- and cost-efficiency than a traditional SAS experiment, we propose to perform SAS during the second phase of MSAS and only for identifying the substrates within the set of hits identified during the inhibitor screening experiment (**Scheme 4.6, step 2**). Furthermore, it is important to stipulate that MSAS's experimental setup, like that of the parent methodology, is not limited to protease inhibitor discovery. The same strategy can directly be applied to any other type of enzyme target studied, provided that the members of the screened library each contain a suitable enzyme-processable functionality.

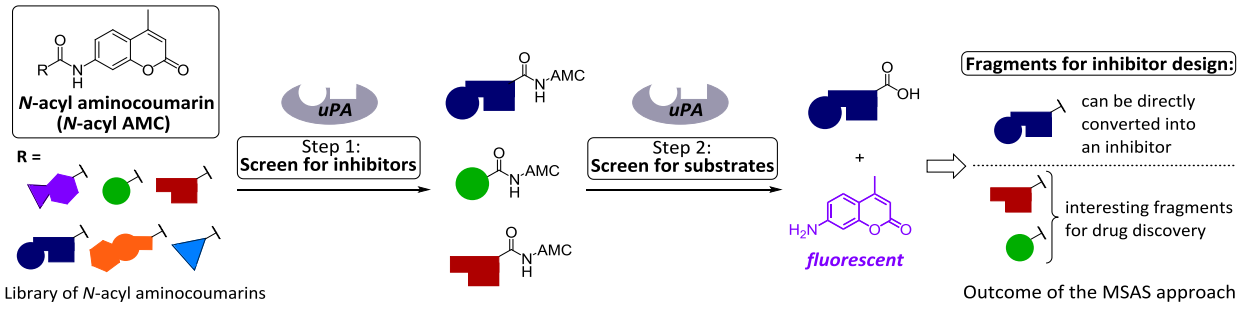

Scheme 4.6. Outline of the MSAS approach demonstrated for a protease target.

The affinity data obtained after step 1 and the substrate property data obtained after step 2 can theoretically be validated in several orthogonal approaches for transforming fragments into inhibitors. To investigate and validate the results of the MSAS setup further, representative examples of such approaches are preliminarily explored in the following part. Library member **4.133**, possessing both significant uPA affinity and substrate properties, was selected as the common starting point. The 4-guanidinophenethyl portion of this compound had already been reported earlier by our group as a constituent of nanomolar and highly selective peptide-derived diaryl phosphonate inhibitors of uPA.[33] It was therefore included in the "biased" portion of the library. Its status as a positive control element also justified its selection for the experiments dealing with translating fragments into inhibitors.

4.4. Validation of the "inhibitor screening" (step 1, MSAS)

In order to validate the affinity data produced during step 1 of MSAS, we proposed a generally applicable strategy based on the preparation of scaffold-based inhibitors. With specific regard to protease targets, such scaffold-based compounds have the potential to circumvent several of the inherent liabilities of classical, peptide-based protease inhibitors (mainly related to ADME: absorption, distribution, metabolism and excretion). Also on a much more general level, many of the recently approved small-molecule drugs share an overall comparable architecture consisting of a central scaffold decorated with several substituents that confer additional affinity for the biomolecules they target. A generalized routine for obtaining such compounds is proposed. Firstly, a fragment identified during the first step of MSAS is chemically grafted onto a limited set of different, drug-like scaffolds (**Scheme 4.7**). If a compound with uPA affinity significantly higher than that of the original fragment is found within this small set of monosubstituted scaffolds, that compound is selected for further optimization. During the optimization, one to several additional substituents are introduced on the selected monosubstituted scaffold to increase target affinity further. For maximum efficiency, it is advisable to select scaffold types onto which several additional substituents can readily be introduced, preferentially in a regioselective fashion and by combinatorial chemistry techniques.

To elaborate this concept, we chose the imidazopyridine and pyrimidine scaffolds, already present in, for example, the hypnotic drug zolpidem and the HIV-RT inhibitor rilpivirine.[37,38] A wealth of efficient chemical decoration strategies that allow efficient production of diversely substituted analogues exist in both cases.[39,40] Firstly, the guanidinophenethyl fragment was attached through an amine linker (**Scheme 4.7**). The two scaffolded inhibitors **4.139** and **4.140** were then evaluated, and they displayed roughly comparable affinities for uPA (19.39 ± 1.22 μM and 9.26 ± 1.05 μM, respectively). This corresponds to a relative increase in affinity of about one order of magnitude relative to library member **4.133** and indicates that both the imidazopyridine and pyrimidine scaffolds could be used for construction of scaffold-based uPA inhibitors. For obtaining molecules with increased affinity, further optimization could be performed by introducing one or several additional substituents. The synthesis and chemical characterization of the scaffold-based inhibitors can be found in the Experimental section of this chapter as well as, in case of the imidazopyridine compound **4.139**, in Chapter 5.

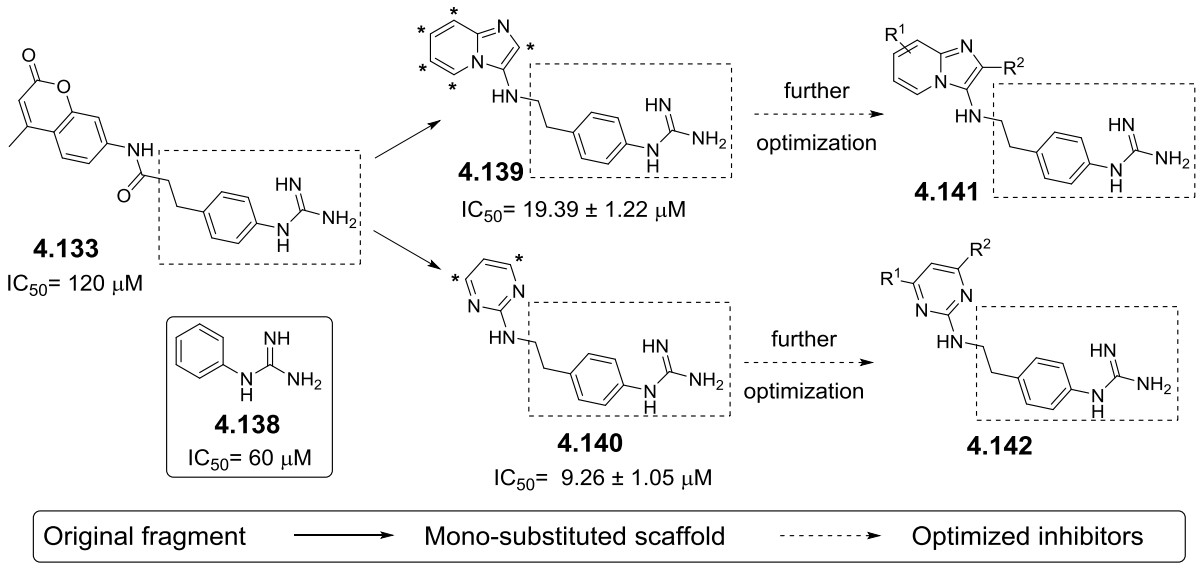

*= suitable derivatization point; R^1, R^2 = additional substituents

Scheme 4.7. Introduction of the 4-guanidinophenethyl fragment onto an imidazopyridine and a pyrimidine scaffold to afford 4.139 and 4.140, respectively. Scaffold positions that, from a synthetic point of view, allow easy substituent introduction for further optimization are marked with asterisks; R^1, R^2 = additional substituents.

4.5. Validation of the 'substrate screen' (step 2, MSAS)

4.5.1. Chemistry

The original data validation strategy of the SAS approach (step 2, MSAS) was based on the preparation of diphenyl phosphonate inhibitors of urokinase. To this end, the potentially irreversibly binding diphenyl phosphonate warhead was grafted onto the 4-guanidinophenethyl moiety and also, as a control, onto the homologous 4-guanidinophenylmethyl residue of **4.129**. Diaryl phosphonate inhibitor **4.143** was obtained using a general protocol for base-promoted alkylation of *H*-phosphonates (the Michaelis-Becker reaction), and the homologous compound **4.144**, was prepared by the modified version of the classical Arbuzov reaction protocol, from previously synthesized starting materials (**Schemes 4.8, 4.9**).[41,42] Chemical characterization of the prepared phosphonate inhibitors can be found in the Experimental section of this chapter (Part 4.7).

Scheme 4.8. Synthesis of diaryl phosphonate inhibitor 4.143.[a]

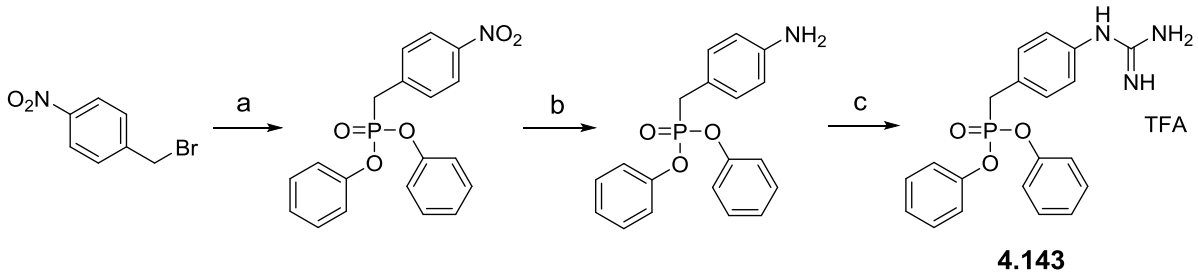

4.143

[a]Reagents and conditions: (a) 1-(bromomethyl)-4-nitrobenzene, diphenylphosphite, DBU, 0 °C, 2 h; (b) Zn/HCl, THF, 0 °C; (c) (i) *N,N'*-di-Boc-1*H*-pyrazole-1-carboxamidine, TEA, THF, rt, (ii) TFA/DCM (1:1), rt, 1 h.

Scheme 4.9. Synthesis of diaryl phosphonate inhibitor 4.144.[a]

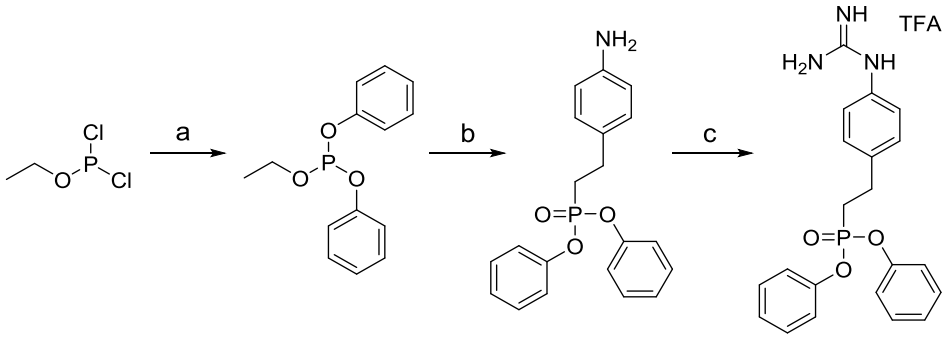

4.144

[a]Reagents and conditions: (a) phenol, TEA, toluene; (b) (i) 1-(2-bromoethyl)-4-nitrobenzene, pressure tube, 120 °C, (ii) Zn/HCl, THF, 0 °C; (c) (i) *N,N'*-di-Boc-1*H*-pyrazole-1-carboxamidine, TEA, THF, rt, (ii) TFA/DCM (1:1), rt.

4.5.2. Results and discussion

Biochemical evaluation of the prepared phosphonates revealed that compound **4.144** derived from fragment "hit" identified during substrate screening is a potent mechanism-based inhibitor of uPA, in contrast to compound **4.143**. The latter was derived from a fragment which, although still possessing uPA affinity, was not processed as a substrate in the corresponding assay. As suggested by Ellman and co-workers, this would translate either into an inhibitor with significantly reduced potency, or at least into a compound with compromised capability of mechanism-based enzyme blocking.[19] Indeed, compounds **4.143** and **4.144** displayed an approximately 140-fold difference in potency (**Table 4.4**). Furthermore, both compounds were subsequently demonstrated to be irreversible inhibitors. This typically implies that the inhibitory potencies of **4.143** and **4.144** should not be interpreted as a strict

indication of their affinities but rather as a measure for their respective second-order rate constants of the irreversible step in enzyme inactivation. In any case, these results agree well with SAS's assumptions, and on a broader level, with the fundamental assumptions of more canonical approaches in substrate-based drug discovery.

Table 4.4. Comparison of IC_{50} values for uPA inhibition of different benzylguanidine-containing compounds derived from fragments 4.129 and 4.133.

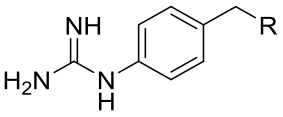

Cpd	R =	IC_{50} (uPA) [µM]	Inhibition type
4.143	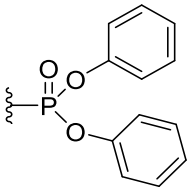	1.37 ± 0.05	irreversible[a]
4.144	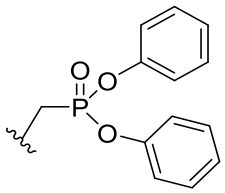	0.0097 ± 0.0003	irreversible[a]
4.145[b]	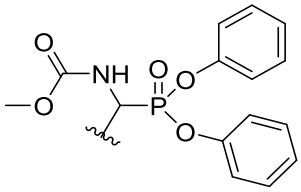	0.0031 ± 0.0005	irreversible[a]
4.146	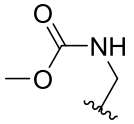	250	reversible
4.147	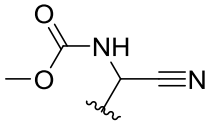	5.0 ± 0.01	reversible

[a]Validated experimentally by dilution assay.[36] [b]Previously reported as UAMC-00150.[33]

It is also remarkable that the potency displayed by compound **4.144** broadly compares with that of diaryl phosphonate **4.145** (**UAMC-00150**), reported earlier by our group as one of the best representatives of known uPA inhibitors.[33] This reference inhibitor contains an additional methoxycarbamoyl group mimicking the P2-P1 amide bond of uPA's peptide substrates. On the basis of this higher degree of similarity with compound types that are naturally processed by uPA, one could reasonably assume that both the kinetic and the thermodynamic parameters of target binding could be favorable in the case of **4.145**, thus resulting in a higher net potency. However, the absence of the methoxycarbamoyl fragment in **4.144** does not seem to interfere significantly with the overall process of target recognition and irreversible covalent bond formation.

Additionally, compounds **4.146** and **4.147**, containing identical methoxycarbamoyl substituents, were evaluated as potential uPA inhibitors. The first, compound **4.146**, lacks a warhead functionality and served mainly to assess the contribution of the reactive functionality to inhibitory potencies, as discussed earlier. Compound **4.146** similar as the phenylguanidine fragment **4.138** has IC_{50} value in the high micromolar range; this indicates that the potencies observed for **4.143-4.145** are mainly driven by an efficiently occurring irreversible step after initial binding of the inhibitor to uPA.[43]

With this information available, compound **4.147** was evaluated as a second test case for the SAS protocol. This molecule contains a carbonitrile group, a potentially reversible, covalent warhead type very often used in inhibitors of serine proteases. Its low micromolar affinity indicates that the nitrile group in this molecule might not be suitably oriented to allow covalent bond formation with uPA in a low energy inhibitor conformation. This result does not raise any critical doubts as to the validity of the SAS protocol, but it warns that for transformation of SAS "hits" into inhibitors, evaluation of several warheads might be mandatory in order to identify a type that performs well with the selected protease and inhibitor.

4.6. Conclusions

In conclusion, the SAS approach has been investigated for the discovery of inhibitors of oncology target urokinase (uPA). Although the obtained results were supportive of the fundamental hypotheses formulated earlier for SAS, we also encountered a number of unreported limitations of the approach. In response, we propose a simple, efficient modified methodology: "MSAS" (modified substrate activity screening). This methodology not only circumvents limitations of the parent approach, but also broadens its scope by providing additional fragments and more coherent SAR data. As well as introducing MSAS as a generally applicable method for enzyme inhibitor discovery, this study has expanded existing SAR knowledge on S1-pocket- binding fragments of uPA. In addition,

hitherto unreported uPA inhibitor scaffolds are presented and have been used to obtain new reversible and irreversible compounds.

4.7. Experimental section

4.7.1. Chemistry

Unless otherwise stated, laboratory reagent grade solvents were used. Reagents were obtained from Sigma-Aldrich (St. Louis, MO, USA), Acros (Geel, Belgium), Fluorochem (Hadfield, Derbyshire, UK), or Apollo Scientific (Bredbury, Stockport, Cheshire, UK) and were used without further purification. Synthesized compounds were characterized by ^{1}H NMR, ^{13}C NMR and mass spectrometry. ^{1}H NMR and ^{13}C NMR spectra were recorded with a Bruker Avance DRX 400 spectrometer, and analyzed with use of MestReNova analytical chemistry software. Chemical shifts are in ppm, and coupling constants are in Hertz (Hz). NMR spectra of a number of prepared starting materials which are not included in this section were agreeing with the available reported data. Electrospray ionization (ESI) mass spectra were obtained with an Esquire 3000plus ion trap mass spectrometer from Bruker Daltonics (Billerica, MA, USA). Purities were determined with two diverse HPLC systems based either on mass detection or on UV detection. Water (A) and acetonitrile (B) were used as eluents. Formic acid 0.1% was added to solvents A and B. LC/MS spectra were recorded on an Agilent (Santa Clara, CA, USA) 1100 Series HPLC system using a Alltech Prevail C18 column (2.1 × 50 mm, 3 µm) coupled with an Esquire 3000plus as MS detector and a 5-100% B, 20 min gradient was used with a flow rate from 0.2 mL/min. A Waters (Milford, MA, USA) Acquity UPLC® system coupled to a Waters TUV detector and a Waters TQD ESI mass spectrometer was used. A Waters Acquity UPLC® BEH C18 1.7 µm, 2.1 mm x 50 mm column was used. Solvent A: water with 0.1% formic acid; solvent B: acetonitrile with 0.1% formic acid. Method I: flow 0.35 mL/min, 0.15 min 95% A, 5% B then in 1.85 min from 95% A, 5% B to 95% B, 5% A, then 0.25 min, 95% B, 5% A. Method II: flow 0.4 mL/min, 0.25 min 95% A, 5% B, then in 4.75 min to 95% B, 5% A, then 0.25 min 95% B, 5% A, followed by 0.75 min 95% A, 5% B. The wavelength for UV detection was 254 nm. Purity of the final products was determined based on the combined interpretation of ^{1}H NMR and, if available, ^{13}C NMR spectra, and UPLC results.

Where necessary, flash purification was performed with a Biotage® (Uppsala, Sweden) Isolera One flash system equipped with an internal variable dual-wavelength diode array detector (200-400 nm). Biotage® SNAP flash cartridges for normal phase purifications KP-Sil (10-50 g) were used. Gradients used varied for each purification.

General Procedure A (Synthesis of *N*-acyl aminocoumarins (*N*-acyl AMCs) using Ghosez's reagent). Carboxylic acid (0.35 g, 1.4 equiv) was dissolved in a 1:1 mixture of dry DCM/THF (40 mL). To this solution Ghosez's reagent was added (1.4 equiv) and the reaction mixture was stirred for 30 min. Next, 7-amino-4-methylcoumarin (1 equiv), and TEA (1 equiv) were added. The reaction mixture was stirred at room temperature for at least 24 h. Volatiles were evaporated. Target compound was purified by recrystallization or column chromatography. In some cases an additional Boc-deprotection step was required to obtain the desired library members. General procedure A was used to obtain compounds **4.1-4.13**, **4.95-4.126** in **Table 4.5**.

General Procedure B (Preparation of *N*-Acyl AMCs *via* bromoacetylated 7-amino-4-methylcoumarin intermediate step).

Preparation of a bromoacetylated AMC (step 1). To a solution of 2-bromoacetyl bromide (2.62 g, 1.3 equiv) in DCM (65 mL) was added 7-amino-4-methylcoumarin (1.75 g, 1 equiv) and TEA (1.52 g, 2.09 mL, 1.5 equiv). The reaction mixture was stirred for 40 min at room temperature. Volatiles were evaporated. The crude product was washed with small portions of acetone, dried, and subsequently washed with distilled water to afford a pure product in form of a white powder.

General Procedure B-I (step 2). Product of the first step (1 g, 1 equiv) was dissolved in a mixture of toluene/DMF (1:1). To this solution a corresponding phenol derivative (1.3 equiv) and K_2CO_3 (4 equiv) were added. The reaction mixture was stirred at room temperature for 24 h. The crude product was purified by recrystallization or by using the Isolera purification system. General procedure B-I was used to obtain compounds **4.14-4.20** in **Table 4.5**.

General Procedure B-II (step 2). Product of the first step (1.2 g, 1 equiv) was dissolved in a mixture of toluene/DMF (1:1). To this solution a corresponding thiol derivative (1.3 equiv), and K_2CO_3 (4 equiv) were added. The reaction mixture was stirred at room temperature for 24 h. Volatiles were evaporated. Obtained product was purified by recrystallization or by using the Isolera purification system. General procedure B-II was used to obtain compounds **4.21-4.22** in **Table 4.5**.

General Procedure B-III (step 2). Product of the first step (1 g, 1 equiv) was dissolved in DMF and 2 equiv of the corresponding primary or secondary amine were added. The solution was stirred until the reaction was completed (usually 24-48 h). The crude product was purified by recrystallization or by using the Isolera purification system. In some cases an additional Boc-deprotection step was required to obtain the desired library members. General procedure B-III was used to obtain compounds **4.26-4.72** in **Table 4.5.**

General Procedure C (Preparation of AMCs with (I) *N*-alkyl-amino-azaheteroaromatic *N*-acyl groups or (II) guanidine-containing *N*-acyl groups).

Standard procedure for Boc-protection of aminocarboxylic acids (step 1). To a solution of aminocarboxylic acid (3 g, 1 equiv) in a mixture of 1,4-dioxane/water (1:1) was added NaOH (1.1 equiv). Subsequently, a Boc-anhydride (1 equiv) was added, and the reaction mixture was stirred overnight at room temperature. Volatiles were evaporated. The crude product was dissolved in water; the pH of the solution was around 9. Aqueous layer was washed with diethyl ether and acidified to pH = 2 with a 2 M HCl solution. The aqueous layer was extracted with ethyl acetate (3 × 30 mL). The organic phase was separated, washed with brine, dried with anhydrous Na_2SO_4, and evaporated under reduced pressure to afford a Boc-protected aminocarboxylic acid. **One-pot coupling reaction (step 2; see general procedure A). Deprotection of Boc-groups using TFA/DCM (step 3).** Product of the second step was dissolved in a mixture of TFA/DCM (1:1), and the reaction mixture was left stirring for 1 h. Volatiles were evaporated. Precipitation from diethyl ether afforded a pure target compound. General procedure C was used to obtain compounds **4.23, 4.73-4.74, 4.81-4.82, 4.86, 4.88-4.89, 4.93-4.94, 4.127-4.128, 4.130-4.131, 4.134-4.135** in **Table 4.5.**

General Procedure C-I (step 4, Guanidylation of an amine). Product of the third step (0.31 g, 1 equiv) was dissolved in DMF. To this solution *N,N'*-di-Boc-1*H*-pyrazole-1-carboxamidine (1.2 equiv), and TEA (3 equiv) were added. The reaction mixture was stirred at room temperature for 3 days. Volatiles were evaporated. Recrystallization from acetone afforded a pure compound. **Deprotection of Boc-groups using TFA/DCM (step 5). General Procedure C-I** (either including the Boc-deprotection step or not) was used to obtain compounds **4.24-4.25, 4.75-4.76, 4.87, 4.90-4.91, 4.129, 4.132-4.133, 4.136-4.137** in **Table 4.5**.

Procedure C-II (step 4, Standard nucleophilic substitution). Product of the third step (0.32 g, 1 equiv) was dissolved in DMF. To this solution an alkyl chloride derivative (1.1 equiv) and TEA (3 equiv) were added. The reaction mixture was stirred at room temperature for 4 days. Volatiles were evaporated, and the crude product was purified by column chromatography. **General Procedure C-II** was used to obtain compounds **4.77, 4.84** in **Table 4.5**.

Procedure C-III (step 4, Nucleophilic aromatic substitution). Product of the third step (0.35 g, 1 equiv) was dissolved in DMF. To this solution a 2-chloropyridine derivative or, in case of compound **4.80**, 2-chloropyrimidine (1.1 equiv) and $KHCO_3$ (2.2 equiv) were added. The reaction mixture was stirred for around 20 h under reflux under an inert atmosphere of nitrogen. Recrystallization from acetone yielded a pure target compound. **General Procedure C-III** was used to obtain compounds **4.78-4.80, 4.85, 4.92** in **Table 4.5**.

Table 4.5. Chemical characterization of all *N*-acyl AMCs prepared and tested in this study.

Cpd	Structure	General Procedure	Analytical data
4.1	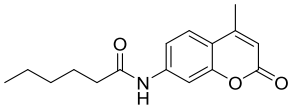	A	^{1}H NMR (400 MHz, DMSO,) δ 0.93 (t, *J* = 8.0 Hz, 3H), 1.36 (d, *J* = 4.0 Hz, 4H), 1.65-1.70 (m, 2H), 2.39-2.45 (m, 5H), 6.3 (s, 1H), 7.54 (dd, *J* = 4.0, 8.0 Hz, 1H), 7.76 (d, *J* = 8.00 Hz, 1H), 7.83 (s, 1H), 10.38 (s, 1H). LC/MS: t_r 16.3 min, *m/z* 295.9 $[M+Na]^+$, 568.9 $[2M+Na]^+$, purity 98%.
4.2	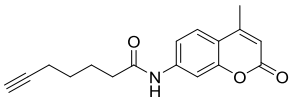	A	^{1}H NMR (400 MHz, DMSO) δ 1.49 (p, *J* = 7.44 Hz, 2H), 1.69 (p, *J* = 7.39 Hz, 2H), 2.16-2.23 (m, 2H), 2.35-2.42 (m, 5H), 2.78 (t, *J* = 2.58 Hz, 1H), 6.25 (s, 1H), 7.49 (dd, *J* = 1.92, 8.63 Hz, 1H), 7.70 (d, *J* = 8.69 Hz, 1H), 7.77 (d, *J* = 1.84 Hz, 1H), 10.35 (s, 1H). LC/MS: t_r 14.9 min, *m/z* 589.1 $[2M+Na]^+$, purity 90%. Yield: 24.9%.
4.3	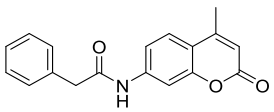	A	^{1}H NMR (400 MHz, DMSO) δ 2.39 (d, *J* = 1.02 Hz, 3H), 3.70 (s, 2H), 6.26 (d, *J* = 1.21 Hz, 1H), 7.25 (m, 1H), 7.31-7.36 (m, 4H), 7.50 (dd, *J* = 2.05, 8.69 Hz, 1H), 7.70 (d, *J* = 8.67 Hz, 1H), 7.75 (d, *J* = 2.01 Hz, 1H), 10.61 (s, 1H). LC/MS: t_r 15.2 min, *m/z* 291.2 $[M-H]^-$, purity 99%. Yield: 29.9%.
4.4	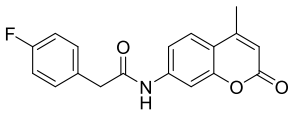	A	^{1}H NMR (400 MHz, DMSO) δ 2.39 (d, *J* = 1.14 Hz, 3H), 3.71 (s, 2H), 6.26 (d, *J* = 1.19 Hz, 1H), 7.12-7.18 (m, 2H), 7.33-7.40 (m, 2H), 7.50 (dd, *J* = 2.61, 8.69 Hz, 1H), 7.71 (d, *J* = 8.69 Hz, 1H), 7.76 (d, *J* = 2.0, 1H), 10.61 (s, 1H). LC/MS: t_r 15.4 min, *m/z* 309.9 $[M-H]^-$, purity 97%. Yield: 13.1%.
4.5	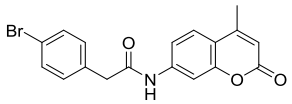	A	^{1}H NMR (400 MHz, DMSO) δ 2.39 (s, 3H), 3.7 (s, 2H), 6.26 (s, 1H), 7.31 (d, *J* = 8.26 Hz, 2H), 7.48-7.54 (m, 3H), 7.71-7.75 (m, 2H), 10.61 (s, 1H). LC/MS: t_r 16.7 min, *m/z* 373.9 $[M+H]^+$, purity 99%. Yield: 33.6%.
4.6	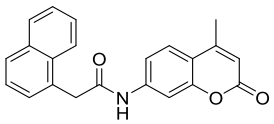	A	^{1}H NMR (400 MHz, DMSO) δ 2.37 (d, *J* = 0.96 Hz, 3H), 4.18 (s, 2H), 6.23 (s, 1H), 7.46-7.54 (m, 5H), 7.69-7.73 (m, 2H), 7.84 (dd, *J* = 1.79, 7.03 Hz, 2H), 7.92 (d, *J* = 7.65 Hz, 1H), 8.07 (d, *J* = 8.07 Hz, 1H), 10.75 (s, 1H). LC/MS: t_r 16.8 min, *m/z* 342.0 $[M-H]^-$, purity >99%.
4.7	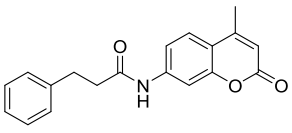	A	^{1}H NMR (400 MHz, DMSO) δ 2.36 (s, 3H), 2.65 (t, *J* = 8.06 Hz, 2H), 2.89 (t, *J* = 7.93 Hz, 2H), 6.22 (s, 1H), 7.15-7.17 (m, 1H), 7.21-7.27 (m, 4H), 7.44 (dd, *J* =1.98, 8.67 Hz, 1H), 7.68 (d, *J* = 8.67 Hz, 1H), 7.73 (d, *J* = 1.91 Hz, 1H), 10.36 (s, 1H). LC/MS: t_r 16.2 min, *m/z* 305.9 $[M-H]^-$, purity >99%. Yield: 57%.

4.8	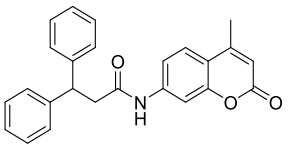	A	^{1}H NMR (400 MHz, DMSO) δ 2.37 (d, J = 1.2 Hz, 3H), 3.16 (d, J = 8.4 Hz, 2H), 4.59 (t, J = 8 Hz, 1H), 6.24 (d, J = 1.2 Hz, 1H), 7.16 (m, 2H), 7.32 (m, 9H), 7.4 (dd, J =2.4, 8.8 Hz, 1H), 7.67 (t, 2H), 10.42 (s, 1H). LC/MS: t_r 17.5 min, m/z 381.9 $[M-H]^-$, purity >99%. Yield: 22.9%.
4.9	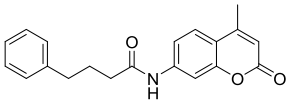	A	^{1}H NMR (400 MHz, DMSO) δ 1.93 (p, J = 7.64 Hz, 2H), 2.37-2.42 (m, 5H), 2.63 (t, J = 7.76 Hz, 2H), 6.26 (d, J = 1.18 Hz, 1H), 7.17-7.32 (m, 5H), 7.52 (dd, J =2.7, 8.68 Hz, 1H), 7.71 (d, J = 8.69 Hz, 1H), 7.80 (d, J = 1.98 Hz, 1H), 10.48 (s, 1H). LC/MS: t_r 16.6 min, m/z 320.0 $[M-H]^-$, purity >99%. Yield: 54.4%.
4.10	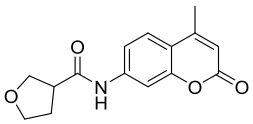	A	^{1}H NMR (DMSO, 400 MHz) δ 2.05-2.13 (m, 2H), 2.39 (d, J = 1.2 Hz, 3H), 3.19 (p, J = 6.93 Hz, 1H), 3.68-3.81 (m, 3H), 3.94 (t, J = 8.21 Hz, 1H), 6.26 (d, J = 1.21 Hz, 1H), 7.49 (dd, J = 2.05, 8.66 Hz, 1H), 7.73 (d, J = 8.68 Hz, 1H), 7.77 (d, J = 2.0 Hz, 1H), 10.51 (s, 1H). LC/MS: t_r 12.4 min, m/z 271.9 $[M-H]^-$, purity 99%. Yield: 38.5%.
4.11	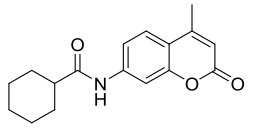	A	^{1}H NMR (400 MHz, DMSO) δ 1.15-1.48 (m, 6H), 1.72-1.88 (m, 4H), 2.31-2.42 (m, 4H), 6.25 (d, J = 1.12 Hz, 1H), 7.50 (dd, J = 1.99, 8.67 Hz, 1H), 7.71 (d, J = 8.68 Hz, 1H), 7.77 (d, J = 1.95 Hz, 1H), 10.25 (s, 1H). LC/MS: t_r 16.1 min, m/z 283.9 $[M-H]^-$, purity 95%. Yield: 52.2%.
4.12	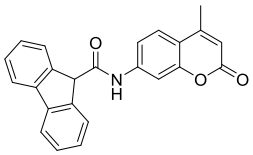	A	^{1}H NMR (400 MHz, DMSO) δ 2.42 (m, 3H), 5.20 (s, 1H), 6.28 (d, J = 1.22 Hz, 1H), 7.29-7.48 (m, 4H), 7.56-7.94 (m, 7H), 11.48 (s, 1H). LC/MS: t_r 17.4 min, m/z 368 $[M+H]^+$, purity >99%. Yield: 57.2%.
4.13	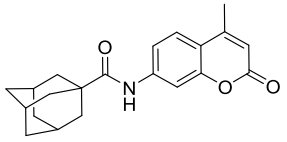	A	^{1}H NMR (400 MHz, DMSO) δ 1.62 (s, 9H), 1.77 (m, 3H), 1.99 (m, 2H), 2.41 (d, 1H), 2.44 (d, 3H), 6.32 (d, 1H), 7.06 (d, 1H), 7.54-7.63 (m, 2H), 7.69 (d, 1H), 12.9 (s, 1H). LC/MS: t_r 18.3 min, m/z 335.8 $[M-H]^-$, purity 90%. Yield: 62.3%.
4.14	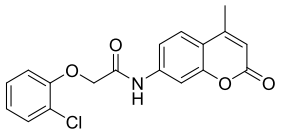	B-I	^{1}H NMR (400 MHz, DMSO) δ 2.41 (s, 3H), 4.23 (s, 2H), 6.33 (s, 1H), 6.73-6.83 (m, 1H), 6.96 (dd, J = 1.3, 8.11 Hz, 1H), 7.09-7.17 (m, 1H), 7.31 (dd, J =1.4, 7.93 Hz, 1H), 7.47 (d, J = 7.78 Hz, 1H), 7.72-7.84 (m, 3H), 11.06 (s, 1H). LC/MS: t_r 10.6 min, m/z 361 $[M+K]^+$, purity >99%.
4.15	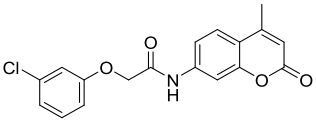	B-I	^{1}H NMR (400 MHz, DMSO) δ 2.41 (s, 3H), 4.81 (s, 2H), 6.29 (s, 1H), 7.00 (dd, J = 2.0, 8.40 Hz,1H), 7.05 (dd, J = 1.97, 7.97 Hz, 1H), 7.12 (t, J = 2.19 Hz, 1H), 7.35 (t, J = 8.18 Hz, 1H), 7.58 (dd, J =2.05, 8.68 Hz, 1H), 7.72-7.81 (m, 2H), 10.53 (s, 1H). LC/MS: t_r 16.8 min, m/z 342.1 $[M-H]^-$, purity >99%.

4.16	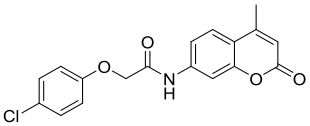	B-I	^{1}H NMR (400 MHz, DMSO) δ 2.40 (s, 3H), 4.78 (s, 2H), 6.29 (s, 1H), 7.00-7.08 (m, 2H), 7.33-7.41 (m, 2H), 7.58 (dd, *J* = 2.05, 8.68 Hz, 1H), 7.71-7.81 (m, 2H), 10.55 (s, 1H). LC/MS: t_r 16.7 min, *m/z* 342.5 $[M-H]^-$, purity 93%.
4.17	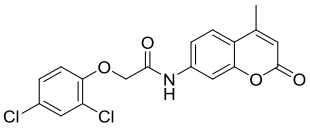	B-I	^{1}H NMR (400 MHz, DMSO) δ 2.41 (s, 3H), 4.09 (s, 2H), 6.3 (s, 1H), 6.96 (d, *J* = 8.73 Hz, 1H), 7.2 (dd, *J* = 2.59, 8.72 Hz, 1H), 7.44 (d, *J* = 2.58 Hz, 1H), 7.48 (dd, *J* = 2.09, 8.67 Hz, 1H), 7.73 (d, *J* = 2.02 Hz, 1H), 7.75 (d, J = 8.67 Hz, 1H), 10.46 (s, 1H). LC/MS: t_r 13.2 min, *m/z* 378.7 $[M-H]^-$, purity >99%.
4.18	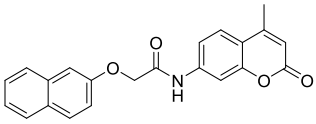	B-I	^{1}H NMR (400 MHz, DMSO) δ 2.40 (s, 3H), 4.88 (s, 2H), 6.28 (s, 1H), 7.28-7.41 (m, 3H), 7.42-7.51 (m, 1H), 7.61 (dd, *J* = 1.98, 8.66 Hz, 1H), 7.74 (d, *J* = 8.7 Hz, 1H), 7.77-7.92 (m, 4H), 10.62 (s, 1H). LC/MS: t_r 17.6 min, *m/z* 358.5 $[M-H]^-$, purity >99%.
4.19	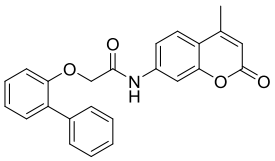	B-I	^{1}H NMR (400 MHz, DMSO) δ 2.41 (s, 3H), 4.79 (s, 2H), 6.29 (s, 1H), 7.07 (d, *J* = 7.96 Hz, 2H), 7.31-7.37 (m, 3H), 7.40-7.45 (m, 2H), 7.49 (dd, *J* = 1.99, 8.65 Hz, 1H), 7.63 (dd, *J* = 1.34, 8.25 Hz, 2H), 7.72-7.79 (m, 2H), 10.41 (s, 1H). LC/MS: t_r 18.8 min, *m/z* 386.1 $[M+H]^+$, purity 95%.
4.20	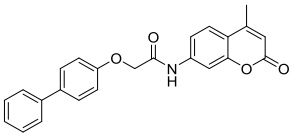	B-I	^{1}H NMR (400 MHz, DMSO) δ 2.41 (s, 3H), 4.82 (s, 2H), 6.29 (s, 1H), 7.10 (d, *J* = 8.78 Hz, 2H), 7.24-7.35 (m, 1H), 7.40-7.45 (m, 3H), 7.52-7.66 (m, 4H), 7.72-7.85 (m, 2H), 10.56 (s, 1H). LC/MS: t_r 18.3 min, *m/z* 384.7 $[M-H]^-$, purity 90%.
4.21	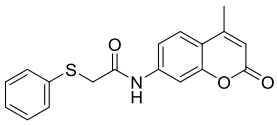	B-II	^{1}H NMR (400 MHz, DMSO) δ 2.39 (d, *J* = 1.26 Hz, 3H), 3.91 (s, 2H), 4.65 (s, 2H), 6.27 (d, *J* = 1.36 Hz, 1H), 7.18-7.27 (m, 3H), 7.29-7.38 (m, 7H), 7.38-7.43 (m, 7H), 7.46 (dd, *J* = 2.11, 8.65 Hz, 1H), 7.51-7.55 (m, 1H), 7.70-7.74 (m, 2H), 10.64 (s, 1H). LC/MS: t_r 15.7 min, *m/z* 324.7 $[M-H]^-$, purity >99%.
4.22	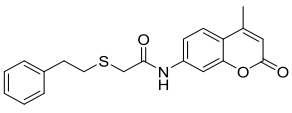	B-II	^{1}H NMR (400 MHz, DMSO) δ 2.40 (d, *J* = 1.29 Hz, 3H), 2.82-3.02 (m, 4H), 3.39 (s, 2H), 6.27 (d, *J* = 1.43 Hz, 1H), 7.16-7.32 (m, 5H), 7.49 (dd, *J* = 2.06, 8.67 Hz, 1H), 7.73 (d, *J* = 8.71 Hz, 1H), 7.76 (d, *J* = 2.02 Hz, 1H), 10.64 (s, 1H). LC/MS: t_r 15.8 min, *m/z* 352.6 $[M-H]^-$, purity >99%.
4.23	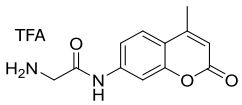	C (steps 1-3)	^{1}H NMR (400 MHz, DMSO) δ 2.41 (d, *J* = 0.8 Hz, 3H), 3.85 (s, 2H), 6.31 (d, *J* = 1.01 Hz, 1H), 7.47 (dd, *J* = 1.98, 8.63 Hz, 1H), 7.77-7.79 (m, 2H), 8.18 (brs, 3H), 10.91 (s, 1H). LC/MS: t_r 7.9 min, *m/z* 233.0 $[M+H]^+$, purity 99%.

4.24	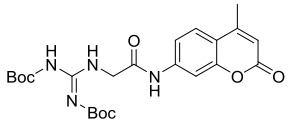	C-I (steps 1-4)	^{1}H NMR (400 MHz, DMSO) δ 1.38 (s, 9H), 1.51 (s, 9H), 2.40 (d, J = 1.15 Hz, 3H), 4.21 (d, J = 4.55 Hz, 2H), 6.28 (d, J = 1.22 Hz, 1H), 7.48 (dd, J = 2.06, 8.66 Hz, 1H), 7.70-7.75 (m, 2H), 8.75(t, J = 4.52 Hz, 1H), 10.57 (s, 1H), 11.46 (s, 1H). LC/MS: t_r 19.1 min, *m/z* 475.1 $[M+H]^+$, purity >99%. Yield: 73%.
4.25	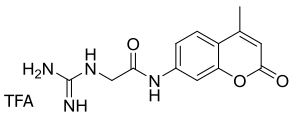	C-I	^{1}H NMR (400 MHz, DMSO) δ 2.41 (s, 3H), 4.10 (d, J = 6.27 Hz, 2H), 6.29 (s, 1H), 7.30 (brs, 3H), 7.49 (dd, J = 1.81, 8.6 Hz, 1H), 7.56 (t, J = 6.01 Hz, 1H), 7.76 (m, 2H), 10.62 (s, 1H). LC/MS: t_r 9 min, *m/z* 275 $[M+H]^+$, purity 99%.
4.26	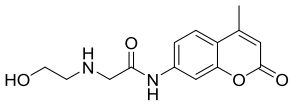	B-III	^{1}H NMR (400 MHz, DMSO) δ 2.40 (s, 3H), 2.65 (m, 2H), 2.82-2.88 (m, 2H), 3.39 (s, 2H), 3.53 (m, 1H), 4.69 (s, 1H), 5.12 (s, 1H), 6.27 (s, 1H), 7.56 (dd, J = 2.04, 8.68 Hz, 1H), 7.73 (d, J = 8.67 Hz, 1H), 7.81 (d, J = 2.01 Hz, 1H). LC/MS: t_r 8.0 min, *m/z* 277.0 $[M+H]^+$, purity 98%.
4.27	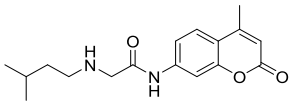	B-III	^{1}H NMR (400 MHz, DMSO) δ 0.90 (d, J = 6.56 Hz, 6H), 1.47-1.58 (m, 2H), 1.58-1.70 (m, 1H), 2.41 (s, 3H), 2.89-3.06 (m, 2H), 3.99 (s, 2H), 6.32 (s, 1H), 7.49 (dd, J = 1.94, 8.62 Hz, 1H), 7.74-7.87 (m, 2H), 8.86 (s, 1H), 11.10 (s, 1H). LC/MS: t_r 11.2 min, *m/z* 303.6 $[M+H]^+$, purity >99%.
4.28	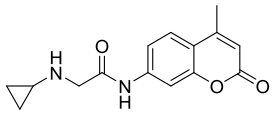	B-III	^{1}H NMR (400 MHz, DMSO) δ 0.74 (d, J = 5.92 Hz, 2H), 0.90 (s, 2H), 2.41 (s, 3H), 2.78 (m, 1H), 4.10 (s, 2H), 6.31 (s, 1H), 7.53 (dd, J = 1.97, 8.68 Hz, 1H), 7.76 (d, J = 8.67 Hz, 1H), 7.81 (d, J = 1.93 Hz, 1H), 7.95 (s, 1H), 9.32 (s, 1H), 11.34 (s, 1H). LC/MS: t_r 9.4 min, *m/z* 273.5 $[M+H]^+$, purity >99%.
4.29	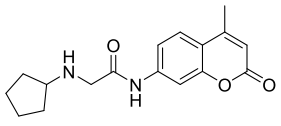	B-III	^{1}H NMR (400 MHz, DMSO) δ 1.52 (m, 2H), 1.67 (m, 4H), 1.93 (d, J = 6.72 Hz, 2H), 2.39 (s, 3H), 3.53 (q, J = 7.09 Hz, 1H), 3.98 (s, 2H), 6.30 (s, 1H), 7.43 (dd, J = 1.89, 8.61 Hz, 1H), 7.75 (m, 2H), 8.99 (brs, 1H), 10.94 (s, 1H). LC/MS: t_r 10.4 min, *m/z* 301.1 $[M+H]^+$, purity >99%.
4.30	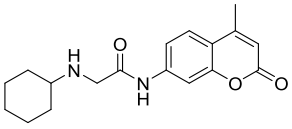	B-III	^{1}H NMR (400 MHz, DMSO) δ 1.10 (t, J = 1.27 Hz, 1H), 1.25 (m, 4H), 1.6 (d, J = 1.28 Hz, 2H), 1.77 (d, J = 1.22 Hz, 2H), 2.0 (d, J = 1.08 Hz, 2H), 2.40 (s, 3H), 6.31 (s, 1H), 7.45 (dd, J = 2.05, 8.62 Hz, 1H), 7.75 (m, 2H), 8.81 (brs, 1H), 10.93 (s, 1H). LC/MS: t_r 11.0 min, *m/z* 315.1 $[M+H]^+$, purity >99%.
4.31	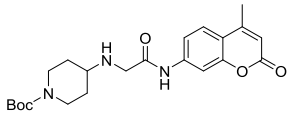	B-III	^{1}H NMR (400 MHz, DMSO) δ 1.38 (s, 9H), 1.73-1.81 (m, 2H), 2.40 (d, J = 1.13 Hz, 3H), 2.52-2.60 (m, 2H), 3.31 (m, 2H), 3.37 (m, 3H), 3.84 (m, 2H), 6.27 (d, J = 1.21 Hz, 1H), 7.58 (dd, J = 2.03, 8.66

			Hz, 1H), 7.71 (d, *J* = 8.68 Hz, 1H), 7.83 (d, *J* = 2.01 Hz, 1H), 10.25 (s,1H). LC/MS: t_r 11.9 min, *m/z* 414.1 $[M-H]^-$, purity 99%.
4.32	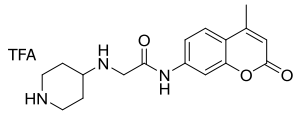	B-III	^{1}H NMR (400 MHz, D_2O) *δ* 1.91-2.05 (m, 2H), 2.39-2.52 (m, 5H), 3.10-3.20 (m, 2H), 3.62-3.70 (m, 3H), 4.21 (s, 2H), 6.31 (d, *J* = 1.1 Hz, 1H), 7.40 (dd, *J* = 2.11, 8.67 Hz, 1H), 7.67 (d, *J* = 2.04 Hz, 1H), 7.74 (d, *J* = 8.70 Hz, 1H). LC/MS: t_r 3 min, *m/z* 316.1 $[M+H]^+$, purity 97%.
4.33	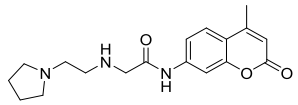	B-III	^{1}H NMR (400 MHz, DMSO) *δ*1.90 (m, 4H), 2.40 (s, 3H), 2.86 (t, *J* = 5.78 Hz, 2H), 3.09-3.16 (m, 7H), 3.58 (s, 2H), 6.28 (s, 1H), 7.53 (dd, *J* = 1.98, 8.66 Hz, 1H), 7.74 (d, *J*= 8.67 Hz, 1H), 7.82 (d, *J* = 1.93, 1H), 10.42 (s, 1H). LC/MS: t_r 7.9 min, *m/z* 330.1 $[M+H]^+$, purity 99%.
4.34	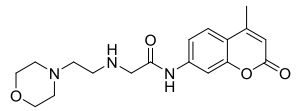	B-III	^{1}H NMR (400 MHz, DMSO) *δ* 2.38 (s, 3H), 2.42 (t, 2H), 2.51 (m, 1H), 2.60 (m, 2H), 3.12 (t, 4H), 3.58 (t, 4H), 3.97 (s, 2H), 6.28 (s, 1H), 7.44 (dd, *J* = 1.97, 8.69 Hz, 1H), 7.74-7.76 (m, 2H), 10.87 (s, 1H). LC/MS: t_r 8.3 min, *m/z* 346.1 $[M+H]^+$, purity >99%.
4.35	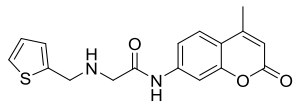	B-III	^{1}H NMR (400 MHz, DMSO) *δ* 2.36 (s, 3H), 3.90 (s, 2H), 4.43 (s, 2H), 6.26 (s, 1H), 7.07 (t, *J* = 3.66 Hz, 1H), 7.27 (d, *J* = 2.69 Hz, 1H), 7.39 (d, *J* = 8.57 Hz, 1H), 7.63 (d, *J* = 1.2 Hz, 1H), 7.71 (m, 2H), 9.34 (brs, 2H), 10.85 (s, 1H). LC/MS: t_r 10.9 min, *m/z* 329 $[M+H]^+$, purity 96%.
4.36	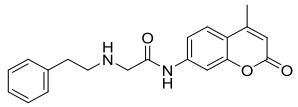	B-III	^{1}H NMR (400 MHz, DMSO) *δ* 2.39 (s, 3H), 2.71-2.85 (m, 4H), 2.98 (d, *J* = 8.45 Hz, 2H), 3.36 (s, 2H), 6.26 (s, 1H), 7.17-7.36 (m, 5H), 7.43 (dd, *J* = 2.04, 8.66 Hz, 1H), 7.70 (d, *J* = 8.66 Hz, 1H), 7.75 (d, *J* = 2.01 Hz, 1H). LC/MS: t_r 11.7 min, *m/z* 337.5 $[M+H]^+$, purity >95%.
4.37	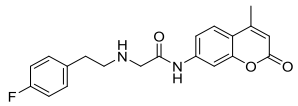	B-III	^{1}H NMR (400 MHz, DMSO) *δ* 2.39 (s, 3H), 2.76 (m, 2H), 2.96-3.04 (m, 2H), 3.36 (s, 2H), 6.25 (s, 1H), 7.12 (m, 4H), 7.24-7.33 (m, 1H), 7.47 (dd, *J* =2.09, 8.66 Hz, 1H), 7.70 (d, *J* = 8.7 Hz, 1H), 7.77 (d, *J* = 2.02 Hz, 1H), 7.95 (s, 1H). LC/MS: t_r 11.8, *m/z* 355.4 $[M+H]^+$, purity >99%.
4.38	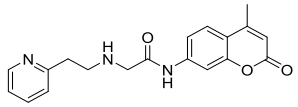	B-III	^{1}H NMR (400 MHz, DMSO) *δ* 2.41 (s, 3H), 3.17 (m, 4H), 4.08 (s, 2H), 6.32 (s, 1H), 7.34 (m, 2H), 7.48 (d, 1H), 7.77 (s, 4H), 8.54 (s, 1H), 9.06 (brs, 1H), 10.93 (s, 1H). LC/MS: t_r 9.6 min, *m/z* 338.1 $[M+H]^+$, purity 99%.
4.39	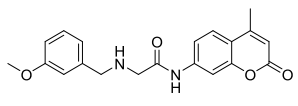	B-III	^{1}H NMR (400 MHz, DMSO) *δ* 2.40 (s, 3H), 3.28 (s, 2H), 3.73 (s, 2H), 3.74 (s, 3H), 4.54 (brs, 1H), 6.26 (s, 1H), 6.80 (dd, *J*= 2.60, 8.20 Hz, 1H), 6.93 (d, *J* =

			7.47 Hz, 1H), 6.95 (s, 1H), 7.23 (t, *J* = 7.82 Hz, 1H), 7.54 (dd, *J* = 2.05, 8.67 Hz, 1H), 7.72 (d, *J* = 8.7 Hz, 1H), 7.80 (d, *J* = 2.01 Hz, 1H). LC/MS: t_r 11.5 min, *m/z* 350.9 $[M-H]^-$, purity 99%.
4.40	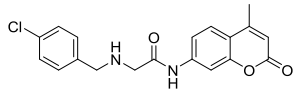	B-III	^{1}H NMR (400 MHz, DMSO) *δ* 2.40 (s, 3H), 2.93 (d, 1H), 3.80 (m, 2H), 4.02 (s, 2H), 6.26 (s, 1H), 7.36-7.46 (m, 2H), 7.45-7.58 (m, 3H), 7.72 (d, *J* = 8.67 Hz, 1H), 7.81 (s, 1H), 10.45 (s, 1H). LC/MS: t_r 12.2 min, *m/z* 357.6 $[M+H]^+$, purity >99%.
4.41	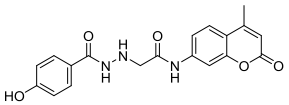	B-III	^{1}H NMR (400 MHz, DMSO) *δ* 1.92 (s, 1H), 1.98 (s, 1H), 2.40 (s, 3H), 3.65 (s, 2H), 6.27 (s, 1H), 6.81 (m, 2H), 7.59 (dd, *J* = 2.02, 8.61 Hz, 1H), 7.68-7.78 (m, 3H), 7.84 (d, *J* = 2.04 Hz, 1H), 9.99 (s, 1H), 10.89 (s, 1H). LC/MS: t_r 12.5 min, *m/z* 368.4 $[M+H]^+$, purity 97%.
4.42	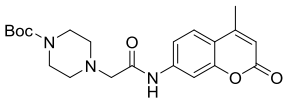	B-III	^{1}H NMR (400 MHz, DMSO) *δ* 1.37 (s, 9H), 2.45 (t, 4H), 2.37 (s, 3H), 3.18 (s, 2H), 3.3 (t, 4H), 6.24 (s, 1H), 7.55 (dd, *J* = 2.05, 8.68 Hz, 1H), 7.70 (d, *J* = 8.70 Hz, 1H), 7.77 (d, *J* = 2.01 Hz, 1H), 10.14 (s, 1H). LC/MS: t_r 12.2 min, *m/z* 399.9 $[M-H]^-$, purity >98%.
4.43	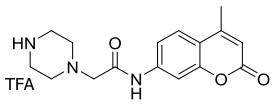	B-III	^{1}H NMR (400 MHz, DMSO) *δ* 2.41 (s, 3H), 2.95 (s, 4H), 3.23 (s, 4H), 3.54 (s, 2H), 6.29 (d, *J* = 1.12 Hz, 1H), 7.56 (dd, *J* = 2.01, 8.68 Hz, 1H), 7.76 (d, *J* = 8.67 Hz, 1H), 7.81 (d, *J* = 1.99 Hz, 1H), 8.74 (brs, 2H), 10.41 (s, 1H). LC/MS: t_r 9.3 min, *m/z* 302.0 $[M+H]^+$, purity >99%.
4.44	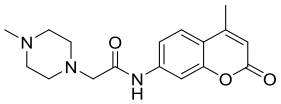	B-III	^{1}H NMR (400 MHz, DMSO) *δ* 2.39 (s, 3H), 2.45 (s, 3H), 2.55-2.85 (m, 8H), 3.4 (s, 2H), 6.26 (s, 1H), 7.56 (dd, *J* = 2.07, 8.67 Hz, 1H), 7.73 (d, *J* = 8.67 Hz, 1H), 7.79 (d, *J* = 2.01 Hz, 1H), 10.17 (s, 1H). LC/MS: t_r 9.8 min, *m/z* 316.1 $[M+H]^+$, purity >99%.
4.45	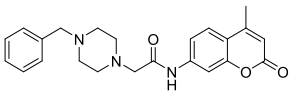	B-III	^{1}H NMR (400 MHz, DMSO) *δ* 2.39 (s, 3H), 2.40-2.45 (m, 4H), 2.50-2.55 (m, 4H), 3.16 (s, 2H), 3.46 (s, 2H), 6.25 (s, 1H), 7.25-7.31 (m, 5H), 7.56 (dd, *J* =2.03, 8.67 Hz, 1H), 7.71 (d, *J* = 8.7 Hz, 1H), 7.79 (d, *J* = 2.01 Hz, 1H), 10.12 (s, 1H). LC/MS: t_r 11.7 min, *m/z* 389.9 $[M+H]^+$, purity 98%.
4.46	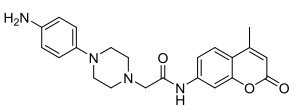	B-III	^{1}H NMR (400 MHz, DMSO) *δ* 2.37 (s, 3H), 2.60 (t, *J* = 4.78 Hz, 4H), 2.94 (t, *J* = 4.93 Hz, 4H), 4.52 (s, 2H), 6.24 (s, 1H), 6.45 (d, *J* = 8.77 Hz, 2H), 6.68 (d, *J* = 8.80 Hz, 2H), 7.55 (dd, *J* = 2.02, 8.67 Hz, 1H), 7.70 (d, *J* = 8.68 Hz, 1H), 7.80 (d, *J* = 2.0 Hz, 1H), 10.15 (s, 1H). LC/MS: t_r 8.8 min, *m/z* 390.9 $[M-H]^-$ purity >99%.

4.47	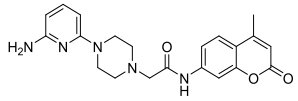	B-III	^{1}H NMR (400 MHz, DMSO) δ 2.42 (s, 3H), 2.59 (t, *J* = 5.09 Hz, 4H), 3.24 (s, 2H), 3.45 (t, *J* = 5.07 Hz, 4H), 5.51 (s, 2H), 5.79 (s, 1H), 5.92 (d, *J* = 7.97, 1H), 6.28 (s, 1H), 7.17 (t, *J* = 7.92 Hz, 1H), 7.62 (dd, *J* = 2.03, 8.67 Hz, 1H), 7.75 (d, *J* = 8.69 Hz, 1H), 7.85 (d, *J* = 1.97 Hz, 1H), 10.21 (s, 1H). LC/MS: t_r 9.6 min, *m/z* 391.9 $[M-H]^-$, purity >95%.
4.48	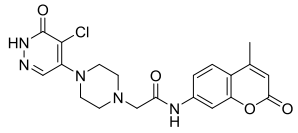	B-III	^{1}H NMR (400 MHz, DMSO) δ 2.38 (s, 3H), 3.30-3.46 (brs, 4H), 3.58-3.76 (brs, 4H), 4.11 (s, 2H), 6.28 (s, 1H), 7.44 (dd, *J* = 1.86, 8.59 Hz, 1H), 7.72-7.78 (m, 2H), 7.89 (s, 1H). LC/MS: t_r 10.2 min, *m/z* 430.1 $[M+H]^+$, purity >99%.
4.49	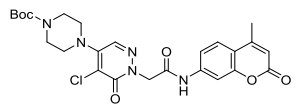	B-III	^{1}H NMR (400 MHz, DMSO) δ 1.42 (s, 9H), 2.40 (d, *J* = 1.1 Hz, 3H), 3.40-3.49 (m, 8H), 4.90 (s, 2H), 6.24 (s, 1H), 7.46 (dd, 1H), 7.68-7.72 (m, 2H), 7.96 (s, 1H), 10.70 (br s, 1H). LC/MS: t_r 16.1 min, *m/z* 568.1 $[M+K]^+$, purity >99%.
4.50	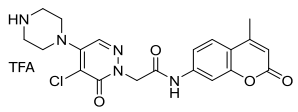	B-III	^{1}H NMR (400 MHz, DMSO) δ 2.45 (s, 3H), 3.23-3.35 (brs, 4H), 3.40 (m, 2H), 3.67 (t, 2H), 6.32 (s, 1H), 7.50 (dd, *J* = 2.03, 8.7 Hz, 1H), 7.75-7.82 (m, 2H), 8.07 (s, 1H), 8.86 (brs, 1H), 10.84 (s, 1H). LC/MS: t_r 10.1 min, *m/z* 468 $[M+K]^+$, purity 99%.
4.51	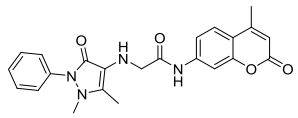	B-III	^{1}H NMR (400 MHz, DMSO) δ 2.21 (s, 3H), 2.39 (d, *J* = 1.17 Hz, 3H), 2.85 (s, 3H), 3.88 (d, *J* = 6.53 Hz, 2H), 4.49 (t, *J* = 6.64 Hz, 1H), 6.26 (d, *J* = 1.21 Hz, 1H), 7.25-7.30 (m, 1H), 7.36-7.42 (m, 2H), 7.44-7.49 (m, 2H), 7.54 (dd, *J* = 2.04, 8.69 Hz, 1H), 7.73 (d, *J* = 8.71 Hz, 1H), 7.80 (d, *J* = 2.01 Hz, 1H), 10.55 (s, 1H). LC/MS: t_r 14.6 min, *m/z* 441.1 $[M+Na]^+$, purity >99%.
4.52	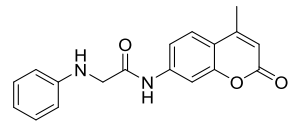	B-III	^{1}H NMR (400 MHz, DMSO) δ 2.39 (s, 3H), 3.92 (d, *J* = 6.16 Hz, 2H), 6.01 (t, *J* = 6.07, 1H), 6.26 (d, *J* = 1.12 Hz, 1H), 6.59 (m, 3H), 7.09 (m, 2H), 7.54 (dd, *J* = 2.06, 8.7 Hz, 1H), 7.73 (d, *J* = 8.69 Hz, 1H), 7.79 (d, *J* = 2.01 Hz, 1H), 10.44 (s, 1H). LC/MS: t_r 15.1 min, *m/z* 309 $[M+H]^+$, purity >99%.
4.53	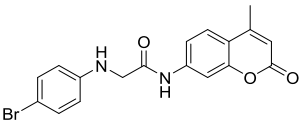	B-III	^{1}H NMR (400 MHz, DMSO) δ 2.39 (s, 3H), 3.61 (s, 1H), 3.94 (s, 2H), 6.26 (s, 1H), 6.58 (d, *J* = 8.86 Hz, 2H), 7.22 (d, *J* = 8.83 Hz, 2H), 7.55 (dd, *J* =2.01, 8.64 Hz, 1H), 7.72 (d, *J* = 8.71 Hz, 1H), 7.80 (d, *J* = 1.93 Hz, 1H), 10.67 (s, 1H). LC/MS: t_r 16.6 min, *m/z* 388.9 $[M+H]^+$, purity >99%.
4.54	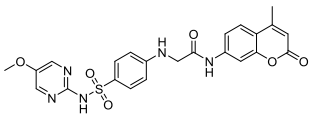	B-III	^{1}H NMR (400 MHz, DMSO) δ 2.40 (d, *J* = 1.19 Hz, 3H), 3.77 (s, 3H), 4.01 (d, *J* = 6.12 Hz, 2H), 6.27 (d, *J* = 1.22 Hz, 1H), 6.65 (d, *J* = 8.65 Hz, 2H), 6.89 (brs, 1H), 7.51 (dd, *J* = 2.04, 8.70 Hz, 1H), 7.67 (d, *J* = 8.76 Hz, 2H), 7.71-7.77 (m, 2H), 8.25 (s, 2H),

			10.53 (s, 1H). LC/MS: t_r 13.8 min, *m/z* 518.1 $[M+Na]^+$, purity 90%.
4.55	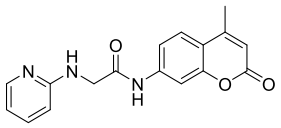	B-III	^{1}H NMR (400 MHz, DMSO) δ 2.41 (s, 3H), 5.17 (s, 2H), 6.30 (s, 1H), 6.94 (s, 1H), 7.10 (d, *J* = 8.57 Hz, 1H), 7.51 (d, *J* = 8.0 Hz, 1H), 7.70 (s, 1H), 7.78 (d, *J* = 7.82 Hz, 1H), 7.93 (t, 1H), 8.06 (d, 1H), 8.56 (brs, 1H), 10.96 (s, 1H). LC/MS: t_r 9.9 min, *m/z* 310 $[M+H]^+$, purity >99%.
4.56	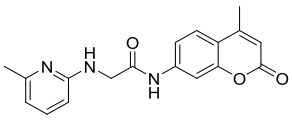	B-III	^{1}H NMR (400 MHz, DMSO) δ 2.22 (s, 3H), 2.39 (d, *J* = 1,12 Hz, 3H), 4.11 (d, *J* = 5.91 Hz, 2H), 6.26 (d, *J* = 1.2 Hz, 1H), 6.38-6.42 (t, *J* = 7.74 Hz, 2H), 6.73-6.76 (t, *J* = 6.17 Hz, 1H), 7.27-7.31 (m, 1H), 7.52 (dd, *J* = 2.04, 8.71 Hz, 1H), 7.73 (d, *J* = 8.67 Hz, 1H), 7.77 (d, *J* = 2.0 Hz, 1H), 10.45 (s, 1H). LC/MS: t_r 10.7 min, *m/z* 346 $[M+Na]^+$, purity 95%.
4.57	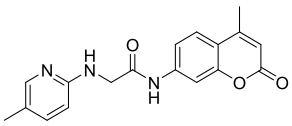	B-III	^{1}H NMR (400 MHz, DMSO) δ 2.16 (s, 3H), 2.41 (s, 3H), 5.11 (s, 2H), 6.29 (d, *J* = 1.11 Hz, 1H), 7.05 (d, *J* = 9.08 Hz, 1H), 7.51 (dd, *J* = 1.99, 8.68 Hz, 1H), 7.70 (d, *J* = 1.94 Hz, 1H), 7.78 (d, *J* = 8.69 Hz, 1H), 7.83 (d, *J* = 1.67 Hz, 1H), 7.92 (s, 1H), 10.96 (s, 1H). LC/MS: t_r 10.5 min, *m/z* 324 $[M+H]^+$, purity 99%.
4.58	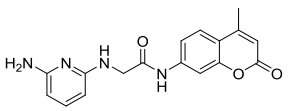	B-III	^{1}H NMR (400 MHz, DMSO) δ 2.39 (s, 3H), 4.02 (d, *J* = 6.06 Hz, 2H), 5.42 (s, 2H), 5.69 (d, *J* = 7.7 Hz, 1H), 5.74 (d, *J* = 7.54 Hz, 1H), 6.25 (d, *J* = 1.19 Hz, 1H), 6.34 (t, 1H), 7.07 (t, *J* = 7.8 Hz, 1H), 7.53 (dd, *J* = 2.03, 8.68 Hz, 1H), 7.73 (d, *J* = 8.68 Hz, 1H), 7.77 (d, *J* = 2.0 Hz, 1H), 10.42 (s, 1H). LC/MS: t_r 10.8 min, *m/z* 325 $[M+H]^+$, purity >99%.
4.59	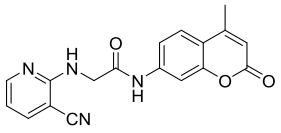	B-III	^{1}H NMR (400 MHz, DMSO) δ 2.42 (d, *J* = 1.1 Hz, 3H), 5.3 (s, 2H), 6.31 (d, *J* = 1.2 Hz, 1H), 7.16 (t, *J* = 7.3 Hz, 1H), 7.53 (dd, *J* = 8.8, 2.1 Hz, 1H), 7.71 (d, *J* = 2.0 Hz, 1H), 7.80 (d, *J* = 8.7 Hz, 1H), 8.47(d, *J* = 6.7 Hz, 1H), 8.68 (d, *J* = 6.7 Hz, 1H), 9.26 (s, 1H), 11.02 (s, 1H). LC/MS: t_r 10.0 min, *m/z* 332.9 $[M-H]^-$, purity 95%.
4.60	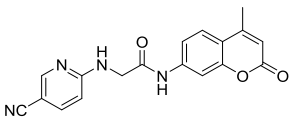	B-III	^{1}H NMR (400 MHz, DMSO) δ 2.42 (s, 3H), 4.09 (s, 1H), 5.21 (s, 2H), 6.32 (s, 1H), 7.20 (d, *J* = 9.46 Hz, 1H), 7.51 (d, *J* = 8.55 Hz, 1H), 7.70 (s, 1H), 7.79 (d, *J* = 8.65 Hz, 1H), 8.90 (s, 1H), 11.03 (s, 1H). LC/MS: t_r 10.3 min, *m/z* 335.0 $[M+H]^+$, purity >99%.
4.61	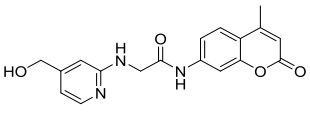	B-III	^{1}H NMR (400 MHz, DMSO) δ 2.42 (d, *J* = 1.1 Hz, 1H), 4.58 (d, *J* = 5.3 Hz, 2H), 5.15 (s, 2H), 5.77 (t, *J* = 5.6 Hz, 1H), 6.31 (d, *J* = 1.2 Hz, 1H), 6.82 (dd, *J* = 1.6, 6.9 Hz, 1H), 7.09 (d, *J* =1.4 Hz, 1H), 7.52 (dd, *J* = 2.0, 8.7 Hz, 1H), 7.72 (d, *J* = 2.0 Hz, 1H), 7.79 (d,

			J = 8.7 Hz, 1H), 7.98 (d, *J* = 6.7 Hz, 1H), 8.48 (s, 1H), 10.96 (s, 1H). LC/MS: t_r 9.8 min, *m/z* 340.0 $[M+H]^+$, purity 98%.
4.62	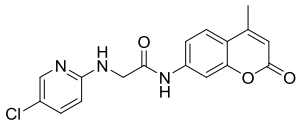	B-III	^{1}H NMR (400 MHz, DMSO) δ 2.41 (s, 3H), 5.15 (s, 2H), 6.30 (s, 1H), 7.16 (d, *J* = 9.59 Hz, 1H), 7.51 (dd, *J* = 1.96, 8.69 Hz, 1H), 7.70 (d, *J* = 1.9 Hz, 1H), 7.90 (d, *J* = 8.69 Hz, 1H), 8.05 (dd, *J* = 2.18, 9.55 Hz, 1H), 8.44 (d, *J* = 2.17 Hz, 1H), 8.85 (brs, 2H), 10.99 (s, 1H). LC/MS: t_r 10.9 min, *m/z* 344.5 $[M+H]^+$, purity >99%.
4.63	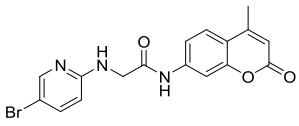	B-III	^{1}H NMR (400 MHz, DMSO) δ 2.41 (s, 3H), 5.17 (s, 2H), 6.30 (s, 1H), 7.10 (d, *J* = 9.56 Hz, 1H), 7.54 (d, *J* = 8.29 Hz, 1H), 7.71 (s, 1H), 7.79 (d, *J* = 8.65 Hz, 1H), 8.07 (d, *J* = 9.54 Hz, 1H), 8.47 (s, 1H), 8.90 (brs, 1H), 11.14 (s, 1H). LC/MS: t_r 10.9 min, *m/z* 389.9 $[M+H]^+$, purity >98%.
4.64	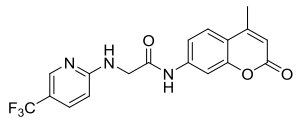	B-III	^{1}H NMR (400 MHz, DMSO) δ 2.41 (s, 3H), 5.24 (s, 2H), 6.30 (s, 1H), 7.27 (d, *J* = 9.45 Hz, 1H), 7.53 (dd, *J* = 1.42, 8.61 Hz, 1H), 7.70 (d, *J* = 1.39 Hz, 1H), 7.79 (d, *J* = 8.63 Hz, 1H), 8.21 (d, *J* = 9.21 Hz, 1H), 8.80 (s, 1H), 9.25 (brs, 1H), 11.03 (s, 1H). LC/MS: t_r 11.3 min, *m/z* 378.4 $[M+H]^+$, purity >99%.
4.65	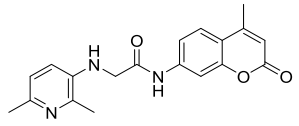	B-III	^{1}H NMR (400 MHz, DMSO) δ 2.41 (s, 3H), 2.5 (s, 6H), 4.16 (d, *J* = 5.81 Hz, 2H), 6.28 (s, 1H), 6.52 (brs, 1H), 7.45-7.50 (m, 3H), 7.73-7.76 (m, 2H), 10.55 (s, 1H). LC/MS: t_r 10.9 min, *m/z* 338 $[M+H]^+$, purity >99%.
4.66	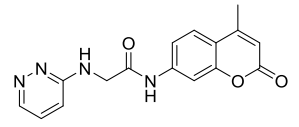	B-III	^{1}H NMR(400 MHz, DMSO) δ 2.41 (d, *J*=1.03, 3H), 5.49 (s, 2H), 6.31 (d, *J* = 1.2 Hz, 1H), 7.49 (dd, *J* = 2.04, 8.67 Hz, 1H), 7.60 (d, *J* = 9.18 Hz, 1H), 7.69 (d, *J* = 2.01 Hz, 1H), 7.79 (d, *J* = 8.68 Hz, 1H), 7.99 (brs, 1H), 8.10-8.16 (m, 1H),9.03 (d, *J* = 5.16 Hz, 1H), 11.12 (s, 1H). LC/MS: t_r 10.7 min, *m/z* 311 $[M+H]^+$, purity >99%.
4.67	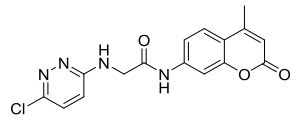	B-III	^{1}H NMR (400 MHz, DMSO) δ 2.42 (d, *J* =1.01 Hz, 3H), 5.28 (s, 2H), 6.32 (d, *J* = 1.15 Hz, 1H), 7.50 (dd, *J* = 2.01, 8.66 Hz, 1H), 7.70-7.73 (m, 2H), 7.80 (d, *J* = 8.68 Hz, 1H), 8.04 (d, *J* = 9.58 Hz, 1H), 11.03 (s, 1H). LC/MS: t_r 11.2 min, *m/z* 345 $[M+H]^+$, purity >99%.
4.68	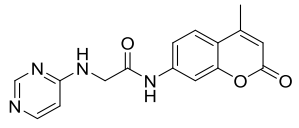	B-III	^{1}H NMR (400 MHz, DMSO) δ 2.41 (s, 3H), 5.16 (s, 2H), 5.75 (s, 1H), 6.30 (s, 1H), 6.83 (d, *J* = 7.4 Hz, 1H), 7.51 (dd, *J* = 2.01, 8.67 Hz, 1H), 7.71 (d, *J* = 1.65 Hz, 1H), 7.77 (d, *J* = 8.61 Hz, 1H), 8.25 (d, *J* = 7.44 Hz, 1H), 8.76 (s, 1H). LC/MS: t_r 9.5 min, *m/z* 311 $[M+H]^+$, purity 99%.

4.69	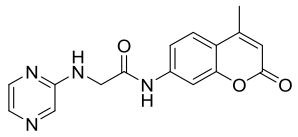	B-III	^{1}H NMR (400 MHz, DMSO) δ 2.42 (s, 3H), 5.55 (s, 2H), 6.32 (s, 1H), 7.51 (dd, *J* = 1.97, 8.71 Hz, 1H), 7.70 (d, *J* = 2.05 Hz, 1H), 7.81 (d, *J* = 8.68 Hz, 1H), 8.06-8.10 (m, 3H), 8.75 (d, *J* = 4.2 Hz, 1H), 11.1 (s, 1H). LC/MS: t_r 9.7 min, *m/z* 311 $[M+H]^+$, purity >99%.
4.70	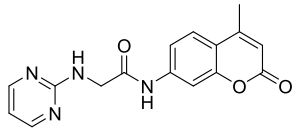	B-III	^{1}H NMR (400 MHz, DMSO) δ 2.36 (s, 3H), 5.10 (s, 2H), 6.26 (s, 1H), 6.49 (m, 1H), 7.45 (dd, *J* =2.11, 8.73 Hz, 1H), 7.65 (d, *J* = 1.99 Hz, 1H), 7.75 (d, *J* = 8.69 Hz, 1H), 8.16 (d, *J* = 4.78 Hz, 1H), 8.50 (dd, *J* = 1.99, 6.61 Hz, 1H), 8.88 (m, 1H), 10.94 (s, 1H). LC/MS: t_r 9.4 min, *m/z* 311 $[M+H]^+$, purity >99%.
4.71	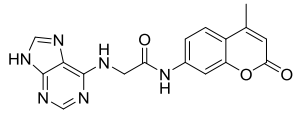	B-III	^{1}H NMR (400 MHz, DMSO) δ 2.41 (s, 3H), 5.40 (s, 2H), 6.30 (s, 1H), 7.49 (d, *J* = 8.58 Hz, 1H), 7.69 (d, *J* = 1.80 Hz, 1H), 7.78 (d, *J* = 8.74 Hz, 1H), 8.20 (s, 1H), 8.56 (s, 1H), 8.79 (s, 1H), 9.46 (s, 1H), 11.12 (s, 1H). LC/MS: t_r 10.0 min, *m/z* 351 $[M+H]^+$, purity 95%.
4.72	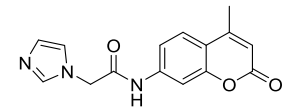	B-III	^{1}H NMR (400 MHz, DMSO) δ 2.40 (d, *J* = 1.17 Hz, 3H), 5.24 (s, 2H), 6.30 (d, *J* = 1.23 Hz, 1H), 7.46-7.52 (m, 1H), 7.59-7.82 (m, 4H), 8.94 (s, 1H), 10.96 (s, 1H). LC/MS: t_r 9.7 min, *m/z* 284.0 $[M+H]^+$, purity 95%.
4.73	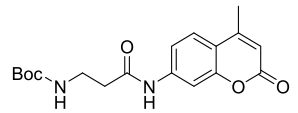	C (steps 1-2)	^{1}H NMR (400 MHz, DMSO) δ 1.38 (s, 9H), 2.40 (s, 3H), 2.53 (t, *J* = 7.02 Hz, 2H), 3.23 (q, *J* = 6.84 Hz, 2H), 6.26 (s, 1H), 6.91 (s, 1H), 7.47 (dd, *J* = 1.95, 8.69 Hz, 1H), 7.72 (d, *J* = 8.68 Hz, 1H), 7.77 (d, 1H), 10.38 (s, 1H). LC/MS: t_r 14.7 min, *m/z* 345 $[M-H]^-$, purity 90%.
4.74	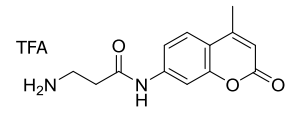	C (steps 1-3)	^{1}H-NMR (400 MHz, DMSO) δ 2.40 (d, *J* = 0.97 Hz, 3H), 2.76 (t, *J* = 6.57 Hz, 2H), 3.11 (m, 2H), 6.28 (d, *J* = 1.1 Hz, 1H), 7.47 (dd, *J* = 1.95, 8.67 Hz, 1H), 7.75 (d, *J* = 8.7 Hz, 1H), 7.79 (d, *J* = 1.9 Hz, 1H), 10.61 (s, 1H). LC/MS: t_r 9.0 min, *m/z* 247 $[M+H]^+$, purity >99%.
4.75	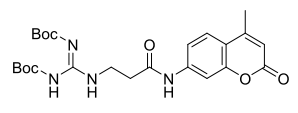	C-I (steps 1-4)	^{1}H NMR (400 MHz, DMSO) δ 1.38 (s, 9H), 1.46 (s, 9H), 2.40 (d, *J* = 0.94 Hz, 3H), 2.67 (t, *J* = 6.23 Hz, 2H), 3.61 (q, *J* = 6.17 Hz, 2H), 6.27 (d, *J* = 1.12 Hz, 1H), 7.47 (dd, *J* = 1.97, 8.7 Hz, 1H), 7.71-7.74(m, 2H), 8.54 (t, *J* = 5.59 Hz, 1H),10.45 (s, 1H), 11.48 (s, 1H). LC/MS: t_r 17.8 min, *m/z* 489.2 $[M+H]^+$.
4.76	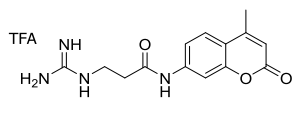	C-I	^{1}H NMR (400 MHz, DMSO) δ 2.37 (s, 3H), 2.63 (t, *J* = 6.34 Hz, 2H), 3.41 (q, *J* = 5.89 Hz, 2H), 6.24 (s, 1H), 7.42 (dd, *J* = 1.61, 8.5 Hz, 1H), 7.72 (d, *J* = 8.68 Hz, 1H), 7.76 (d, *J* = 1.72 Hz, 1H), 10.55 (s, 1H). LC/MS: t_r 9.9 min, *m/z* 289 $[M+H]^+$, purity 95%.

4.77	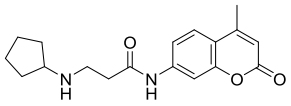	C-II	^{1}H NMR (400 MHz, DMSO) δ 1.50-1.57 (m, 4H), 1.7 (m, 2H), 1.97 (m, 2H), 2.41 (d, *J* = 1.01 Hz, 3H), 2.80 (t, *J* = 6.6 Hz, 2H), 3.20 (t, *J* = 6.8 Hz, 2H), 6.28 (d, *J* = 1.1 Hz, 1H), 7.49 (dd, *J* = 2.0, 8.7 Hz, 1H), 7.76 (d, *J* = 8.7 Hz, 1H), 7.79 (d, *J* = 2.02 Hz, 1H), 10.63(s, 1H). LC/MS: t_r 10.8 min, *m/z* 315.1 $[M+H]^+$, purity >99%.
4.78	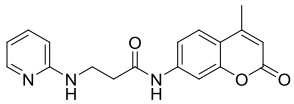	C-III	^{1}H NMR (400 MHz, DMSO) δ 2.4 (d, *J* =0.8 Hz, 3H), 2.98 (t, *J* = 6.5 Hz, 2H), 4.49 (t, *J* = 6.5 Hz, 2H), 6.29 (d, *J* = 1.1 Hz, 1H), 6.92 (t, *J* = 6.9 Hz, 1H), 7.07 (d, *J* = 9.2 Hz, 1H), 7.45 (dd, *J* = 1.9, 8.7 Hz, 1H), 7.74 (d, *J* = 8.9 Hz, 1H), 7.75 (d, *J* = 2.0 Hz, 1H), 7.89 (t, *J* = 7.4 Hz, 1H), 8.10 (d, *J* = 5.8 Hz, 1H), 8.54 (brs, 1H), 10.56 (s, 1H). LC/MS: t_r 10.4 min, *m/z* 324$[M+H]^+$, purity >99%.
4.79	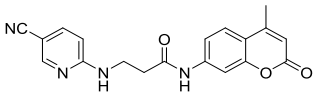	C-III	^{1}H NMR (400 MHz, DMSO) δ 2.36 (d, *J* = 1.02 Hz, 3H), 2.63 (t, *J* = 6.58 Hz, 2H), 3.59 (t, *J* = 6.61 Hz, 2H), 6.21 (d, *J* = 1.14 Hz, 1H), 6.55 (d, *J* = 8.87 Hz, 1H), 7.41 (dd, *J* =2.03, 8.7 Hz, 1H), 7.63 (d, *J* = 9.32 Hz, 1H), 7.69 (d, *J* = 8.70 Hz, 1H), 7.72 (d, *J* = 2.0 Hz, 1H), 8.32 (d, *J* = 2.23 Hz, 1H), 10.39 (s, 1H). LC/MS: t_r 13.8 min, *m/z* 347 $[M-H]^-$, purity 95%.
4.80	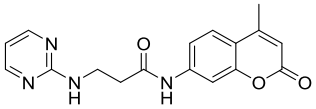	C-III	^{1}H NMR (400 MHz, DMSO) δ 2.46 (s, 3H), 3.10 (t, *J* = 6.1 Hz, 2H),3.35 (m, 2H), 6.24 (s, 1H), 7.02 (dd, *J* =4.7, 6.7 Hz, 1H), 7.44 (dd, *J* =2.0, 8.7 Hz, 1H), 7.70 (d, *J* = 8.5 Hz, 1H), 7.82 (d, *J* = 1.8 Hz, 1H), 7.82 (s, 1H), 8.52 (dd, *J* = 1.6, 6.7 Hz, 1H), 8.78 (dd, *J* = 1.7, 4.3 Hz, 1H). LC/MS: t_r 9.8 min, *m/z* 325.5 $[M+H]^+$, purity 92%.
4.81	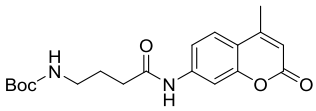	C (steps 1-2)	^{1}H NMR (400 MHz, DMSO) δ 1.37 (s, 9H), 1.70 (p, *J* = 7.16 Hz, 2H), 2.30-2.42 (m, 5H), 2.97 (q, *J* = 6.11 Hz, 2H), 6.26 (d, *J* = 1.18 Hz, 1H), 6.86 (t, *J* = 5.59 Hz, 1H), 7.48 (dd, *J* =2.05, 8.71 Hz, 1H), 7.72 (d, *J* = 8.71 Hz, 1H), 7.77 (d, *J* = 1.95 Hz, 1H), 10.34 (s, 1H). LC/MS: t_r 15.1 min, *m/z* 359 $[M-H]^-$, purity >99%.
4.82	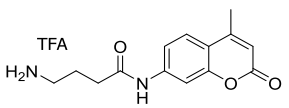	C (steps 1-3)	^{1}H NMR (400 MHz, DMSO) δ 1.86 (m, *J* = 7.61 Hz, 2H), 2.39 (d, *J* = 0.94 Hz, 3H), 2.48 (m, 2H), 2.86 (brs, 2H), 6.25 (d, *J* = 1.11 Hz, 1H), 7.46 (dd, *J* = 2.01, 8.68 Hz, 1H), 7.70-7.78 (m, 4H), 10.44 (s, 1H). LC/MS: t_r 9.5 min, *m/z* 261.0 $[M+H]^+$, purity >99%.
4.83	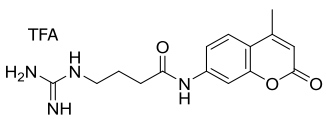	C-I	^{1}H NMR (400 MHz, DMSO) δ 1.80 (p, *J* = 7.12 Hz, 2H), 2.41 (d, *J* = 1.14 Hz, 3H), 2.45 (t, *J* = 7.29 Hz, 2H), 3.17 (q, *J* = 7.43 Hz, 2H), 6.27 (d, *J* = 1.20 Hz, 1H), 7.49 (dd, *J* =2.04, 8.68 Hz, 1H), 7.60 (t, *J* = 4.92 Hz, 1H), 7.74 (d, *J* = 8.69 Hz, 1H), 7.80 (d, *J* = 1.99 Hz, 1H), 10.43 (s, 1H). LC/MS: t_r 10.3 min,

			m/z 303 $[M+H]^+$, purity 99%.
4.84	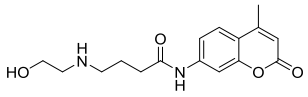	C-II	^{1}H NMR (400 MHz, DMSO) δ 1.91-2.0 (m, 2H), 2.40 (s, 3H), 2.55–2.69 (m, 1H) 2.93-3.03 (m, 2H), 3.40 (m, 2H), 3.13 (q, *J* = 5.84 Hz, 2H) 3.67 (s, 2H), 6.26 (s, 1H), 7.51 (dd, *J* =1.97, 8.69 Hz, 1H), 7.72 (d, *J* = 8.66 Hz, 1H), 7.81 (d, *J* = 1.98 Hz, 1H), 8.0 (s, 1H), 10.63 (s, 1H). LC/MS: t_r 9.7 min, *m/z* 305.6 $[M+H]^+$, purity >99%.
4.85	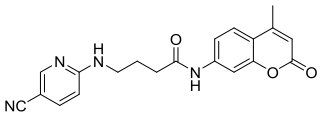	C-III	^{1}H NMR (400 MHz, DMSO) δ 1.86 (t, *J* = 7.03 Hz, 2H), 2.39 (s, 3H), 2.42 (t, *J* = 7.59 Hz, 2H), 3.33 (m, 2H), 6.25 (s, 1H), 6.53 (d, *J* = 9.08 Hz, 1H), 7.46 (dd, *J* = 1.97, 8.69 Hz, 1H), 7.64-7.72 (m, 3H), 7.77 (d, *J* = 1.89 Hz, 1H), 8.37 (d, *J* = 2.13 Hz, 1H), 10.37 (s, 1H). LC/MS: t_r 14 min, *m/z* 363.1 $[M+H]^+$, purity >99%.
4.86	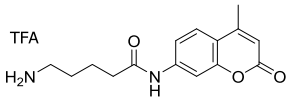	C (steps 1-3)	^{1}H NMR (400 MHz, DMSO) δ 1.53-1.65 (m, 4H), 2.40-2.43 (m, 5H), 2.83 (t, *J* = 8.68 Hz, 2H), 6.27 (d, *J* = 1.22 Hz, 1H), 7.47 (dd, *J* =2.04, 8.70 Hz, 1H), 7.64 (brs, 2H), 7.71 (d, *J* = 8.67 Hz, 1H), 7.80 (d, *J* = 2.0 Hz, 1H), 10.38 (s, 1H). LC/MS: t_r 9.8 min, *m/z* 275.1 $[M+H]^+$, purity 97%.
4.87	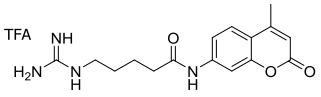	C-I	^{1}H NMR (400 MHz, DMSO) δ 1.49-1.55 (p, *J* = 7.38 Hz, 2H), 1.60-1.67 (p, *J* = 7.27 Hz, 2H), 2.40-2.43 (m, 5H), 3.11 (q, *J* = 6.42 Hz, 2H), 6.26 (d, *J* = 1.18 Hz, 1H), 6.8-7.4 (brs, 3H), 7.49 (dd, *J* = 2.02, 8.70 Hz, 1H), 7.58 (t, *J* = 5.35 Hz, 1H), 7.72 (d, *J* = 8.71 Hz, 1H), 7.80 (d, *J* = 1.98 Hz, 1H), 10.44 (s, 1H). LC/MS: t_r 10.7 min, *m/z* 317.1 $[M+H]^+$, purity >99%.
4.88	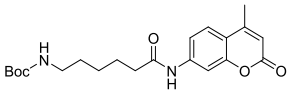	C (steps 1-2)	^{1}H NMR (400 MHz, DMSO) δ 1.29 (m, 2H), 1.36 (s, 9H), 1.39 (m, 2H), 1.57 (m, *J* = 7.32 Hz, 2H), 2.35 (t, *J* = 7.29 Hz, 2H), 2.39 (s, 3H), 2.91 (q, *J* = 6.6 Hz, 2H), 6.25 (s, 1H), 6.77 (brs, 1H), 7.48 (dd, *J* = 1.8, 8.63 Hz, 1H), 7.71 (d, *J* = 8.7 Hz, 1H), 7.77 (d, *J* = 1.8 Hz, 1H), 10.30 (s, 1H). LC/MS: t_r 16.0 min, *m/z* 387.1 $[M-H]^-$, purity >99%.
4.89	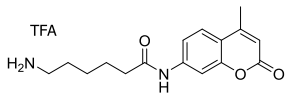	C (steps 1-3)	^{1}H NMR (400 MHz, DMSO) δ 1.36 (m, 2H), 1.52-1.66 (m, 4H), 2.36-2.40 (m, 5H), 2.80 (q, *J* = 7.33 Hz, 2H), 6.26 (d, *J* = 1.09 Hz, 1H), 7.47 (dd, *J* = 2.0, 8.67 Hz, 1H), 7.65-7.72 (m, 3H), 7.79 (d, *J* = 1.93 Hz, 1H), 10.35 (s, 1H). LC/MS: t_r 10.2 min, *m/z* 289 $[M+H]^+$, purity 99%.
4.90	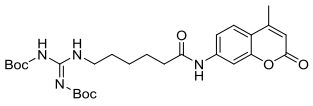	C-I (steps 1-4)	^{1}H NMR (400 MHz, DMSO) δ 1.30-1.35 (m, 2H), 1.38 (s, 9H), 1.46 (s, 9H), 1.49-1.66 (m, 4H), 2.35-2.39 (m, 5H), 3.30 (m, 2H), 6.25 (d, *J* = 1.16, 1H), 7.48 (dd, *J* = 2.01, 8.69, 1H), 7.69 (d, *J* = 8.68, 1H), 7.77 (d, *J* = 1.96, 1H),8.30 (d, *J* = 5.38, 1H), 10.30

			(s, 1H), 11.48 (s, 1H). LC/MS: t_r 18.3 min, *m/z* 531.2 $[M+H]^+$, purity 90%.
4.91	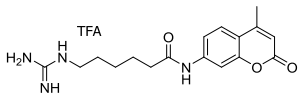	C-I	^{1}H NMR (400 MHz, DMSO) δ 1.29-1.36 (m, 2H), 1.46-1.53 (m, 2H), 1.58-1.66 (m, 2H), 2.36-2.40 (m, 5H), 3.07-3.12 (q, *J* = 6.05 Hz, 2H), 6.26 (d, *J* = 1.18 Hz, 1H), 6.98 (brs, 3H), 7.44-7.48 (m, 2H), 7.72 (d, *J* = 8.68 Hz, 1H), 7.79 (d, *J* = 1.97 Hz, 1H), 10.33 (s, 1H). LC/MS: t_r 11.1 min, *m/z* 331.1 $[M+H]^+$, purity 99%.
4.92	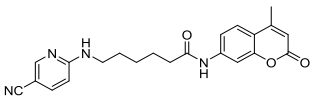	C-III	^{1}H NMR (400 MHz, DMSO) δ 1.27-1.35 (m, 2H), 1.47-1.63 (m, 4H), 2.30-2.36 (m, 5H), 3.23 (t, 2H), 6.21 (d, *J* = 1.16 Hz, 1H), 6.48 (d, *J* = 8.89 Hz, 1H), 7.40 (dd, *J* = 2.03, 8.68 Hz, 1H), 7.54 (d, 1H), 7.66-7.70 (m, 2H), 8.24 (d, *J*=2.19 Hz, 1H), 10.36 (s, 1H). LC/MS: t_r 14.8 min, *m/z* 391.1 $[M+H]^+$, purity 98%.
4.93	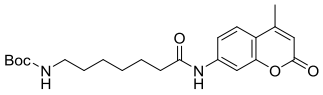	C (steps 1-2)	^{1}H NMR (400 MHz, DMSO) δ 1.20-1.32 (m, 4H), 1.33 (m, 2H), 1.36 (s, 9H), 1.59 (p, *J* = 7.49 Hz, 2H), 2.35 (t, *J* = 7.44 Hz, 2H), 2.39 (d, *J* = 1.3 Hz, 3H), 2.89 (q, *J* = 6.58 Hz, 2H), 6.25 (d, *J* = 1.48 Hz, 1H), 6.76 (t, *J* = 5.42 Hz, 1H), 7.47 (dd, *J* = 2.08, 8.68 Hz, 1H), 7.70 (d, *J* = 8.59 Hz, 1H), 7.76 (d, *J*=2.05, 1H), 10.30 (s, 1H). LC/MS: t_r 16.6 min, *m/z* 403.8 $[M+H]^+$, purity >99%.
4.94	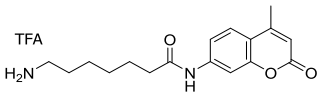	C (steps 1-3)	^{1}H NMR (400 MHz, DMSO) δ 1.27-1.37 (m, 4H), 1.48-1.64 (m, 4H), 2.36 (d, *J* = 7.32 Hz, 2H), 2.39 (d, *J* = 1.33 Hz, 3H), 2.71-2.82 (m, 2H), 6.26 (q, *J* = 1.20 Hz, 1H), 7.46 (dd, *J* = 2.05, 8.68 Hz, 1H), 7.66 (s, 3H), 7.71 (d, *J* = 8.67 Hz, 1H), 7.79 (d, *J* = 2.02 Hz, 1H), 10.34 (s, 1H). LC/MS: t_r 10.8 min, *m/z* 303.1 $[M+H]^+$, purity 99%. Yield: 43.5%.
4.95	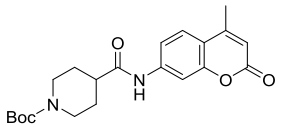	A	^{1}H NMR (400 MHz, DMSO) δ 1.41 (s, 9H), 1.46-1.53 (m, 2H), 1.82 (d, *J* = 1.08 Hz, 2H), 2.39 (s, 3H), 2.56 (m, 1H), 3.3 (m, 4H), 6.26 (s, 1H), 7.52 (dd, *J* =2.03, 8.69 Hz, 1H), 7.72 (d, *J* = 8.7 Hz, 1H), 7.77 (d, *J* = 1.99 Hz, 1H), 10.41 (s, 1H). LC/MS: t_r 16.2 min, *m/z* 385 $[M-H]^-$, purity >99%.
4.96	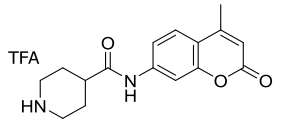	A	^{1}H NMR (400 MHz, DMSO) δ 1.75-1.86 (m, 2H), 1.97-2.0 (m, 2H), 2.39 (s, 3H), 2.67 (m, 1H), 3.3 (m, 4H), 6.27 (s, 1H), 7.49 (dd, *J* =2.04, 8.69 Hz, 1H), 7.73 (d, *J* = 8.7 Hz, 1H), 7.77 (d, *J* = 2.01 Hz, 1H), 10.49 (s, 1H). LC/MS: t_r 9.8 min, *m/z* 287 $[M+H]^+$, purity 99%.
4.97	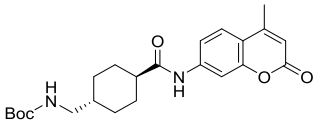	A	^{1}H NMR (400 MHz, DMSO) δ 0.90 (q, 2H), 1.14 (s, 12H), 1.72 (d, *J* = 1.03 Hz, 2H), 1.80 (d, *J* = 1.08 Hz, 2H), 2.25 (m, 1H), 2.34 (s, 3H), 2.72 (t, *J* = 6.32 Hz, 2H), 6.19 (s, 1H), 6.77 (t, *J* = 5.82 Hz, 1H), 7.45

			(dd, *J* = 2.03, 8.72 Hz, 1H), 7.65 (d, *J* = 8.71 Hz, 1H), 7.72 (d, *J* = 2.0 Hz, 1H), 10.23 (s, 1H). LC/MS: t_r 16.6 min, *m/z* 413.1 $[M-H]^-$, purity >99%.
4.98	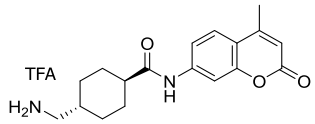	A	^{1}H NMR (400 MHz, DMSO) *δ* 1.02 (m, 2H), 1.45 (m, 2H), 1.57 (s, 1H), 1.87 (d, *J* = 1.04 Hz, 2H),1.93 (d, *J* = 3.58 Hz, 2H), 2.35 (m, 1H), 2.40 (s, 3H), 2.72 (p, *J* = 6.19 Hz, 2H), 6.27 (s, 1H),7.50 (dd, *J* =2.03, 8.70 Hz, 1H), 7.73 (d, *J* = 8.7 Hz, 1H), 7.73 (brs, 2H), 7.80 (d, *J* = 2.0 Hz, 1H), 10.32 (s, 1H). LC/MS: t_r 7.6 min, *m/z* 315.1 $[M+H]^+$, purity 99%.
4.99	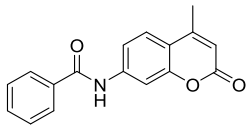	A	^{1}H NMR (400 MHz, DMSO) *δ* 2.44 (s, 3H), 6.31 (s, 1H), 7.57 (t, *J* = 7.63 Hz, 2H), 7.64 (d, *J* = 7.35 Hz, 1H), 7.79 (d, *J* = 1.08 Hz, 2H), 7.96-8.0 (m, 3H), 10.65 (s, 1H). LC/MS: t_r 15.3 min, *m/z* 277.8 $[M-H]^-$, purity >99%. Yield: 50.2%.
4.100	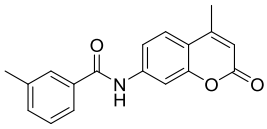	A	^{1}H NMR (400 MHz, DMSO) *δ* 2.36 (s, 3H), 2.37 (d, *J* = 1.17 Hz, 3H), 6.24 (d, *J* = 1.2 Hz, 1H), 7.39 (m, 2H), 7.70-7.74 (m, 3H), 7.75 (s, 1H), 7.90 (t, 1H), 10.58 (s, 1H). LC/MS: t_r 16.3 min, *m/z* 291.8 $[M-H]^-$, purity >99%. Yield: 53.8%.
4.101	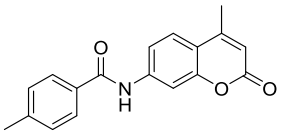	A	^{1}H NMR (400 MHz, DMSO) *δ* 2.40 (s, 3H), 2.43 (d, *J* = 1.14 Hz, 3H), 6.29 (d, *J* = 1.2 Hz, 1H), 7.38 (d, *J* = 7.96 Hz, 2H), 7.76-7.79 (m, 2H), 7.89-7.93 (d, *J* = 8.19 Hz, 2H), 7.96 (s, 1H), 10.57 (s, 1H). LC/MS: t_r 16.2 min, *m/z* 291.8 $[M-H]^-$, purity >99%. Yield: 84%.
4.102	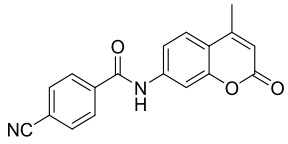	A	^{1}H NMR (400 MHz, DMSO) *δ* 2.37(d, *J* = 1.16 Hz, 2H), 6.25(d, *J* = 1.21 Hz, 1H), 7.69 (dd, *J* = 1.97, 8.71 Hz, 1H), 7.74(d, *J* = 8.7 Hz, 1H), 7.86 (d, *J* = 1.92 Hz, 1H), 8.08-7.98 (m, 4H), 10.81 (s, 1H). LC/MS: t_r 15.5 min, *m/z* 305.4 $[M+H]^+$, purity >99%. Yield: 46.1%.
4.103	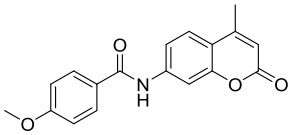	A	^{1}H NMR (DMSO 400 MHz) *δ* 2.42 (d, *J* = 4.0 Hz, 3H), 3.86 (s, 3 H), 6.28 (d, *J* = 4.0 Hz, 1H), 7.10 (d, *J* = 8.0 Hz, 2H), 7.77 (s, 2H), 7.96 (s, 1H), 8.0 (d, *J* = 8.0 Hz, 2H), 10.51 (s, 1H). LC/MS: t_r 15.5 min, *m/z* 307.8 $[M-H]^-$, purity 98%. Yield: 51%.
4.104	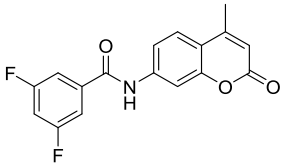	A	^{1}H NMR (400 MHz, DMSO) *δ* 2.39 (s, 3H), 6.28 (s, 1H), 7.50-7.56 (m, 1H), 7.67-7.71 (m, 3H), 7.77 (d, *J* = 8.70 Hz, 1H), 7.89 (d, *J* = 1.89 Hz, 1H), 10.72 (s, 1H). LC/MS: t_r 16.4 min, *m/z* 313.8 $[M-H]^-$, purity 98%. Yield: 78%.
4.105	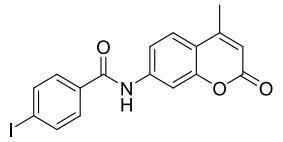	A	^{1}H NMR (400 MHz, DMSO) *δ* 2.42 (s, 3H), 6.30 (s, 1H), 7.72-7.82 (m, 4H), 7.9-8.0 (m, 3H), 10.69 (s, 1H). LC/MS: t_r 17.5 min, *m/z* 404.4 $[M-H]^-$, purity 99%. Yield: 54%.

4.106	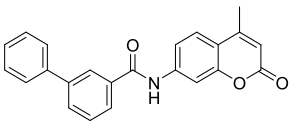	A	^{1}H NMR (400 MHz, DMSO) δ 2.43 (d, J = 1.13 Hz, 3H), 6.31 (d, J = 1.21 Hz, 1H), 7.41-7.46 (m, 1H), 7.49-7.56 (m, 2H), 7.66 (t, J = 7.75 Hz, 1H), 7.76-7.82 (m, 4H), 7.90-8.0 (m, 3H), 8.25 (t, J = 1.58 Hz, 1H), 10.73 (s, 1H). LC/MS: t_r 18.3 min, m/z 353.8 $[M-H]^-$, purity >99%. Yield: 49.3%.
4.107	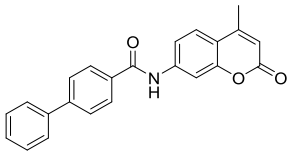	A	^{1}H NMR (400 MHz, DMSO) δ 2.44 (s, 3H), 6.30 (s, 1H), 7.44 (t, J = 7.29 Hz, 1H), 7.52 (t, J = 7.29 Hz, 2H), 7.77-7.81 (m, 4H), 7.87 (d, J = 8.37 Hz, 2H), 8.0 (d, J = 1.54 Hz, 1H), 8.11 (d, J = 8.36 Hz, 2H), 10.73 (s, 1H). LC/MS: t_r 18.5 min, m/z 353.8 $[M-H]^-$, purity 97%. Yield: 71%.
4.108	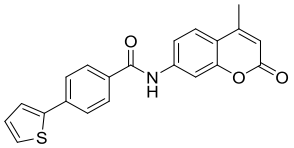	A	^{1}H NMR (400 MHz, DMSO) δ 2.43 (d, J = 1.13 Hz, 3H), 6.30 (d, J = 1.18 Hz, 1H), 7.65-7.68 (m, 2H), 7.71 (dd, J =1.09, 3.61 Hz, 1H), 7.79 (m, 2H), 7.85 (d, J = 8.5 Hz, 2H), 7.94-7.98 (m, 2H), 8.05 (d, J = 8.54 Hz, 2H), 10.67 (s, 1H). LC/MS: t_r 18.2 min, m/z 359.8 $[M-H]^-$, purity 92%. Yield: 20%.
4.109	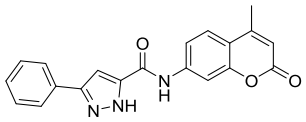	A	^{1}H NMR (400 MHz, DMSO) δ 2.29 (d, J = 1.09 Hz, 3H), 6.41 (d, J = 2.15 Hz, 1H), 5.9 (s, 1H), 6,28 (d, J = 1.21 Hz, 1H) 6.57 (dd, J = 2.18, 8.62 Hz, 1H), 7.33 (s, 1H), 7.40 (d, J = 8.57 Hz, 1H), 7.49 (t, J = 7.56 Hz, 1H), 7.76 (d, J = 8.73 Hz, 1H), 7.81-7.89 (m, 3H), 8.0 (d, J = 1.99 Hz, 1H), 10.60 (s, 1H). LC/MS: t_r 16.5 min, m/z 346.6 $[M+H]^+$, purity 99%. Yield: 76%.
4.110	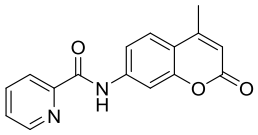	A	^{1}H NMR (400 MHz, DMSO) δ 2.40 (s, 3H), 6.28 (s, 1H), 7.69 (t, J = 6.59 Hz, 1H), 7.76 (d, J = 8.71 Hz, 1H), 7.95 (dd, J = 1.78, 8.67 Hz, 1H), 8.04-8.10 (m, 2H), 8.18 (d, J = 7.83 Hz, 1H), 8.75 (d, J = 4.21 Hz, 1H), 11.06 (s, 1H). LC/MS: t_r 15.8 min, m/z 278.8 $[M-H]^-$, purity 99%. Yield: 25%.
4.111	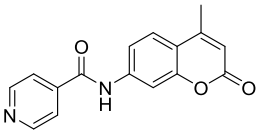	A	^{1}H NMR (400 MHz, DMSO) δ 2.44 (s, 3H), 6.33 (s, 1H), 7.74-7.83 (m, 2H), 7.94 (d, J = 1.74 Hz, 1H), 7.98 (d, J = 6.02 Hz, 2H), 8.87 (d, J = 5.74 Hz, 2H), 10.96 (s, 1H). LC/MS: t_r 13 min, m/z 278.8 $[M-H]^-$, purity >99%. Yield: 75%.
4.112	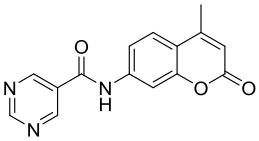	A	^{1}H NMR (400 MHz, DMSO) δ 2.43 (s, 3H), 6.32 (s, 1H), 7.69-7.72 (dd, J =1.87, 8.61 Hz, 1H), 7.82 (d, J = 8.70 Hz, 1H), 7.92 (d, J = 2.02 Hz, 1H), 8.98 (s, 1H), 9.30 (s, 2H), 9.38 (s, 1H). LC/MS: t_r 12.6 min, m/z 279.8 $[M-H]^-$, purity >99%. Yield: 31%.
4.113	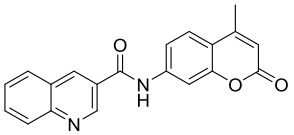	A	^{1}H NMR (400 MHz, DMSO) δ 2.44 (d, J = 1.19 Hz, 3H), 6.32 (d, J = 1.22 Hz, 1H), 7.72-7.84 (m, 3H), 7.92 (m, 1H), 7.99 (d, J = 1.77 Hz, 1H), 8.15 (d, J = 8.32 Hz, 1H), 8.19 (dd, J =0.87, 8.43 Hz, 1H), 9.01 (d, J = 1.85 Hz, 1H), 9.38 (d, J = 2.27 Hz, 1H), 11.01 (s, 1H). LC/MS: t_r 15.8 min, m/z 328.9 $[M-H]^-$,

			purity >99%. Yield: 88%.
4.114	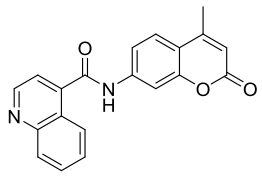	A	^{1}H NMR (400 MHz, DMSO) δ 2.44 (d, J = 1.19 Hz, 3H), 6.34 (d, J = 1.23 Hz, 1H), 7.63-7.75 (m, 2H), 7.78-7.88 (m, 3H), 7.97 (d, J = 1.86 Hz, 1H), 8.13-8.19 (m, 2H), 9.08 (d, J = 4.32 Hz, 1H), 11.30 (s, 1H). LC/MS: t_r 14.8 min, m/z 328.9 $[M-H]^-$, purity >99%.
4.115	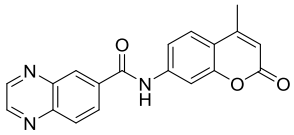	A	^{1}H NMR (400 MHz, DMSO) δ 2.44 (s, 3H), 6.32 (s, 1H), 7.83 (m, 2H), 8.01 (d, J = 1.56 Hz, 1H), 8.26 (d, J = 8.74 Hz, 1H), 8.39 (dd, J = 2.01; 8.75, 1H), 8.81 (d, J = 1.93 Hz, 1H), 9.09 (dd, J = 1.8, 6.05 Hz, 2H), 11.01 (s, 1H). LC/MS: t_r 15.0 min, m/z 329.9 $[M-H]^-$, purity >99%. Yield: 47.6%.
4.116	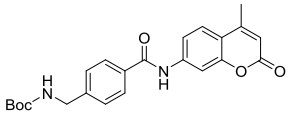	A	^{1}H NMR (400 MHz, DMSO) δ1.41 (s, 9H), 2.43 (s, 3H), 4.22 (d, 2H),6.30 (s, 1H), 7.41 (d, J = 8.21 Hz, 2H), 7.50 (t, J = 6.1 Hz, 1H), 7.77 (brs, 2H), 7.91 (m, 3H), 10.59 (s, 1H). LC/MS: t_r 16.6 min, m/z 431.1 $[M+Na]^+$, purity 90%. Yield: 30%.
4.117	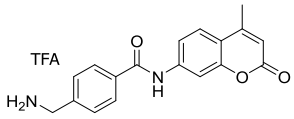	A	^{1}H NMR (400 MHz, DMSO) δ 2.46 (d, J = 1.19 Hz, 3H), 4.18 (m, 2H), 6.34 (d, J = 1.12 Hz, 1H), 7.65 (d, J = 8.42 Hz, 2H), 7.80 (m, 2H), 7.99 (d, J = 1.52 Hz, 1H), 8.08 (d, J = 8.39 Hz, 2H), 8.27 (brs, 3H), 10.70 (s, 1H). LC/MS: t_r 10.8 min, m/z 309.1 $[M+H]^+$, purity >99%.
4.118	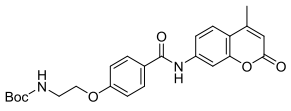	A	^{1}H NMR (400 MHz, DMSO) δ 1.39 (s, 9H), 2.42 (s, 3H), 3.3 (m, 2H), 4.06 (t, J = 5.14 Hz, 2H), 6.28 (s, 1H), 7.0-7.15 (m, 3H), 7.72-7.80 (m, 2H), 7.92-8.05 (m, 3H), 10.5 (s, 1H). LC/MS: t_r 17.1 min, m/z 437 $[M-H]^-$, purity >99%.
4.119	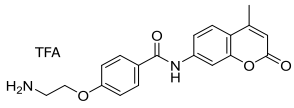	A	^{1}H NMR (400 MHz, DMSO) δ 2.33 (s, 3H), 3.19 (q, J = 5.44 Hz, 2H), 4.17 (t, J = 5.25 Hz, 2H), 6.20 (s, 1H), 7.05 (d, J = 8.92 Hz, 2H), 7.67 (s, 2H), 7.86 (s, 1H), 7.87-7.98(m, 5H), 10.42 (s, 1H). LC/MS: t_r 11.3 min, m/z 339.1 $[M+H]^+$, purity 99%.
4.120	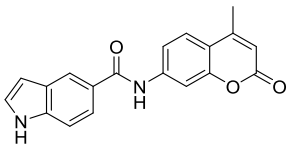	A	^{1}H NMR (400 MHz, DMSO) δ 2.43 (s, 3H), 6.28 (s, 1H), 6.61 (s, 1H), 7.48-7.53 (m, 2H), 7.77 (d, J = 8.87 Hz, 2H), 7.84 (dd, J = 1.95, 8.74 Hz, 1H), 8.0 (d, J = 1.87 Hz, 1H), 8.31 (s, 1H), 10.53 (s, 1H), 11.46 (s, 1H). LC/MS: t_r 15.3 min, m/z 316.8 $[M-H]^-$, purity 99%. Yield: 88%.
4.121	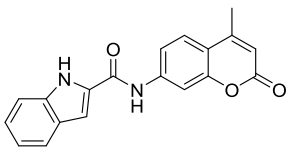	A	^{1}H NMR (400 MHz, DMSO) δ 2.38 (s, 3H), 6.24 (s, 1H), 7.04 (t, J = 7.45 Hz, 1H), 7.20 (t, J = 7.57 Hz, 1H), 7.42-7.45 (m, 2H), 7.66 (d, J = 7.97 Hz, 1H), 7.73 (s, 2H), 7.96 (s, 1H), 10.57 (s, 1H), 11.81 (s, 1H). LC/MS: t_r 16.7 min, m/z 316.8 $[M-H]^-$, purity 97%. Yield: 55%.

4.122	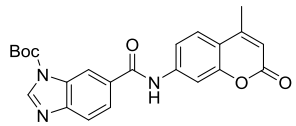	A	^{1}H NMR (400 MHz, DMSO) δ 1.68 (s, 9H), 2.44 (d, J = 1.19 Hz, 3H), 6.30 (d, J = 1.22 Hz, 1H), 7.77-7.84 (m, 2H), 7.99 (d, J = 1.74 Hz, 1H), 8.08 (s, 2H), 8.47 (t, J = 1.14 Hz, 1H), 8.80 (s, 1H), 10.72 (s, 1H). LC/MS: t_r 17.7 min, m/z 417.9 $[M-H]^-$, purity 95%. Yield: 21%.
4.123	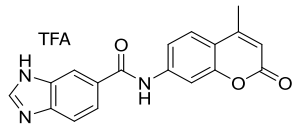	A	^{1}H NMR (400 MHz, DMSO) δ 2.43 (s, 3H), 6.30 (s, 1H), 7.77-7.79 (m, 2H), 7.86 (d, J = 8.54 Hz, 1H), 7.97 (s, 1H), 8.03 (dd, J = 1.62, 8.56 Hz, 1H), 8.39 (s, 1H), 9.0 (s, 1H), 10.74 (s, 1H). LC/MS: t_r 11.4 min, m/z 320 $[M+H]^+$, purity 99%.
4.124	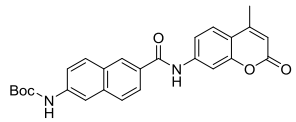	A	^{1}H NMR (400 MHz, DMSO) δ 1.53 (s, 9H), 2.44 (s, 3H), 6.31 (s, 1H), 7.62 (dd, J =2.09, 8.92 Hz, 1H), 7.81 (m, 2H), 7.93 (d, J = 8.8 Hz, 1H), 7.97-8.01 (m, 3H), 8.21 (s, 1H), 8.52 (s, 1H), 9.77 (s, 1H), 10.75 (s, 1H). LC/MS: t_r 18.8 min, m/z 443.1 $[M-H]^-$, purity >99%. Yield: 39.4%.
4.125	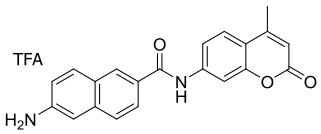	A	^{1}H NMR (400 MHz, DMSO) δ 2.44 (s, 3H), 6.29 (s, 1H), 6.96 (s, 1H), 7.09 (dd, J = 2.12, 8.75 Hz, 1H), 7.67 (d, J = 8.71 Hz, 1H), 7.77-7.82 (m, 3H), 7.88 (dd, J = 1.82, 8.66 Hz, 1H), 8.0 (d, J = 1.72 Hz, 1H), 8.40 (s, 1H), 10.6 (s, 1H). LC/MS: t_r 15.6 min, m/z 345 $[M+H]^+$, purity 99%.
4.126	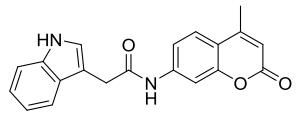	A	^{1}H NMR (400 MHz, DMSO) δ 2.39 (s, 3H), 3.79 (s, 2H), 6.25 (s, 1H), 6.96-7.0 (m, 1H), 7.05-7.09 (m, 1H), 7.28 (d, J = 2.31 Hz, 1H), 7.37 (d, J = 8.05 Hz, 1H), 7.51-7.54 (dd, J = 2.05, 8.71 Hz, 1H), 7.61 (d, J = 7.68 Hz, 1H), 7.72 (d, J = 8.70 Hz, 1H), 7.78 (d, J = 1.99 Hz, 1H), 10.60 (s, 1H), 10.95 (s, 1H). LC/MS: t_r 15.2 min, m/z 333.5 $[M+H]^+$, purity >99%. Yield: 53%.
4.127	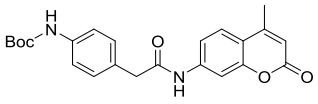	C (steps 1-2)	^{1}H NMR (400 MHz, DMSO) δ 1.46 (s, 9H), 2.39 (s, 3H), 3.61 (s, 2H), 6.26 (s, 1H), 7.2 (d, J = 7.84 Hz, 2H), 7.33-7.52 (m, 3H), 7.68-7.75 (m, 2H), 9.29 (s, 1H), 10.55 (s, 1H); MS (ESI): m/z 407.4 $[M-H]^-$; LC/MS: t_r 16.5 min, purity 97%; yield: 35.5%
4.128	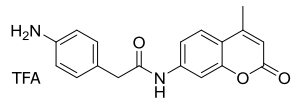	C (steps 1-3)	^{1}H NMR (400 MHz, DMSO) δ 2.39 (s, 3H), 3.66 (s, 2H), 6.26 (s, 1H), 7.04 (d, J = 8.17 Hz, 2H), 7.27 (d, J = 9.08 Hz, 2H), 7.49 (dd, J = 1.88, 8.60 Hz, 1H), 7.71-7.77 (m, 2H), 10.58 (s, 1H). LC/MS: t_r 10.6 min, m/z 309 $[M+H]^+$, purity 99%.
4.129	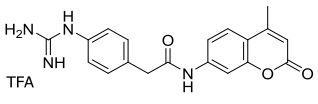	C-I	^{1}H NMR (400 MHz, DMSO) δ 2.40 (d, J = 1.11 Hz, 3H), 3.72 (s, 2H), 6.27 (d, J = 1.09 Hz, 1H), 7.22 (d, J = 8.39 Hz, 2H), 7.36 (brs, 3H), 7.43 (d, J = 8.43 Hz, 2H), 7.49 (dd, J = 2.05, 8.70 Hz, 1H), 7.74 (d, J = 8.69 Hz, 1H), 7.78 (d, J = 2.01 Hz, 1H), 9.62 (s, 1H), 10.64 (s, 1H). LC/MS: t_r 11.2 min, m/z 351

			$[M+H]^+$ purity >99%.
4.130	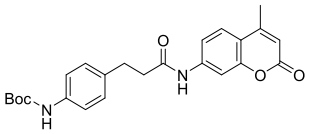	C (steps 1-2)	^{1}H NMR (400 MHz, DMSO) δ 1.46 (s, 9H), 2.39 (s, 3H), 2.63 (t, *J* = 7.55 Hz, 2H), 2.85 (t, *J* = 7.32 Hz, 2H), 6.25 (s, 1H), 7.13 (d, *J* = 8.15 Hz, 2H), 7.36 (d, *J* = 7.49 Hz, 2H), 7.47 (d, *J* = 8.88 Hz, 1H), 7.69-7.76 (m, 2H), 9.23 (s, 1H), 10.34 (s, 1H). LC/MS: t_r 17.2 min, *m/z* 421.1 $[M-H]^-$, purity 98%. Yield: 58.6%.
4.131	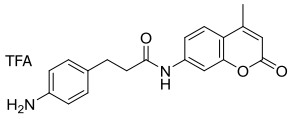	C (steps 1-3)	^{1}H NMR (400 MHz, DMSO) δ 2.39 (d, *J* = 1.05 Hz, 3H), 2.67 (t, *J* = 7.63 Hz, 2H), 2.90 (t, *J* = 7.61 Hz, 2H), 6.26 (d, *J* = 1.17 Hz, 1H), 7.07 (d, *J* = 8.29 Hz, 2H), 7.26 (d, *J* = 8.33 Hz, 2H), 7.46 (dd, *J* = 2.0, 8.67 Hz, 1H), 7.71 (d, *J* = 8.7 Hz, 1H), 7.76 (d, *J* = 1.97 Hz, 1H), 10.36 (s, 1H). LC/MS: t_r 11.1 min, *m/z* 323 $[M+H]^+$, purity 99%.
4.132	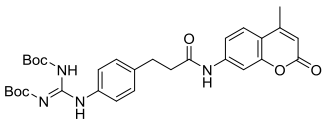	C-I (steps 1-4)	^{1}H NMR (400 MHz, DMSO) δ 1.38 (s, 9H), 1.50 (s, 9H), 2.39 (s, 3H), 2.68 (t, *J* = 7.67 Hz, 2H), 2.91 (t, *J* = 7.34 Hz, 2H), 6.26 (s, 1H), 7.25 (d, *J* = 8.36 Hz, 2H), 7.43-7.47 (m, 3H), 7.72(d, *J* = 8.67 Hz, 1H), 7.76 (d, *J* = 1.76 Hz, 1H), 9.94 (s, 1H), 10.36 (s, 1H), 11.42 (s, 1H). LC/MS: t_r 20.3 min, *m/z* 565.2, purity >99%. Yield: 58%.
4.133	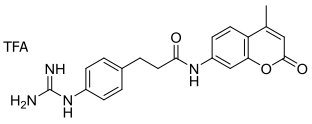	C-I	^{1}H-NMR (400 MHz, DMSO) δ 2.39 (d, *J* = 0.86 Hz, 3H), 2.71 (t, *J* = 7.56 Hz, 2H), 2.95 (t, *J* = 7.71 Hz, 2H), 6.26 (d, *J* = 1.07 Hz, 1H), 7.15 (d, *J* = 8.28 Hz, 2H), 7.33-7.35 (m, 5H), 7.47 (dd, *J* = 1.94, 8.67 Hz, 1H), 7.72 (d, *J* = 8.68 Hz, 1H), 7.78 (d, *J* = 1.91 Hz, 1H), 9.57 (s, 1H), 10.39 (s, 1H). LC/MS: t_r 11.5 min, *m/z* 365.1 $[M+H]^+$, purity 99%.
4.134	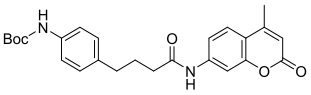	C (steps 1-2)	^{1}H NMR (400 MHz, DMSO) δ 1.47 (s, 9H), 1.89 (p, *J* = 7.16 Hz, 2H), 2.33-2.39 (m, 5H), 2.56 (m, 2H), 6.25 (s, 1H), 7.10 (d, *J* = 8.46 Hz, 2H), 7.35 (d, *J* = 8.13 Hz, 2H), 7.49 (dd, *J* = 1.59, 8.78 Hz, 1H), 7.69-7.76 (m, 2H), 9.22 (s, 1H), 10.31 (s, 1H). LC/MS: t_r 17.7 min, *m/z* 435.1 $[M-H]^-$, purity >99%. Yield: 23%.
4.135	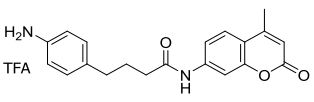	C (steps 1-3)	^{1}H NMR (400 MHz, DMSO) δ 1.88 (p, *J* = 7.56 Hz, 2H), 2.36-2.40 (m, 5H), 2.61 (t, *J* = 7.39 Hz, 2H), 6.26 (d, *J* = 1.18 Hz, 1H), 7.06 (d, *J* = 8.29 Hz, 2H), 7.24 (d, *J* = 8.34 Hz, 2H), 7.48 (dd, *J* = 2.02, 8.69 Hz, 1H), 7.72 (d, *J* = 8.7 Hz, 1H), 7.77 (d, *J* = 1.99 Hz, 1H), 10.34 (s, 1H). LC/MS: t_r 11.7 min, *m/z* 337.1 $[M+H]^+$, purity >99%.
4.136	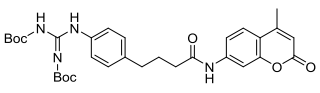	C-I (steps 1-4)	^{1}H NMR (400 MHz, DMSO) δ 1.4 (s, 9H), 1,51 (s, 9H), 1.95 (p, *J* = 7.35 Hz, 2H), 2.36-2.39 (m,5H), 2.62 (t, *J* = 6.87 Hz, 2H), 6.25 (d, *J* = 1.16 Hz, 1H), 7.21 (d, *J* = 8.36 Hz, 2H), 7.43-7.49 (m, 3H), 7.71 (d, *J* = 8.68 Hz, 1H), 7.76 (d, *J* = 1.98 Hz, 1H), 9.95

			(s, 1H), 10.32 (s, 1H), 11.43 (s, 1H). LC/MS: t_r 20.9 min, *m/z* 579.3 $[M+H]^+$, purity 90%. Yield: 48.6%.
4.137	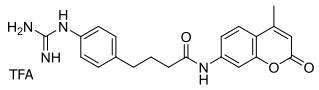	C-I	^{1}H NMR (400 MHz, $CDCl_3$) δ 1.87 (p, *J* = 7.71 Hz, 2H), 2.24-2.27 (m, 5H), 2.56 (t, *J* = 7.70 Hz, 2H), 6.03 (s, 1H), 7.0 (d, *J* = 8.35 Hz, 2H), 7.14 (d, *J* = 8.34 Hz, 2H), 7.36-7.40 (m, 2H), 7.53 (d, *J* = 1.71 Hz, 1H). LC/MS: t_r 11.2 min, *m/z* 379.1 $[M+H]^+$, purity >99%.

Characterization of other compounds described in this chapter

1-Phenylguanidine (4.138). The title compound was prepared according to a standard guanidylation procedure (see general procedure C-I). ^{1}H NMR (400 MHz, DMSO) δ 7.22-7.32 (m, 3H), 7.42-7.46 (m, 2H), 7.56-7.61 (brs, 3H), 10.02 (s, 1H). UPLC/MS: t_r 0.27 min, *m/z* 136.1 $[M+H]^+$, purity >99%.

1-(4-(2-(Imidazo[1,2-*a*]pyridin-3-ylamino)ethyl)phenyl)guanidine (4.139). Detailed synthetic procedure for preparation of the title compound together with its characterization can be found in Chapter 5 (*vide infra*).

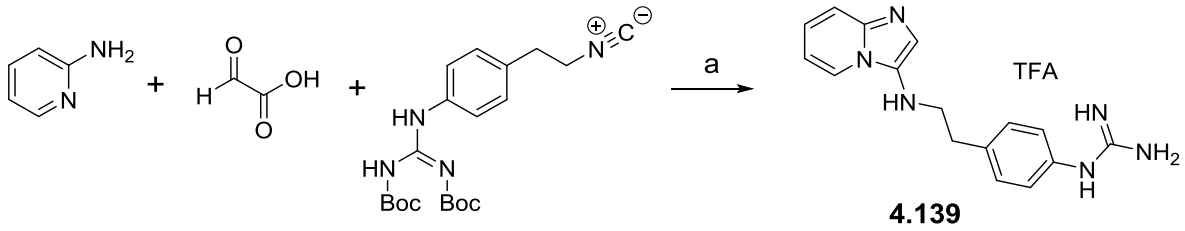

[a]Reagents and conditions: (a) (i) MeOH, $HClO_4$ (cat), rt, (ii) TFA/DCM (1:1), rt.

1-(4-(2-(Pyrimidin-2-ylamino)ethyl)phenyl)guanidine (4.140). The title compound was prepared in three synthetic steps using a standard nucleophilic aromatic substitution reaction from previously prepared starting material.[39] ^{1}H NMR (400 MHz, DMSO) δ 2.85 (t, *J* = 7.70 Hz, 2H), 3.49 (t, *J* = 7.63 Hz, 2H), 6.61 (t, *J* = 4.85 Hz, 1H), 7.15 (d, *J* = 8.40 Hz, 2H), 7.29-7.32 (brs, 4H), 7.32 (d, *J* = 8.41 Hz, 2H), 8.29 (d, *J* = 4.82 Hz, 2H), 9.55 (s, 1H). UPLC/MS: t_r 0.30 min, *m/z* 257.2 $[M+H]^+$, purity >99%.

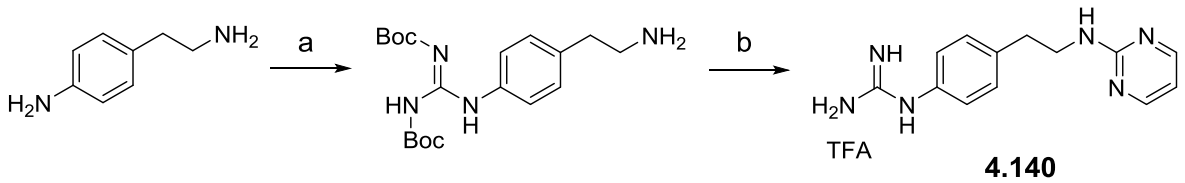

[a]Reagents and conditions: (a) *N,N'*-di-Boc-1*H*-pyrazole-1-carboxamidine, 1,4-dioxane, 10% aq AcOH; (b) (i) 2-chloropyrimidine, TEA, THF, rt, (ii) TFA/DCM (1:1).

Diphenyl (4-guanidinobenzyl)phosphonate (4.143). The title compound was prepared in four synthetic steps according to a general protocol for the Michaelis-Becker reaction from previously prepared starting material.[41] ^{1}H NMR (400 MHz, $CDCl_3$) δ 3.37 (brs, 2H), 3.76 (d, J = 21.61 Hz, 2H), 7.22-7.31 (m, 6H), 7.35-7.40 (m, 2H), 7.47-7.54 (m, 5H), 7.61 (dd, J = 2.38, 8.17 Hz, 2H), 10.11 (s, 1H). ^{13}C NMR (101 MHz, $CDCl_3$) δ 33.8, 120.4, 120.5, 125.7, 125.9, 129.8, 130.1, 131.8, 131.9, 133.8, 150.0, 156.7. UPLC/MS: t_r 1.75 min, *m/z* 382.1 $[M+H]^+$, purity >99%.

Diphenyl (4-guanidinophenethyl)phosphonate (4.144). The title compound was prepared in five synthetic steps according to a modified version of the classical Arbuzov reaction protocol from previously prepared starting material.[42] ^{1}H NMR (400 MHz, $CDCl_3$) δ 2.37-2.45 (m, 2H), 3.07-3.14 (m, 2H), 4.31 (brs, 2H), 7.07-7.33 (m, 15H), 9.82 (s, 1H). ^{13}C NMR (101 MHz, $CDCl_3$,) δ 26.6, 28.0, 120.5, 125.7, 126.0, 130.1, 132.7, 140.0, 150.0, 156.9. UPLC/MS: t_r 1.81 min, *m/z* 396.1 $[M+H]^+$, purity >99%.

4.7.2. Biochemical assays

Enzymatic assays were performed with a BioTek (Winooski, VT, USA) Microplate Reader (Synergy MX). Data collection and analysis were performed with Gen5 Microplate Software and Microsoft Excel. Human enzyme, the urokinase plasminogen activator (uPA), was obtained from HYPHEN BioMed (Neuville-Sur-Oise, France). A fluorogenic substrate screening against uPA was performed with recombinant human uPA purchased from R&D Systems (Minneapolis, MN, USA). Inhibitor kinetic assays were carried out with urokinase chromogenic substrate BIOPHEN CS-61(44) (pyro-Glu-Gly-Arg-pNA, K_m= 80 µM) purchased from HYPHEN BioMed. A 50 mM HEPES buffer (Sigma-Aldrich), pH 8.2, was used. All enzymatic activity measurements were routinely performed in duplicate. *N*-Acyl AMC stock solutions and inhibitor stock solutions (10 mM) were prepared in DMSO and stored at -20 ^{o}C. Enzymatic assays contained less than 5% (v/v) of DMSO.

Inhibitor Kinetic Assays. Enzymatic activity was measured over 5 min at 37 ^{o}C using urokinase chromogenic substrate BIOPHEN CS-61(44). Absorbance was monitored at λ = 405 nm. The assay mixture contained the *N*-acyl AMC compound (50-500 µM depending on solubility; 5 µL), ca. 20 nM of non-recombinant uPA solution in buffer (145 µL) and substrate BIOPHEN CS-61(44) (100 µM; 50 µL) in a final volume of 200 µL. Concentration of the chromogenic substrate used (100 µM) allowed for sufficiently high initial substrate processing rate, while limiting competition between substrate and inhibitor.

Fluorogenic Substrate Screening Against uPA. Screening of the library of *N*-acyl AMCs for substrates of uPA was performed over 6 h at 37 ^{o}C. The excitation wavelength was 383 nm, and the emission wavelength was 455 nm. Because of false positives appearing in assays based on a non-recombinant

enzyme, the substrate screening was performed with a recombinant human uPA. Initial screening of the library was performed at the highest substrate concentration possible (for most of the library members 100-500 μM), uPA concentration was around 200 nM. Final screening was performed using subsaturating levels of substrate.[18,44] Final substrate screening and ranging hits based on the enzymatic cleavage efficiency were determined at 100 μM substrate and approximately 200 nM uPA concentration. Relative fluorescence units (RFUs) were measured for each substrate at regular intervals over a 6 h period of time with and without enzyme (blank). Blank was subtracted from the enzymatic activity measurements. The slope of the plotted line gave the relative k_{cat}/K_m value for each substrate.[19] The identified substrates were tested for the presence of false positives using a simple enzyme denaturation experiment.

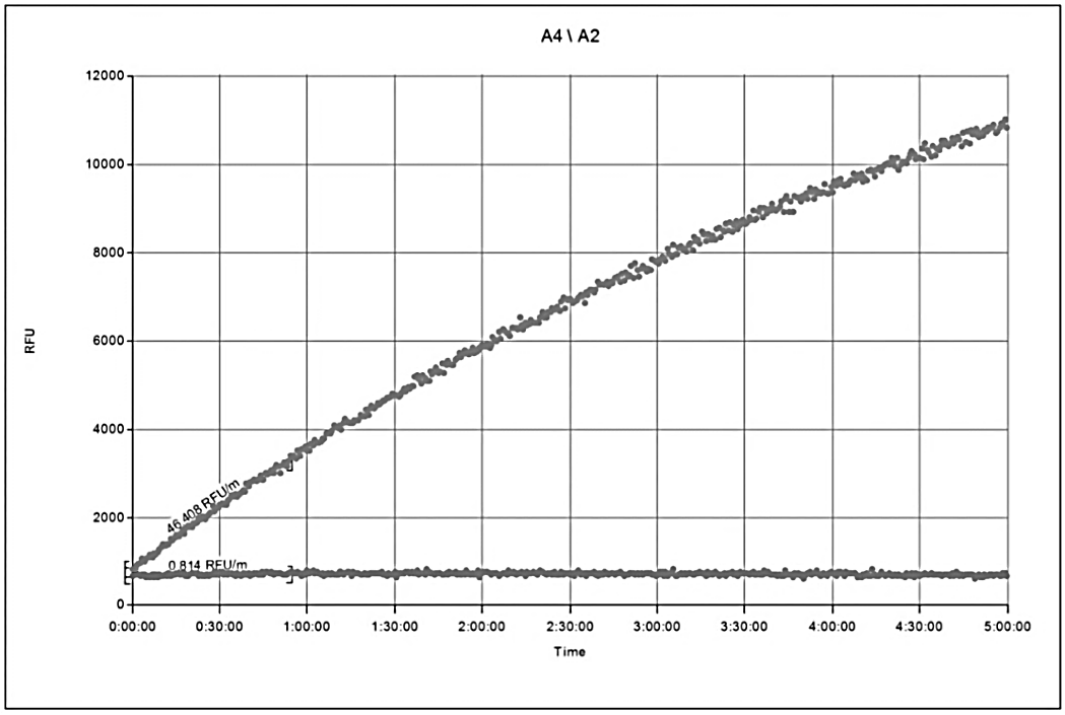

Figure 4.2. Substrate screening against uPA: plot of fluorescence [RFU] versus time [min] for the best substrate identified, compound 4.133 (blank represented by a nearly horizontal line).

Determination of the IC_{50} values. Enzymatic activity was measured at 37 °C using uPA chromogenic substrate BIOPHEN CS-61(44). Absorbance was monitored at λ = 405 nm. Each reaction mixture had a total volume of 200 μL and contained the chromogenic substrate (250 μM), the non-recombinant urokinase solution (ca. 20 nM) in buffer (145 μL) and the inhibitor (5 μL). The initial screening was performed at three inhibitor concentrations (250 μM, 2.5 μM and 25 nM) in order to estimate the IC_{50} range. For the exact IC_{50} determination, at least four inhibitor concentrations above and four

concentrations below the estimated IC_{50} value were used. IC_{50} values were determined by fitting the obtained data with a four-parameter logistics equation using GraFit7 Erithacus Software. Two independent IC_{50} measurements were performed, each of them in duplicate. Based on those two independent measurements, we estimated error in the IC_{50} value.

$$V_0 = V_{min} + \left(\frac{v_{max} - v_{min}}{1 + \left(\frac{[I]_0}{IC_{50}} \right)} \right)$$

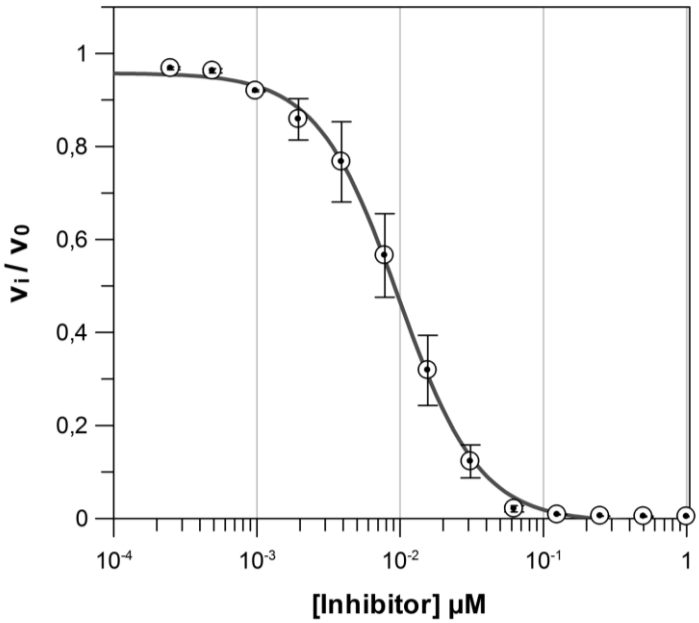

Parameter	Value	Std. Error
Y Range	9,65e-1	1,44e-2
IC 50	9,74e-3	3,5e-4
Slope factor	1,53	7,6e-2
Background	-7,4e-3	8,26e-3

Figure 4.3. Determination of the IC_{50} (uPA) value of compound 4.144.

Determination of inhibition type: To monitor the dissociation of the inhibitor-enzyme complex, aliquots of enzyme were incubated at 37 °C (1) without and (2) with the inhibitor, at a concentration 50 times higher than its IC_{50}. Enzyme was used at a 2.5 times higher concentration than for the IC_{50} determination. After 15 min, the aliquots were diluted 50-fold with the substrate (250 µM) solution in assay buffer. Dissociation of the enzyme-inhibitor complex was determined spectrophotometrically by monitoring hydrolysis of the chromogenic substrate over time.[36]

References

(1) Bollag, G.; Hirth, P.; Tsai, J.; Zhang, J.; Ibrahim, P. N.; Cho, H.; Spevak, W.; Zhang, C.; Zhang, Y.; Habets, G.; Burton, E. A.; Wong, B.; Tsang, G.; West, B. L.; Powell, B.; Shellooe, R.; Marimuthu, A.; Nguyen, H.; Zhang, K. Y. J.; Artis, D. R.; Schlessinger, J.; Su, F.; Higgins, B.; Iyer, R.; D'Andrea, K.; Koehler, A.; Stumm, M.; Lin, P. S.; Lee, R. J.; Grippo, J.; Puzanov, I.; Kim, K. B.; Ribas, A.; McArthur, G. A.; Sosman, J. A.; Chapman, P. B.; Flaherty, K. T.; Xu, X.; Nathanson, K. L.; Nolop, K. Clinical Efficacy of a RAF Inhibitor Needs Broad Target Blockade in BRAF-Mutant Melanoma. *Nature* **2010**, *467*, 596–599.

(2) Congreve, M.; Carr, R.; Murray, C.; Jhoti, H. A "Rule of Three" for Fragment-Based Lead Discovery? *Drug Discov. Today* **2003**, *8*, 876–877.

(3) Congreve, M.; Chessari, G.; Tisi, D.; Woodhead, A. J. Recent Developments in Fragment-Based Drug Discovery. *J. Med. Chem.* **2008**, *51*, 3661–3680.

(4) Murray, C. W.; Rees, D. C. The Rise of Fragment-Based Drug Discovery. *Nature Chemistry* **2009**, *1*, 187–192.

(5) Hajduk, P. J.; Greer, J. A Decade of Fragment-Based Drug Design: Strategic Advances and Lessons Learned. *Nat. Rev. Drug Discov.* **2007**, *6*, 211–219.

(6) Murray, C. W.; Verdonk, M. L.; Rees, D. C. Experiences in Fragment-Based Drug Discovery. *Trends Pharmacol. Sci.* **2012**, *33*, 224–232.

(7) Rees, D. C.; Congreve, M.; Murray, C. W.; Carr, R. Fragment-Based Lead Discovery. *Nat. Rev. Drug Discov.* **2004**, *3*, 660–672.

(8) Murray, C. W.; Blundell, T. L. Structural Biology in Fragment-Based Drug Design. *Curr. Opin. Struct. Biol.* **2010**, *20* (4), 497–507.

(9) Hartshorn, M. J.; Murray, C. W.; Cleasby, A.; Frederickson, M.; Tickle, I. J.; Jhoti, H. Fragment-Based Lead Discovery Using X-Ray Crystallography. *J. Med. Chem.* **2005**, *48*, 403–413.

(10) Huber, W.; Mueller, F. Biomolecular Interaction Analysis in Drug Discovery Using Surface Plasmon Resonance Technology. *Curr. Pharm. Des.* **2006**, *12*, 3999–4021.

(11) Lambruschini, C.; Veronesi, M.; Romeo, E.; Garau, G.; Bandiera, T.; Piomelli, D.; Scarpelli, R.; Dalvit, C. Development of Fragment-Based N-FABS NMR Screening Applied to the Membrane Enzyme FAAH. *ChemBioChem* **2013**, *14*, 1611–1619.

(12) Dias, D. M.; Ciulli, A. NMR Approaches in Structure-Based Lead Discovery: Recent Developments and New Frontiers for Targeting Multi-Protein Complexes. *Prog. Biophys. Mol. Biol.* **2014**, *116*, 101–112.

(13) Shepherd, C. A.; Hopkins, A. L.; Navratilova, I. Fragment Screening by SPR and Advanced Application to GPCRs. *Prog. Biophys. Mol. Biol.* **2014**, *116*, 113–123.

(14) Neumann, T.; Junker, H.-D.; Schmidt, K.; Sekul, R. SPR-Based Fragment Screening: Advantages and Applications. *Curr. Top. Med. Chem.* **2007**, *7*, 1630–1642.

(15) Vulpetti, A.; Dalvit, C. Design and Generation of Highly Diverse Fluorinated Fragment Libraries and Their Efficient Screening with Improved ^{19}F NMR Methodology. *ChemMedChem* **2013**, *8*, 2057–2069.

(16) Dalvit, C. Ligand- and Substrate-Based ^{19}F NMR Screening: Principles and Applications to Drug Discovery. *Prog. Nucl. Magn. Reson. Spectrosc.* **2007**, *51*, 243–271.

(17) Drinkwater, N.; Vu, H.; Lovell, K. M.; Criscione, K. R.; Collins, B. M.; Prisinzano, T. E.; Poulsen, S.-A.; McLeish, M. J.; Grunewald, G. L.; Martin, J. L. Fragment-Based Screening by X-Ray Crystallography, MS and Isothermal Titration Calorimetry to Identify PNMT (phenylethanolamine N-Methyltransferase) Inhibitors. *Biochem. J.* **2010**, *431*, 51–61.

(18) Wood, W. J. L.; Patterson, A. W.; Tsuruoka, H.; Jain, R. K.; Ellman, J. A. Substrate Activity Screening: A Fragment-Based Method for the Rapid Identification of Nonpeptidic Protease Inhibitors. *J. Am. Chem. Soc.* **2005**, *127*, 15521–15527.

(19) Salisbury, C. M.; Ellman, J. A. Rapid Identification of Potent Nonpeptidic Serine Protease Inhibitors. *ChemBioChem* **2006**, *7*, 1034–1037.

(20) Soellner, M. B.; Rawls, K. A.; Grundner, C.; Alber, T.; Ellman, J. A. Fragment-Based Substrate Activity Screening Method for the Identification of Potent Inhibitors of the *Mycobacterium tuberculosis* Phosphatase PtpB. *J. Am. Chem. Soc.* **2007**, *129*, 9613–9615.

(21) Drag, M.; Bogyo, M.; Ellman, J. A.; Salvesen, G. S. Aminopeptidase Fingerprints, an Integrated Approach for Identification of Good Substrates and Optimal Inhibitors. *J. Biol. Chem.* **2010**, *285*, 3310–3318.

(22) Leyva, M. J.; Degiacomo, F.; Kaltenbach, L. S.; Holcomb, J.; Zhang, N.; Gafni, J.; Park, H.; Lo, D. C.; Salvesen, G. S.; Ellerby, L. M.; Ellman, J. A. Identification and Evaluation of Small Molecule Pan-Caspase Inhibitors in Huntington's Disease Models. *Chem. Biol.* **2010**, *17*, 1189–1200.

(23) Baguley, T. D.; Xu, H.-C.; Chatterjee, M.; Nairn, A. C.; Lombroso, P. J.; Ellman, J. A. Substrate-Based Fragment Identification for the Development of Selective, Nonpeptidic Inhibitors of Striatal-Enriched Protein Tyrosine Phosphatase. *J. Med. Chem.* **2013**, *56*, 7636–7650.

(24) Jamali, H.; Khan, H. A.; Stringer, J. R.; Chowdhury, S.; Ellman, J. A. Identification of Multiple Structurally Distinct, Nonpeptidic Small Molecule Inhibitors of Protein Arginine Deiminase 3 Using a Substrate-Based Fragment Method. *J. Am. Chem. Soc.* **2015**, *137*, 3616–3621.

(25) Chapelat, J.; Berst, F.; Marzinzik, A. L.; Moebitz, H.; Drueckes, P.; Trappe, J.; Fabbro, D.; Seebach, D. The Substrate-Activity-Screening Methodology Applied to Receptor Tyrosine Kinases: A Proof-of-Concept Study. *Eur. J. Med. Chem.* **2012**, *57*, 1–9.

(26) Rawls, K. A.; Lang, P. T.; Takeuchi, J.; Imamura, S.; Baguley, T. D.; Grundner, C.; Alber, T.; Ellman, J. A. Fragment-Based Discovery of Selective Inhibitors of the *Mycobacterium tuberculosis* Protein Tyrosine Phosphatase PtpA. *Bioorg. Med. Chem. Lett.* **2009**, *19*, 6851–6854.

(27) Patterson, A. W.; Wood, W. J. L.; Ellman, J. A. Substrate Activity Screening (SAS): A General Procedure for the Preparation and Screening of a Fragment-Based Non-Peptidic Protease Substrate Library for Inhibitor Discovery. *Nat. Protoc.* **2007**, *2*, 424–433.

(28) Mekkawy, A. H.; Pourgholami, M. H.; Morris, D. L. Involvement of Urokinase-Type Plasminogen Activator System in Cancer : An Overview. *Med. Res. Rev.* **2014**, *34*, 918–956.

(29) Mekkawy, A. H.; Morris, D. L.; Pourgholami, M. H. Urokinase Plasminogen Activator System as a Potential Target for Cancer Therapy. *Futur. Oncol.* **2009**, *5*, 1487–1499.

(30) Dass, K.; Ahmad, A.; Azmi, A. S.; Sarkar, S. H.; Sarkar, F. H. Evolving Role of uPA/uPAR System in Human Cancers. *Cancer Treat. Rev.* **2008**, *34*, 122–136.

(31) Roodbeen, R.; Paaske, B.; Jiang, L.; Jensen, J. K.; Christensen, A.; Nielsen, J. T.; Huang, M.; Mulder, F. A. A.; Nielsen, N. C.; Andreasen, P. A.; Jensen, K. J. Bicyclic Peptide Inhibitor of Urokinase-Type Plasminogen Activator: Mode of Action. *ChemBioChem* **2013**, *14*, 2179–2188.

(32) Chen, S.; Gfeller, D.; Buth, S. A.; Michielin, O.; Leiman, P. G.; Heinis, C. Improving Binding Affinity and Stability of Peptide Ligands by Substituting Glycines with D-Amino Acids. *ChemBioChem* **2013**, *14*, 1316–1322.

(33) Joossens, J.; Ali, O. M.; El-Sayed, I.; Surpateanu, G.; Van der Veken, P.; Lambeir, A.-M.; Setyono-Han, B.; Foekens, J. A.; Schneider, A.; Schmalix, W.; Haemers, A.; Augustyns, K. Small, Potent, and Selective Diaryl Phosphonate Inhibitors for Urokinase-Type Plasminogen Activator with in Vivo Antimetastatic Properties. *J. Med. Chem.* **2007**, *50*, 6638–6646.

(34) Munyemana, F.; Frisque-Hesbain, A.-M.; Devos, A.; Ghosez, L. Synthesis of Alkyl Halides under Neutral Conditions. *Tetrahedron Lett.* **1989**, *30*, 3077–3080.

(35) Montalbetti, C. A. G. N.; Falque, V. Amide Bond Formation and Peptide Coupling. *Tetrahedron* **2005**, *61*, 10827–10852.

(36) Joossens, J.; Van der Veken, P.; Surpateanu, G.; Lambeir, A.-M.; El-Sayed, I.; Ali, O. M.; Augustyns, K.; Haemers, A. Diphenyl Phosphonate Inhibitors for the Urokinase-Type Plasminogen Activator: Optimization of the P4 Position. *J. Med. Chem.* **2006**, *49*, 5785–5793.

(37) Johnson, D. S.; Li, J. J. *The Art of Drug Synthesis*; Wiley, New York, 2007.

(38) Sharma, M.; Saravolatz, L. D. Rilpivirine: A New Non-Nucleoside Reverse Transcriptase Inhibitor. *J. Antimicrob. Chemother.* **2013**, *68*, 250–256.

(39) Brown, D. J., Evans, R. F., Cowden, W. B., Fenn, M. D. *Chemistry of Heterocyclic Compounds: The Pyrimidines*; Wiley, New York, 1994.

(40) Ruijter, E.; Scheffelaar, R.; Orru, R. V. A. Multicomponent Reaction Design in the Quest for Molecular Complexity and Diversity. *Angew. Chem. Int. Ed.* **2011**, *50*, 6234–6246.

(41) Gavara, L.; Petit, C.; Montchamp, J.-L. DBU-Promoted Alkylation of Alkyl Phosphinates and *H*-Phosphonates. *Tetrahedron Lett.* **2012**, *53*, 5000–5003.

(42) Arbusow, B. A. Michaelis-Arbusow- und Perkow-Reaktionen. *Pure Appl. Chem.* **1964**, *9*, 307–336.

(43) Powers, J. C.; Asgian, J. L.; Ekici, O. D.; James, K. E. Irreversible Inhibitors of Serine, Cysteine, and Threonine Proteases. *Chem. Rev.* **2002**, *102*, 4639–4750.

(44) Gervais, F. G. Caspases Cleave Focal Adhesion Kinase during Apoptosis to Generate a FRNK-like Polypeptide. *J. Biol. Chem.* **1998**, *273*, 17102–17108.

Chapter 5

Novel and selective inhibitors of uPA with an imidazo[1,2-a]pyridine scaffold

The content of this chapter is based on:

Gladysz, R.; Adriaenssens, Y.; De Winter, H., Joossens, J.; Lambeir, A.-M.; Augustyns, K.; Van der Veken, P. Discovery and SAR of novel and selective inhibitors of urokinase plasminogen activator (uPA) with an imidazo[1,2-*a*]pyridine scaffold, *Journal of Medicinal Chemistry*, **2015**, *58*, 9238–9257.

5. Novel and selective inhibitors of uPA with an imidazo[1,2-*a*]pyridine scaffold

5.1. Introduction

Urokinase plasminogen activator is a biomarker and therapeutic target for several cancer types. Its inhibition is regarded as a promising, noncytotoxic approach in cancer therapy by blocking growth and/or metastasis of solid tumors. Despite the significant role of uPA as oncology target, the clinical development of uPA inhibitors has been hampered by doubtful biopharmaceutical performance of compounds developed so far and their insufficient selectivity with respect to related proteases. Nonetheless, the field of urokinase inhibitor discovery still delivers a number of relevant compounds, mostly small molecules with a competitive, reversible inhibition profile, but also irreversible uPA ligands, antibodies or peptide-based molecules. Relevant examples of uPA inhibitors are presented in Chapter 2 (*vide supra*, Part 2.1.7).

This chapter focuses on the discovery of a novel class of reversible, nonpeptidic uPA inhibitors with an imidazo[1,2-*a*]pyridine scaffold. It is directly based on the results obtained during our modified substrate activity screening (MSAS) approach, which was validated by identifying several fragment-sized ligands of the uPA S1 pocket.[1] Detailed description of this methodology was given in Chapter 4 (*vide supra*). Validation of the MSAS approach has shown that an S1-binding fragment could be transformed into a druglike uPA inhibitor by grafting it onto a suitable scaffold and by further decorating this scaffold with additional affinity-conferring substituents. This chapter presents an extensive investigation of this hypothesis and confirms it by the preparation of potent uPA inhibitors. Since no earlier examples of imidazopyridine inhibitors of urokinase have been reported evaluation of the inhibitory potencies under the assay conditions of this chapter included the reference compounds UK-122 (**5.1**), gabexate (**5.2**), and amiloride (**5.3**) (**Figure 5.1**).

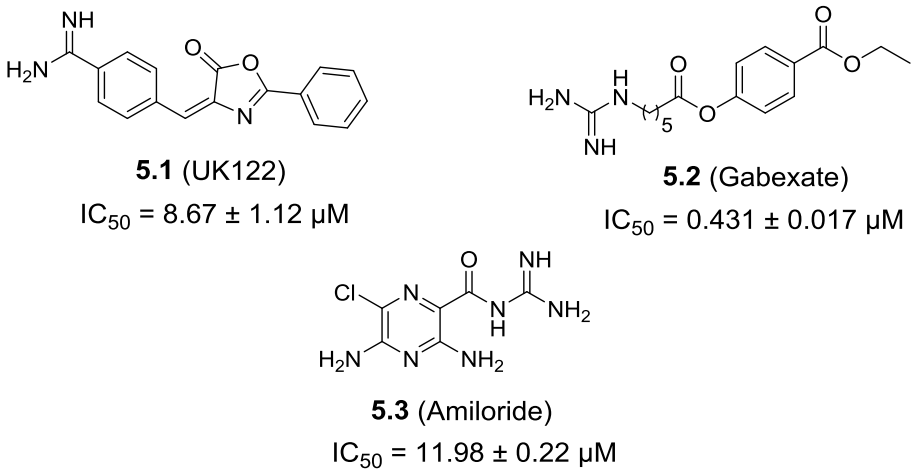

Figure 5.1. Inhibitory activities of the reference compounds against uPA determined under the assay conditions of this chapter.

5.2. General methods

The S1-binding fragments used in this chapter were demonstrated during the MSAS screening to possess high micromolar uPA affinity. Their structures are summarized in **Figure 5.2 (entry A)**. The previous chapter included a proof-of-concept example where fragment **R^{1b}** was grafted onto the 3-position of an imidazopyridine scaffold. A comparison of the IC_{50} values of the separate and the scaffolded fragment indicated the imidazopyridine system to be a novel, potentially useful scaffold for uPA inhibitors.

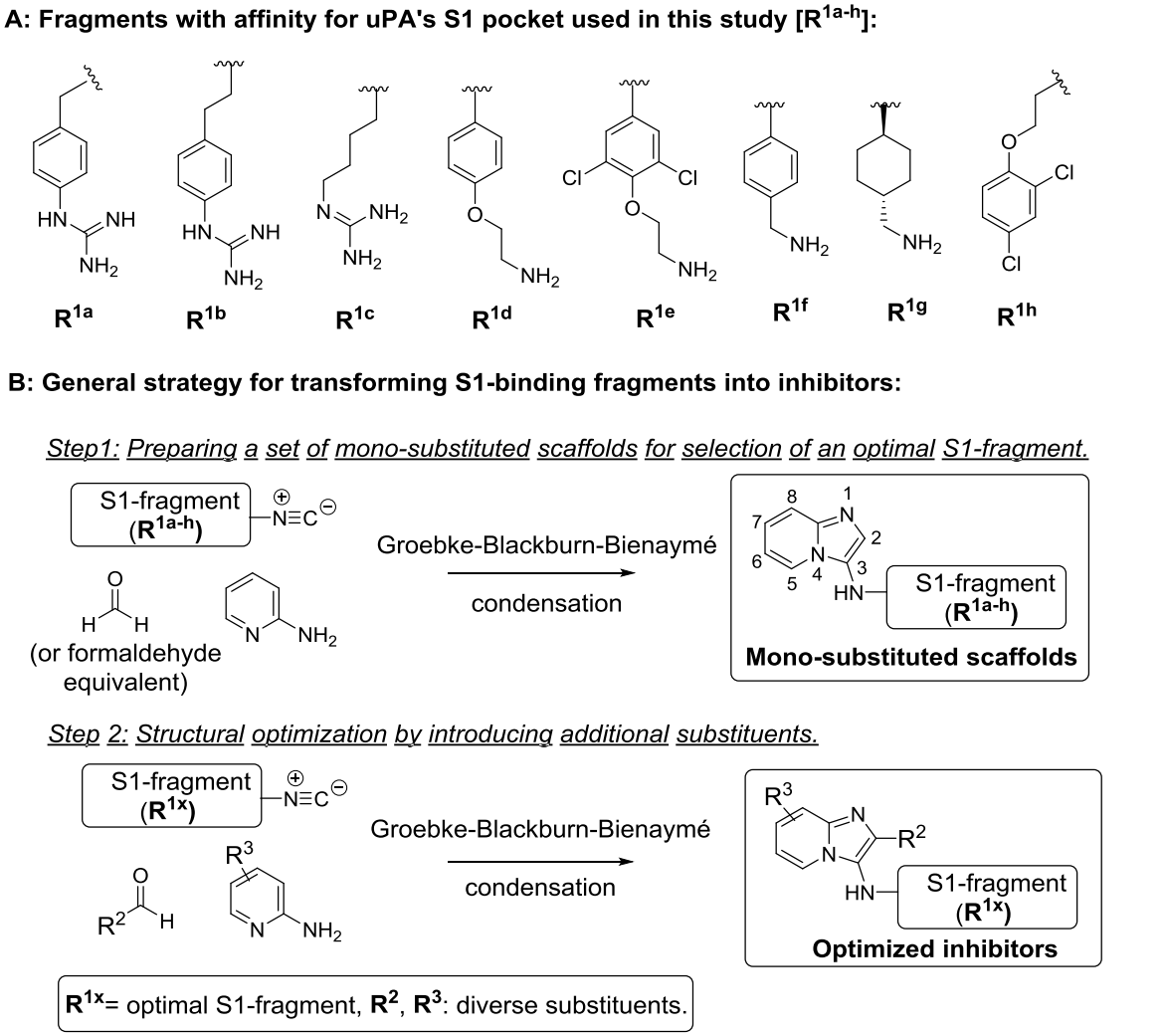

Figure 5.2. Overview of the strategy followed for the preparation of potent uPA inhibitors with an imidazopyridine scaffold.

The general strategy that was followed for obtaining potent uPA inhibitors consists of two parts. In the first part (**Figure 5.2, entry B, step1**), a set of imidazo[1,2-*a*]pyridines was prepared, each bearing one of the S1-binding fragments (**R^{1a-h}**). The choice to introduce the S1-binders at the 3-position of the imidazopyridine was mainly governed by practical synthetic considerations (*vide infra*), although

our earlier proof-of-concept work already indicated this to be a viable approach for preparing compounds with appreciable uPA-affinity. Comparison of the target potencies of the monosubstituted scaffolds obtained in this manner was then used to identify the optimal S1-binding substituent. Further optimization (**Figure 5.2, entry B, step 2**) is achieved by combining the optimal S1-substituent with additional substituents (R^2 and R^3) on the imidazopyridine ring system. Although we extensively relied on molecular modeling to guide the selection of the R^2 and R^3 substituents, diversification in terms of steric and electronic parameters was an equally important goal.

5.2.1. The Groebke-Blackburn-Bienaymé reaction for the preparation of uPA inhibitors

The key step in the preparation of all target compounds of this chapter is the so-called Groebke-Blackburn-Bienaymé condensation, a variant of the Ugi reaction, reported for the first time in 1998.[2-4] It is based on the three-component coupling of (1) an isocyanide, (2) an aldehyde, and (3) a 2-aminoazine in the presence of a suitable catalyst, usually a Lewis acid or Brønsted acid, to generate fused imidazo[1,2-*a*]heterocycles in a one-pot transformation. Carbene-based mechanistic rationale for the Groebke-Blackburn-Bienaymé reaction is presented on **Scheme 5.1**; alternatively an ionic mechanism can be proposed to explain the formation of fused 3-aminoimidazoles.

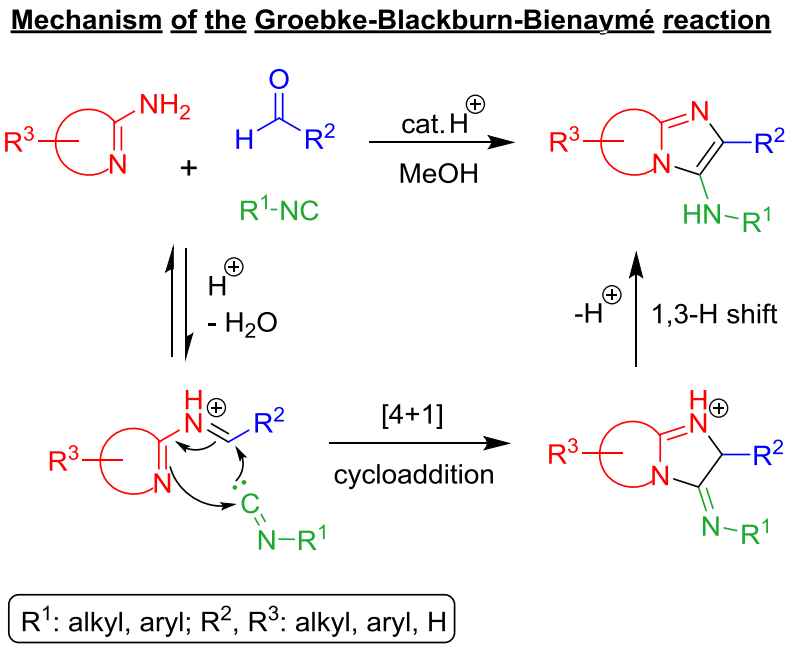

Scheme 5.1. Carbene-based mechanistic rationale for the Groebke-Blackburn-Bienaymé reaction for the synthesis of fused 3-aminoimidazoles (adapted from Bienaymé et al.[4]).

Taking into account the limited number of commercially available isocyanides and their often non-straightforward synthesis, we considered the latter reaction component the least suited as a source of molecular diversity. As mentioned, this practical consideration was instrumental to reserve the isocyanide-derived R^1 group for the S1-binding fragments identified in the MSAS hits. Conversely, aldehydes are commercially available in abundant numbers. Therefore, the aldehyde-derived R^2-substituent was deemed an appropriate source of steric and electronic diversity. Finally, we also found the commercial availability of decorated 2-aminopyridines to be rather limited. Nonetheless, a significant number of 2-aminopyridines equipped with functional groups (e.g., carboxylates, halides) that can easily be derivatized using standard chemical transformations were found to be available. This approach was used to generate sufficient diversity in the produced compound series.

5.2.2. Imidazo[1,2-*a*]pyridine as a relevant scaffold in drug discovery

On a general level, imidazo[1,2-*a*]pyridines have already been applied successfully as scaffold moieties in drug discovery, and the Groebke-Blackburn-Bienaymé reaction represents one of the simplest routes for the diversity-oriented synthesis of this pharmacophore. Compounds of this type have been in clinical investigation for various therapeutic targets resulting in several drugs entering the market, as for instance the hypnotic $GABA_A$ receptor ligand zolpidem, the selective phosphodiesterase 3 (PDE3) inhibitor olprinone, or the CXC chemokine receptor 4 (CXCR4) antagonist GSK812397.[5] Our group, to the best of our knowledge, is the first to report the application of an imidazo[1,2-*a*]pyridine scaffold for the construction of uPA inhibitors. In addition to producing novel and potent uPA-inhibitors, this study also discloses a significant amount of structure-activity relationship data for this class of compounds. Finally, the present study also successfully exemplifies a novel strategy for transforming low-affinity fragments into potent, druglike compounds with a decorated scaffold architecture. Theoretically, the same strategy (fragment scaffolding, followed by optimization through diversity-oriented introduction of additional substituents) could be applied to all targets where a fragment-based approach to drug discovery is followed.

5.3. Monosubstituted scaffold-based inhibitors of uPA

5.3.1. Chemistry

First, the set of imidazo[1,2-*a*]pyridines linked with S1-binding fragments $\mathbf{R^{1a-h}}$ was synthesized relying on the Groebke-Blackburn-Bienaymé (GBB) reaction (**Scheme 5.2**).

Scheme 5.2. Synthetic steps leading to the monosubstituted scaffold-based inhibitors 5.7h, 5.8a-g.[a]

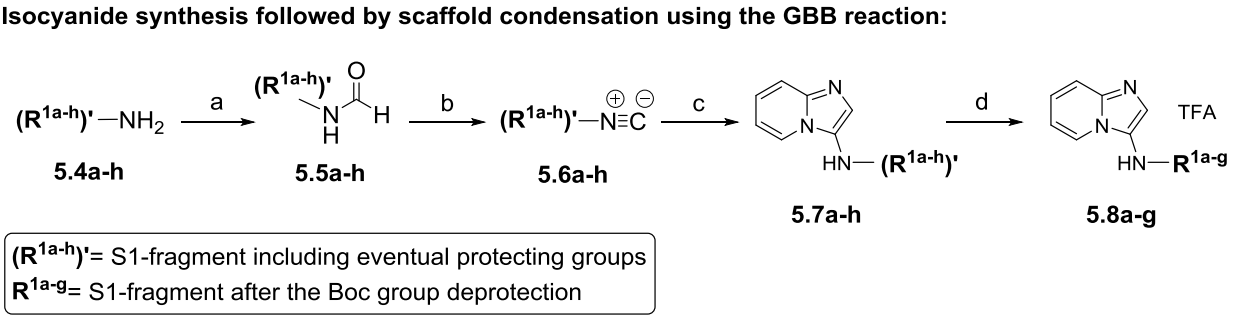

[a]Reagents and conditions: (a) ethyl formate, TEA, 55 °C, 24 h, 55-90%; (b) $POCl_3$, DIPA, DCM, 60-85%; (c) pyridin-2-amine, glyoxylic acid monohydrate, $HClO_4$ (cat), MeOH, rt, 24 h, 38-66%; (d) TFA/DCM (1:1), rt, 1 h, 95-100%.

The isocyanides (**5.6a-h**) required for this reaction were synthesized from amines **5.4a-h** by consecutive formylation and dehydration. The formylation reaction was carried out by refluxing the corresponding amines overnight in ethyl formate and in the presence of triethylamine as previously described by Hartman et al.[6], to afford the desired formamides (**5.5a-h**) in 55-90% yield. Dehydration in the presence of $POCl_3$ led to the formation of the isocyanides (**5.6a-h**) in low to moderate yields (**Table 5.1**).

Careful optimization of the reaction conditions, including the nature of base and the reaction medium, were therefore necessary. Following the protocol described by Ugi et al.[7], we replaced triethylamine by diisopropylamine, which increased not only the average yields (60-85%), but also purity, making chromatographic purification in some cases avoidable. Detailed experimental procedures and characterization data for preparation of amines **5.4a-h**, formamides **5.5a-h**, and isocyanides **5.6a-h** can be found in the Experimental section of this chapter.

Table 5.1. Isocyanide synthesis.

R=	Amine		Formamide 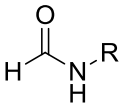		Isocyanide 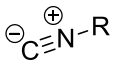	
	Entry	Yield [%]	Entry	Yield [%]	Entry	Yield [%]
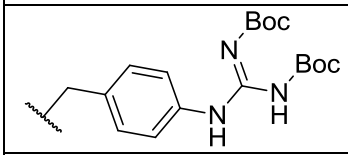	**5.4a**	80	**5.5a**	68	**5.6a**	85
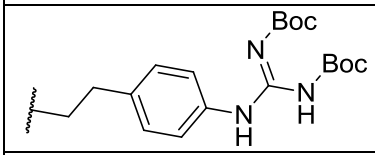	**5.4b**	78	**5.5b**	55	**5.6b**	63
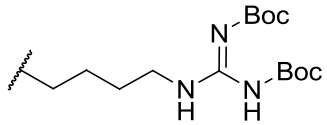	**5.4c**	85	**5.5c**	56.7	**5.6c**	65
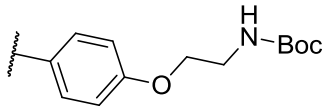	**5.4d**	-	**5.5d**	90	**5.6d**	70
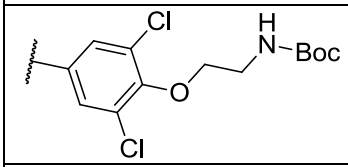	**5.4e**	45	**5.5e**	72	**5.6e**	73
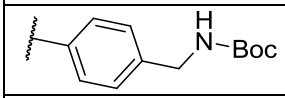	**5.4f**	65	**5.5f**	56	**5.6f**	68
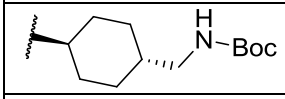	**5.4g**	82	**5.5g**	57	**5.6g**	80
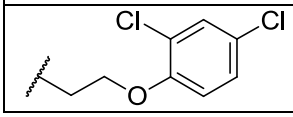	**5.4h**	68	**5.5h**	62.2	**5.6h**	60

For obtaining the monosubstituted imidazopyridines (R^2=R^3=H), the GBB-reaction requires formaldehyde as the aldehyde component. However, the scope of this non-concerted [4+1] cycloaddition is rather limited to formaldehyde.[8,9] This is due to formation of unstable imines, resulting in poor conversions. Our initial attempts to use formaldehyde hydrate and paraformaldehyde as potential formaldehyde equivalents did not produce satisfactory results and afforded the desired product in poor yields (< 30%). Following the protocol reported by Kercher et al.[10], we then applied glyoxylic acid as a formaldehyde equivalent and reacted it with 2-aminopyridine and the set of isocyanides. Glyoxylic acid was indeed found to be an efficient and experimentally more convenient reagent. Further optimization of the original experimental protocol was achieved by using $HClO_4$ as the catalyst and MeOH as the solvent. This resulted in conditions

applicable to all isocyanides that were evaluated and yields for the desired products (**5.7h, 5.8a-g**) ranging between 38 and 65% yield. All reactions were completed within 24 h.

5.3.2. Results and discussion

Evaluation of the uPA inhibitory potency of these monosubstituted imidazo[1,2-*a*]pyridines revealed that the most potent analogues were guanidinophenyl derivatives **5.8a** and **5.8b** (bearing fragments $\mathbf{R^{1a}}$ and $\mathbf{R^{1b}}$) (**Table 5.2**). These displayed IC_{50}-values of 9.04 ± 0.62 µM and 19.39 ± 1.22 µM, respectively. The hypothetical binding modes of these closely related molecules were investigated by docking studies. Results suggested the guanidine side chain of both compounds to interact through hydrogen bonds with Gly-219, Ser-190, and as reasonably expectable, with the anionic carboxylate function of uPA's Asp189. In addition, a hydrogen bond between the amine nitrogen of the imidazopyridine ring system and the catalytically important Ser-195 is also predicted both in the case of compounds **5.8a** and **5.8b** (**Figure 5.3**).

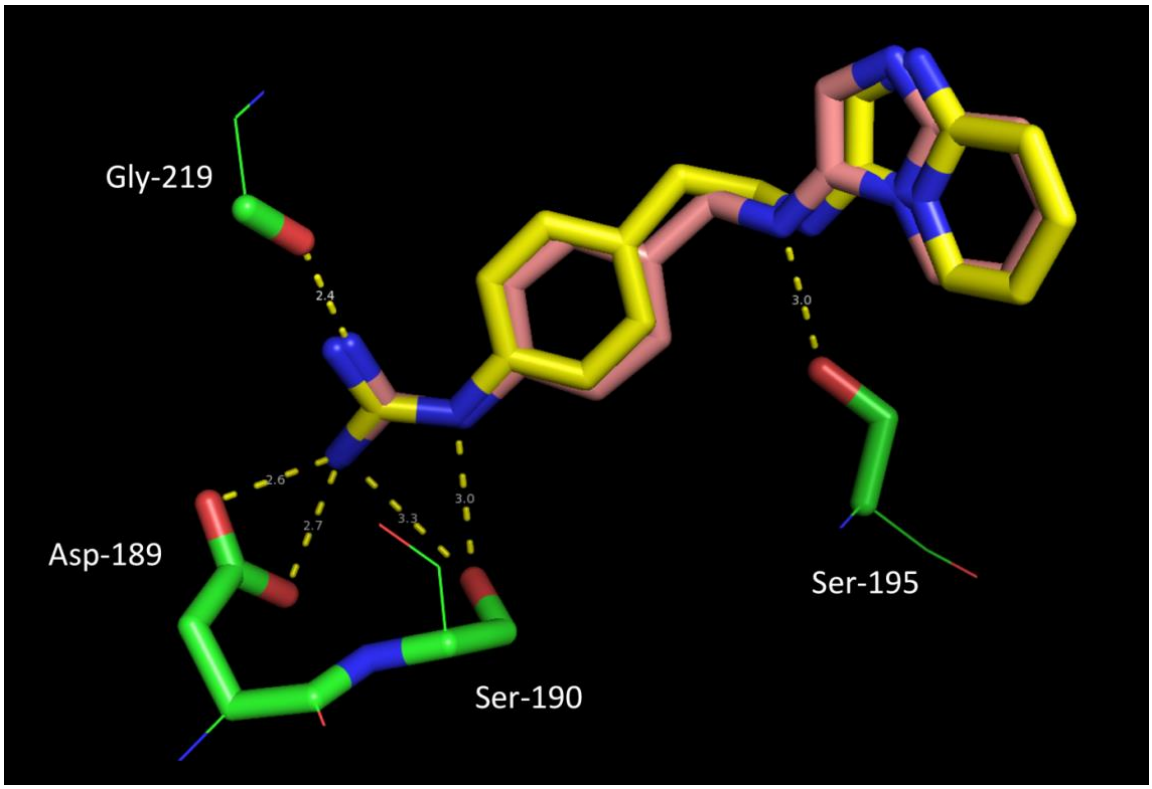

Figure 5.3. Predicted binding mode of compounds 5.8a (light brown) and 5.8b (yellow) in the active site of uPA (PDB code 2O8W). Proposed hydrogen bonds between ligands and labeled protein residues are indicated by yellow dashed lines. Both compounds overlay quite well and show an almost identical binding pattern.

Table 5.2. Biochemical evaluation of the monosubstituted analogues 5.7h, 5.8a-g against uPA.

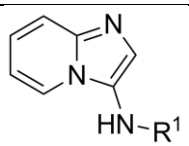

Cpd	R^1=	IC_{50} (uPA) [µM]
5.7h	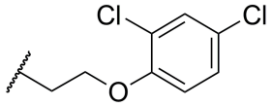	~250
5.8a	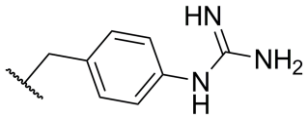	9.04 ± 0.62
5.8b	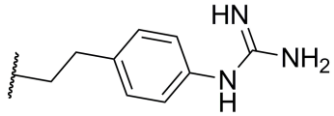	19.39 ± 1.22
5.8c	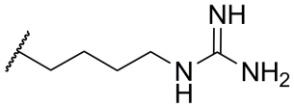	~200
5.8d	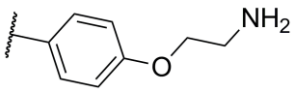	>1000
5.8e	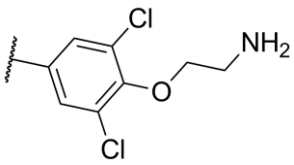	500
5.8f	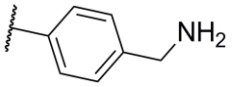	>500
5.8g	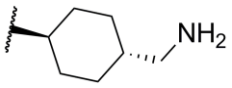	500

A helicopter view of the predicted binding of compound **5.8a** within the active site pocket of uPA is given in **Figure 5.4a**, showing complementarity between ligand and pocket. The guanidine moiety of the compound is deeply buried in the active site, while the imidazole nitrogen of the imidazopyridine ring system is pointing into the solvent and not participating in any hydrogen bonding to the protein. The imidazopyridine scaffold in these simulations was found not to contribute to target affinity *via* directed interactions with the enzyme, although it also does not negatively interfere with binding of **5.8a** and **5.8b** to the active center.

The significant potency of **5.8a** and **5.8b** also reflects the ranking of their corresponding S1-fragments $\mathbf{R^{1a}}$ and $\mathbf{R^{1b}}$ during the modified SAS (MSAS) experiments mentioned earlier, where both displayed among the highest affinities in the collection of „hits". For the other inhibitors in **Table 5.2**, however, the translation of fragment ranking data into potency of the corresponding imidazopyridine inhibitors seems less straightforward. In general, affinities for compounds **5.7h, 5.8c-g** are in the high micromolar range. Noteworthy, the presence of a guanidinobutyl fragment in **5.8c** did not lead to potent inhibition despite this fragment's resemblance to the arginine side chain that is used by uPA for recognition of its natural substrates. Likewise, the aminoethoxyphenyl fragments present in **5.8d** and **5.8e** displayed satisfactory potency during our earlier MSAS experiments but did not result in potent imidazopyridine inhibitors. In addition, these fragments also occur in the mexiletine analogue and/or its like, and both of them were confirmed as ligands of uPA's S1 pocket using X-ray crystallography.[11] Comparable discrepancy is present for the dichlorophenoxy fragment in **5.7h**; while this moiety was ranked close to $\mathbf{R^{1a}}$ and $\mathbf{R^{1b}}$ in the MSAS experiments, grafting it onto an imidazopyridine scaffold leads to a relatively poor inhibitor. Finally, evaluation data for the aminomethyl-substituted **5.8f** and **5.8g** also demonstrated these compounds to be weak uPA inhibitors. Taken together, these biochemical evaluation data led to prioritization of **5.8a** and **5.8b** in the optimization effort. The slightly higher uPA potency, lower molecular weight, and reduced conformational flexibility of **5.8a** were decisive for focusing on this compound during optimization by introducing additional substituents on different positions of the monosubstituted scaffold.

5.4. Optimization of the initial hit: influence of the C2 substituent

Optimization of the initial hit **5.8a** began with investigating the influence of an additional substituent at the 2-position of the imidazo[1,2-*a*]pyridine scaffold (compounds **5.10a**-**k**, **Table 5.3**). For preparing these compounds, 2-aminopyridine and the corresponding isocyanide **5.6a** were reacted with different commercially available aldehydes (**Scheme 5.3**). Selection of the latter was mainly done in a nontarget-biased manner, aiming to cover as much of druglike chemical space as possible by taking steric, electronic and electrostatic parameters into account.

5.4.1. Chemistry

Preparation of the 2-substituted-3-amino-imidazo[1,2-*a*]pyridines (**Scheme 5.3**) followed the classical GBB reaction experimental protocol.[4] Reactions were performed in MeOH and included preformation of the imine intermediate in the presence of a catalytic amount of $HClO_4$ in order to suppress the formation of byproducts. Although the applied experimental protocol in most cases gave satisfactory results (60-86% yield), reaction with some aliphatic aldehydes (e.g., propionaldehyde, 2-amino-acetaldehyde, 3-chlorophenylacetaldehyde) led to poor or moderate yields for compounds **5.9d-f** (49%, 32%, and 22%, respectively), while 2-methoxyaldehyde and 3-(2,4-dichlorophenyl)propanal failed to react under these conditions.

Scheme 5.3. Synthesis of analogues modified at the 2-position 5.10a-k.[a]

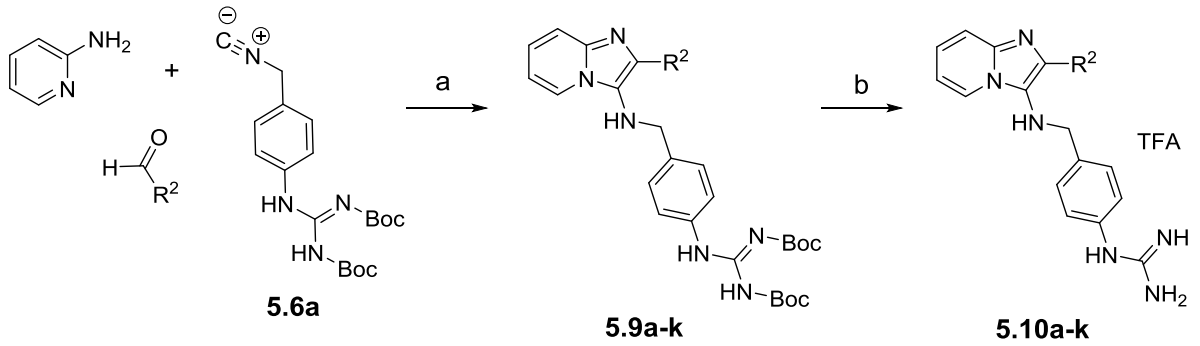

R^2 = 3-pyridyl-, 4-ethylphenyl-, benzyl-, ethyl-, aminomethyl-, 3-chlorobenzyl-, 4-piperidinyl-, 3,5-dichlorophenyl-, phenyl-, 3-fluophenyl-, 4-fluophenyl-

[a]Reagents and conditions: (a) $HClO_4$ (cat), MeOH, rt, 24 h, 22-86%; (b) TFA/DCM (1:1), rt, 1 h, 94-100%.

Additionally, two analogues of **5.8b** (**5.12a** and **5.12b)** with a guanidinophenethyl substituent at the 3-position were prepared (**Scheme 5.4**) for comparison of the inhibitory potency (**Table 5.4**). Compound **5.12a** has an ethyl substituent at the 2-position of the imidazo[1,2-*a*]pyridine ring, whereas analogue **5.12b** comprises the imidazo[1,2-*a*]pyrazine core and carries a 3-chlorophenyl substituent at the 2-position. Preparation of compounds **5.12a** and **5.12b** involved the previously used GBB reaction protocol affording intermediates **5.11a** and **5.11b** in moderate yields (54 and 49%, respectively).

Scheme 5.4. Synthesis of analogues 5.12a-b.[a]

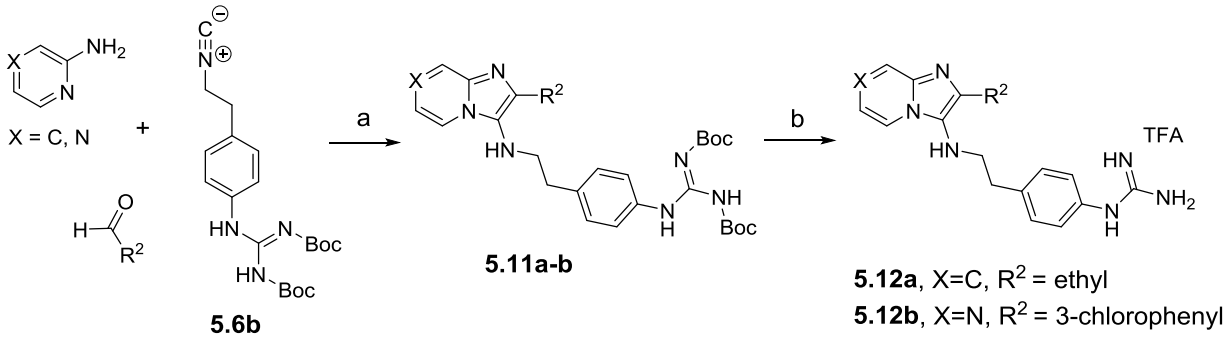

[a]Reagents and conditions: (a) $HClO_4$ (cat), MeOH, rt, 24 h, 49-54%; (b) TFA/DCM (1:1), rt, 1 h, 96-98%.

Most of the performed GBB reactions were complete within 24 h. The final step involved a simple Boc deprotection to afford the desired products in quantitative yields in the form of TFA-salts.

5.4.2. Results and discussion

The uPA potency of the prepared set of 2-substituted analogues was then evaluated (**Table 5.3**). In general, most of the compounds within the 2-substituted imidazo[1,2-*a*]pyridines set displayed reduced uPA affinity. Especially aromatic substituents and sterically demanding aliphatic substituents at the 2-position were not favorable. This detrimental effect is tentatively explained by the computational model used (*vide supra*), suggesting that sterically demanding substituents at the 2-position counteract the conformation that is optimal for binding to the uPA S1 pocket. For instance, the 3-pyridyl (**5.10a**), 3-fluophenyl (**5.10j**), 4-fluophenyl (**5.10k**), and 3,5-dichlorophenyl (**5.10h**) analogues have IC_{50} values ≥100 μM, indicating at least 10-fold decrease in potency in comparison to the initial hit **5.8a**. The same is holds for the 4-piperidinyl-substituted compound **5.10g**, displaying an IC_{50} of more than 100 μM. Interestingly, the benzylic substituents in **5.10c** and **5.10f** caused a relatively less pronounced affinity decrease in comparison to **5.8a**, probably due to increased conformational flexibility. Finally, only the aminomethyl-substituted compound **5.10e** retained the initial binding affinity with an IC_{50} value of 9.30 ± 2.67 μM.

Table 5.3. Biochemical evaluation of the 2-substituted-3-amino-imidazo[1,2-*a*]pyridines set 5.10a-k against uPA.

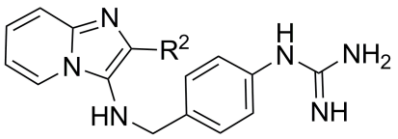

Cpd	R^2=	IC_{50} (uPA) [µM]
5.10a	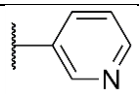	250 ± 2.23
5.10b	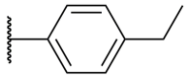	63.92 ± 9.42
5.10c	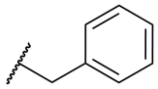	30.25 ± 4.71
5.10d		48.47 ± 8.47
5.10e	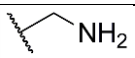	9.30 ± 2.67
5.10f	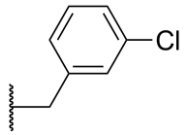	18.03 ± 0.95
5.10g	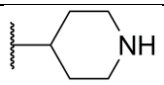	~250
5.10h	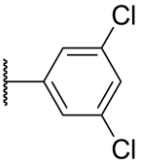	99.16 ± 8.69
5.10i	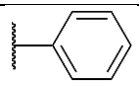	30.15 ± 1.92
5.10j	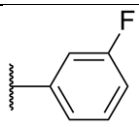	~100
5.10k	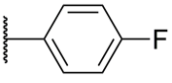	~125

The guanidinophenethyl derivatives **5.12a**, **5.12b** followed a grossly comparable potency pattern (**Table 5.4**), although **5.12a**'s significant drop in potency compared to **5.8b** cannot be readily rationalized by taking only steric factors into account.

Table 5.4. Biochemical evaluation of the C3-guanidinophenethyl-substituted analogues 5.12a, 5.12b against uPA.

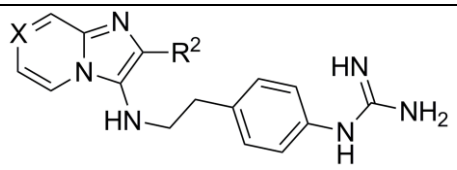

Cpd	R^2=	X=	IC_{50} (uPA) [µM]
5.12a		C	~150
5.12b	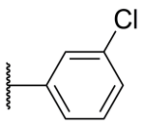	N	53.78 ± 3.72

5.5. Optimization of the initial hit: influence of substitution at the C6-C8 position

Before evaluation data for the 2-substituted imidazo[1,2-*a*]pyridines set were obtained (**Table 5.3**), we decided to explore substitution at the C6-C8 position conserving the C2 3-pyridyl substituent (**Scheme 5.5**). The reason to conserve the latter was inspired by the practically very straightforward synthesis and purification of the compound.

5.5.1. Chemistry

Nine additional C2 3-pyridyl substituted analogues (**5.15a-i**) (**Table 5.5**) were prepared by varying the aminopyridine reaction partner of the GBB reaction. Aminopyridine building blocks were either commercially available or synthesized separately. Accordingly, 2-amino-*N*-butylisonicotinamide **(5.13a)** and 6-amino-*N*-butylnicotinamide **(5.13b)** used for the preparation of compounds **5.15d** and **5.15h**, were synthesized by the aminolysis reaction in the presence of an organocatalyst (1,5,7- triazabicyclo[4.4.0]dec-5-ene, TBD), as reported by Kiesewetter and co-workers[12] (**Table 5.6, entry 2**). Details on the preparation of the latter can be found in the Experimental section.

Scheme 5.5. Synthesis of analogues 5.15a-i.[a]

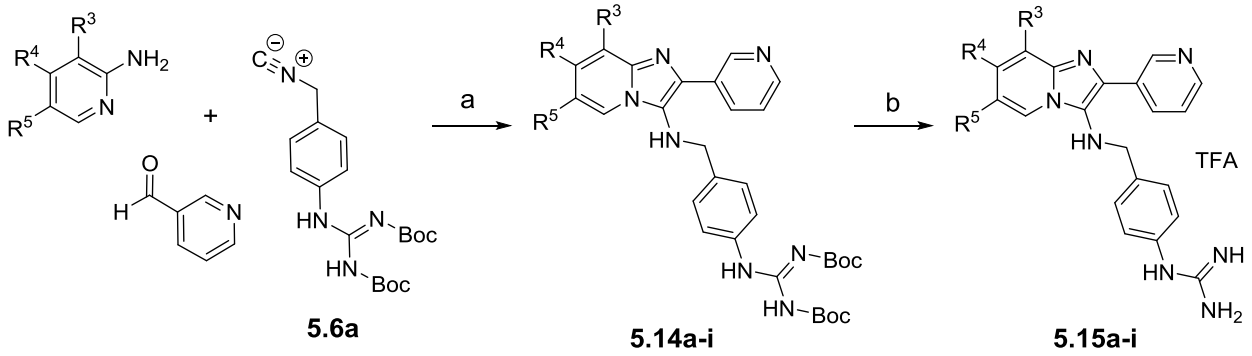

R^3 = methyl-
R^4 = methyl carboxylate, carboxylate, *N*-butylcarboxamide
R^5 = methyl-, trifluoromethyl-, fluoro-, *N*-butylcarboxamide, carboxamide

[a]Reagents and conditions: (a) $HClO_4$ (cat), MeOH, rt, 24 h, 25-68% (in case of compound **5.14d** (i) methyl 2-aminopyridine-4-carboxylate, TBD, DMF, 120 °C, 20 h, 52.5%; (ii) $HClO_4$ (cat), MeOH, rt, 24 h, 60%; compound **5.14h** (i) methyl 6-aminonicotinate, TBD, DMF, 120 °C, 24 h, 42%; (ii) $HClO_4$ (cat), MeOH, rt, 24 h, 47%); (b) TFA/DCM (1:1), rt, 1 h, 94-100% (in case of compound **5.15c** (i) NaOH (2 M), DCM/MeOH (9:1), 12 h, rt, 69%; (ii) TFA/DCM (1:1), rt, 1 h, 93%).

Noteworthy, aminopyridines substituted at the 4- or 5-position (e.g., compounds **5.14d** and **5.14i**) provided better yields in the GBB reaction (60 and 68%, respectively), whereas 2-aminopyridines substituted at the 3- or 6-position performed worse or failed to react under these conditions. For instance, reaction with 3-methylpyridin-2-amine provided **5.14a** only in 25% yield, and 3-(trifluoromethyl)pyridin-2-amine was found not to react at all under these conditions. Replacing the reaction solvent (MeOH) by the non-nucleophilic trifluoroethanol, as originally proposed by Bienaymé et al.[4], still did not afford the desired product.

5.5.2. Results and discussion

The uPA-evaluation results of inhibitors **5.15a-i** are presented in **Table 5.5**. These results demonstrate that the detrimental effect of the C2 3-pyridyl substituent on uPA potency, as observed with **5.10a**, can be significantly reduced by introducing additional affinity-conferring substituents (**Table 5.5**) on the scaffold. Nonetheless, the position of a substituent was found to have a significant effect on inhibitory activity. Generally, analogues substituted at the 7-position of the imidazopyridine scaffold displayed a higher affinity than compounds bearing a substituent at the 6-position. For instance, the C7 methyl carboxylate moiety in **5.15b** caused an increase of binding affinity of almost one order of magnitude relative to **5.10a**. Replacement of the 7-methyl carboxylate group by an

N-butylcarboxamide group in **5.15d** leads to a further increase in affinity. On the other hand, introducing the *N*-butylcarboxamide at the 6-position resulted in analogue **5.15h** with a significantly reduced uPA affinity (60.84 ± 3.39 µM) compared to **5.15d**. Also compounds with C6 electron-withdrawing groups like trifluoromethyl- and fluoro-substituted analogues **5.15f** and **5.15g** displayed reduced inhibitory potency (IC_{50} ~ 200 µM and IC_{50} = 57.55 ± 6.58 µM, respectively).

Again, the more favorable results of the 7-substituted congeners can be tentatively explained by a molecular docking study. **Figure 5.4** clearly indicates that the 6-position of the imidazopyridine scaffold approaches the surface of the pocket and might therefore be compatible with only very small substituent types. On the contrary, the 7-position is more accessible for attaching alternative substituents.

Table 5.5. Biochemical evaluation of the C2 3-pyridyl substituted analogues 5.15a-i against uPA.

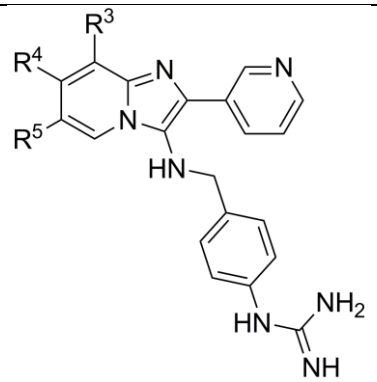

Cpd	R^3=	R^4=	R^5=	IC_{50} (uPA) [µM]
5.15a	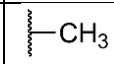	H	H	27.44 ± 1.34
5.15b	H	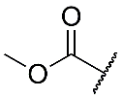	H	14.95 ± 0.81
5.15c	H	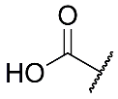	H	26.85 ± 1.57
5.15d	H	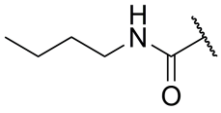	H	6.89 ± 0.80
5.15e	H	H		23.89 ± 2.69
5.15f	H	H		~200
5.15g	H	H		57.55 ± 6.58

5.15h	H	H	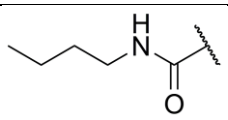	60.84 ± 3.39
5.15i	H	H	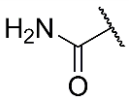	27.26 ± 2.19

5.6. Optimization of the initial hit: amide-substituted analogues 5.18a-f

After obtaining the evaluation results, we decided to synthesize a set imidazo[1,2-*a*]pyridines lacking the C2 3-pyridyl substituent, but with diverse amide groups at the scaffold's 7-position (compounds **5.18a-f**). The *N*-butylcarboxamide substituent that was already present in **5.15d** was included in this series.

5.6.1. Chemistry

The synthetic strategy for these molecules involved formation of the required amide substituent *via* aminolysis of methyl 2-aminopyridine-4-carboxylate, prior to the GBB reaction with glyoxylic acid and isocyanide **5.6a** (**Scheme 5.6**). Although this strategy does not introduce molecular diversity during the final synthetic step, it was selected for two reasons. First, the aminolysis reaction was found to require harsh reaction conditions (high temperature and pressure, long reaction times) that were not compatible with the labile di-Boc-protecting groups of the guanidine function, resulting in poor yields of the desired product (**Table 5.6, entry 1**). Second, performing the GBB further on in the synthesis allowed us to reduce the reaction scale and therefore to consume less of the synthetically more demanding guanidinophenyl-derived isocyanide **5.6a**. Again, the aminolysis was carried out in the presence of TBD. Optimization of the experimental conditions used for preparation of amides **5.13a-b** (**Table 5.6, entry 2**) revealed that by reacting methyl 2-aminopyridine-4-carboxylate with a 2-fold excess of the amine component, increasing the catalyst amount (0.3 equiv) and performing the reaction in dry toluene at 110 °C, the desired amides (**5.16a-e)** were obtained in very good to excellent yields and without the need of chromatographic purification (exemplified in **Table 5.6, entry 4**). The devised protocol does not require protection of the amino group in aminopyridine and was found to be applicable with comparable outcome to methyl 2-aminopyridine-3-carboxylate, methyl 6-aminopyridine-3-carboxylate. Detailed experimental procedures and characterization data for amides **5.16a-e** can be found in the Experimental section. Next to aminolysis, direct coupling of 2-aminopyridine-4-carboxylate with the corresponding amine in DMF in the presence of EDC and HOBt was also tried. However, this resulted in the desired amide only in 10% yield (**Table 5.6, entry 5**).

Table 5.6. Conditions applied to amide bond formation.

Entry	Amine	Carbonyl compound	Catalyst or coupling reagent	Solvent	Conditions	Yield [%]
1	*n*-butylamine (2 eq)	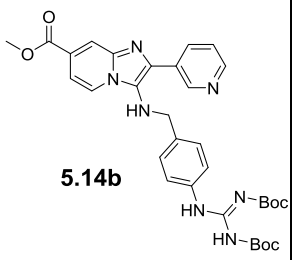 **5.14b**	TBD (0.2 eq)	DMF	pressure tube, 120 °C, 24 h	<10
2	*n*-butylamine (2 eq)	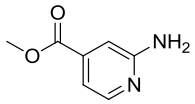	TBD (0.2 eq)	DMF	pressure tube, 120 °C, 20 h	52.5
3	cyclopropyl amine (2.2 eq)	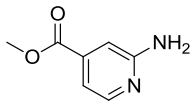	TBD (0.2 eq)	DMF	pressure tube, 120 °C, 21 h	17.2
4	cyclopropyl amine (2.2 eq)	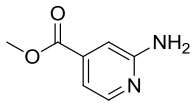	TBD (0.3 eq)	Toluene	pressure tube, 110 °C, 17 h	**89**
5	cyclopropyl amine (1.5 eq)	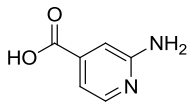	EDC and HOBt	DMF	65 °C, 20 h	10

The prepared amide-substituted aminopyridines were then reacted with glyoxylic acid and isocyanide **5.6a** following the previously used GBB reaction protocol (**Scheme 5.6**). Interestingly, reactions involving 2-aminopyridines with 4-substituent proceeded faster and most of them were complete within 6 h. Products of the three-component coupling (3CC) **5.17a-f** were then subjected to a simple Boc deprotection to afford the desired compounds in the form of TFA-salts, or in case of compound **5.18e**, HCl-salt. Finally, six analogues (**5.18a-f**) were synthesized in moderate yields (42-60%) (**Table 5.7**).

Scheme 5.6. Synthesis of the amide-substituted analogues 5.18a-f.[a]

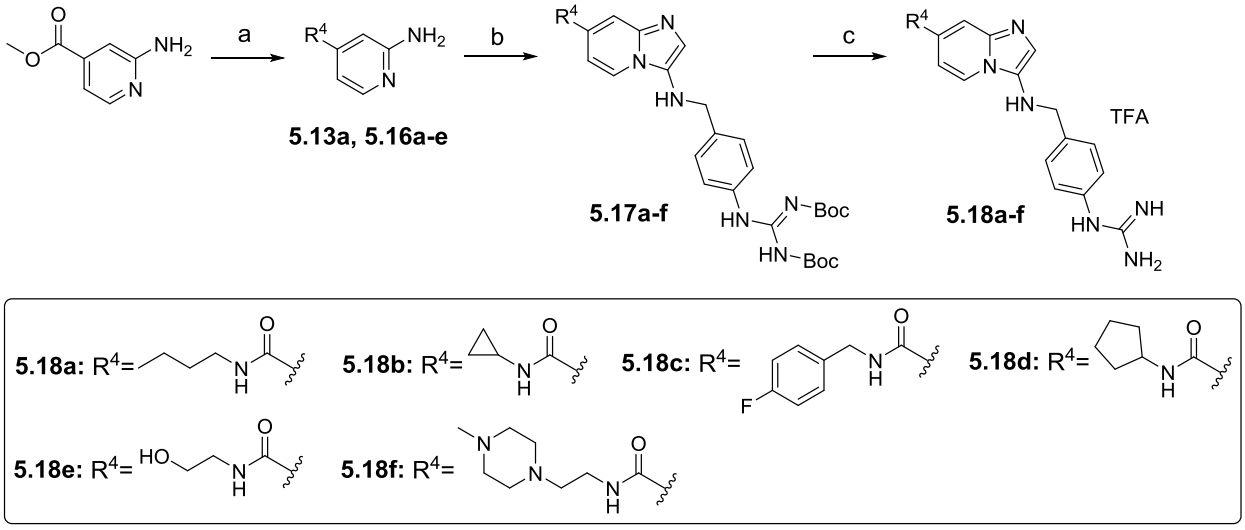

[a]Reagents and conditions: (a) TBD, toluene, 110 °C, 20 h, 86-97% (in case of compound **5.13a** TBD, DMF, 120 °C, 20 h, 52.5%); (b) glyoxylic acid monohydrate, isocyanide **5.6a**, $HClO_4$ (cat), MeOH, rt, 6 h, 42-61%; (c) TFA/DCM (1:1), rt, 1 h, 96-100%.

5.6.2. Results and discussion

The uPA inhibitory potency of the prepared set of amide-substituted analogues **5.18a-f** was then evaluated (**Table 5.7**). Affinities of compounds within this series were in the nanomolar range, indicating an optimal substitution pattern for the scaffold-based uPA inhibitors. The most potent analogue **5.18a** (IC_{50} = 97 ± 10 nM) displays an increase in uPA affinity of about two orders of magnitude relative to initial hit **5.8a**. Similar potency was demonstrated by the cyclopropylamide-substituted analogue **5.18b** (IC_{50} = 184 ± 7 nM), whereas the 2-(4-methylpiperazine) ethylamide group in compound **5.18f** (IC_{50} = 404 ± 20 nM) caused a 4-fold affinity decrease in comparison to **5.18a**.

Table 5.7. Biochemical evaluation of the amide-substituted analogues 5.18a-f against uPA.

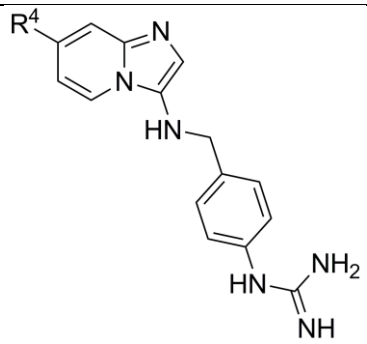

Cpd	R^4=	IC_{50} (uPA) [µM]
5.18a	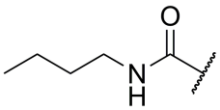	0.097 ± 0.010
5.18b	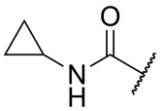	0.184 ± 0.007
5.18c	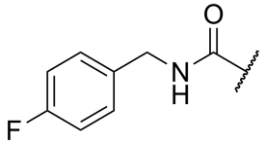	0.254 ± 0.016
5.18d	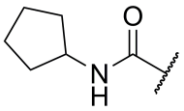	0.174 ± 0.021
5.18e	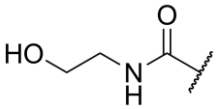	0.366 ± 0.017
5.18f	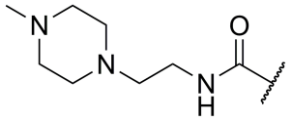	0.404 ± 0.020

The modeling study of the *N*-butylamide fragment of compound **5.18a** in the active site of uPA highlights the available space in this region (**Figure 5.4b**). Besides, formation of an additional hydrogen bond between the amide nitrogen of the *N*-butylamide fragment and the hydroxyl group of Tyr-151 can be observed and could potentially explain the increase in binding affinity that is observed when comparing compound **5.8a** with compound **5.18a** (**Figure 5.4a,b**). The modeling study of compounds **5.18b-f** revealed similar interactions occurring in the uPA's active site (**Figure 5.4c**). This additional interaction might also contribute favorably to the compounds' selectivity with respect to related proteases (*vide infra*).

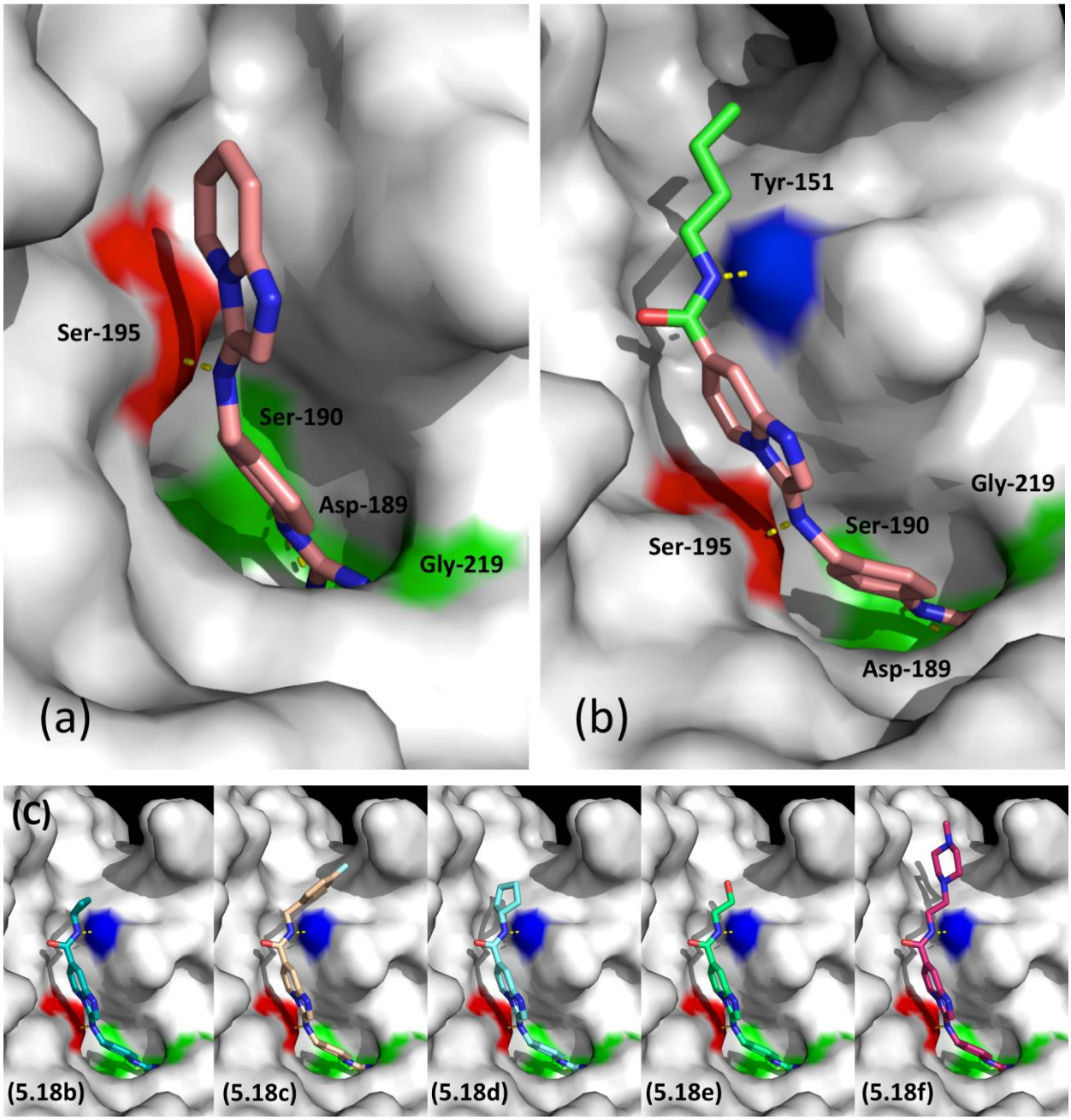

Figure 5.4. Helicopter view of uPA's active site (PDB code 2O8W) showing the proposed binding mode of (a) compound 5.8a, (b) compound 5.18a, and (c) compounds 5.18b-f. The protein surface is colored white, while the surface generated by residue Ser-195 is colored red and the surface generated by residues Ser-190, Asp-189 and Gly-219 is colored green. Putative hydrogen bonds are shown as dashed yellow lines. Docking of compound 5.18a (panel b) reveals an additional hydrogen bond between the ligand and the hydroxyl group of Tyr-151 (colored blue). The R^4 group (Table 5.7) of compound 5.18a is colored green and has been docked using idealized geometrical bond and torsion angles.

Kinetic analysis of the identified inhibitors **5.18a-f** indicated that they are reversible, tight-binding, slow-dissociating inhibitors of uPA. In addition, selectivity of the most potent analogues for uPA was determined with respect to a panel of closely related proteases (tissue-type plasminogen activator (tPA), thrombin, factor Xa (FXa), plasmin, plasma kallikrein, trypsin, factor VIIa (FVIIa)). The results are summarized in **Table 5.8**. Compound **5.8a** was found to be at least 10-fold more selective for uPA than for the other assayed enzymes, while the amide-substituted compounds **5.18a-f** were found selective over all specified enzymes. High specificity of these compounds for uPA can probably be related to interacting with Tyr in position 151 of uPA (**Figure 5.4b, c**). Compound **5.18a** demonstrated the best affinity as well as selectivity profile among this set: with an IC_{50} > 100 µM for all of the related enzymes, this compound has a uPA selectivity index of more than 10^3.

Besides, since the phenylguanidine (**5.19**) fragment is an essential part of the identified inhibitors, we decided to evaluate its contribution to selectivity. Given the fact that no inhibition of thrombin, tPA, FXa, plasmin, plasma kallikrein and FVIIa was observed at 100 µM concentration of compound **5.19**, we can conclude that indeed the phenylguanidine fragment is crucial for selectivity of the identified inhibitors for uPA.

5.7. Conclusions

In conclusion, we have developed a straightforward synthetic strategy for the synthesis of substituted imidazo[1,2-*a*]pyridines as efficient and selective uPA inhibitors. To the best of our knowledge, this is the first reported application of an imidazo[1,2-*a*]pyridine scaffold to the discovery of uPA inhibitors. Compounds **5.18a-f** have nanomolar uPA potencies and are among the most selective inhibitors reported to date. The presence of a guanidine group in **5.18a-f** might nonetheless hamper further development. If required, a prodrug strategy involving the use of a hydroxyguanidine precursor could offer an effective way to overcome bioavailability issues of this kind. Finally, this study presents a novel and efficient strategy for transforming low-affinity fragments into potent, druglike compounds with a decorated scaffold architecture. The same strategy can be readily applied to inhibitor discovery for other enzyme targets.

Table 5.8. Inhibitory activities against uPA and related enzymes (including the reference compounds: UK122 (5.1), gabexate (5.2), amiloride (5.3)).

Cpd	IC_{50} [µM] or % of enzyme inhibition at 100 µM concentration[a]							
	uPA	**thrombin**	**tPA**	**FXa**	**plasmin**	**plasma kallikrein**	**trypsin**	**FVIIa**
5.1	8.67 ± 1.12	56.1 ± 3.65	68.51 ± 5.05	6.47 ± 0.58	0.34 ± 0.01	1.34 ± 0.19	3.18 ± 0.17	0%
5.2	0.431 ± 0.017	0.687 ± 0.048	15.36 ± 0.94	4.61 ± 0.54	1.55 ± 0.06	1.35 ± 0.24	7.12 ± 0.13	-
5.3	11.98 ± 0.22	5.2%	1%	3.5%	0%	0%	31.76 ± 2.88	7.4%
5.8a	9.04 ± 0.62	23%	33.6%	42%	29.8%	39.4%	114.88 ± 6.78	2.5%
5.10a	250 ± 2.23	6.6%	9.4%	24.6%	0%	0%	3.3%	0%
5.18a	0.097 ± 0.010	19.2%	8%	41.8%	13.6%	2.8%	42.7%	1.4%
5.18b	0.184 ± 0.007	8%	0%	45.4%	3.3%	0%	46%	2.6%
5.18c	0.254 ± 0.016	19.5%	11.9%	45.7%	8.3%	0%	43.2%	4.2%
5.18d	0.174 ± 0.021	17.8%	11.2%	47.8%	0%	0%	37.1%	4%
5.18e	0.366 ± 0.017	4.7%	0%	51.58 ± 2.39	15.6%	0%	43.3%	5%
5.18f	0.404 ± 0.020	6.6%	2.8%	12.2%	0%	0%	32%	2%
5.19	57.49 ± 5.20	0%	0%	0%	0%	0%	38.8%	0%

[a]The IC_{50} values and % of enzyme inhibition were determined under the assay conditions of this manuscript.

5.8. Experimental section

5.8.1. Chemistry

All commercially available starting materials, solvents and other research consumables were obtained as described in the Experimental section of Chapter 4, as well as information with regard to the analytical techniques and equipment used for the synthesis, purification, and characterization of synthesized compounds. Purity determination was based on the combined interpretation of ^{1}H NMR, ^{13}C NMR spectra, and UPLC results. All final products have a purity of at least 95% with the exception of compound **5.8c** (purity: 90%). A Waters Acquity UPLC® system was used in two different UPLC methods. Water (A) and acetonitrile (B) were used as eluents. Formic acid 0.1% was added to solvents A and B. Method I: flow 0.7 mL/min, 0.15 min 95% A, 5% B then in 1.85 min from 95% A, 5% B to 100% B, 0% A, then 0.25 min, 100% B, 0% A, 0.75 min (0.350 mL/min) 95% A, 5% B. Method II (purity method): flow 0.4 mL/min, 0.15 min 95% A, 5% B then in 4.85 min from 95% A, 5% B to 100% B, 0% A, then 0.25 min, 100% B, 0% A, 0.75 min 95% A, 5% B.

Where necessary, flash purification was performed with a Biotage® Isolera One flash system. Biotage® SNAP flash cartridges were used for normal phase purifications KP-Sil (10 g, 25 g, 50 g, flow rate of 10-50 mL/min), and for reversed phase purifications KP-C18-HS (12 g, 30 g, flow rate of 10-30 mL/min). Dry sample loading was done by self-packing samplet cartridges using silica and Celite 545 for normal and reversed phase purifications, respectively. Gradients used varied for each purification.

High resolution mass spectrometry (HRMS) involved the following: the dry samples were dissolved in 1 mL of methanol to obtain 10 mM stock solutions, and next diluted 100-fold with methanol to a final concentration of 10 µM. Then 10 µL of each sample was injected using the CapLC system (Waters, Manchester, UK) and electrosprayed using a standard electrospray source. Samples were injected with an interval of 3 min. Positive ion mode accurate mass spectra were acquired using a Q-TOF II instrument (Waters, Manchester, UK). The mass spectrometer was calibrated prior to use with a 0.2% H_3PO_4 solution. The spectra were lock-mass- corrected using the known mass of the nearest H_3PO_4 cluster.

Melting points were determined with a Buchi 530 melting point apparatus and are uncorrected.

The following section comprises the synthetic procedures and analytical data for intermediates and all final compounds reported in this manuscript. Most of the final products were obtained in the form of TFA salts. All TFA-related resonances are omitted in the ^{13}C NMR characterization. The experimental procedures for all the steps in the synthesis of several final products are summarized here as the general procedures.

General Procedure A (**Formamide synthesis).** To a round-bottomed flask fitted with a reflux condenser were added the corresponding amine (13.50 mmol) and ethyl formate (20 equiv). The reaction mixture was stirred and heated under reflux while triethylamine (1.5 equiv) was added. After overnight stirring under reflux the reaction was completed. Subsequently, volatiles were evaporated and the crude product was redissolved in DCM (50 mL). The resulting solution was washed with H_2O (50 mL) and then with brine (50 mL). The organic phase was separated, dried over anhydrous $MgSO_4$ and condensed under reduced pressure. In some cases, further purification was avoidable, otherwise the corresponding formamide was purified using an Isolera purification system with a gradient of 20-100% of EtOAc in heptane, affording the corresponding formamides **5.5a-h** in 55-90% yield.

General Prodecure B (**Isocyanide synthesis).** To a suspension of formamide (4.08 mmol) in dry DCM (25 mL) was added diisopropylamine (2.7 equiv), and the reaction mixture was stirred at 0 °C under a nitrogen atmosphere. To this solution $POCl_3$ (1.1 equiv) was slowly added with a syringe, and stirring was continued for 1 h at 0 °C, and then for 2 h at rt. After completion of the reaction, a solution of Na_2CO_3 in water (2 g/20 mL) was slowly added to maintain 25-30 °C. Stirring was continued for 1 h at rt. More water (20 mL) and DCM (50 mL) was added. The organic phase was separated, dried over anhydrous $MgSO_4$, and concentrated under reduced pressure. In some cases further purification was avoidable, otherwise the corresponding isocyanide was purified using an Isolera purification system with a gradient of 0-50% of EtOAc in heptane, affording the corresponding isocyanides **5.6a-h** in 60-85% yield.

General Prodecure C (**TBD-catalyzed aminolysis reaction)**. To a solution of methyl 2-aminopyridine-4-carboxylate (0.5 g, 3.29 mmol) in dry toluene (10 mL) were added amine (2.2 equiv) and 1,5,7-triazabicyclo[4.4.0]dec-5-ene (TBD) (0.137 g, 0.986 mmol, 0.3 equiv), and the reaction mixture was stirred in a pressure tube at 110 °C for 20 h. After that time the reaction mixture was cooled down and stirred at ambient temperature for a few hours. The desired product precipitated in the form of white crystals, which were subsequently filtered and washed with cold diethyl ether (3 x 20 mL). The desired amides **5.16a-e** were obtained in very good to excellent yields (86-97%) and without the need of chromatographic purification.

General Prodecure D (**Preparation of substituted imidazo[1,2-*a*]pyridines using the Groebke-Blackburn-Bienaymé (GBB) reaction).** To a solution 2-aminoazine (e.g., 1.104 mmol) in MeOH (10 mL), aldehyde (or formaldehyde equivalent: glyoxylic acid monohydrate, 1.5 equiv)) and $HClO_4$ (cat.) (70% aq solution, 8.48 µL, 0.1 equiv) were added at rt, and the reaction was left stirring for 30 min. After that time the isonitrile component (1.1 equiv) was introduced, and the reaction mixture

was stirred at ambient temperature until it was completed, usually within 5-24 h. After that time, the reaction mixture was concentrated under reduced pressure and the crude product was directly purified using an Isolera purification system with a gradient varying by purification, usually 20-100% of EtOAc in heptane (1.5% TEA). In some cases, reversed phase purification was used and applied gradient of 10-100% of MeOH in water. The general procedure D was used to prepare compounds **5.7a-h**, **5.9a-k, 5.11a-b, 5.14a-i, 5.17a-f.**

General Prodecure E (Standard procedure for deprotection of Boc groups using TFA/DCM). Product of the GBB reaction (0.195 mmol) containing a basic function protected with the Boc group was dissolved in a mixture of DCM (1.5 mL) and TFA (1.5 mL) in 1:1 ratio, and the reaction mixture was stirred at rt for 1 h. After that time, volatiles were evaporated and the obtained product was washed with diethyl ether (2 x 10 mL), yielding the pure final compound in the form of a TFA-salt.

1-(4-(Aminomethyl)phenyl)-2,3-di-Boc-guanidine (5.4a). To a solution of 4-(aminomethyl)aniline (0.6 g, 4.91 mmol) in 10% aq acetic acid (40 mL) was added a solution of *N,N'*-di-Boc-1*H*-pyrazole-1-carboxamidine (1.68 g, 5.40 mmol) in 1,4-dioxane (40 mL). After overnight stirring at rt, water (100 mL) was added and the mixture was washed with diethyl ether (3 x 60 mL). The aqueous phase was basicified with 2 M NaOH to pH 13 and extracted with ethyl acetate (3 x 75 mL). The combined extract was washed with water (2 x 50 mL), dried with anhydrous Na_2SO_4, filtered and concentrated under reduced pressure to give the expected product **5.4a** in a form of white solid (0.46 g, 80%). ^{1}H NMR (400 MHz, $CDCl_3$) δ 11.65 (s, 1H), 10.31 (s, 1H), 7.56 (d, *J* = 8.5 Hz, 2H), 7.27 (d, *J* = 8.5 Hz, 2H), 3.83 (s, 2H), 1.54 (s, 9H), 1.51 (s, 9H). UPLC/MS: t_r 1.94 min, *m/z* 365.3 $[M+H]^+$.

1-(4-(Aminoethyl)phenyl)-2,3-di-Boc-guanidine (5.4b). The title compound was prepared from 4-(aminoethyl)aniline (0.3 g, 2.203 mmol) using the same synthetic procedure that was applied to the preparation of 1-(4-(aminomethyl)phenyl)-*N,N'*-bis-Boc-guanidine (**5.4a**), yielding a colorless oil (0.65 g, 78%). ^{1}H NMR (400 MHz, $CDCl_3$) δ 11.64 (s, 1H), 10.26 (s, 1H), 7.50 (d, *J* = 8.4 Hz, 2H), 7.15 (d, *J* = 8.4 Hz, 2H), 3.07 – 2.86 (m, 2H), 2.72 (t, *J* = 6.0 Hz, 2H), 1.53 (s, 9H), 1.49 (s, 9H). UPLC/MS: t_r 1.60 min, *m/z* 379.3 $[M+H]^+$.

1-(4-Aminobutyl)-2,3-di-Boc-guanidine (5.4c). The title amine was prepared from tetramethylenediamine as presented in **Scheme 5.7**. To a solution of tetramethylenediamine (1.14 mL, 11.34 mmol) in 20:1 mixture of THF (16 mL) and H_2O (0.8 mL) was added dropwise a solution of *N,N'*-bis-Boc-methylisothiourea (1.098 g, 3.78 mmol) in THF (10 mL) at 25 °C. After addition the reaction was heated at 50 °C for 2 h, and then the solvent was evaporated under reduced pressure. The resulting crude product was partitioned between DCM and saturated aq $NaHCO_3$. The organic extracts were dried over anhydrous Na_2SO_4, filtered and concentrated under

reduced pressure to give the desired product (**5.4c**) in the form of a cloudy oil (1.05 g, 85%). ^{1}H NMR (400 MHz, $CDCl_3$) δ 11.45 (brs, 1H), 8.30 (s, 1H), 3.44 – 3.31 (m, 2H), 2.69 (t, *J* = 6.6 Hz, 2H), 1.63 – 1.52 (m, 2H), 1.51 – 1.37 (m, 2H), 1.51 – 1.37 (m, 20H). UPLC/MS: t_r 1.51 min, *m/z* 331.6 $[M+H]^+$.

Scheme 5.7. Preparation of aniline 5.4c as intermediate in the synthesis of isocyanide 5.6c.[a]

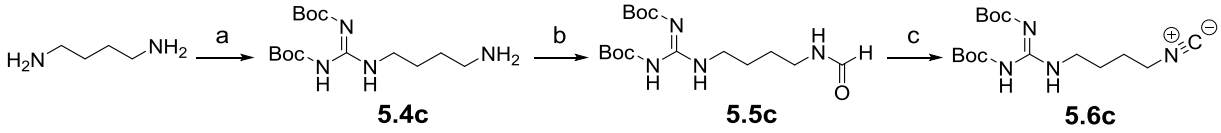

[a]Reagents and conditions: (a) *N,N'*-bis-Boc-methylisothiourea, THF, 50 °C, 2 h; (b) ethyl formate, TEA, reflux; (c) $POCl_3$, TEA, dry DCM, 0 °C, 2 h.

3,5-Dichloro-4-(2-(Boc-amino)ethoxy)aniline (5.4e). Amine **5.4e** was obtained in three synthetic steps from the previously prepared starting material (**Scheme 5.8**). **Step 1: Preparation of *N*-Cbz-4-amino-2,6-dichlorophenol (standard Cbz-protection procedure)**. To a suspension of 4-amino-2,6-dichlorophenol (2.2 g, 12.36 mmol) and $NaHCO_3$ (1.142 g, 13.59 mmol, 1.1 equiv) in THF (20 mL) benzyl chloroformate (1.669 ml, 11.74 mmol) was added dropwise at 0 °C. The reaction was left stirring overnight. After that time EtOAc (70 mL) was added and the organic layer was extracted with 2M HCl (50 mL), washed with brine, dried over anhydrous $MgSO_4$, and evaporated under reduced pressure. The title compound was purified using an Isolera purification system with a gradient of 0-20% of EtOAc in heptane to afford *N*-Cbz-4-amino-2,6-dichlorophenol (2 g, 52%). **Step 2: Preparation of 3,5-dichloro-*N*-Cbz-4-(2-(Boc-amino)ethoxy)aniline.** To a solution of *N*-Boc-2-bromoethanamine (2.202 g, 8.84 mmol) in DMF (40 mL) *N*-Cbz-4-amino-2,6-dichlorophenol (2.3 g, 7.37 mmol) was added. To this reaction mixture K_2CO_3 (2.037 g, 14.74 mmol) was added in portions. After 4 h stirring at 60 °C, the reaction was completed. The reaction mixture was quenched with water and the aqueous phase was extracted with EtOAc (3 x 50 mL). The combined organic extract was washed with water (50 mL), then with brine (50 mL), dried over anhydrous $MgSO_4$, and concentrated under reduced pressure to afford a transparent oil. The title compound was purified using an Isolera purification system with a gradient of 0-25% of EtOAc in heptane (1.7 g, 51%). **Step 3: 3,5-dichloro-4-(2-(Boc-amino)ethoxy)aniline (5.4e) (standard hydrogenolysis procedure).** First, 3,5-dichloro-*N*-Cbz-4-(2-(Boc-amino)ethoxy)aniline (1.5 g, 3.29 mmol) was dissolved in MeOH (30 mL). After 30 min of bubbling nitrogen gas through the solution, Pd/C (0.631 g, 2.96 mmol) was added, and the reaction was flushed again for 15 min with nitrogen before hydrogen gas was added *via* a balloon. The reaction was stirred under a hydrogen atmosphere for 50 min. The obtained product was purified using an Isolera purification system with a gradient of 10-100% of EtOAc in heptane to afford the title amine (0.835 g, 75%). The product was directly used in the next step, i.e., formamide synthesis.

Scheme 5.8. Preparation of aniline 5.4e as intermediate in the synthesis of isocyanide 5.6e.[a]

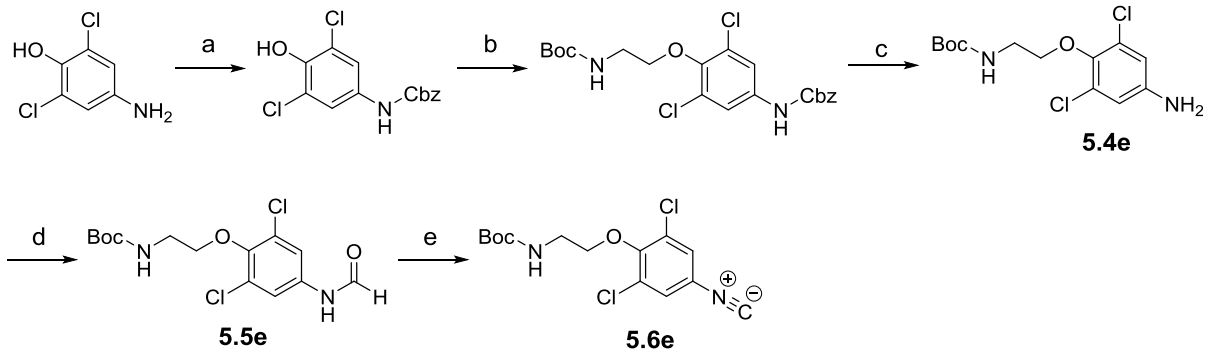

[a]Reagents and conditions: (a) CbzCl, $NaHCO_3$, THF; (b) *N*-Boc-2-bromoethanamine, K_2CO_3, DMF; (c) H_2, Pd/C, MeOH; (d) ethyl formate, TEA, reflux; (e) $POCl_3$, DIPA, dry DCM, 0°C, 2 h.

(1*R*,4*R*)-4-((Boc-amino)methyl)cyclohexan-1-amine (5.4g). Amine **5.4g** was obtained using a Curtius rearrangement (**Scheme 5.9**). To a solution of (1*R*,4*R*)-4-((Boc-amino)methyl)cyclohexane-1-carboxylic acid (2.15 g, 8.36 mmol) in anhydrous THF (25 mL) stirred under a nitrogen atmosphere were added triethylamine (2.329 mL, 16.71 mmol, 2 equiv) and diphenylphosphonic azide (2.7 ml, 12.53 mmol, 1.5 equiv). The reaction mixture was stirred under reflux for 1 h for full conversion of the starting material to occur. The reaction mixture was cooled down, the solvent was evaporated under vacuum, and the obtained residue was redissolved in a small amount of THF. The obtained solution was poured into a 2M NaOH aq (50 mL) and stirred for 1h at rt. Next EtOAc (75 mL) was added and the aqueous phase was washed thoroughly with EtOAc (3 x 75 mL). The organic phase was dried over anhydrous $MgSO_4$ and concentrated under reduced pressure, washed with a small portion of cold diethyl ether (30 mL) to afford the desired amine as a white solid (1.73 g, 82%). ^{1}H NMR (400 MHz, DMSO) δ 2.81 – 2.67 (m, 3H), 1.91 – 1.78 (m, 2H), 1.70 – 1.58 (m, 2H), 1.37 (s, 9H), 1.30 – 1.08 (m, 3H), 0.94 – 0.78 (m, 2H). ^{13}C NMR (101 MHz, DMSO) δ 155.72, 77.35, 49.51, 45.58, 36.85, 30.67, 28.28, 28.23. UPLC/MS: t_r 1.14 min, *m/z* 229.1 $[M+H]^+$, 457.4 $[2M+H]^+$.

Scheme 5.9. Preparation of amine 5.4g as intermediate in the synthesis of isocyanide 5.6g.[a]

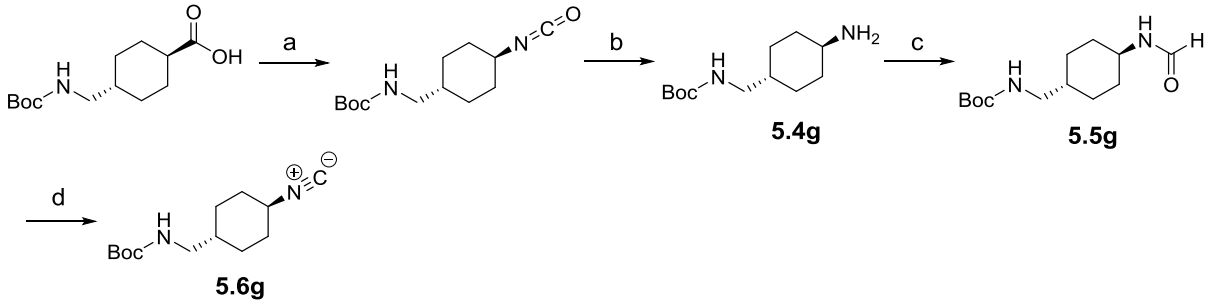

[a]Reagents and conditions: (a) TEA (2 equiv), DPPA (1.5 equiv), THF, reflux, 1 h; (b) NaOH aq (2M), rt, 1 h; (c) ethyl formate, TEA, reflux; (d) $POCl_3$, DIPA, dry DCM, 0°C, 2 h.

2-(2,4-Dichlorophenoxy)ethanamine (5.4h). Amine **5.4h** was obtained in three synthetic steps as presented on **Scheme 5.10**.To a solution of 2,4-dichlorophenol (0.58 g, 3.56 mmol) in DMF (20 mL) were added *N*-Boc-2-bromoethanamine (0.957 g, 4.27 mmol, 1.2 equiv) and K_2CO_3 (0.984 g, 7.12 mmol, 2 equiv). After overnight stirring at 60 °C, the reaction was quenched with water, and the aqueous phase was extracted with EtOAc (3 x 50 mL). The combined organic extract was washed with water (50 mL), then with brine (50 mL), dried over anhydrous $MgSO_4$, and concentrated under reduced pressure to yield the desired product in a form of transparent oil which rapidly crystallized into white solid material (1.02 g, 65.5%). Next, the obtained *N*-Boc-(2-(2,4-dichlorophenoxy) ethaneamine (1 g, 3.27 mmol) was dissolved in 1:1 mixture of TFA and DCM and the reaction mixture was stirred for 1 h at rt. After that time, volatiles were evaporated under reduced pressure affording the title amine (**5.4h**) in quantitative yield in the form of a TFA-salt (1.493 g, 100%). ^{1}H NMR (400 MHz, $CDCl_3$) δ 7.97 (brs, 3H), 7.32 (d, *J* = 2.5 Hz, 1H), 7.16 (dd, *J* = 8.8, 2.5 Hz, 1H), 6.82 (d, *J* = 8.8 Hz, 1H), 4.20 (t, *J* = 5 Hz, 2H), 3.48 – 3.37 (m, 2H). UPLC/MS: t_r 1.43 min, *m/z* 206.0 $[M+H]^+$.

Scheme 5.10. Preparation of amine 5.4h as intermediate in the synthesis of isocyanide 5.6h.[a]

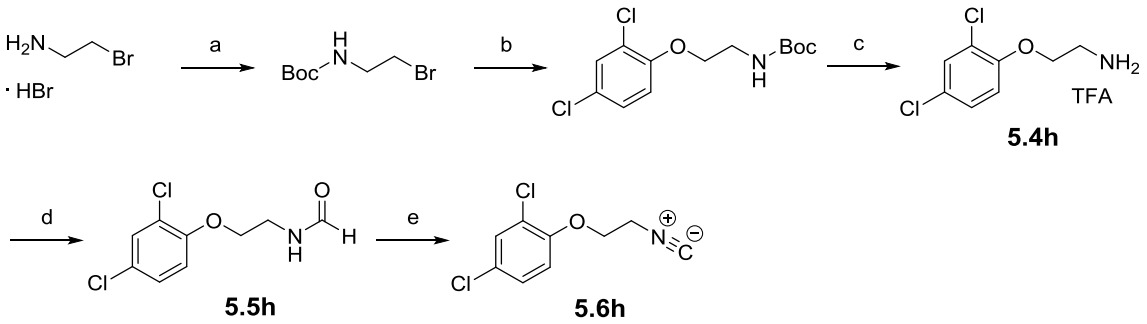

[a]Reagents and conditions: (a) Boc_2O (1.1 equiv), DCM, TEA (2.2 equiv); (b) 2,4-dichlorophenol, K_2CO_3 (2 equiv), DMF, 60 °C; (c) TFA/DCM (1:1), rt, 1 h; (d) ethyl formate, TEA, reflux; (e) $POCl_3$, DIPA, dry DCM, 0 °C, 2 h.

***N*-(4-(2,3-di-Boc-guanidino)benzyl)formamide (5.5a).** The title compound was prepared using the general procedure A to afford a white solid in 68% yield. ^{1}H NMR (400 MHz, $CDCl_3$) δ 11.61 (s, 1H), 10.29 (s, 1H), 8.17 (s, 1H), 7.53 (d, *J* = 8.5 Hz, 2H), 7.22 (d, *J* = 8.4 Hz, 2H), 6.07 (s, 1H), 4.39 (d, *J* = 5.8 Hz, 2H), 1.53 (s, 9H), 1.48 (s, 9H). UPLC/MS: t_r 2.00 min, *m/z* 393.3 $[M+H]^+$.

***N*-(4-(2,3-di-Boc-guanidino)phenethyl)formamide (5.5b).** The title compound was prepared using the general procedure A to afford a white solid in 55% yield. ^{1}H NMR (400 MHz, $CDCl_3$) δ 11.62 (s, 1H), 10.26 (s, 1H), 8.06 (s, 1H), 7.49 (d, *J* = 8.5 Hz, 2H), 7.14 (d, *J* = 8.5 Hz, 2H), 5.82 (brs, 1H), 3.51 (q, *J* = 6.5 Hz, 2H), 2.79 (t, *J* = 6.7 Hz, 2H), 1.53 (s, 9H), 1.49 (s, 9H). UPLC/MS: t_r 2.16 min, *m/z* 407.5 $[M+H]^+$.

***N*-(4-(2,3-di-Boc-guanidino)butyl)formamide (5.5c).** The title compound was prepared using the general procedure A to afford a white solid in 56.7% yield. ^{1}H NMR (400 MHz, $CDCl_3$) δ 11.49 (s, 1H), 8.29 (t, *J* = 5.5 Hz, 1H), 7.99 (s, 1H), 3.31 – 3.22 (m, 2H), 3.15 – 3.02 (m, 2H), 1.55 – 1.30 (m, 22H). UPLC/MS: t_r 1.83 min, *m/z* 359.6 $[M+H]^+$.

***N*-(4-(2-(Boc-amino)ethoxy)phenyl)formamide (5.5d).** The title compound was prepared using the general procedure A to afford a white solid in 90% yield. ^{1}H NMR (400 MHz, DMSO) δ 10.01 (s, 1H), 8.19 (d, *J* = 1.9 Hz, 1H), 7.52 – 7.45 (m, 2H), 6.98 (t, *J* = 5.3 Hz, 1H), 6.93 – 6.85 (m, 2H), 3.91 (t, *J* = 5.9 Hz, 2H), 3.26 (q, *J* = 5.8 Hz, 2H), 1.38 (s, 9H). UPLC/MS: t_r 1.54 min, *m/z* 281.2 $[M+H]^+$, 561.4 $[2M+H]^+$.

***N*-(3,5-Dichloro-4-(2-(Boc-amino)ethoxy)phenyl)formamide (5.5e).** The title compound was prepared using the general procedure A to afford a yellow solid in 72% yield. The product was directly used in the next step, isocyanide synthesis.

***N*-(4-((Boc-amino)methyl)phenyl)formamide (5.5f).** The title compound was prepared using the general procedure A to afford a white solid in 56% yield. ^{1}H NMR (400 MHz, DMSO) δ 10.13 (s, 1H), 8.24 (s, 1H), 7.51 (d, *J* = 8.4 Hz, 2H), 7.32 (brs, 1H), 7.17 (d, *J* = 8.5 Hz, 2H), 4.06 (d, *J* = 6.1 Hz, 2H), 1.38 (s, 9H). UPLC/MS: t_r 1.51 min, *m/z* 251.3 $[M+H]^+$, 501.3 $[2M+H]^+$.

***N*-((1*R*,4*R*)-4-((Boc-amino)methyl)cyclohexyl)formamide (5.5g).** The title compound was prepared using the general procedure A to afford a white solid in 57% yield. ^{1}H NMR (400 MHz, DMSO) δ 7.91 (m, 1H), 6.80 (t, *J* = 5.6 Hz, 1H), 3.60 – 3.40 (m, 1H), 2.75 (t, *J* = 6.3 Hz, 2H), 1.83 – 1.60 (m, 4H), 1.37 (s, 9H), 1.33 – 1.02 (m, 3H), 0.98 – 0.81 (m, 2H). ^{13}C NMR (101 MHz, DMSO) δ 159.98, 155.70, 77.30, 46.55, 45.77, 37.10, 31.86, 28.95, 28.27. UPLC/MS: t_r 1.45 min, *m/z* 257.1 $[M+H]^+$, 513.4 $[2M+H]^+$.

***N*-(2-(2,4-Dichlorophenoxy)ethyl)formamide (5.5h).** The title compound was prepared using the general procedure A to afford a white solid in 62.2% yield. ^{1}H NMR (400 MHz, $CDCl_3$) δ 8.18 (s, 1H), 7.30 (s, 1H), 7.12 (d, *J* = 8.8 Hz, 1H), 6.79 (d, *J* = 8.8 Hz, 1H), 4.03 (t, *J* = 5.1 Hz, 2H), 3.68 (q, *J* = 5.3 Hz, 2H). ^{13}C NMR (101 MHz, $CDCl_3$) δ 161.60, 152.73, 130.00, 127.78, 126.41, 123.70, 114.49, 68.19, 37.37. UPLC/MS: t_r 1.98 min, *m/z* 234.0 $[M+H]^+$, 469.1 $[2M+H]^+$.

1-(4-(Isocyanomethyl)phenyl)-2,3-di-Boc-guanidine (5.6a). The title compound was prepared using the general procedure B to afford a white solid in 85% yield. ^{1}H NMR (400 MHz, $CDCl_3$) δ 11.63 (s, 1H), 10.39 (s, 1H), 7.66 (d, *J* = 8.6 Hz, 2H), 7.29 (d, *J* = 8.7 Hz, 2H), 4.59 (s, 2H), 1.54 (s, 9H), 1.50 (s, 9H). ^{13}C NMR (101 MHz, $CDCl_3$) δ 163.53, 153.61, 153.41, 137.17, 128.53, 127.35, 122.61, 84.01, 79.89, 45.23, 28.28, 28.18. UPLC/MS: t_r 2.44 min, *m/z* 375.2 $[M+H]^+$.

1-(4-(2-Isocyanoethyl)phenyl)-2,3-di-Boc-guanidine (5.6b). The title compound was prepared using the general procedure B to afford a white solid in 63% yield. ^{1}H NMR (400 MHz, $CDCl_3$) δ 11.63 (s, 1H), 10.33 (s, 1H), 7.57 (d, *J* = 8.5 Hz, 2H), 7.18 (d, *J* = 8.5 Hz, 2H), 3.57 (t, *J* = 7.1 Hz, 2H), 2.95 (t, *J* = 7.1 Hz, 2H), 1.53 (s, 9H), 1.50 (s, 9H). UPLC/MS: t_r 2.43 min, *m/z* 389.2 $[M+H]^+$.

1-(4-Isocyanobutyl)-2,3-di-Boc-guanidine (5.6c). The title compound was prepared using the general procedure B to afford a white solid in 65% yield. ^{1}H NMR (400 MHz, $CDCl_3$) δ 11.48 (s, 1H), 8.35 (s, 1H), 3.52 – 3.38 (m, 4H), 1.80 – 1.67 (m, 4H), 1.49 (d, *J* = 1.9 Hz, 18H). UPLC/MS: t_r 2.22 min, *m/z* 341.6 $[M+H]^+$.

2-(4-Isocyanophenoxy)-*N*-Boc-ethanamine (5.6d). The title compound was prepared using the general procedure B to afford a white solid in 70% yield. ^{1}H NMR (400 MHz, $CDCl_3$) δ 7.33 – 7.27 (m, 2H), 6.88 – 6.83 (m, 2H), 4.01 (t, *J* = 5.2 Hz, 2H), 3.53 (q, *J* = 5.3 Hz, 2H), 1.44 (s, 9H). ^{13}C NMR (101 MHz, $CDCl_3$) δ 162.92, 158.99, 155.95, 127.93, 119.91, 115.17, 79.85, 67.66, 40.03, 28.49. UPLC/MS: t_r 1.79 min, *m/z* 263.2 $[M+H]^+$.

2-(2,6-Dichloro-4-isocyanophenoxy)-*N*-Boc-ethanamine (5.6e). The title compound was prepared using the general procedure B to afford a white solid in 73% yield. ^{1}H NMR (400 MHz, $CDCl_3$) δ 7.36 (s, 2H), 4.11 (t, *J* = 5.0 Hz, 2H), 3.54 (q, *J* = 5.2 Hz, 2H), 1.45 (s, 9H).

1-(4-Isocyanophenyl)-*N*-Boc-methanamine (5.6f). The title compound was prepared using the general procedure B to afford a white solid in 68% yield. ^{1}H NMR (400 MHz, $CDCl_3$) δ 7.36 – 7.27 (m, 4H), 4.94 (s, 1H), 4.32 (d, *J* = 5.7 Hz, 2H), 1.45 (s, 9H). ^{13}C NMR (101 MHz, $CDCl_3$) δ 164.14, 155.97, 140.95, 128.32, 126.69, 80.06, 44.14, 28.49. UPLC/MS: t_r 1.84 min, *m/z* 233.0 $[M+H]^+$, 465.2 $[2M+H]^+$.

1-((1*R*,4*R*)-4-Isocyanocyclohexyl)-*N*-Boc-methanamine (5.6g). The title compound was prepared using the general procedure B to afford a white solid in 80% yield. ^{1}H NMR (400 MHz, $CDCl_3$) δ 4.59 (brs, 1H), 3.42 – 3.29 (m, 1H), 2.95 (t, *J* = 6.5 Hz, 2H), 2.22 – 2.11(m, 2H), 1.87 – 1.71 (m, 2H), 1.63 – 1.31 (m, 12H), 1.02 – 0.85 (m, 2H). ^{13}C NMR (101 MHz, $CDCl_3$) δ 156.12, 154.14, 79.38, 52.10, 45.86, 36.99, 32.83, 28.49, 28.22. UPLC/MS: t_r 1.81 min, *m/z* 239.0 $[M+H]^+$, 477.3 $[2M+H]^+$.

2,4-Dichloro-1-(2-isocyanoethoxy)benzene (5.6h). The title compound was prepared using the general procedure B to afford a white solid in 60% yield. ^{1}H NMR (400 MHz, $CDCl_3$) δ 7.39 (d, *J* = 2.5 Hz, 1H), 7.20 (dd, *J* = 8.8, 2.5 Hz, 1H), 6.87 (d, *J* = 8.8 Hz, 1H), 4.21 (t, *J* = 5.6 Hz, 2H), 3.84 (t, *J* = 5.6 Hz, 2H). ^{13}C NMR (101 MHz, $CDCl_3$) δ 159.02, 152.49, 130.52, 127.86, 127.55, 124.79, 115.53, 67.24, 41.28. UPLC/MS: t_r 2.58 min, *m/z* 216.1 $[M+H]^+$.

1-(4-((Imidazo[1,2-*a*]pyridin-3-ylamino)methyl)phenyl)-2,3-di-Boc-guanidine (5.7a). The title compound was prepared according to the general procedure D from pyridin-2-amine, glyoxylic acid monohydrate, isocyanide **5.6a** (0.35 g, 47.5%). ^{1}H NMR (400 MHz, $CDCl_3$) δ 11.61 (s, 1H), 10.32 (s, 1H), 8.24 (d, *J* = 6.9 Hz, 1H), 7.56 (d, *J* = 9.1 Hz, 1H), 7.50 – 7.35 (m, 3H), 7.26 (d, *J* = 8.5 Hz, 2H), 7.05 (td, *J* = 6.9, 1.0 Hz, 1H), 6.83 (s, 1H), 4.20 (s, 2H), 1.54 (s, 9H), 1.43 (s, 9H). ^{13}C NMR (101 MHz, $CDCl_3$) δ 154.39, 138.09, 135.93, 135.14, 132.63, 128.42, 128.19, 123.58, 123.50, 114.55, 114.46, 84.35, 80.14, 49.97, 28.24. UPLC/MS: t_r 1.92 min, *m/z* 481.4 $[M+H]^+$.

1-(4-((Imidazo[1,2-*a*]pyridin-3-ylamino)ethyl)phenyl)-2,3-di-Boc-guanidine (5.7b). The title compound was prepared according to the general procedure D from pyridin-2-amine, glyoxylic acid monohydrate, isocyanide **5.6b** (0.40 g, 64%). UPLC/MS: t_r 2.07 min, *m/z* 495.6 $[M+H]^+$.

1-(4-(Imidazo[1,2-*a*]pyridin-3-ylamino)butyl)-2,3-di-Boc-guanidine (5.7c). The title compound was prepared according to the general procedure D using pyridin-2-amine, glyoxylic acid monohydrate, isocyanide **5.6c** (0.28 g, 42%). ^{1}H NMR (400 MHz, DMSO) δ 11.50 (s, 1H), 8.33 (t, *J* = 5.4 Hz, 1H), 8.13 (d, *J* = 6.9 Hz, 1H), 7.43 (d, *J* = 9.1 Hz, 1H), 7.10 (ddd, *J* = 9.1, 6.6, 1.1 Hz, 1H), 6.95 (s, 1H), 6.87 (td, *J* = 6.8, 1.0 Hz, 1H), 5.40 (t, *J* = 5.6 Hz, 1H), 3.37 – 3.26 (m, 2H), 3.14 – 3.01 (m, 2H), 1.69 – 1.51 (m, 4H), 1.43 (s, 9H), 1.33 (s, 9H). UPLC/MS: t_r 1.76 min, *m/z* 447.6 $[M+H]^+$.

***N*-(4-(2-(Boc-amino)ethoxy)phenyl)imidazo[1,2-*a*]pyridin-3-amine (5.7d).** The title compound was prepared according to the general procedure D using pyridin-2-amine, glyoxylic acid monohydrate, isocyanide **5.6d** (0.42 g, 65%). ^{1}H NMR (400 MHz, $CDCl_3$) δ 7.87 (dt, *J* = 6.8, 1.2 Hz, 1H), 7.62 (dt, *J* = 9.1, 1.1 Hz, 1H), 7.50 (s, 1H), 7.24-7.18 (m, 1H), 6.83 – 6.70 (m, 3H), 6.53 – 6.46 (m, 2H), 5.44 (s, 1H), 4.99 (brs, 1H), 3.93 (t, *J* = 5.1 Hz, 2H), 3.52 – 3.44 (m, 2H), 1.44 (s, 9H). ^{13}C NMR (101 MHz, $CDCl_3$) δ 156.04, 152.72, 142.96, 139.25, 127.65, 125.34, 124.30, 123.10, 117.73, 115.97, 115.06, 112.76, 79.63, 67.89, 40.30, 28.53. UPLC/MS: t_r 1.37 min, *m/z* 369.2 $[M+H]^+$.

***N*-(3,5-Dichloro-4-(2-(Boc-amino)ethoxy)phenyl)imidazo[1,2-*a*]pyridin-3-amine (5.7e).** The title compound was prepared according to the general procedure D using pyridin-2-amine, glyoxylic acid monohydrate, isocyanide **5.6e** (0.26 g, 42%). ^{1}H NMR (400 MHz, $CDCl_3$) δ 7.92 (dt, *J* = 6.8, 1.1 Hz, 1H), 7.69 (d, *J* = 9.1 Hz, 1H), 7.54 (s, 1H), 7.34 – 7.28 (m, 1H), 6.91 (td, *J* = 6.8, 0.9 Hz, 1H), 6.52 (s, 2H), 5.80 (s, 1H), 5.18 (s, 1H), 4.01 (t, *J* = 5.0 Hz, 2H), 3.56 – 3.44 (m, 2H), 1.45 (s, 9H). ^{13}C NMR (101 MHz, $CDCl_3$) δ 156.22, 144.10, 143.91, 142.88, 130.24, 129.99, 125.20, 122.54, 121.73, 118.39, 113.67, 112.94, 79.53, 72.81, 50.92, 28.55. UPLC/MS: t_r 1.55 min, *m/z* 437.1 $[M+H]^+$.

***N*-(4-((Boc-amino)methyl)phenyl)imidazo[1,2-*a*]pyridin-3-amine (5.7f).** The title compound was prepared according to the general procedure D from pyridin-2-amine, glyoxylic acid monohydrate, isocyanide **5.6f** (0.40g, 66%). ^{1}H NMR (400 MHz, DMSO) δ 8.00 (s, 1H), 7.95 (d, *J* = 6.8 Hz, 1H), 7.60 (dt, *J* = 9.1, 1.0 Hz, 1H), 7.51 (s, 1H), 7.30 (ddd, *J* = 9.1, 6.7, 1.2 Hz, 1H), 7.23 (t, *J* = 6.0 Hz, 1H), 7.02 (d, *J* = 8.4 Hz, 2H), 6.95 (td, *J* = 6.8, 1.0 Hz, 1H), 6.50 (d, *J* = 8.4 Hz, 2H), 3.98 (d, *J* = 6.1 Hz, 2H), 1.37 (s, 9H). ^{13}C NMR (101 MHz, DMSO) δ 155.68, 144.59, 141.71, 128.28, 126.21, 124.71, 124.10, 123.17, 117.04, 113.08, 112.37, 77.58, 42.91, 28.26. UPLC/MS: t_r 1.38 min, *m/z* 339.1 $[M+H]^+$.

***N*-((1*R*,4*R*)-4-((Boc-amino)methyl)cyclohexyl)imidazo[1,2-*a*]pyridin-3-amine (5.7g**). The title compound was prepared according to the general procedure D from pyridin-2-amine, glyoxylic acid monohydrate, isocyanide **5.6g** (0.26 g, 43%). ^{1}H NMR (400 MHz, $CDCl_3$) δ 8.19 (d, *J* = 6.9 Hz, 1H), 7.68 (d, *J* = 9.1 Hz, 1H), 7.42 – 7.33 (m, 1H), 7.23 (s, 1H), 7.02 (t, *J* = 6.8 Hz, 1H), 4.62 (brs, 1H), 3.03 – 2.89 (m, 3H), 2.13 – 2.04 (m, 2H), 1.86 – 1.76 (m, 2H), 1.44 (s, 9H), 1.36 – 1.22 (m, 3H), 1.07 – 0.92 (m, 2H). ^{13}C NMR (101 MHz, $CDCl_3$) δ 156.22, 140.85, 130.18, 125.13, 122.87, 116.55, 112.71, 79.26, 56.63, 46.43, 37.95, 33.16, 29.28, 28.54. UPLC/MS: t_r 1.42 min, *m/z* 345.2 $[M+H]^+$.

***N*-(2-(2,4-Dichlorophenoxy)ethyl)imidazo[1,2-*a*]pyridin-3-amine (5.7h).** The title compound was prepared according to the general procedure D from pyridin-2-amine, glyoxylic acid monohydrate, isocyanide **5.6h**, yielding a yellow solid (0.25 g, 38%), mp 98-100 °C. ^{1}H NMR (400 MHz, $CDCl_3$) δ 8.03 (d, *J* = 6.9 Hz, 1H), 7.55 (d, *J* = 9.1 Hz, 1H), 7.40 (d, *J* = 2.5 Hz, 1H), 7.23 –7.17 (m, 2H), 7.15 – 7.08 (m, 1H), 6.88 (d, *J* = 8.8 Hz, 1H), 6.80 (td, *J* = 6.8, 0.9 Hz, 1H), 4.21 (t, *J* = 5.1 Hz, 2H), 3.60 – 3.51 (m, 2H). ^{13}C NMR (101 MHz, $CDCl_3$) δ 152.86, 137.39, 132.91, 130.18, 129.52, 127.99, 126.65, 124.04, 123.65, 115.18, 114.59, 114.02, 68.96, 46.18. UPLC/MS: t_r 1.85 min, *m/z* 322.1 $[M+H]^+$, purity: 98%. HRMS: mass calculated for $C_{15}H_{14}N_3OCl_2$: 322.0514; found: 322.0514.

1-(4-((Imidazo[1,2-*a*]pyridin-3-ylamino)methyl)phenyl)guanidine (5.8a). Boc deprotection of compound **5.7a** was done using the general procedure E to afford the title compound **(5.8a)** as a yellow oil (0.12 g, 98%). ^{1}H NMR (400 MHz, DMSO) δ 9.98 (s, 1H), 8.63 (d, *J* = 6.9 Hz, 1H), 7.89 – 7.75 (m, 2H), 7.59 – 7.42 (m, 7H), 7.32 (s, 1H), 7.23 (d, *J* = 8.4 Hz, 2H), 4.41 (s, 2H). ^{13}C NMR (101 MHz, DMSO) δ 155.86, 136.50, 135.53, 134.50, 133.91, 131.08, 128.89, 124.44, 124.39, 115.90, 112.37, 47.46. UPLC/MS: t_r 0.27 min, *m/z* 281.2 $[M+H]^+$, purity: 96%. HRMS: mass calculated for $C_{15}H_{17}N_6$: 281.1515; found: 281.1524.

1-(4-(2-(Imidazo[1,2-*a*]pyridin-3-ylamino)ethyl)phenyl)guanidine (5.8b). Boc deprotection of compound **5.7b** was done using the general procedure E to afford the title compound **(5.8b)** as an orange oil (0.09 g, 97%). ^{1}H-NMR (400 MHz, DMSO) δ 9.85 (s, 1H), 8.54 (d, *J* = 6.93, 1H), 7.86 – 7.76 (m, 2H), 7.50 (s, 1H), 7.47 – 7.43 (m, 4H), 7.41 (d, *J* = 8.37, 2H), 7.19 (d, *J* = 8.37, 2H), 6.39 (brs, 1H),

3.39 (t, *J* = 7.3 Hz, 2H), 2.97 (t, *J* = 7.4 Hz, 2H). ^{13}C NMR (101 MHz, DMSO) δ 155.96, 144.01, 137.64, 135.53, 134.14, 133.54, 130.92, 130.11, 124.58, 124.26, 115.80, 112.36, 101.40, 46.18, 34.12. UPLC/MS: t_r 0.28 min, *m/z* 295.3 $[M+H]^+$, purity: 95%. HRMS: mass calculated for $C_{16}H_{19}N_6$: 295.1671; found: 295.1679.

1-(4-(Imidazo[1,2-*a*]pyridin-3-ylamino)butyl)guanidine (5.8c). Boc deprotection of compound **5.7c** was done using the general procedure E to afford the title compound **(5.8c)** as an orange oil (0.10 g, 96%). ^{1}H NMR (400 MHz, DMSO) δ 8.57 (d, *J*=6.90 Hz, 1H), 7.96 – 7.67 (m, 4H), 7.44 (td, *J* = 6.9, 1.2 Hz, 1H), 7.41 (s, 1H), 6.26 (s, 1H), 3.21 – 3.04 (m, 5H), 1.72 – 1.53 (m, 4H). ^{13}C NMR (101 MHz, DMSO) δ 156.93, 135.46, 134.44, 130.85, 124.30, 115.71, 112.32, 100.88, 45.72, 44.26, 26.07, 25.59. UPLC/MS: t_r 0.27 min, *m/z* 247.2 $[M+H]^+$, purity: 90%. HRMS: mass calculated for $C_{12}H_{19}N_6$: 247.1671; found: 247.1662.

***N*-(4-(2-Aminoethoxy)phenyl)imidazo[1,2-*a*]pyridin-3-amine (5.8d).** Boc deprotection of compound **5.7d** was done using the general procedure E to afford the title compound **(5.8d)** as a yellow oil (0.11 g, 100%). ^{1}H NMR (400 MHz, DMSO) δ 8.43 (d, *J* = 6.8 Hz, 1H), 8.11 (brs, 3H), 8.08 (s, 1H), 8.02 (d, *J* = 9.1 Hz, 1H), 7.97 – 7.89 (m, 1H), 7.48 (t, *J* = 6.4 Hz, 1H), 6.89 (d, *J* = 9.0 Hz, 2H), 6.80 (d, *J* = 9.0 Hz, 2H), 4.08 (t, *J* = 5.1 Hz, 2H), 3.20 (q, *J* = 5.1 Hz, 2H). ^{13}C NMR (101 MHz, DMSO) δ 152.06, 138.21, 137.50, 132.85, 127.05, 125.06, 116.77, 116.05, 115.84, 114.56, 112.95, 64.95, 30.71. UPLC/MS: t_r 0.18 min, *m/z* 269.0 $[M+H]^+$, purity: 97%. HRMS: mass calculated for $C_{15}H_{17}N_4O$: 269.1402; found: 269.1408.

***N*-(4-(2-Aminoethoxy)-3,5-dichlorophenyl)imidazo[1,2-*a*]pyridin-3-amine (5.8e).** Boc deprotection of compound **5.7e** was done using the general procedure E to afford the title compound **(5.8e)** as a white solid (0.12 g, 97%), mp 195-197 °C. ^{1}H NMR (400 MHz, MeOD) δ 8.47 (dt, *J* = 6.9, 1.1 Hz, 1H), 8.07 – 7.95 (m, 3H), 7.52 (td, *J* = 6.7, 1.4 Hz, 1H), 6.87 (s, 2H), 4.18 (t, *J* = 5.1, 2H), 3.38 (t, *J* = 5.0, 2H). ^{13}C NMR (101 MHz, MeOD) δ 144.91, 143.93, 140.06, 135.18, 131.21, 126.57, 126.17, 118.66, 118.58, 115.50, 113.92, 70.17, 40.97. UPLC/MS: t_r 0.24 min, *m/z* 337.0 $[M+H]^+$, purity: 99%. HRMS: mass calculated for $C_{15}H_{15}N_4OCl_2$: 337.0623; found: 337.0623.

***N*-(4-(Aminomethyl)phenyl)imidazo[1,2-*a*]pyridin-3-amine (5.8f).** Boc deprotection of compound **5.7f** was done using the general procedure E to afford the title compound **(5.8f)** as a colorless oil (0.26 g, 95%). ^{1}H NMR (400 MHz, DMSO) δ 8.73 (s, 1H), 8.39 (dt, *J* = 6.8, 1.0 Hz, 1H), 8.24 – 8.10 (m, 4H), 8.05 (dt, *J* = 9.1, 1.0 Hz, 1H), 7.97 (ddd, *J* = 9.0, 6.9, 1.1 Hz, 1H), 7.49 (td, *J* = 6.9, 1.1 Hz, 1H), 7.30 (d, *J* = 8.6 Hz, 2H), 6.82 (d, *J* = 8.6 Hz, 2H), 3.93 (q, *J* = 5.5 Hz, 2H). ^{13}C NMR (101 MHz, DMSO) δ 144.75, 137.91, 133.10, 130.49, 125.47, 125.20, 124.99, 116.90, 116.47, 114.08, 113.10, 41.93. UPLC/MS: t_r 0.22 min, *m/z* 239.1 $[M+H]^+$, purity: 97%. HRMS: mass calculated for $C_{14}H_{15}N_4$: 239.1297; found: 239.1292.

***N*-((1*R*,4*R*)-4-(Aminomethyl)cyclohexyl)imidazo[1,2-*a*]pyridin-3-amine (5.8g).** Boc deprotection of compound **5.7g** was done using the general procedure E to afford the title compound **(5.8g)** as an orange oil (0.10 g, 98%). ^{1}H NMR (400 MHz, DMSO) δ 8.60 (d, *J* = 6.9 Hz, 1H), 8.04 – 7.82 (m, 5H), 7.81 – 7.74 (m, 1H), 7.52 (s, 1H), 7.43 (t, *J* = 6.8 Hz, 1H), 3.22 – 3.03 (m, 1H), 2.80 – 2.59 (m, 2H), 2.22 – 2.02 (m, 2H), 1.92 – 1.72 (m, 2H), 1.66 – 1.50 (m, 1H), 1.35 – 1.19 (m, 2H), 1.15 – 0.97 (m, 2H). ^{13}C NMR (101 MHz, DMSO) δ 135.49, 133.05, 130.92, 124.43, 115.75, 112.27, 102.65, 53.49, 44.14, 35.17, 31.49, 28.42. UPLC/MS: t_r 0.25 min, *m/z* 245.0 $[M+H]^+$, 489.3 $[2M+H]^+$, purity: 98%. HRMS: mass calculated for $C_{14}H_{21}N_4$: 245.1766; found: 245.1775.

1,2-Di-Boc-3-(4-(((2-(pyridin-3-yl)imidazo[1,2-*a*]pyridin-3-yl)amino)methyl)phenyl)guanidine (5.9a). The title compound was prepared using general procedure D from pyridin-2-amine, nicotinaldehyde, isocyanide **5.6a** (0.67 g, 72%). ^{1}H NMR (400 MHz, DMSO) δ 11.40 (s, 1H), 9.96 (s, 1H), 9.30 (d, *J* = 1.4 Hz, 1H), 8.48 (dd, *J* = 4.7, 1.4 Hz, 1H), 8.40 (d, *J* = 8.0 Hz, 1H), 8.24 (d, *J* = 6.8 Hz, 1H), 7.54 – 7.38 (m, 4H), 7.28 (d, *J* = 8.3 Hz, 2H), 7.19 (t, *J* = 8.1 Hz, 1H), 6.87 (t, *J* = 6.5 Hz, 1H), 5.45 (t, *J* = 6.2 Hz, 1H), 4.09 (d, *J* = 6.1 Hz, 2H), 1.50 (s, 9H), 1.40 (s, 9H). ^{13}C NMR (101 MHz, DMSO) δ 152.80, 147.71, 147.62, 140.94, 136.23, 135.62, 133.47, 131.87, 130.33, 128.49, 127.21, 124.37, 123.56, 123.37, 122.49, 116.91, 111.64, 83.38, 78.83, 50.76, 27.87, 27.69. UPLC/MS: t_r 1.84 min, *m/z* 558.5 $[M+H]^+$.

1,2-Di-Boc-3-(4-(((2-(4-ethylphenyl)imidazo[1,2-*a*]pyridin-3-yl)amino)methyl)phenyl)guanidine (5.9b). The title compound was prepared according to the general procedure D from pyridin-2-amine, 4-ethylbenzaldehyde, isocyanide **5.6a** (0.50 g, 82%). ^{1}H NMR (400 MHz, DMSO) δ 11.41 (s, 1H), 9.97 (s, 1H), 8.20 (d, *J* = 6.9 Hz, 1H), 8.06 (d, *J* = 8.2 Hz, 2H), 7.55 – 7.37 (m, 3H), 7.38 – 7.21 (m, 4H), 7.18 – 7.09 (m, 1H), 6.82 (td, *J* = 6.8, 1.0 Hz, 1H), 5.27 (t, *J* = 6.2 Hz, 1H), 4.06 (d, *J* = 6.2 Hz, 2H), 2.64 (q, *J* = 7.6 Hz, 2H), 1.51 (s, 9H), 1.40 (s, 9H), 1.22 (t, *J* = 7.6 Hz, 3H). ^{13}C NMR (101 MHz, DMSO) δ 162.69, 152.83, 142.41, 140.38, 136.47, 135.57, 134.53, 132.04, 128.48, 127.75, 126.58, 126.13, 123.70, 123.10, 122.51, 116.65, 111.24, 83.42, 78.82, 50.73, 27.98, 27.92, 27.67, 15.55. UPLC/MS: t_r 2.12 min, *m/z* 585.6 $[M+H]^+$.

1-(4-(((2-Benzylimidazo[1,2-*a*]pyridin-3-yl)amino)methyl)phenyl)-2,3-di-Boc-guanidine (5.9c). The title compound was prepared according to the general procedure D from pyridin-2-amine, 2-phenylacetaldehyde, isocyanide **5.6a** (0.40 g, 60%). ^{1}H NMR (400 MHz, DMSO) δ 11.41 (s, 1H), 9.97 (s, 1H), 8.14 (d, *J* = 6.8 Hz, 1H), 7.45 (d, *J* = 8.4 Hz, 2H), 7.38 – 7.18 (m, 7H), 7.17 – 7.04 (m, 2H), 6.81 (td, *J* = 6.7, 1.1 Hz, 1H), 5.13 (t, *J* = 6.4 Hz, 1H), 3.99 (d, *J* = 6.5 Hz, 2H), 3.90 (s, 2H), 1.51 (s, 9H), 1.40 (s, 9H). ^{13}C NMR (101 MHz, DMSO) δ 152.82, 140.63, 140.09, 136.35, 135.54, 128.79, 128.55, 128.03, 126.45, 125.62, 122.85, 122.64, 122.47, 116.40, 110.94, 83.39, 78.80, 51.12, 32.70, 27.90, 27.66. UPLC/MS: t_r 1.94 min, *m/z* 571.5 $[M+H]^+$.

1,2-Di-Boc-3-(4-(((2-ethylimidazo[1,2-*a*]pyridin-3-yl)amino)methyl)phenyl)guanidine (5.9d). The title compound was prepared according to the general procedure D from pyridin-2-amine, propionaldehyde, isocyanide **5.6a** (0.30 g, 49%). ^{1}H NMR (400 MHz, DMSO) δ 11.40 (s, 1H), 9.97 (s, 1H), 8.12 (d, *J* = 6.8 Hz, 1H), 7.46 (d, *J* = 8.2 Hz, 2H), 7.38 – 7.24 (m, 3H), 7.13 – 7.00 (m, 1H), 6.79 (t, *J* = 6.7 Hz, 1H), 5.03 (t, *J* = 6.4 Hz, 1H), 4.03 (d, *J* = 6.2 Hz, 2H), 2.54 (q, *J* = 7.6 Hz, 2H), 1.50 (s, 9H), 1.39 (s, 9H), 1.11 (t, *J* = 7.6 Hz, 3H). UPLC/MS: t_r 1.96 min, *m/z* 509.5 $[M+H]^+$.

1,2-Di-Boc-3-(4-(((2-((Boc-amino)methyl)imidazo[1,2-*a*]pyridin-3-yl)amino)methyl)phenyl) guanidine (5.9e). The title compound was prepared according to the general procedure D from pyridin-2-amine, 2-(Boc-amino)acetaldehyde, isocyanide **5.6a** (0.21 g, 32%). ^{1}H NMR (400 MHz, $CDCl_3$) δ 11.62 (s, 1H), 10.34 (s, 1H), 8.00 (d, *J* = 6.8 Hz, 1H), 7.57 (d, *J* = 8.5 Hz, 2H), 7.50 (d, *J* = 9.0 Hz, 1H), 7.25 – 7.14 (m, 3H), 6.82 (t, *J* = 6.7 Hz, 1H), 5.43 – 5.22 (m, 1H), 4.54 – 4.33(m, 1H), 4.17 (d, *J* = 6.1 Hz, 2H), 4.10 (d, *J* = 6.5 Hz, 2H), 1.54 (s, 9H), 1.50 (s, 9H), 1.39 (s, 9H). UPLC/MS: t_r 2.02 min, *m/z* 610.7 $[M+H]^+$.

1-(4-(((2-(3-Chlorobenzyl)imidazo[1,2-*a*]pyridin-3-yl)amino)methyl)phenyl)-2,3-di-Boc-guanidine (5.9f). The title compound was prepared according to the general procedure D from pyridin-2-amine, 2-(3-chlorophenyl)acetaldehyde, isocyanide **5.6a** (0.14 g, 22%). ^{1}H NMR (400 MHz, $CDCl_3$) δ 11.61 (s, 1H), 10.33 (s, 1H), 8.09 (d, *J* = 7.0 Hz, 1H), 7.63 – 7.50 (m, 3H), 7.37 – 7.30 (m, 1H), 7.23 – 7.06 (m, 7H), 6.96 (t, *J* = 6.7 Hz, 1H), 4.04 – 3.91 (m, 4H), 3.31 (s, 1H), 1.54 (s, 9H), 1.49 (s, 9H). UPLC/MS: t_r 2.15 min, *m/z* 605.7 $[M+H]^+$.

1-(4-(((2-(1-Boc-piperidin-4-yl)imidazo[1,2-*a*]pyridin-3-yl)amino)methyl)phenyl)-2,3-di-Boc-guanidine (5.9g). The title compound was prepared according to the general procedure D from pyridin-2-amine, 1-Boc-piperidine-4-carbaldehyde, isocyanide **5.6a** (0.35 g, 72%). ^{1}H NMR (400 MHz, $CDCl_3$) δ 11.62 (s, 1H), 10.34 (s, 1H), 8.05 (d, *J* = 6.4 Hz, 1H), 7.82 – 7.66 (m, 1H), 7.63 – 7.55 (m, 2H), 7.29 – 7.20 (m, 3H), 6.97 – 6.82 (m, 1H), 4.10 (d, *J* = 6.4 Hz, 2H), 3.42 – 3.18 (m, 1H), 2.93 – 2.62 (m, 2H), 2.02 – 1.82 (m, 2H), 1.76 – 1.65 (m, 2H), 1.61 – 1.41 (m, 29H). UPLC/MS: t_r 2.16 min, *m/z* 664.8 $[M+H]^+$.

1-(4-(((2-(3,5-Dichlorophenyl)imidazo[1,2-*a*]pyridin-3-yl)amino)methyl)phenyl)-2,3-di-Boc-guanidine (5.9h). The title compound was prepared according to the general procedure D from pyridin-2-amine, 3,5-dichlorobenzaldehyde, isocyanide **5.6a** (0.42 g, 86%). ^{1}H NMR (400 MHz, $CDCl_3$) δ 11.61 (s, 1H), 10.32 (s, 1H), 8.12 – 8.02 (m, 1H), 7.96 (d, *J* = 1.9 Hz, 2H), 7.66 – 7.59 (m, 1H), 7.55 – 7.48 (m, 2H), 7.30 – 7.18 (m, 4H), 6.87 (t, *J* = 6.5 Hz, 1H), 4.15 – 4.08 (m, 2H), 1.54 (s, 9H), 1.50 (s, 9H). UPLC/MS: t_r 2.29 min, *m/z* 625.6 $[M+H]^+$.

1,2-Di-Boc-3-(4-(((2-phenylimidazo[1,2-*a*]pyridin-3-yl)amino)methyl)phenyl)guanidine (5.9i). The title compound was prepared according to the general procedure D from pyridin-2-amine, benzaldehyde, isocyanide **5.6a** (0.14 g, 34%). ^{1}H NMR (400 MHz, $CDCl_3$) δ 11.61 (s, 1H), 10.30 (s, 1H), 8.13 (d, *J* = 6.6 Hz, 1H), 8.06 – 8.00 (m, 2H), 7.94 (brs, 1H), 7.86 – 7.73 (m, 1H), 7.55 – 7.41 (m, 4H), 7.40 – 7.32 (m, 2H), 7.20 (d, *J* = 8.2 Hz, 2H), 7.01 – 6.92 (m, 1H), 4.15 (d, *J* = 5.2 Hz, 2H), 1.54 (s, 9H), 1.50 (s, 9H). UPLC/MS: t_r 2.08 min, *m/z* 557.5 $[M+H]^+$.

1-(4-(((2-(3-Fluorophenyl)imidazo[1,2-*a*]pyridin-3-yl)amino)methyl)phenyl)-2,3-di-Boc-guanidine (5.9j). The title compound was prepared according to the general procedure D from pyridin-2-amine, 3-fluorobenzaldehyde, isocyanide **5.6a** (0.36 g, 75%). ^{1}H NMR (400 MHz, $CDCl_3$) δ 11.63 (s, 1H), 10.32 (s, 1H), 8.01 (d, *J* = 6.8 Hz, 1H), 7.83 – 7.72 (m, 2H), 7.65 – 7.51(m, 3H), 7.45 – 7.36 (m, 1H), 7.28 (d, *J* = 8.4 Hz, 2H), 7.18 (ddd, *J* = 8.9, 6.7, 1.1 Hz, 1H), 7.02 (tdd, *J* = 8.4, 2.6, 0.9 Hz, 1H), 6.80 (td, *J* = 6.8, 0.9 Hz, 1H), 4.15 (d, *J* = 6.1 Hz, 2H), 3.57 (s, 1H), 1.54 (s, 9H), 1.51 (s, 9H). ^{13}C NMR (101 MHz, $CDCl_3$) δ 163.63, 163.3 (d, *J* = 242.4 Hz), 153.68, 153.46, 136.54, 135.17, 130.38 (d, *J* = 8.5 Hz), 128.83, 126.13, 122.70 (d, *J* = 6.3 Hz), 122.64 (d, *J* = 6.1 Hz), 122.61, 117.24, 114.67 (d, *J* = 21.5 Hz), 114.02 (d, *J* = 23.1 Hz), 112.62, 83.97, 79.86, 52.01, 28.34, 28.23. UPLC/MS: t_r 1.97 min, *m/z* 575.6 $[M+H]^+$.

1-(4-(((2-(4-Fluorophenyl)imidazo[1,2-*a*]pyridin-3-yl)amino)methyl)phenyl)-2,3-di-Boc-guanidine (5.9k). The title compound was prepared according to the general procedure D from pyridin-2-amine, 4-fluorobenzaldehyde, isocyanide **5.6a** (0.27 g, 63%). ^{1}H NMR (400 MHz, DMSO) δ 11.41 (s, 1H), 9.96 (s, 1H), 8.25 – 8.12 (m, 3H), 7.50 – 7.40 (m, 3H), 7.34 – 7.22 (m, 4H), 7.16 (ddd, *J* = 9.0, 6.6, 1.2 Hz, 1H), 6.84 (td, *J* = 6.8, 1.1 Hz, 1H), 5.32 (t, *J* = 6.2 Hz, 1H), 4.06 (d, *J* = 6.2 Hz, 2H), 1.51 (s, 9H), 1.40 (s, 9H). ^{13}C NMR (101 MHz, DMSO) δ 161.30 (d, *J* = 243.9 Hz), 152.83, 152.18, 140.46, 136.35, 135.59, 133.61, 131.07 (d, *J* = 3.0 Hz), 128.50, 128.46 (d, *J* = 9.1 Hz), 126.19, 123.98, 123.25, 122.55, 116.72, 115.17 (d, *J* = 21.1 Hz), 111.37, 83.39, 78.80, 50.69, 27.90, 27.66. UPLC/MS: t_r 1.97 min, *m/z* 575.6 $[M+H]^+$.

1-(4-(((2-(Pyridin-3-yl)imidazo[1,2-*a*]pyridin-3-yl)amino)methyl)phenyl)guanidine (5.10a). Boc deprotection of compound **5.9a** was done using the general procedure E to afford the title compound **(5.10a)** as a yellow solid (0.30 g, 95%), mp 146 °C. ^{1}H NMR (400 MHz, DMSO) δ 10.01 (s, 1H), 9.07 (d, *J* = 1.8 Hz, 1H), 8.68 (dd, *J* = 5.0, 1.5 Hz, 1H), 8.64 (d, *J* = 6.8 Hz, 1H), 8.39 (d, *J* = 8.1 Hz, 1H), 7.91 – 7.73 (m, 2H), 7.72 – 7.65 (m, 1H), 7.57 (brs, 4H), 7.39 (t, *J* = 6.8 Hz, 1H), 7.29 (d, *J* = 8.4 Hz, 2H), 7.08 (d, *J* = 8.3 Hz, 2H), 4.17 (s, 2H). ^{13}C NMR (101 MHz, DMSO) δ 155.85, 147.87, 146.29, 138.05, 137.09, 136.25, 134.51, 131.44, 129.46, 128.29, 125.03, 124.52, 124.15, 115.65, 113.47, 50.10. UPLC/MS: t_r 0.23 min, *m/z* 358.4 $[M+H]^+$, purity: 99%. HRMS: mass calculated for $C_{20}H_{20}N_7$: 358.1780; found: 358.1778.

1-(4-(((2-(4-Ethylphenyl)imidazo[1,2-*a*]pyridin-3-yl)amino)methyl)phenyl)guanidine (5.10b). Boc deprotection of compound **5.9b** was done using the general procedure E to afford the title compound **(5.10b)** as a yellow solid (0.10 g, 98%), mp 165-166 °C. ^{1}H NMR (400 MHz, DMSO) δ 10.01 (s, 1H), 8.68 (d, *J* = 6.8 Hz, 1H), 7.92 – 7.82 (m, 4H), 7.54 (brs, 4H), 7.49 – 7.40 (m, 3H), 7.33 (d, *J* = 8.4 Hz, 2H), 7.12 (d, *J* = 8.4 Hz, 2H), 5.98 (brs, 1H), 4.16 (s, 2H), 2.70 (q, *J* = 7.6 Hz, 2H), 1.24 (t, *J* = 7.6 Hz, 3H). ^{13}C NMR (101 MHz, DMSO) δ 155.85, 145.61, 137.07, 136.54, 134.55, 132.63, 129.37, 128.51, 127.35, 127.11, 125.58, 125.19, 124.50, 124.10, 116.44, 112.13, 49.96, 28.03, 15.39. UPLC/MS: t_r 1.12 min, *m/z* 385.5 $[M+H]^+$, 769.8 $[2M+H]^+$, purity > 99%. HRMS: mass calculated for $C_{23}H_{25}N_6$: 385.2141; found: 385.2139.

1-(4-(((2-Benzylimidazo[1,2-*a*]pyridin-3-yl)amino)methyl)phenyl)guanidine (5.10c).
Boc deprotection of compound **5.9c** was done using the general procedure E to afford the title compound **(5.10c)** as a white solid (0.31 g, 100%), mp 110 °C. ^{1}H NMR (400 MHz, DMSO) δ 10.15 (s, 1H), 8.64 (d, *J* = 6.8 Hz, 1H), 7.92 – 7.79 (m, 2H), 7.64 (brs, 4H), 7.47 (td, *J* = 6.8, 1.4 Hz, 1H), 7.41 (d, *J* = 8.4 Hz, 2H), 7.37 – 7.12 (m, 7H), 4.18 (s, 2H), 4.07 (s, 2H). ^{13}C NMR (101 MHz, DMSO) δ 155.90, 137.38, 137.15, 136.28, 134.64, 132.44, 129.51, 128.67, 128.61, 128.34, 126.89, 125.71, 125.25, 124.19, 116.48, 111.97, 50.30, 29.11. UPLC/MS: t_r 0.97 min, *m/z* 371.4 $[M+H]^+$, purity > 99%. HRMS: mass calculated for $C_{22}H_{23}N_6$: 371.1984; found: 371.1978.

1-(4-(((2-Ethylimidazo[1,2-*a*]pyridin-3-yl)amino)methyl)phenyl)guanidine (5.10d). Boc deprotection of compound **5.9d** was done using the general procedure E, affording the title compound **(5.10d)** as a colorless oil (0.10 g, 98%). ^{1}H NMR (400 MHz, DMSO) δ 10.01 (s, 1H), 8.62 (d, *J* = 6.8 Hz, 1H), 7.90 – 7.82 (m, 2H), 7.54 (brs, 4H), 7.49 – 7.43 (m, 1H), 7.40 (d, *J* = 8.4 Hz, 2H), 7.19 (d, *J* = 8.4 Hz, 2H), 5.78 (brs, 1H), 4.17 (s, 2H), 2.64 (q, *J* = 7.6 Hz, 2H), 1.12 (t, *J* = 7.6 Hz, 3H). ^{13}C NMR (101 MHz, DMSO) δ 155.88, 137.50, 135.97, 134.59, 132.08, 129.56, 128.97, 126.98, 125.01, 124.14, 116.39, 111.84, 50.37, 16.82, 12.93. UPLC/MS: t_r 0.24 min, *m/z* 309.4 $[M+H]^+$, purity: 96%. HRMS: mass calculated for $C_{17}H_{21}N_6$: 309.1828; found: 309.1812.

1-(4-(((2-(Aminomethyl)imidazo[1,2-*a*]pyridin-3-yl)amino)methyl)phenyl)guanidine (5.10e). Boc deprotection of compound **5.9e** was done using the general procedure E, affording the title compound **(5.10e)** as an orange oil (0.08 g, 94%). ^{1}H NMR (400 MHz, MeOD) δ 8.18 (dt, *J* = 6.9, 1.2 Hz, 1H), 7.48 (dt, *J* = 9.1, 1.1 Hz, 1H), 7.44 (d, *J* = 8.5 Hz, 2H), 7.31 (ddd, *J* = 9.1, 6.7, 1.3 Hz, 1H), 7.24 (d, *J* = 8.5 Hz, 2H), 6.93 (td, *J* = 6.8, 1.1 Hz, 1H), 4.23 (s, 2H), 4.06 (s, 2H). ^{13}C NMR (101 MHz, DMSO) δ 155.97, 137.57, 137.26, 134.71, 131.03, 130.08, 129.50, 124.85, 124.23, 115.51, 113.54, 50.18, 48.62. UPLC/MS: t_r 0.16 min, *m/z* 310.3 $[M+H]^+$, purity: 97%. HRMS: mass calculated for $C_{16}H_{20}N_7$: 310.1780; found: 310.1775.

1-(4-(((2-(3-Chlorobenzyl)imidazo[1,2-*a*]pyridin-3-yl)amino)methyl)phenyl)guanidine (5.10f). Boc deprotection of compound **5.9f** was done using the general procedure E, affording the title compound **(5.10f)** as an orange oil (0.09 g, 97%). ^{1}H NMR (400 MHz, MeOD) δ 8.61 (d, *J* = 6.8 Hz, 1H), 7.93 – 7.83 (m, 1H), 7.74 (d, *J* = 9.0 Hz, 1H), 7.51 – 7.39 (m, 3H), 7.36 – 7.07 (m, 6H), 4.27 (s, 2H), 4.09 (s, 2H). ^{13}C NMR (101 MHz, MeOD) δ 158.01, 140.11, 139.93, 138.63, 135.75, 135.67, 134.05, 131.47, 131.01, 129.90, 129.73, 128.45, 128.17, 128.05, 126.43, 126.27, 117.80, 112.98, 51.99, 30.33. UPLC/MS: t_r 1.24 min, *m/z* 405.4 $[M+H]^+$, purity: 98%. HRMS: mass calculated for $C_{22}H_{22}N_6Cl$: 405.1594; found: 405.1602.

1-(4-(((2-(Piperidin-4-yl)imidazo[1,2-*a*]pyridin-3-yl)amino)methyl)phenyl)guanidine (5.10g). Boc deprotection of compound **5.9g** was done using the general procedure E, affording the title compound **(5.10g)** as a white solid (0.25 g, 94%), mp 108 °C. ^{1}H NMR (400 MHz, DMSO) δ 10.28 (s, 1H), 9.13 – 8.94 (m, 1H), 8.80 – 8.63 (m, 1H), 8.60 (d, *J* = 6.8 Hz, 1H), 7.94 – 7.79 (m, 2H), 7.67 (brs, 4H), 7.50 – 7.35 (m, 3H), 7.19 (d, *J* = 8.2 Hz, 2H), 4.18 (s, 2H), 3.46 – 3.29 (m, 2H), 3.17 – 3.02 (m, 1H), 3.00 – 2.84 (m, 2H), 1.99 – 1.79 (m, 2H), 1.75 – 1.59 (m, 2H). ^{13}C NMR (101 MHz, DMSO) δ 155.95, 137.42, 136.72, 134.63, 129.77, 126.92, 125.01, 124.17, 116.22, 112.38, 50.41, 43.03, 29.91, 27.41. UPLC/MS: t_r 0.23 min, *m/z* 364.4 $[M+H]^+$, purity > 99%. HRMS: mass calculated for $C_{20}H_{26}N_7$: 364.2250; found: 364.2242.

1-(4-(((2-(3,5-Dichlorophenyl)imidazo[1,2-*a*]pyridin-3-yl)amino)methyl)phenyl)guanidine (5.10h). Boc deprotection of compound **5.9h** was done using the general procedure E, affording the title compound **(5.10h)** as a yellow solid (0.19 g, 100%), mp 151-153 °C. ^{1}H NMR (400 MHz, DMSO) δ 10.03 (s, 1H), 8.58 (d, *J* = 6.8 Hz, 1H), 8.01 (d, *J* = 1.9 Hz, 2H), 7.80 – 7.73 (m, 1H), 7.71 – 7.62 (m, 2H), 7.57 (brs, 4H), 7.35 (d, *J* = 8.4 Hz, 2H), 7.27 (t, *J* = 6.8 Hz, 1H), 7.14 (d, *J* = 8.4 Hz, 2H), 4.16 (s, 2H). ^{13}C NMR (101 MHz, DMSO) δ 155.83, 138.41, 137.07, 134.53, 133.27, 130.19, 129.45, 128.22, 127.68, 125.24, 124.77, 123.99, 114.81, 114.15, 50.25. UPLC/MS: t_r 1.29 min, *m/z* 425.4 $[M+H]^+$, purity > 99%. HRMS: mass calculated for $C_{21}H_{19}N_6Cl_2$: 425.1048; found: 425.1059.

1-(4-(((2-Phenylimidazo[1,2-*a*]pyridin-3-yl)amino)methyl)phenyl)guanidine (5.10i).

Boc deprotection of compound **5.9i** was done using the general procedure E, affording the title compound **(5.10i)** as an orange oil (0.09 g, 97%). ^{1}H NMR (400 MHz, MeOD) δ 8.69 (dt, *J* = 6.9, 1.0 Hz, 1H), 7.96 – 7.89 (m, 1H), 7.87 – 7.80 (m, 3H), 7.62 – 7.53 (m, 3H), 7.48 (td, *J* = 6.9, 1.1 Hz, 1H), 7.28 (d, *J* = 8.4 Hz, 2H), 7.10 (d, *J* = 8.4 Hz, 2H), 4.24 (s, 2H). ^{13}C NMR (101 MHz, MeOD) δ 157.96, 139.42, 138.31, 135.49, 134.47, 131.17, 130.91, 130.36, 128.93, 128.04, 126.28, 118.01, 112.87, 51.34. UPLC/MS: t_r 1.02 min, *m/z* 357.4 $[M+H]^+$, purity: 96%. HRMS: mass calculated for $C_{21}H_{21}N_6$: 357.1828; found: 357.1810.

1-(4-(((2-(3-Fluorophenyl)imidazo[1,2-*a*]pyridin-3-yl)amino)methyl)phenyl)guanidine (5.10j). Boc deprotection of compound **5.9j** was done using the general procedure E, affording the title compound **(5.10j)** as a white solid (0.16 g, 96%), mp 153 °C. ^{1}H NMR (400 MHz, DMSO) δ 10.04 (s, 1H), 8.65 (d, *J* = 6.8 Hz, 1H), 7.91 – 7.76 (m, 4H), 7.65 – 7.59 (m, 1H), 7.57 (brs, 4H), 7.41 (td, *J* = 6.7, 1.3 Hz, 1H), 7.37 – 7.29 (m, 3H), 7.11 (d, *J* = 8.4 Hz, 2H), 6.03 (s, 1H), 4.17 (s, 2H). ^{13}C NMR (101 MHz, DMSO) δ, 162.30 (d, *J* = 243.8 Hz), 155.83, 137.25, 137.05, 134.54, 132.07, 131.13 (d, *J* = 8.5 Hz), 129.39, 127.92, 125.12, 124.09, 123.34 (d, *J* = 2.6 Hz), 116.04 (d, *J* = 20.6 Hz), 113.92 (d, *J* = 23.8 Hz), 112.86, 50.04. UPLC/MS: t_r 0.99 min, *m/z* 375.5 $[M+H]^+$, purity > 99%. HRMS: mass calculated for $C_{21}H_{20}N_6F$: 375.1733; found: 375.1721.

1-(4-(((2-(4-Fluorophenyl)imidazo[1,2-*a*]pyridin-3-yl)amino)methyl)phenyl)guanidine (5.10k). Boc deprotection of compound **5.9k** was done using the general procedure E, affording the title compound **(5.10k)** as a light-yellow oil (0.15 g, 95%). ^{1}H NMR (400 MHz, DMSO) δ 10.09 (s, 1H), 8.69 – 8.62 (m, 1H), 8.03 – 7.93 (m, 2H), 7.90 – 7.78 (m, 2H), 7.73 – 7.50 (m, 4H), 7.46 – 7.37 (m, 3H), 7.31 (d, *J* = 8.4 Hz, 2H), 7.11 (d, *J* = 8.4 Hz, 2H), 5.96 (brs, 1H), 4.15 (s, 2H). ^{13}C NMR (101 MHz, DMSO) δ 162.54 (d, *J* = 247.8 Hz), 155.92, 137.06, 136.92, 134.59, 132.19, 129.79 (d, *J* = 8.6 Hz), 129.40, 127.30, 125.32, 125.16, 124.24, 124.09, 116.16, 116.11 (d, *J* = 21.9 Hz), 112.57, 49.98. UPLC/MS: t_r 0.97 min, *m/z* 375.3 $[M+H]^+$, purity: 99%. HRMS: mass calculated for $C_{21}H_{20}N_6F$: 375.1733; found: 375.1751.

1-(4-(2-((2-Ethylimidazo[1,2-*a*]pyridin-3-yl)amino)ethyl)phenyl)-2,3-di-Boc-guanidine (5.11a). The title compound was prepared according to the general procedure D from pyridin-2-amine, 4-propionaldehyde, isocyanide **5.6b** (0.35 g, 54%). ^{1}H NMR (400 MHz, DMSO) δ 11.43 (s, 1H), 9.94 (s, 1H), 7.96 (d, *J* = 6.8 Hz, 1H), 7.43 (d, *J* = 8.4 Hz, 2H), 7.34 (dt, *J* = 9.0, 1.0 Hz, 1H), 7.20 (d, *J* = 8.5 Hz, 2H), 7.05 (ddd, *J* = 9.0, 6.6, 1.3 Hz, 1H), 6.77 (td, *J* = 6.7, 1.1 Hz, 1H), 4.61 (t, *J* = 6.2 Hz, 1H), 3.16 – 3.07 (m, 2H), 2.76 (t, *J* = 7.5 Hz, 2H), 2.66 (q, *J* = 7.5 Hz, 2H), 1.50 (s, 9H), 1.39 (s, 9H), 1.21 (t, *J* = 7.5 Hz, 3H). ^{13}C NMR (101 MHz, DMSO) δ 152.93, 139.90, 138.73, 136.56, 134.58, 128.86, 125.62, 122.85, 122.52, 122.19, 116.24, 110.73, 83.36, 49.75, 36.02, 27.87, 27.67, 19.88, 14.22. UPLC/MS: t_r 2.03 min, *m/z* 523.6 $[M+H]^+$.

1-(4-(2-((2-(3-Chlorophenyl)imidazo[1,2-*a*]pyrazin-3-yl)amino)ethyl)phenyl)-2,3-di-Boc-guanidine (5.11b). The title compound was prepared according to the general procedure D from pyrazin-2-amine, 3-chlorobenzaldehyde, isocyanide **5.6b** (0.18 g, 49%). ^{1}H NMR (400 MHz, $CDCl_3$) δ 11.62 (s, 1H), 8.85 (s, 1H), 8.16 – 8.07 (m, 1H), 7.96 – 7.90 (m, 1H), 7.79 – 7.69 (m, 2H), 7.46 – 7.34 (m, 4H), 7.10 (d, *J* = 8.3 Hz, 2H), 4.31 (brs, 1H), 3.42 – 3.32 (m, 2H), 2.83 (t, *J* = 6.4 Hz, 2H), 1.55 (s, 9H), 1.49 (s, 9H). UPLC/MS: t_r 1.44 min, *m/z* 606.5 $[M+H]^+$.

1-(4-(2-((2-Ethylimidazo[1,2-*a*]pyridin-3-yl)amino)ethyl)phenyl)guanidine (5.12a). Boc deprotection of compound **5.11a** was done using the general procedure E, affording the title compound **(5.12a)** as a colorless oil (0.24 g, 98%). ^{1}H NMR (400 MHz, DMSO) δ 10.01 (s, 1H), 8.47 (d, *J* = 6.8 Hz, 1H), 7.90 – 7.80 (m, 2H), 7.53 (brs, 4H), 7.43 (ddd, *J* = 6.8, 5.9, 2.2 Hz, 1H), 7.31 (d, *J* = 8.4 Hz, 2H), 7.15 (d, *J* = 8.4 Hz, 2H), 3.29 – 3.16 (m, 2H), 2.92 – 2.76 (m, 4H), 1.28 (t, *J* = 7.6 Hz, 3H). ^{13}C NMR (101 MHz, DMSO) δ 156.06, 137.67, 135.91, 133.50, 131.91, 129.95, 128.44, 127.39, 124.90, 124.50, 116.27, 111.82, 48.95, 35.77, 16.93, 13.16. UPLC/MS: t_r 0.28 min, *m/z* 323.4 $[M+H]^+$, purity: 97%. HRMS: mass calculated for $C_{18}H_{23}N_6$: 323.1984; found: 323.1986.

1-(4-(2-((2-(3-Chlorophenyl)imidazo[1,2-*a*]pyrazin-3-yl)amino)ethyl)phenyl)guanidine (5.12b). Boc deprotection of compound **5.11b** was done using the general procedure E, affording the title compound **(5.12b)** as a yellow oil (0.12 g, 96%). ^{1}H NMR (400 MHz, DMSO) δ 9.64 (s, 1H), 8.97 (d, *J* = 1.3 Hz, 1H), 8.31 (dd, *J* = 4.7, 1.4 Hz, 1H), 8.10 (t, *J* = 1.7 Hz, 1H), 8.00 (dt, *J* = 7.7, 1.3 Hz, 1H), 7.87 (d, *J* = 4.7 Hz, 1H), 7.48 (t, *J* = 7.8 Hz, 1H), 7.45 – 7.40 (m, 1H), 7.34 (brs, 4H), 7.18 (d, *J* = 8.4 Hz, 2H), 7.07 (d, *J* = 8.4 Hz, 2H), 5.51 (s, 1H), 3.25 (t, *J* = 7.1 Hz, 2H), 2.81 (t, *J* = 7.4 Hz, 2H). ^{13}C NMR (101 MHz, DMSO) δ 155.97, 140.46, 137.52, 135.38, 135.19, 134.91, 133.48, 133.31, 130.64, 130.54, 129.77, 127.93, 126.54, 125.58, 124.58, 116.87, 48.17, 35.92. UPLC/MS: t_r 1.38 min, *m/z* 406.4 $[M+H]^+$, purity: 99%. HRMS: mass calculated for $C_{21}H_{21}N_7Cl$: 406.1547; found: 406.1548.

2-Amino-*N*-butylisonicotinamide (5.13a). The title compound was prepared according to the TBD-catalysed aminolysis reaction. To a solution of methyl 2-aminopyridine-4-carboxylate (0.3 g, 1.972 mmol) in dry DMF (10 mL) were added butan-1-amine (0.391 mL, 3.94 mmol, 2 equiv) and 1,5,7-triazabicyclo[4.4.0]dec-5-ene (TBD) (54.9 mg, 0.394 mmol, 0.2 equiv), and the reaction mixture was stirred in a pressure tube at 120 °C for 20 h. The crude product was purified by an Isolera, using normal phase chromatography and by applying gradient from 0-10% of MeOH in EtOAc, to afford a white solid (0.20 g, 52.5%). ^{1}H NMR (400 MHz, $CDCl_3$) δ 8.10 (dd, *J* = 5.3, 0.5 Hz, 1H), 6.93 – 6.89 (s, 1H), 6.84 (dd, *J* = 5.4, 1.4 Hz, 1H), 6.20 (brs, 1H), 3.48 – 3.38 (m, 2H), 1.64 – 1.54 (m, 2H), 1.46 – 1.34 (m, 2H), 0.95 (t, *J* = 7.3 Hz, 3H). ^{13}C NMR (101 MHz, $CDCl_3$) δ 165.97, 158.91, 148.07, 144.47, 110.69, 107.11, 40.02, 31.70, 20.27, 13.89. UPLC/MS: t_r 0.31 min, *m/z* 194.3 $[M+H]^+$.

6-Amino-*N*-butylnicotinamide (5.13b). The title compound was prepared according to the TBD-catalyzed aminolysis reaction. To a solution of methyl 6-aminonicotinate (0.3 g, 1.972 mmol) in dry DMF (9 mL) were added butan-1-amine (0.391 mL, 3.94 mmol, 2 equiv) and 1,5,7-triazabicyclo[4.4.0]dec-5-ene (TBD) (54.9 mg, 0.394 mmol, 0.2 equiv), and the reaction mixture was stirred in a pressure tube at 120 °C for 24 h. The crude product was purified by an Isolera, using normal phase chromatography and by applying gradient from 10-100% of EtOAc in heptane to 0-15%

of MeOH in EtOAc, to afford a white solid (0.16 g, 42%). ^{1}H NMR (400 MHz, $CDCl_3$) δ 8.45 (d, *J* = 2.3 Hz, 1H), 7.88 (dd, *J* = 8.6, 2.3 Hz, 1H), 6.50 (dd, *J* = 8.6, 0.7 Hz, 1H), 5.94 (brs, 1H), 3.48 – 3.39 (m, 2H), 1.63 – 1.53 (m, 2H), 1.47 – 1.35 (m, 2H), 0.95 (t, *J* = 7.3 Hz, 3H). UPLC/MS: t_r 0.25 min, *m/z* 194.2 $[M+H]^+$.

1-(4-(((8-Methyl-2-(pyridin-3-yl)imidazo[1,2-*a*]pyridin-3-yl)amino)methyl)phenyl)-2,3-di-Boc-guanidine (5.14a). The title compound was prepared according to the general procedure D from 3-methylpyridin-2-amine, nicotinaldehyde, isocyanide **5.6a** (0.09 g, 25%). ^{1}H NMR (400 MHz, $CDCl_3$) δ 11.62 (s, 1H), 10.30 (s, 1H), 9.22 (d, *J* = 2.0 Hz, 1H), 8.53 (dd, *J* = 4.8, 1.4 Hz, 1H), 8.32 (d, *J* = 7.9 Hz, 1H), 7.90 (d, *J* = 6.8 Hz, 1H), 7.52 (d, *J* = 8.4 Hz, 2H), 7.37 (ddd, *J* = 7.9, 4.8, 0.8 Hz, 1H), 7.23 (d, *J* = 8.3 Hz, 2H), 6.98 (d, *J* = 6.8 Hz, 1H), 6.73 (t, *J* = 6.8 Hz, 1H), 4.12 (s, 2H), 2.63 (s, 3H), 1.53 (s, 9H), 1.50 (s, 9H). ^{13}C NMR (101 MHz, $CDCl_3$) δ 153.61, 147.97, 147.91, 142.03, 136.47, 135.30, 135.09, 130.15, 129.42, 128.85, 127.37, 126.70, 124.29, 123.84, 122.52, 120.62, 112.76, 83.93, 79.83, 52.07, 28.24, 16.81. UPLC/MS: t_r 1.95 min, *m/z* 572.6 $[M+H]^+$.

Methyl 3-((4-(2,3-di-Boc-guanidino)benzyl)amino)-2-(pyridin-3-yl)imidazo[1,2-*a*]pyridine-7-carboxylate (5.14b). The title compound was prepared according to the general procedure D from methyl 2-aminoisonicotinate, nicotinaldehyde, isocyanide **5.6a** (0.40 g, 49%). ^{1}H NMR (400 MHz, $CDCl_3$) δ 11.61 (brs, 1H), 9.12 (d, *J* = 1.6 Hz, 1H), 8.52 (dd, *J* = 4.9, 1.5 Hz, 1H), 8.32 (dt, *J* = 8.0, 1.9 Hz, 1H), 8.28 (dd, *J* = 1.5, 0.9 Hz, 1H), 8.03 (dd, *J* = 7.2, 0.9 Hz, 1H), 7.48 (d, *J* = 8.5 Hz, 2H), 7.45 – 7.36 (m, 2H), 7.22 (d, *J* = 8.5 Hz, 2H), 4.16 (d, *J* = 5.9 Hz, 2H), 3.96 (s, 3H), 1.59 – 1.45 (m, 18H). ^{13}C NMR (101 MHz, $CDCl_3$) δ 165.90, 154.42, 153.86, 148.25, 147.68, 140.89, 136.44, 135.97, 135.28, 135.19, 130.26, 128.96, 127.90, 125.90, 124.09, 122.86, 122.16, 120.54, 111.62, 84.08, 80.14, 52.70, 50.96, 28.24. UPLC/MS: t_r 2.08 min, *m/z* 616.6 $[M+H]^+$.

3-((4-(2,3-Di-Boc-guanidino)benzyl)amino)-2-(pyridin-3-yl)imidazo[1,2-*a*]pyridine-7-carboxylic acid (5.14c). The title compound was prepared by base hydrolysis of an ester function in compound **5.14b**. To a solution of compound **5.14b** (0.10 g, 0.194 mmol) in a 9:1 mixture of DCM (1.8 mL) and MeOH (0.2 mL), was added a 2 M solution of sodium hydroxide (0.145 mL, 0.291 mmol, 1.5 equiv) and the reaction was left stirring for 12 h at rt. The crude product was purified by an Isolera, using reversed phase chromatography and by applying gradient of 10-100% of MeOH in water, to afford a yellow solid (0.08 g, 69%). ^{1}H NMR (400 MHz, MeOD) δ 9.03 (d, *J* = 1.7 Hz, 1H), 8.57 (dd, *J* = 5.0, 1.1 Hz, 1H), 8.52 – 8.46 (m, 1H), 8.37 (dd, *J* = 7.2, 0.9 Hz, 1H), 8.21 (dd, *J* = 1.4, 1.0 Hz, 1H), 7.68 (dd, *J* = 7.9, 5.0 Hz, 1H), 7.53 (dd, *J* = 7.2, 1.5 Hz, 1H), 7.33 (d, *J* = 8.5 Hz, 2H), 7.10 (d, *J* = 8.5 Hz, 2H), 4.19 (s, 2H), 1.57 – 1.45 (m, 18H). UPLC/MS: t_r 1.89 min, *m/z* 602.7 $[M+H]^+$.

***N*-Butyl-3-((4-(2,3-di-Boc-guanidino)benzyl)amino)-2-(pyridin-3-yl)imidazo[1,2-*a*]pyridine-7-carboxamide (5.14d).** The title compound was prepared according to the general procedure D from aminopyridine **5.13a**, nicotinaldehyde, isocyanide **5.6a** to afford a light-yellow solid (0.41 g, 60%). ^{1}H NMR (400 MHz, $CDCl_3$) δ 11.61 (s, 1H), 10.29 (s, 1H), 9.26 – 9.19 (m, 1H), 8.56 (dd, *J* = 4.9, 1.6 Hz, 1H), 8.36 – 8.29 (m, 1H), 8.05 (dd, *J* = 7.1, 0.8 Hz, 1H), 7.98 – 7.94 (m, 1H), 7.48 (d, *J* = 8.5 Hz, 2H), 7.42 (ddd, *J* = 8.0, 4.9, 0.7 Hz, 1H), 7.30 (dd, *J* = 7.1, 1.6 Hz, 1H), 7.16 (d, *J* = 8.5 Hz, 2H), 6.67 (t, *J* = 5.5 Hz, 1H), 4.16 – 4.06 (m, 2H), 3.98 – 3.83 (m, 1H), 3.52 – 3.43 (m, 2H), 1.69 – 1.58 (m, 2H), 1.54 (s, 9H), 1.50 (s, 9H), 1.46 – 1.36 (m, 2H), 0.97 (t, *J* = 7.3 Hz, 3H). ^{13}C NMR (101 MHz, $CDCl_3$) δ 165.57, 153.76, 148.17, 147.50, 140.49, 136.59, 135.21, 134.80, 129.70, 128.88, 127.49, 124.15, 122.77, 122.74, 115.47, 111.56, 84.05, 79.85, 52.00, 40.20, 31.77, 28.24, 20.33, 13.94. UPLC/MS: t_r 2.02 min, *m/z* 657.7 $[M+H]^+$.

1,2-Di-Boc-3-(4-(((6-methyl-2-(pyridin-3-yl)imidazo[1,2-*a*]pyridin-3-yl)amino)methyl)phenyl) guanidine (5.14e). The title compound was prepared according to the general procedure D from 5-methylpyridin-2-amine, nicotinaldehyde, isocyanide **5.6a** to afford a yellow solid (0.17 g, 46%). UPLC/MS: t_r 1.98 min, *m/z* 572.6 $[M+H]^+$.

1,2-Di-Boc-3-(4-(((2-(pyridin-3-yl)-6-(trifluoromethyl)imidazo[1,2-*a*]pyridin-3-yl)amino)methyl) phenyl)guanidine (5.14f). The title compound was prepared according to the general procedure D from 5-(trifluoromethyl)pyridin-2-amine, nicotinaldehyde, isocyanide **5.6a** to afford a yellow solid (0.13 g, 37%). ^{1}H NMR (400 MHz, $CDCl_3$) δ 11.61 (s, 1H), 10.30 (brs, 1H), 9.26 (s, 1H), 8.57 (d, *J* = 4.0 Hz, 1H), 8.38 – 8.28 (m, 2H), 7.62 (d, *J* = 9.4 Hz, 1H), 7.53 – 7.47 (m, 2H), 7.47 – 7.41 (m, 1H), 7.29 (dd, *J* = 9.4, 1.8 Hz, 1H), 7.21 – 7.14 (m, 2H), 4.20 – 4.13 (m, 2H), 3.77 (t, *J* = 5.3 Hz, 1H), 1.53 (s, 9H), 1.50 (s, 9H). UPLC/MS: t_r 2.18 min, *m/z* 626.7 $[M+H]^+$.

1-Boc-3-(4-(((6-fluoro-2-(pyridin-3-yl)imidazo[1,2-*a*]pyridin-3-yl)amino)methyl)phenyl)guanidine (5.14g). The title compound was prepared according to the general procedure D from 5-fluoropyridin-2-amine, nicotinaldehyde, isocyanide **5.6a** and using 2,2,2-trifluoroethanol (8 mL) as a solvent, to afford a yellow solid (0.25 g, 65%). ^{1}H NMR (400 MHz, MeOD) δ 9.06 (dd, *J* = 2.2, 0.8 Hz, 1H), 8.46 (dd, *J* = 4.9, 1.6 Hz, 1H), 8.32 (ddd, *J* = 8.0, 2.2, 1.7 Hz, 1H), 8.21 (ddd, *J* = 4.2, 2.4, 0.7 Hz, 1H), 7.54 – 7.45 (m, 2H), 7.31 –7.23 (m, 1H), 7.14 (d, *J* = 8.5 Hz, 2H), 7.04 (d, *J* = 8.5 Hz, 2H), 4.13 (s, 2H), 1.47 (s, 9H). ^{13}C NMR (101 MHz, MeOD) δ 153.73, 148.64 (d, *J* = 3.1 Hz), 140.94, 137.64, 136.39, 135.16, 131.77, 130.68, 129.86, 125.04 (d, *J* = 32.7 Hz),124.87, 118.64, 118.42 (d, *J* = 8.9 Hz), 111.04 (d, *J* = 42.1 Hz), 79.98, 52.05, 28.64. UPLC/MS: t_r 1.28 min, *m/z* 476.5 $[M+H]^+$.

***N*-Butyl-3-((4-(2,3-di-Boc-guanidino)benzyl)amino)-2-(pyridin-3-yl)imidazo[1,2-*a*]pyridine-6-carboxamide (5.14h).** The title compound was prepared according to the general procedure D from

aminopyridine **5.13b**, nicotinaldehyde, isocyanide **5.6a** to afford a yellow solid (0.23 g, 47%). ^{1}H NMR (400 MHz, $CDCl_3$) δ 11.67 (s, 1H), 9.43 (d, *J* = 1.4 Hz, 1H), 9.24 (s, 1H), 8.55 (dd, *J* = 4.8, 1.5 Hz, 1H), 8.50 – 8.42 (m, 1H), 7.65 (d, *J* = 9.5 Hz, 1H), 7.54 (d, *J* = 9.4 Hz, 1H), 7.41 (dd, *J* = 7.9, 4.8 Hz, 1H), 7.30 (d, *J* = 8.3 Hz, 2H), 7.18 (d, *J* = 8.3 Hz, 2H), 7.04 – 6.88 (m, 1H), 4.59 – 4.40 (m, 1H), 4.08 (d, *J* = 5.6 Hz, 2H), 3.31 – 3.16 (m, 2H), 1.62 – 1.47 (m, 11H), 1.45 (s, 9H), 1.41 – 1.30 (m, 2H), 0.92 (t, *J* = 7.3 Hz, 3H). ^{13}C NMR (101 MHz, $CDCl_3$) δ 164.95, 155.02, 153.40, 148.22, 148.00, 141.87, 136.22, 135.73, 134.69, 130.10, 129.13, 128.29, 125.24, 124.69, 123.92, 123.56, 120.76, 116.29, 84.18, 80.26, 52.47, 40.31, 31.58, 28.29, 28.25, 20.42, 13.97. UPLC/MS: t_r 2.00 min, *m/z* 657.7 $[M+H]^+$.

3-((4-(2,3-Di-Boc-guanidino)benzyl)amino)-2-(pyridin-3-yl)imidazo[1,2-*a*]pyridine-6-carboxamide (5.14i). The title compound was prepared according to the general procedure D from 6-aminonicotinamide, nicotinaldehyde, isocyanide **5.6a**. The crude product was purified by an Isolera, using reversed phase chromatography and by applying gradient of 10-100% of MeOH in water, to afford a yellow solid (0.30 g, 68%). UPLC/MS: t_r 1.76 min, *m/z* 601.7 $[M+H]^+$.

1-(4-(((8-Methyl-2-(pyridin-3-yl)imidazo[1,2-*a*]pyridin-3-yl)amino)methyl)phenyl)guanidine (5.15a). Boc deprotection of compound **5.14a** was done using the general procedure E, affording the title compound **(5.15a)** as an orange oil (0.04 g, 99%). ^{1}H NMR (400 MHz, MeOD) δ 8.77 (brs, 1H), 8.65 (dd, *J* = 4.9, 1.4 Hz, 1H), 8.57 (d, *J* = 6.8 Hz, 1H), 8.28 – 8.23 (m, 1H), 7.73 (d, *J* = 7.2 Hz, 1H), 7.63 (dd, *J* = 8.0, 5.0 Hz, 1H), 7.40 (t, *J* = 7.0 Hz, 1H), 7.21 (d, *J* = 8.4 Hz, 2H), 7.09 (d, *J* = 8.4 Hz, 2H), 4.24 (s, 2H), 2.67 (s, 3H). ^{13}C NMR (101 MHz, MeOD) δ 158.03, 149.97, 148.98, 139.47, 139.41, 138.74, 135.56, 133.41, 130.91, 130.05, 126.35, 125.61, 124.96, 124.79, 123.87, 117.88, 51.42, 15.99. UPLC/MS: t_r 0.26 min, *m/z* 372.5 $[M+H]^+$, purity: 98%. HRMS: mass calculated for $C_{21}H_{22}N_7$: 372.1937; found: 372.1935.

Methyl 3-((4-guanidinobenzyl)amino)-2-(pyridin-3-yl)imidazo[1,2-*a*]pyridine-7-carboxylate (5.15b). Boc deprotection of compound **5.14b** was done using the general procedure E, affording the title compound **(5.15b)** as an orange oil (0.09 g, 94%). ^{1}H NMR (400 MHz, MeOD) δ 9.13 (brs, 1H), 8.73 – 8.59 (m, 2H), 8.39 (dd, *J* = 7.2, 0.7 Hz, 1H), 8.25 – 8.20 (m, 1H), 7.84 – 7.73 (m, 1H), 7.53 (dd, *J* = 7.2, 1.5 Hz, 1H), 7.26 (d, *J* = 8.4 Hz, 2H), 7.10 (d, *J* = 8.4 Hz, 2H), 4.26 (s, 2H), 3.98 (s, 3H). UPLC/MS: t_r 1.09 min, *m/z* 416.5 $[M+H]^+$, purity: 97%. HRMS: mass calculated for $C_{22}H_{22}N_7O_2$: 416.1835; found: 416.1846.

3-((4-Guanidinobenzyl)amino)-2-(pyridin-3-yl)imidazo[1,2-*a*]pyridine-7-carboxylic acid (5.15c). Boc deprotection of compound **5.14c** was done using the general procedure E, affording the title compound **(5.15c)** as a yellow solid (0.05 g, 93%). ^{1}H NMR (400 MHz, MeOD) δ 9.12 (brs, 1H), 8.72 – 8.58 (m, 2H), 8.42 (dd, *J* = 7.2, 0.7 Hz, 1H), 8.28 – 8.21 (m, 1H), 7.85 – 7.75 (m, 1H), 7.58 (dd, *J* = 7.2,

1.5 Hz, 1H), 7.26 (d, *J* = 8.4 Hz, 2H), 7.11 (d, *J* = 8.4 Hz, 2H), 4.27 (s, 2H). ^{13}C NMR (101 MHz, MeOD) δ 158.01, 157.23, 146.21, 145.55, 140.02, 139.75, 137.59, 137.31, 135.57, 131.09, 126.35, 124.95, 121.19, 118.91, 114.16, 51.83. UPLC/MS: t_r 0.17 min, *m/z* 402.3 $[M+H]^+$, purity: 98%. HRMS: mass calculated for $C_{21}H_{20}N_7O_2$: 402.1678; found: 402.1673.

***N*-Butyl-3-((4-guanidinobenzyl)amino)-2-(pyridin-3-yl)imidazo[1,2-*a*]pyridine-7-carboxamide (5.15d).** Boc deprotection of compound **5.14d** was done using the general procedure E, affording the title compound **(5.15d)** as a light-yellow solid (0.08 g, 100%), mp 148-150 °C. ^{1}H NMR (400 MHz, DMSO) δ 9.84 (s, 1H), 9.26 – 9.17 (m, 1H), 8.75 (t, *J* = 5.5 Hz, 1H), 8.68 (d, *J* = 4.3 Hz, 1H), 8.61 (d, *J* = 8.0 Hz, 1H), 8.45 (d, *J* = 7.1 Hz, 1H), 8.11 (s, 1H), 7.76 (dd, *J* = 8.0, 5.2 Hz, 1H), 7.55 – 7.38 (m, 5H), 7.30 (d, *J* = 8.3 Hz, 2H), 7.09 (d, *J* = 8.3 Hz, 2H), 5.90 (s, 1H), 4.17 (s, 2H), 3.37 – 3.23 (m, 2H), 1.60 – 1.47 (m, 2H), 1.42 – 1.28 (m, 2H), 0.92 (t, *J* = 7.3 Hz, 3H). UPLC/MS: t_r 1.13 min, *m/z* 457.5 $[M+H]^+$, purity > 99%. HRMS: mass calculated for $C_{25}H_{29}N_8O$: 457.2464; found: 457.2446.

1-(4-(((6-Methyl-2-(pyridin-3-yl)imidazo[1,2-*a*]pyridin-3-yl)amino)methyl)phenyl)guanidine (5.15e). Boc deprotection of compound **5.14e** was done using the general procedure E, affording the title compound **(5.15e)** as an orange oil (0.07 g, 95%). ^{1}H NMR (400 MHz, MeOD) δ 8.82 (s, 1H), 8.64 (d, *J* = 4.5 Hz, 1H), 8.52 – 8.46 (m, 1H), 8.28 – 8.20 (m, 1H), 7.87 – 7.74 (m, 2H), 7.63 (dd, *J* = 8.0, 5.0 Hz, 1H), 7.25 (d, *J* = 8.5 Hz, 2H), 7.10 (d, *J* = 8.5 Hz, 2H), 4.26 (s, 2H), 2.52 (d, *J* = 0.9 Hz, 3H). ^{13}C NMR (101 MHz, MeOD) δ 158.03, 149.95, 148.35, 139.43, 138.13, 137.99, 137.33, 135.62, 131.05, 129.50, 128.95, 126.33, 125.81, 124.74, 123.98, 112.80, 51.54, 18.15. UPLC/MS: t_r 0.28 min, *m/z* 372.4 $[M+H]^+$, purity: 98%. HRMS: mass calculated for $C_{21}H_{22}N_7$: 372.1937; found: 372.1938.

1-(4-(((2-(Pyridin-3-yl)-6-(trifluoromethyl)imidazo[1,2-*a*]pyridin-3-yl)amino)methyl)phenyl) guanidine (5.15f). Boc deprotection of compound **5.14f** was done using the general procedure E, affording the title compound **(5.15f)** as a colorless oil (0.08 g, 95%). ^{1}H NMR (400 MHz, MeOD) δ 9.17 (s, 1H), 8.66 (d, *J* = 8.2 Hz, 1H), 8.64 – 8.56 (m, 2H), 7.74 (dd, *J* = 8.0, 5.2 Hz, 1H), 7.69 (d, *J* = 9.5 Hz, 1H), 7.52 (dd, *J* = 9.5, 1.7 Hz, 1H), 7.26 (d, *J* = 8.4 Hz, 2H), 7.10 (d, *J* = 8.4 Hz, 2H), 4.24 (s, 2H). UPLC/MS: t_r 1.24 min, *m/z* 426.5 $[M+H]^+$, purity > 99%.

1-(4-(((6-Fluoro-2-(pyridin-3-yl)imidazo[1,2-*a*]pyridin-3-yl)amino)methyl)phenyl)guanidine (5.15g). Boc deprotection of compound **5.14g** was done using the general procedure E, affording the title compound **(5.15g)** as a yellow solid (0.17 g, 96%), mp 141 °C. ^{1}H NMR (400 MHz, MeOD) δ 9.03 (d, *J* = 1.7 Hz, 1H), 8.70 (dd, *J* = 5.3, 1.4 Hz, 1H), 8.68 – 8.64 (m, 1H), 8.60 – 8.54 (m, 1H), 7.88 – 7.72 (m, 3H), 7.26 (d, *J* = 8.4 Hz, 2H), 7.10 (d, *J* = 8.4 Hz, 2H), 4.25 (s, 2H). ^{13}C NMR (101 MHz, MeOD) δ 157.96, 157.35, 154.95, 146.61, 145.43, 140.42, 139.40, 138.42, 135.65, 131.16, 131.01 (d, *J* = 2.3 Hz), 129.26, 128.06, 126.84, 126.27, 123.85 (d, *J* = 26.4 Hz), 116.36 (d, *J* = 8.7 Hz), 113.06 (d, *J* = 42.6 Hz),

51.58. UPLC/MS: t_r 0.26 min, *m/z* 376.3 $[M+H]^+$, purity > 99%. HRMS: mass calculated for $C_{20}H_{19}N_7F$: 376.1686; found: 376.1685.

***N*-Butyl-3-((4-guanidinobenzyl)amino)-2-(pyridin-3-yl)imidazo[1,2-*a*]pyridine-6-carboxamide (5.15h).** Boc deprotection of compound **5.14h** was done using the general procedure E, affording the title compound **(5.15h)** as a yellow oil (0.13 g, 96%). ^{1}H NMR (400 MHz, DMSO) δ 9.91 (s, 1H), 9.21 (d, *J* = 1.7 Hz, 1H), 8.82 (s, 1H), 8.75 (t, *J* = 5.5 Hz, 1H), 8.65 (dd, *J* = 5.0, 1.3 Hz, 1H), 8.58 (d, *J* = 8.0 Hz, 1H), 7.85 (d, *J* = 9.4 Hz, 1H), 7.75 – 7.66 (m, 2H), 7.53 (brs, 4H), 7.31 (d, *J* = 8.3 Hz, 2H), 7.10 (d, *J* = 8.3 Hz, 2H), 4.18 (s, 2H), 3.36 – 3.25 (m, 2H), 1.59 – 1.49 (m, 2H), 1.42 – 1.30 (m, 2H), 0.92 (t, *J* = 7.3 Hz, 3H). ^{13}C NMR (101 MHz, DMSO) δ 163.53, 155.85, 145.69, 144.78, 140.28, 137.58, 136.99, 134.43, 129.55, 128.91, 125.42, 124.94, 124.19, 120.83, 115.08, 50.71, 40.15, 31.22, 19.69, 13.76. UPLC/MS: t_r 1.12 min, *m/z* 457.5 $[M+H]^+$, purity > 99%. HRMS: mass calculated for $C_{25}H_{29}N_8O$: 457.2464; found: 457.2477.

3-((4-Guanidinobenzyl)amino)-2-(pyridin-3-yl)imidazo[1,2-*a*]pyridine-6-carboxamide (5.15i). Boc deprotection of compound **5.14i** was done using the general procedure E, affording the title compound **(5.15i)** as an orange oil (0.11 g, 100%). ^{1}H NMR (400 MHz, MeOD) δ 9.17 (brs, 1H), 8.95 (dd, *J* = 1.6, 1.0 Hz, 1H), 8.77 – 8.70 (m, 2H), 8.10 (dd, *J* = 9.4, 1.7 Hz, 1H), 7.96 – 7.88 (m, 1H), 7.79 (dd, *J* = 9.4, 0.9 Hz, 1H), 7.28 (d, *J* = 8.4 Hz, 2H), 7.11 (d, *J* = 8.4 Hz, 2H), 4.28 (s, 2H). ^{13}C NMR (101 MHz, MeOD) δ 167.86, 157.93, 145.44, 144.35, 141.52, 141.47, 139.61, 135.72, 131.22, 131.16, 130.22, 130.01, 127.65, 127.58, 127.35, 126.34, 123.81, 114.99, 52.23. UPLC/MS: t_r 0.17 min, *m/z* 401.4 $[M+H]^+$, purity: 98%. HRMS: mass calculated for $C_{21}H_{21}N_8O$: 401.1838; found: 401.1838.

2-Amino-*N*-cyclopropylisonicotinamide (5.16a). The title compound was prepared according to the general procedure C using cyclopropanamine to afford a white solid (0.51 g, 89%). ^{1}H NMR (400 MHz, MeOD) δ 7.96 (dd, *J* = 5.4, 0.8 Hz, 1H), 6.87 (dd, *J* = 1.5, 0.8 Hz, 1H), 6.84 (dd, *J* = 5.4, 1.5 Hz, 1H), 2.87 – 2.79 (m, 1H), 0.84 – 0.77 (m, 2H), 0.66 – 0.59 (m, 2H). ^{13}C NMR (101 MHz, MeOD) δ 170.31, 161.43, 148.75, 145.18, 110.95, 108.14, 23.97, 6.48. UPLC/MS: t_r 0.18 min, *m/z* 178.2 $[M+H]^+$.

2-Amino-*N*-(4-fluorobenzyl)isonicotinamide (5.16b). The title compound was prepared according to the general procedure C using (4-fluorophenyl)methanamine to afford a white solid (0.70 g, 87%). ^{1}H NMR (400 MHz, DMSO) δ 9.08 (brs, 1H), 8.00 (d, *J* = 5.1 Hz, 1H), 7.39 – 7.28 (m, 2H), 7.21 – 7.09 (m, 2H), 6.89 – 6.80 (m, 2H), 6.14 (s, 2H), 4.42 (s, 2H). ^{13}C NMR (101 MHz, DMSO) δ 165.61, 161.18 (d, *J* = 242.1 Hz), 160.31, 148.35, 142.70, 135.59 (d, *J* = 3.0 Hz), 129.21 (d, *J* = 8.1 Hz), 115.01 (d, *J* = 21.3 Hz), 109.04, 106.08, 41.86. UPLC/MS: t_r 1.09 min, *m/z* 246.3 $[M+H]^+$.

2-Amino-*N*-cyclopentylisonicotinamide (5.16c). The title compound was prepared according to the general procedure C using cyclopentanamine to afford a white solid (0.61 g, 90%). ^{1}H NMR (400 MHz, MeOD) δ 7.96 (d, *J* = 5.0, 1H), 6.89 – 6.83 (m, 2H), 4.28 (p, *J* = 6.9 Hz, 1H), 2.08 – 1.95 (m, 2H), 1.83 – 1.71 (m, 2H), 1.69 – 1.50 (m, 4H). ^{13}C NMR (101 MHz, MeOD) δ 168.67, 161.36, 148.66, 145.75, 111.14, 108.23, 53.04, 33.32, 24.93. UPLC/MS: t_r 0.18 min, *m/z* 206.3 $[M+H]^+$.

2-Amino-*N*-(2-hydroxyethyl)isonicotinamide (5.16d). The title compound was prepared according to the general procedure C using 2-aminoethan-1-ol to afford a white solid (0.49 g, 86%). ^{1}H NMR (400 MHz, DMSO) δ 8.41 (t, *J* = 5.5 Hz, 1H), 7.97 (d, *J* = 5.2 Hz, 1H), 6.84 – 6.79 (m, 2H), 6.10 (s, 2H), 4.72 (t, *J* = 5.6 Hz, 1H), 3.49 (q, *J* = 6.0 Hz, 2H), 3.29 (q, *J* = 6.1 Hz, 2H). ^{13}C NMR (101 MHz, DMSO) δ 165.65, 160.27, 148.22, 142.95, 109.10, 106.07, 59.59, 42.09. UPLC/MS: t_r 0.17 min, *m/z* 182.3 $[M+H]^+$.

2-Amino-*N*-(2-(4-methylpiperazin-1-yl)ethyl)isonicotinamide (5.16e). The title compound was prepared according to the general procedure C using 2-(4-methylpiperazin-1-yl)ethan-1-amine to afford a white solid (0.45 g, 97%). ^{1}H NMR (400 MHz, MeOD) δ 7.98 (dd, *J* = 5.4, 0.7 Hz, 1H), 6.90 (dd, *J* = 1.5, 0.7 Hz, 1H), 6.87 (dd, *J* = 5.4, 1.5 Hz, 1H), 3.51 (t, *J* = 6.8 Hz, 2H), 2.60 (t, *J* = 6.8 Hz, 2H), 2.57 – 2.34 (m, 8H), 2.28 (s, 3H). ^{13}C NMR (101 MHz, MeOD) δ 168.70, 161.47, 148.81, 145.28, 110.89, 108.14, 57.90, 55.65, 53.67, 45.98, 37.95. UPLC/MS: t_r 0.16 min, *m/z* 264.3 $[M+H]^+$.

***N*-Butyl-3-((4-(2,3-di-Boc-guanidino)benzyl)amino)imidazo[1,2-*a*]pyridine-7-carboxamide (5.17a).** The title compound was prepared according to the general procedure D from aminopyridine **5.13a**, glyoxylic acid monohydrate, isocyanide **5.6a** to afford a light-yellow solid (0.24 g, 42%). ^{1}H NMR (400 MHz, $CDCl_3$) δ 11.61 (s, 1H), 10.27 (brs, 1H), 8.29 (d, *J* = 6.7 Hz, 1H), 7.98 (s, 1H), 7.58 (brs, 1H), 7.51 (d, *J* = 6.8 Hz, 1H), 7.37 (d, *J* = 8.3 Hz, 2H), 7.21 (d, *J* = 8.3 Hz, 2H), 6.88 (s, 1H), 5.09 (brs, 1H), 4.12 (s, 2H), 3.52 – 3.34 (m, 2H), 1.68 – 1.59 (m, 2H), 1.54 (s, 9H), 1.46 – 1.32 (m, 11H), 0.92 (t, *J* = 7.3 Hz, 3H). UPLC/MS: t_r 1.94 min, *m/z* 580.6 $[M+H]^+$.

***N*-Cyclopropyl-3-((4-(2,3-di-Boc-guanidino)benzyl)amino)imidazo[1,2-*a*]pyridine-7-carboxamide (5.17b).** The title compound was prepared according to the general procedure D from aminopyridine **5.16a**, glyoxylic acid monohydrate, isocyanide **5.6a** to afford a light-yellow solid (0.30 g, 48%). UPLC/MS: t_r 1.85 min, *m/z* 564.6 $[M+H]^+$.

3-((4-(2,3-Di-Boc-guanidino)benzyl)amino)-*N*-(4-fluorobenzyl)imidazo[1,2-*a*]pyridine-7-carboxamide (5.17c). The title compound was prepared according to the general procedure D from aminopyridine **5.16b**, glyoxylic acid monohydrate, isocyanide **5.6a** to afford a light-yellow solid (0.32 g, 50%). ^{1}H NMR (400 MHz, $CDCl_3$) δ 11.61 (s, 1H), 10.28 (s, 1H), 8.09 – 7.98 (m, 2H), 7.50 (d, *J* = 8.4

Hz, 2H), 7.43 – 7.30 (m, 5H), 7.03 – 6.95 (m, 2H), 6.91 (s, 1H), 4.57 (d, *J* = 5.6 Hz, 2H), 4.23 (s, 2H), 1.54 (s, 9H), 1.39 (s, 9H). UPLC/MS: t_r 1.97 min, *m/z* 632.6 $[M+H]^+$.

***N*-Cyclopentyl-3-((4-(2,3-di-Boc-guanidino)benzyl)amino)imidazo[1,2-*a*]pyridine-7-carboxamide (5.17d).** The title compound was prepared according to the general procedure D from aminopyridine **5.16c**, glyoxylic acid monohydrate, isocyanide **5.6a** to afford a light-yellow solid (0.26 g, 43%). ^{1}H NMR (400 MHz, $CDCl_3$) δ 7.96 (d, *J* = 7.2 Hz, 1H), 7.84 (brs, 1H), 7.53 (d, *J* = 8.5 Hz, 2H), 7.29 (d, *J* = 8.5 Hz, 2H), 7.23 (dd, *J* = 7.2, 1.4 Hz, 1H), 7.04 (s, 1H), 4.42 – 4.30 (m, 1H), 4.22 (s, 2H), 2.14 – 1.98 (m, 2H), 1.81 – 1.60 (m, 4H), 1.58 – 1.49 (m, 11H), 1.46 (s, 9H). ^{13}C NMR (101 MHz, $CDCl_3$) δ 165.68, 163.44, 153.56, 139.62, 136.15, 135.05, 132.75, 129.24, 128.55, 122.83, 122.72, 121.81, 115.79, 110.64, 83.99, 79.88, 51.99, 50.36, 33.17, 33.14, 28.28, 28.20, 24.00. UPLC/MS: t_r 1.91 min, *m/z* 592.6 $[M+H]^+$.

3-((4-(2,3-Di-Boc-guanidino)benzyl)amino)-*N*-(2-hydroxyethyl)imidazo[1,2-*a*]pyridine-7-carboxamide (5.17e). The title compound was prepared according to the general procedure D from aminopyridine **5.16d**, glyoxylic acid monohydrate, isocyanide **5.6a** to afford a light-yellow solid (0.38 g, 61%). UPLC/MS: t_r 1.74 min, *m/z* 568.6 $[M+H]^+$.

3-((4-(2,3-Di-Boc-guanidino)benzyl)amino)-*N*-(2-(4-methylpiperazin-1-yl)ethyl)imidazo[1,2-*a*]pyridine-7-carboxamide (5.17f). The title compound was prepared according to the general procedure D from aminopyridine **5.16e**, glyoxylic acid monohydrate, isocyanide **5.6a** to afford a light-yellow solid (0.40 g, 58%). ^{1}H NMR (400 MHz, $CDCl_3$) δ 11.63 (s, 1H), 10.33 (s, 1H), 7.98 (d, *J* = 5.6 Hz, 1H), 7.89 (brs, 1H), 7.58 (d, *J* = 8.4 Hz, 2H), 7.36 (d, *J* = 8.4 Hz, 2H), 7.23 – 7.16 (m, 1H), 7.10 (s, 1H), 4.32 (d, *J* = 4.0 Hz, 2H), 3.67 – 3.50 (m, 2H), 2.96 – 2.48 (m, 10H), 2.33 (s, 3H), 1.53 (s, 9H), 1.49 (s, 9H). UPLC/MS: t_r 1.58 min, *m/z* 650.9 $[M+H]^+$.

***N*-Butyl-3-((4-guanidinobenzyl)amino)imidazo[1,2-*a*]pyridine-7-carboxamide (5.18a).**

Boc deprotection of compound **5.17a** was done using the general procedure E, affording the title compound **(5.18a)** as a yellow oil (0.08 mg, 100%). ^{1}H NMR (400 MHz, MeOD) δ 8.61 (dd, *J* = 7.2, 0.7 Hz, 1H), 8.24 – 8.20 (m, 1H), 7.77 (dd, *J* = 7.2, 1.6 Hz, 1H), 7.58 (d, *J* = 8.5 Hz, 2H), 7.32 – 7.27 (m, 3H), 4.52 (s, 2H), 3.43 (t, *J* = 7.2 Hz, 2H), 1.69 – 1.58 (m, 2H), 1.50 – 1.37 (m, 2H), 0.98 (t, *J* = 7.4 Hz, 3H). ^{13}C NMR (101 MHz, MeOD) δ 165.84, 158.08, 138.72, 137.64, 136.82, 136.31, 135.56, 130.33, 126.66, 125.32, 115.16, 112.36, 105.46, 49.35, 41.16, 32.40, 21.17, 14.10. UPLC/MS: t_r 0.62 min, *m/z* 380.4 $[M+H]^+$, purity > 99%. HRMS: mass calculated for $C_{20}H_{26}N_7O$: 380.2199; found: 380.2214.

***N*-Cyclopropyl-3-((4-guanidinobenzyl)amino)imidazo[1,2-*a*]pyridine-7-carboxamide (5.18b).**

Boc deprotection of compound **5.17b** was done using the general procedure E, affording the title compound **(5.18b)** as a yellow solid (0.11 mg, 96%), mp 80 °C. ^{1}H NMR (400 MHz, MeOD) δ 8.61 (d, *J* = 7.3 Hz, 1H), 8.25 – 8.18 (m, 1H), 7.76 (dd, *J* = 7.3, 1.6 Hz, 1H), 7.58 (d, *J* = 8.5 Hz , 2H), 7.34 – 7.25 (m, 3H), 4.52 (s, 2H), 2.96 – 2.87 (m, 1H), 0.89 – 0.82 (m, 2H), 0.73 – 0.66 (m, 2H). ^{13}C NMR (101 MHz, MeOD) δ 167.35, 158.09, 138.70, 137.38, 136.71, 136.37, 135.59, 130.33, 126.67, 125.31, 115.23, 112.34, 105.28, 49.34, 24.38, 6.53. UPLC/MS: t_r 0.26 min, *m/z* 364.3 $[M+H]^+$, purity > 99%. HRMS: mass calculated for $C_{19}H_{22}N_7O$: 364.1886; found: 364.1879.

***N*-(4-Fluorobenzyl)-3-((4-guanidinobenzyl)amino)imidazo[1,2-*a*]pyridine-7-carboxamide (5.18c).**

Boc deprotection of compound **5.17c** was done using the general procedure E, affording the title compound **(5.18c)** as a yellow oil (0.08 mg, 97%). ^{1}H NMR (400 MHz, MeOD) δ 8.62 (dd, *J* = 7.3, 0.8 Hz, 1H), 8.30 – 8.21 (m, 1H), 7.80 (dd, *J* = 7.3, 1.6 Hz, 1H), 7.58 (d, *J* = 8.4 Hz, 2H), 7.45 – 7.36 (m, 2H), 7.35 – 7.24 (m, 3H), 7.12 – 7.00 (m, 2H), 4.59 (s, 2H), 4.52 (s, 2H). ^{13}C NMR (101 MHz, MeOD) δ 165.78, 163.58 (d, *J* = 244.2 Hz), 158.09, 138.70, 137.42, 136.73, 136.40, 135.62 (d, *J* = 3.4 Hz), 135.59, 130.79 (d, *J* = 8.2 Hz), 130.33, 126.68, 125.40, 116.23 (d, *J* = 21.7 Hz), 115.23, 112.49, 105.31, 49.34, 44.24. UPLC/MS: t_r 1.75 min, *m/z* 432.4 $[M+H]^+$, purity > 99%. HRMS: mass calculated for $C_{23}H_{23}N_7OF$: 432.1948; found: 432.1956.

***N*-Cyclopentyl-3-((4-guanidinobenzyl)amino)imidazo[1,2-*a*]pyridine-7-carboxamide (5.18d).**

Boc deprotection of compound **5.17d** was done using the general procedure E, affording the title compound **(5.18d)** as a yellow oil (0.09 mg, 100%). ^{1}H NMR (400 MHz, MeOD) δ 8.61 (dd, *J* = 7.2, 0.9 Hz, 1H), 8.22 (dd, *J* = 1.6, 1.0 Hz, 1H), 7.79 (dd, *J* = 7.2, 1.6 Hz, 1H), 7.59 (d, *J* = 8.5 Hz, 2H), 7.33 – 7.26 (m, 3H), 4.52 (s, 2H), 4.40 – 4.28 (m, 1H), 2.13 – 2.00 (m, 2H), 1.88 – 1.74 (m, 2H), 1.72 – 1.57 (m, 4H). ^{13}C NMR (101 MHz, MeOD) δ 165.69, 158.09, 138.73, 137.93, 136.76, 136.33, 135.59, 130.34, 126.68, 125.26, 115.43, 112.34, 105.22, 53.56, 49.36, 33.32, 24.96. UPLC/MS: t_r 0.60 min, *m/z* 392.6 $[M+H]^+$, purity > 99%). HRMS: mass calculated for $C_{21}H_{26}N_7O$: 392.2199; found: 392.2180.

3-((4-Guanidinobenzyl)amino)-*N*-(2-hydroxyethyl)imidazo[1,2-*a*]pyridine-7-carboxamide (5.18e).

Boc deprotection of compound **5.17e** was done following the standard procedure for deprotection of Boc groups using HCl/Dioxane. A solution of HCl/dioxane (4M, 2 mL) was cooled by an ice-water bath under nitrogen gas. Compound **5.17e** (65 mg, 0.115 mmol) was added in one portion to this solution, and the reaction mixture was stirred for 2 h at rt. After that time, volatiles were evaporated and the obtained product was washed with diethyl ether (2 x 5 mL) yielding HCl-salt of the title compound **5.18e** as a yellow solid (0.05 g, 98%). ^{1}H NMR (400 MHz, MeOD) δ 8.67 (dd, *J* = 7.3, 0.8 Hz, 1H), 8.27 (dd, *J* = 1.5, 0.9 Hz, 1H), 7.81 (dd, *J* = 7.2, 1.6 Hz, 1H), 7.61 (d, *J* = 8.5 Hz, 2H), 7.33 (s, 1H), 7.30 (d, *J* =

8.5 Hz, 2H), 4.53 (s, 2H), 3.75 (t, *J* = 5.7 Hz, 2H), 3.56 (t, *J* = 5.7 Hz, 2H). ^{13}C NMR (101 MHz, DMSO) δ 163.21, 156.09, 136.46, 134.71, 134.44, 134.35, 128.94, 124.47, 124.23, 113.67, 111.30, 102.78, 59.41, 47.11, 42.71. UPLC/MS: t_r 0.25 min, *m/z* 368.4 $[M+H]^+$, purity: 96%. HRMS: mass calculated for $C_{18}H_{22}N_7O_2$: 368.1835; found: 368.1823.

3-((4-Guanidinobenzyl)amino)-*N*-(2-(4-methylpiperazin-1-yl)ethyl)imidazo[1,2-*a*]pyridine-7-carboxamide (5.18f). Boc deprotection of compound **5.17f** was done using the general procedure E, affording the title compound **(5.18f)** as an orange oil (0.06, 97%). ^{1}H NMR (400 MHz, MeOD) δ 8.63 (dd, *J* = 7.3, 0.9 Hz, 1H), 8.29 – 8.25 (m, 1H), 7.80 (dd, *J* = 7.3, 1.6 Hz, 1H), 7.59 (d, *J* = 8.5 Hz, 2H), 7.32 (s, 1H), 7.30 (d, *J* = 8.5 Hz, 2H), 4.52 (s, 2H), 3.73 (t, *J* = 5.9 Hz, 2H), 3.54 –3.26 (m, 8H), 3.12 (t, *J* = 5.9 Hz, 2H), 2.92 (s, 3H). ^{13}C NMR (101 MHz, MeOD) δ 166.40, 158.08, 138.69, 137.06, 136.67, 136.42, 135.60, 130.33, 126.68, 125.30, 115.27, 112.64, 105.18, 57.27, 53.15, 50.70, 49.31, 43.46, 37.11. UPLC/MS: t_r 0.25 min, *m/z* 450.6 $[M+H]^+$, purity: 97%.

5.8.2. Biochemical assays

All commercially available research consumables were obtained as described in the Experimental section of Chapter 4, as well as information with regard to the equipment used for the biochemical assays, and software used for data collection and analysis.

The synthesized imidazo[1,2-*a*]pyridine derivatives **5.7h, 5.8a-g, 5.10a-k, 5.12a-b, 5.15a-i, 5.18a-f** were evaluated for their inhibitory activity against uPA. Inhibitor kinetic assays were using urokinase plasminogen activator (human enzyme; HYPHEN BioMed) and the chromogenic substrate BIOPHEN CS-61(44). The IC_{50} values were determined using a spectrophotometric assay as described in Chapter 4. All compounds were initially screened at three concentrations (100 μM, 10 μM and 1 μM) in order to estimate the range of the IC_{50} value. Those which were able to reduce uPA activity by at least 50% at 100 μM concentration were submitted to an exact IC_{50} determination. Final IC_{50} values of the most potent inhibitors were the average of three independent experimental results (e.g, **Figure 5.5**). Additionally, control experiments using commercial inhibitors were included, and they involved: guanidinophenyl fragment (**5.19**), uPA Inhibitor II: UK122 (**5.1**, Santa Cruz Biotechnology), gabexate mesylate (**5.2**, Enzo Life Sciences), amiloride (**5.3**, Selleckchem).[14-17]

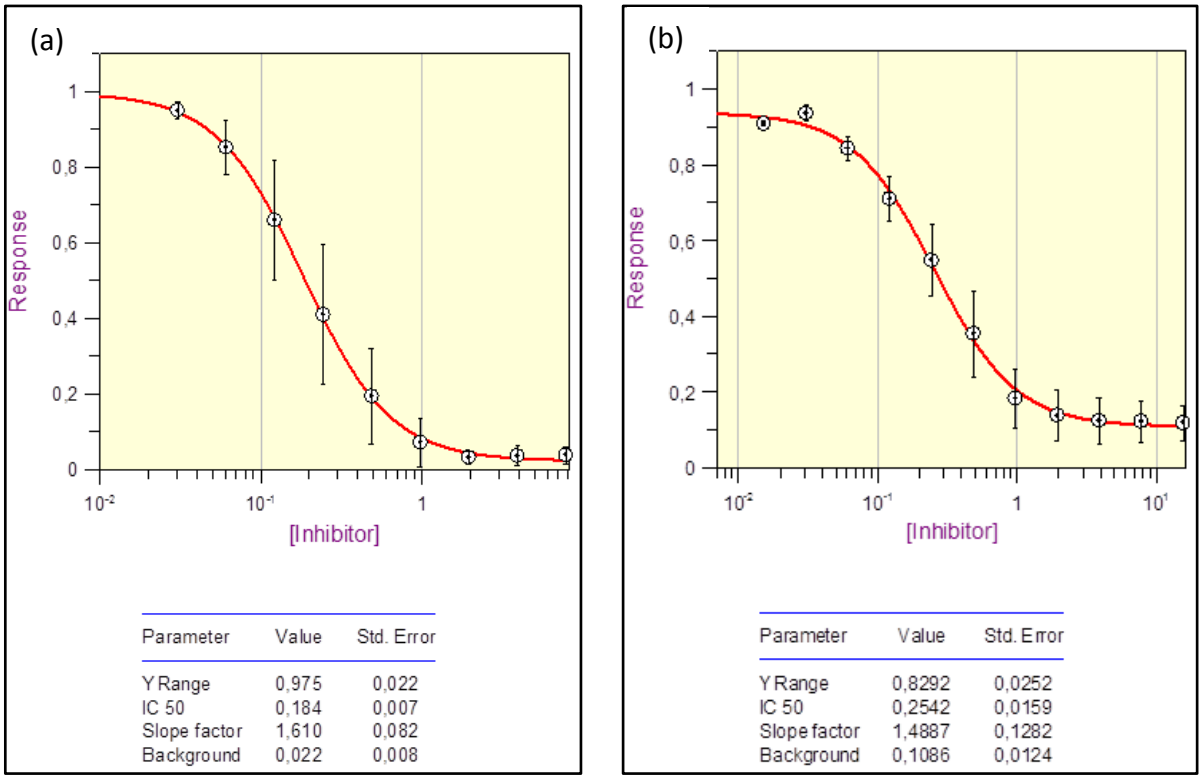

Figure 5.5. Determination of the IC_{50} (uPA) value exemplified for (a) compound 5.18b and (b) compound 5.18c.

Determination of the selectivity for uPA

The inhibitor kinetic assays and determination of the IC_{50} values for thrombin, tPA, FXa, plasmin, plasma kallikrein, trypsin, and FVIIa were performed in the same manner as for uPA, using HEPES buffer at pH 8.2 for thrombin, tPA, and FXa, at pH 7.0 for plasmin, at pH 7.4 for plasma kallikrein, trypsin, and HEPES buffer at pH 7.5 (50 mM HEPES, 100 mM NaCl, 5 mM $CaCl_2$, 0.1% BSA) for FVIIa. In case of the latter, the enzymatic assay was performed in the presence of tissue factor Innovin® from Dade Behring (Deerfield, IL, USA). For each of the enzymes a specific chromogenic substrate was used. The substrates were obtained from HYPHEN BioMed or Sigma-Aldrich. In case of thrombin (from human plasma, Sigma), the activated protein C chromogenic substrate Biophen CS-21(66) (pyro-Glu-Pro-Arg-pNA-HCl, K_m = 400 µM) was used at 415 µM concentration in assay. In case of tPA (recombinant human tPA, HYPHEN BioMed), the tPA and broad spectrum chromogenic substrate Biophen CS-05(88) (H-D-Ile-Pro-L-Arg-pNA-2HCl, K_m = 1 mM) was used at 1 mM concentration. As for Factor Xa (purified human Factor Xa, HYPHEN BioMed), the factor Xa chromogenic substrate Biophen CS-11(32) (Suc-Ile-Glu(γPip)-Gly-Arg-pNa-HCl) was used at 411 µM concentration. In case of plasmin (from human plasma, Sigma-Aldrich), the activated protein C chromogenic substrate, Biophen

CS-21(66) (pyro-Glu-Pro-Arg-pNA-HCl, K_m = 400 µM) was used at 400 µM concentration. In case of plasma kallikrein (from human plasma, Sigma-Aldrich), the kallikrein chromogenic substrate, Biophen CS-31(02) (D-Pro-Phe-Arg-pNA-2HCl, K_m = 269 µM) was used at 269 µM concentration. In case of trypsin (from bovine pancreas, Sigma), the trypsin chromogenic substrate, BAPNA (*N*α-benzoyl-D,L-Arg-pNA-HCl, K_m = 1 mM) was used at 425 µM concentration. As for FVIIa (from human plasma, purified, Enzo), the factor VIIa chromogenic substrate ($MeSO_2$-Cha-Abu-Arg-pNA) was used at 800 µM concentration. Selectivity assays included the guanidinophenyl fragment (**5.19**), as well as previously reported uPA inhibitors UK-122 (**5.1**), gabexate (**5.2**), and amiloride (**5.3**) as positive controls.[14-17] Selectivity data are summarized in **Table 5.8**.

5.8.3. Molecular modeling

Proposed binding conformations of compounds **5.8a, 5.8b** and **5.18a-f** in the binding pocket of uPA were generated starting from the protein crystal structure of human uPA in a complex with 1-phenylguanidine (PDB code 2O8W[18,19]). Visualization of the crystal structure was done with PyMol,[20] and compounds **5.8a** and **5.8b** were docked in the active site using **AutoDock 4.2**[21] with standard parameters and after manually removing the 1-phenylguanidine ligand from its crystal structure. Compounds **5.18a-f** were generated from the docked structure of compound **5.8a** by manually building the *N*-substituted amide fragment onto the imidazopyridine ring system of compound **5.8a** using optimal bond lengths, bond angles, and torsion angles.

References

(1) Gladysz, R.; Cleenewerck, M.; Joossens, J.; Lambeir, A.-M.; Augustyns, K.; Van der Veken, P. Repositioning the Substrate Activity Screening (SAS) Approach as a Fragment-Based Method for Identification of Weak Binders. *ChemBioChem* **2014**, *15*, 2238–2247.

(2) Groebke, K.; Weber, L.; Mehlin, F. Synthesis of Imidazo[1,2-*a*] Annulated Pyridines, Pyrazines and Pyrimidines by a Novel Three-Component Condensation. *Synlett* **1998**, 661–663.

(3) Blackburn, C.; Guan, B.; Fleming, P.; Shiosaki, K.; Tsai, S. Parallel Synthesis of 3-Amino-imidazo[1,2-*a*]pyridines and Pyrazines by a New Three-Component Condensation. *Tetrahedron Lett.* **1998**, *39*, 3635–3638.

(4) Bienaymé, H.; Bouzid, K. A New Heterocyclic Multicomponent Reaction for the Combinatorial Synthesis of Fused 3-Aminoimidazoles. *Angew. Chem. Int. Ed.* **1998**, *37*, 2234–2237.

(5) (a) Bagdi, A. K.; Santra, S.; Monir, K.; Hajra, A. Synthesis of Imidazo[1,2-*a*]pyridines: A Decade Update. *Chem. Commun.* **2015**, *51*, 1555-1575. (b) Devi, N.; Rawal, R. K.; Singh, V. Diversity-Oriented Synthesis of Fused-Imidazole Derivatives via Groebke–Blackburn–Bienaymé Reaction: A Review. *Tetrahedron* **2015**, *71*, 183–232. (c) Crestani, F.; Martin, J. R.; Möhler, H.; Rudolph, U. Mechanism of Action of the Hypnotic Zolpidem *in vivo*. *Br. J. Pharmacol.* **2000**, *131*, 1251-1254. (d) Mizushige, K.; Ueda, T.; Yukiri, K.; Suzuki, H. Olprinone: A Phosphodiesterase III Inhibitor with Positive Inotropic and Vasodilator Effects. *Cardiovasc. Drug Rev.* **2002**, *20*, 163-174. (e) Boggs, S.; Elitzin, V. I.; Gudmundsson, K.; Martin, M. T.; Sharp; M. J. CXCR4 Antagonist (GSK812397). *Synfacts* **2010**, 0011.

(6) Hartman, G. D.; Weinstock, L. M. Thiazoles from Ethyl Isocyanoacetate and Thiono Esters: Ethyl Thiazole-4-Carboxylate. *Organic Syntheses*; John Wiley & Sons: Hoboken, NJ, 1988; Vol. 6, p 620, 10.1002/0471264180.os059.26.

(7) Obrecht, R.; Herrmann, R.; Ugi, I. Isocyanide Synthesis with Phosphoryl Chloride and Diisopropylamine. *Synthesis* **1985**, 400.

(8) Dömling, A. Recent Developments in Isocyanide Based Multicomponent Reactions in Applied Chemistry. *Chem. Rev.* **2006**, *106*, 17–89.

(9) DiMauro, E. F.; Kennedy, J. M. Rapid Synthesis of 3-Amino-imidazopyridines by a Microwave-Assisted Four-Component Coupling in One Pot. *J. Org. Chem.* **2007**, *72*, 1013–1016.

(10) Lyon, M. A; Kercher, T. S. Glyoxylic Acid and MP-Glyoxylate: Efficient Formaldehyde Equivalents in the 3-CC of 2-Aminoazines, Aldehydes, and Isonitriles. *Org. Lett.* **2004**, *6*, 4989-4992.

(11) Frederickson, M.; Callaghan, O.; Chessari, G.; Congreve, M.; Cowan, S. R.; Matthews, J. E.; McMenamin, R.; Smith, D.-M.; Vinković, M.; Wallis, N. G. Fragment-Based Discovery of Mexiletine Derivatives as Orally Bioavailable Inhibitors of Urokinase-Type Plasminogen Activator. *J. Med. Chem.* **2008**, *51*, 183–186.

(12) Kiesewetter, M. K.; Scholten, M. D.; Kirn, N.; Weber, R. L.; Hedrick, J. L.; Waymouth, R. M. Cyclic Guanidine Organic Catalysts: What Is Magic about Triazabicyclodecene? *J. Org. Chem.* **2009**, *74*, 9490–9496.

(13) Joossens, J.; Van der Veken, P.; Surpateanu, G.; Lambeir, A.-M.; El-Sayed, I.; Ali, O. M.; Augustyns, K.; Haemers, A. Diphenyl Phosphonate Inhibitors for the Urokinase-Type Plasminogen Activator: Optimization of the P4 Position. *J. Med. Chem.* **2006**, *49*, 5785–5793.

(14) Zhu, M.; Gokhale, V. M.; Szabo, L.; Munoz, R. M.; Baek, H.; Bashyam, S.; Hurley, L. H.; Von Hoff, D. D.; Han, H. Identification of a Novel Inhibitor of Urokinase-Type Plasminogen Activator. *Mol. Cancer Ther.* **2007**, *6*, 1348–1356.

(15) Sperl, S.; Jacob, U.; Arroyo de Prada, N.; Stürzebecher, J.; Wilhelm, O. G.; Bode, W.; Magdolen, V.; Huber, R.; Moroder, L. (4-Aminomethyl)Phenylguanidine Derivatives As Nonpeptidic Highly Selective Inhibitors of Human Urokinase. *Proc. Natl. Acad. Sci. U. S. A.* **2000**, *97*, 5113–5118.

(16) *Inhibitor Expert (Inhibitors, Compound Libraries*; Selleck Chemicals: Houston, TX, 2013; http://www.selleckchem.com.

(17) *Enzo Life Sciences*; Enzo Life Sciences, Inc., 2015; http://www.enzolifesciences.com.

(18) Zhao, G.; Yuan, C.; Jiang, L.; Huang, Z.; Huang, M. (submitted for publication).

(19) Berman, H. M.; Westbrook, J.; Feng, Z.; Gilliland, G.; Bhat, T. N.; Weissig, H.; Shindyalov, I. N.; Bourne, P. E. The Protein Data Bank. *Nucleic Acids Res.* **2000**, *28*, 235–242.

(20) PyMol: *The PyMOL Molecular Graphics System*, version 1.5.0.4; Schrödinger LLC; http://www.pymol.org.

(21) Morris, G. M.; Huey, R.; Lindstrom, W.; Sanner, M. F.; Belew, R. K.; Goodsell, D. S.; Olson, A. J. Autodock4 and AutoDockTools4: Automated Docking with Selective Receptor Flexiblity. *J. Comput. Chem.* **2009**, *30*, 2785–2791.

Chapter 6

Discussion on SAS and related approaches in medicinal chemistry: strategic advances and lessons learned

The content of this chapter is based on:

Gladysz, R.; Lambeir, A.-M.; Joossens, J.; Augustyns, K.; Van der Veken, P. Substrate Activity Screening (SAS) and Related Approaches in Medicinal Chemistry, *ChemMedChem*, **2016**, *11*, 467–476.

6. Discussion on SAS and related approaches in medicinal chemistry: strategic advances and lessons learned

6.1. Introduction

Substrate activity screening (SAS) was presented in 2005 by Ellman and co-workers as a straightforward approach to inhibitor discovery for enzymatically active drug targets.[1-3] SAS draws on the principle that enzymes typically display affinity for the substrates they process, and uses affinity-conferring substructures of optimized substrates as the basis for inhibitor design. In its simplest form, inhibitors can be obtained by replacing the enzyme-processable function in a substrate by a reactive "warhead" group or a non-processable surrogate. While strategies of this kind are well known and have been central to the practice of enzyme inhibitor discovery during the past decades, SAS has several characteristics that set it apart from the traditional approaches. Most importantly, SAS does not depend on screening collections of natural enzyme substrates or derived molecules. The approach typically uses libraries of small molecule constructs, consisting of a druglike residue that is chemically linked to a functional group that can be processed by the enzyme target. The latter requires that the residue has affinity for the target and binds in the proper orientation and conformation to be converted by the catalytic groups in the enzyme's active site. Furthermore, the druglike residues are generally chosen to be small, fragment-sized entities (typically 10-15 heavy atoms or less), allowing for efficient sampling of chemical space. Seen from this perspective, SAS can be regarded as belonging to the realm of fragment-based drug design (FBDD) methodologies. The fact that enzymatic processing is used here as a proxy for target affinity makes the approach complementary and orthogonal to a number of (bio-)physical experiment types that FBDD uses for the identification of promising fragments, such as X-ray crystallography, NMR-based techniques, surface plasmon resonance (SPR), mass spectrometry, and isothermal titration calorimetry (ITC).

A typical SAS campaign consists of three steps (**Scheme 6.1**). First, a SAS-library is screened for substrates of the target (**step 1, Scheme 6.1**). Identified "hits" are ranked using specific protocols (*vide infra*) and the best substrates that are identified in this manner are structurally optimized during the next step (**step 2**). This step consists of (eventually) iterative cycles of analogue synthesis and evaluation. Finally, the optimized substrates are transformed into inhibitors (step 3). As explained, this can be done by replacing the processable bond with a mechanism-based warhead or a non-processable surrogate. Nonetheless, other strategies can be followed as well, and our recent work also demonstrated that SAS "hits" can be used as the structural basis for reversible, competitive small molecule inhibitors that do not rely on interaction with catalytically active residues of the target enzyme.[4]

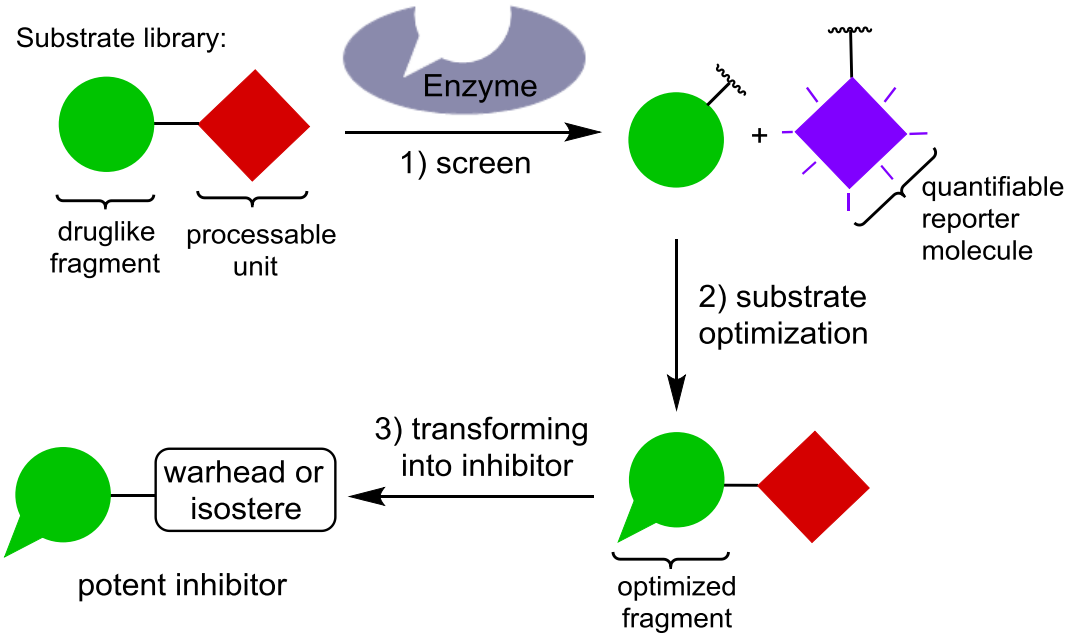

Scheme 6.1. Schematic representation of a typical SAS-approach.

In the following part, an exhaustive literature review will be given of inhibitor discovery studies that have relied on SAS. Relevant aspects of the experimental set-ups of these studies will be highlighted and discussed, including library design and the different screening modes that have been reported for SAS-libraries. The second part of the review will deal with the transformation of SAS-"hits" into potent enzyme inhibitors. Here, the different approaches to substrate ranking based on experimental parameters that define substrate properties, will be discussed (e.g., k_{cat}, K_m, k_{cat}/K_m, substrate processing rate). Thorough understanding of these parameters and ranking systems is crucial for efficiently transforming a substrate into an inhibitor. Finally, considerations on warhead selection will be presented, an issue that is of importance in cases where mechanism-based enzyme inhibitors are specifically desired.

6.2. SAS-studies reported in literature

Most of the reported SAS-based methodologies have focused on the identification of inhibitors for protease targets belonging to the cysteine, serine, and metalloprotease superfamilies. During the past years, a relatively small number of other target classes have been successfully addressed as well, comprising protein tyrosine phosphatases, protein tyrosine kinases, and deiminases. Although these recent reports do confirm the general concept of SAS for enzyme inhibitor discovery, it is certainly too early to claim that the domain has reached maturity and is fully developed. An obvious rationale for the overall limited target scope so far can be sought in the fact that for each new type of

enzymatic activity, a dedicated library has to be synthesized, the members of which contain a functional group that is processable by the enzyme studied. Although the initial effort can therefore be significant, a prepared library can be screened multiple times with different enzyme targets that share the same catalytic principles (**Table 6.1**).

Table 6.1. Overview of the reported SAS-libraries.

Substrate library (R = druglike fragment)	**Enzyme**
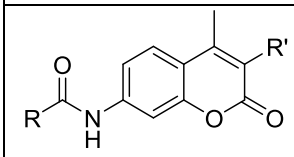 R' = H or CH_2COOH	cysteine protease (cathepsin S, cruzain, caspases)[1,5-7]
	serine protease (chymotrypsin, uPA)[2,17]
	metallopeptidase (APN)[9]
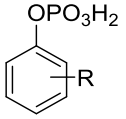	protein tyrosine phosphatase (PTP; PtpB, PtpA, STEP)[3,10,11]
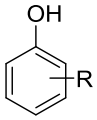	protein tyrosine kinases (receptor tyrosine kinase, c-Src)[13,15]
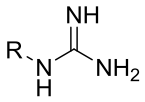	protein arginine deiminase (PAD; PAD3)[16]

The initial publication by Ellman and co-workers[1] describes the application of SAS for the discovery of two distinct classes of novel, nonpeptidic inhibitors of cysteine protease cathepsin S, a target that has been linked to autoimmune diseases such as rheumatoid arthritis and multiple sclerosis. In this study, a library of 105 *N*-acylaminocoumarins was screened. Such molecules release a fluorescent 7-aminocoumarin (AC) derivative upon processing by a protease target, allowing both fluorometric identification of substrates and quantification of the amidolysis rate. Substituted 1,2,3-triazolyl and phenoxyacetyl substrates were identified as "hits". Next, a focused library consisting of analogues of the most efficient substrates was prepared and assayed during the optimization step. Finally, the optimized 1,4-disubstituted-1,2,3-triazole-based substrates were converted into nanomolar inhibitors of cathepsin S *via* the introduction of an aldehyde warhead (**Figure 6.1**, compound **6.1**, K_i = 9 nM). However, the highly reactive aldehyde warhead was found to discount on the selectivity of the obtained inhibitors. As reported by Patterson et al.[5], the SAS approach and substrate optimization guided by a co-crystallized structure of a triazole-based inhibitor and cathepsin S, allowed for a tenfold increase in catalytic efficiency of the 1,4-disubstituted-1,2,3-triazole-based

substrates. Subsequently, the optimized substrate fragments were transformed into potent nitrile cathepsin S inhibitors (compound **6.2**, K_i = 15 nM) with more than 1000-fold selectivity over the highly homologous cathepsins B, K, and L. In another example, the SAS method was used for inhibitor discovery for cruzain, a cysteine protease of *Trypanosoma cruzi*, the causative agent of Chagas disease. The triazole-based substrate library developed for cathepsin S was used again for identification of initial hits.[1,5] The subsequent substrate optimization was guided by structure-based design and resulted in the identification of a quinoline amine substrate. For transformation of this substrate into an inhibitor, a number of warheads were investigated among which a vinyl sulfone, a β-chloro vinyl sulfone, and acyl- and aryloxymethyl ketone. Finally, 2,3,5,6-tetrafluorophenoxymethyl ketone **6.3** was identified as one of the most potent inhibitors of cruzain (compound **6.3**, k_{inact}/K_i = 147 000 ± 6790 M^{-1} s^{-1}).[6] The SAS methodology was also used to identify pan-caspase inhibitors for evaluation in Huntington's Disease (HD) models. In this study, another library of *N*-acylcoumarins was screened against caspase-3 and -6, to identify 1,2,3-triazole-based substrates with high cleavage efficiencies. Subsequently, three substrates with the highest relative k_{cat}/K_m values were converted into novel 2,3,5,6-tetrafluorophenoxymethyl ketone pan-caspase inhibitors, which inhibit proteolysis of the huntingtin gene (Htt) at caspase-3 and -6 cleavage sites (k_{inact}/K_i > 20 000 $M^{-1}s^{-1}$).[7] Application of the SAS approach to serine proteases was first demonstrated for chymotrypsin. Screening of a library of 161 diverse nonpeptidic substrates resulted in the identification of a novel 3-phenyl-isoxazoline scaffold. The optimized substrate was converted into a potent phosphonate inhibitor of chymotrypsin (compound **6.4**, k_{inact}/K_i = 59 000 ± 7000 M^{-1} s^{-1}) with high selectivity over the related serine proteases cathepsin G, elastase, and trypsin.[2]

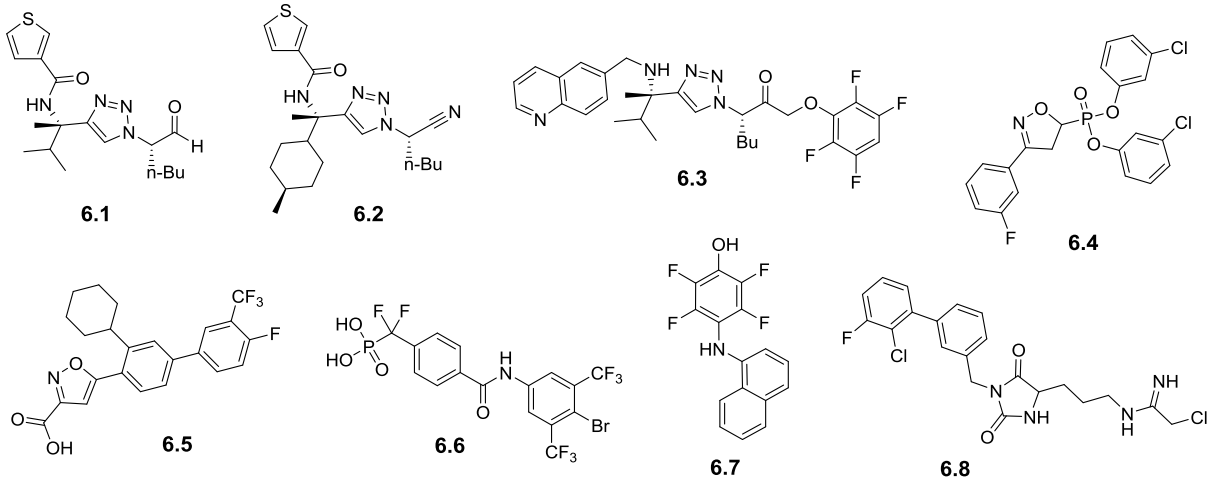

Figure 6.1. Examples of inhibitors discovered using the SAS approach.

Another group of proteases to which SAS was applied are metallopeptidases, relevant pharmaceutical targets implicated in events like cell survival, defense, growth, and development.[8] In this study, a library of 61 individual natural and unnatural amino acid substrates, again equipped with a 7-aminocoumarin fluorophore were screened against human, pig, and rat ortologs of aminopeptidase N (APN), and the identified substrates were converted into the corresponding *α*-aminophosphonate inhibitors.[9]

Furthermore, the SAS methodology has also been successfully used in phosphatase inhibitor development. Initially, it was applied to the *Mycobacterium tuberculosis* protein tyrosine phosphatases (PTPs), PtpA and PtpB. In the report by Soellner and co-workers[3], a 140-member library of *O*-aryl phosphates was screened against PtpB using a spectrophotometric assay for the quantification of inorganic phosphate released upon enzyme-catalyzed substrate hydrolysis. In addition, the optimized substrates were converted into inhibitors by replacement of the phosphate moiety with a non-hydrolyzable phosphate isostere: isoxazole carboxylic acid. The obtained inhibitor showed nanomolar potency against PtpB (compound **6.5**, K_i = 220 nM) as well as good selectivity against a panel of mycobacterial (PtpA) and human PTPs. In another study, the same substrate library was screened against PtpA. The identified fragments were directly used for the construction of inhibitors containing another non-hydrolyzable phosphate isostere: the difluoromethylphosphonate (DFMP) group. Further SAR studies resulted in selective inhibitor of PtpA based on the benzanilide scaffold (compound **6.6**, K_i = 1.4 μM).[10] Additionally, a more recent report describes application of SAS to inhibitor discovery for striatal-enriched protein tyrosine phosphatase (STEP), overexpressed in many neuropsychiatric disorders, such as Alzheimer's disease. Screening the previously used library of *O*-aryl phosphates against STEP identified 4- and 3-biaryl scaffolds, which were transformed into DFMP inhibitors.[3] Further exploration of SAR for these structures yielded nonpeptidic STEP inhibitors with low micromolar inhibition, and 20-fold selectivity over multiple human PTPs.[11]

Another class of enzymes to which the SAS method has been applied, are protein tyrosine kinases, recognized as promising therapeutic targets in cancer, diabetes, rheumatoid arthritis, and hypertension.[12] Seebach and co-workers[13] provided a proof-of-concept for application of SAS to the development of peptidic inhibitors of receptor tyrosine kinase. In this study, a known efficient tetrapeptide substrate was used as a starting point for the synthesis of a focused library of phenols. The library was then screened for kinase-mediated phosphorylation, and further optimized. Finally, the most efficient substrate was converted to the most potent inhibitor (IC_{50} = 2.5 ± 0.8 μM) upon replacement of the tyrosine moiety with a hydroxymethyltyrosine phosphate, being a tyrosine phosphorylation transition state mimetic. In a more recent report, SAS was applied to the discovery of nonpeptidic substrate-competitive inhibitors of c-Src, a protein tyrosine kinase overexpressed in

case of many cancer types.[14] According to the SAS method proposed by Soellner and co-workers[15] first a library of 88 phenols selected by computational clustering analysis was screened by using a luciferase-based assay. Identification of nine substrate hits and subsequent selectivity studies against two homologous kinases led to the selection of *p*-aniline phenol. Fluorinating the selected substrate afforded the initial tetrafluorophenol inhibitor. Its further optimization resulted in a substrate-competitive inhibitor of c-Src (compound **6.7**, K_i = 16 μM).

The most recent application of SAS served the discovery of nonpeptidic small molecule inhibitors of deiminase 3 (PAD3), the protein arginine deiminase (PAD) subtype implicated in the neurodegenerative response to spinal cord injury. In this report, a library of more than 200 guanidine substrates was screened against PAD3 using a colorimetric coupled assay for the detection of urea-containing compounds. It allowed for the identification of hydantoin, benzyl hydantoin and benzylamide scaffolds for further optimization. Finally, the most efficient substrate from each series was converted into the corresponding inhibitor upon replacement of the guanidine moiety with a chloroacetamidine warhead. It resulted in potent, structurally distinct inhibitors of PAD3 with ≥ 10-fold selectivity over PADs 1, 2, and 4 (compound **6.8**, k_{inact}/K_i = 17400 ± 2400 M^{-1} s^{-1}).[16]

A summary of the applications of the "canonical" SAS methodology is given in **Table 6.2**. Although the approach has been remarkably successful, there are a number of aspects which, in our opinion, could benefit from additional attention; (1) the design of the substrate library, (2) the design of an efficient screening assay, (3) the thermodynamic and kinetic analysis of substrate properties, and (4) the selection of an appropriate warhead or isostere.

Table 6.2. Overview of applications of the SAS method in inhibitor discovery.

Enzyme family	Enzyme	Substrate library	Optimization strategy	Derived inhibitor		Ref.
				warhead / isostere	Substrate-inhibitor correlation	
cysteine protease	cathepsin S	*N*-acyl ACs (105 members)	substrate hit optimization (analogue synthesis)	aldehyde	transition-state analogue	Wood et al.[1], 2005
	cathepsin S	*N*-acyl ACs	substrate hit optimization (analogue synthesis)	nitrile	transition-state analogue	Patterson et al.[5], 2006
	cruzain	*N*-acyl ACs (>150-member focused library for cathepsin S)[1,5]	substrate hit optimization (structure-based design)	2,3,5,6-tetrafluoro-phenoxymethyl ketone	transition-state analogue	Brak et al.[6], 2008
	caspases	*N*-acyl ACs	substrate hit optimization (analogue synthesis, structure-based design)	2,3,5,6-tetrafluoro-phenoxymethyl ketone	transition-state analogue	Leyva et al.[7], 2010
serine protease	chymotrypsin	*N*-acyl ACs (initial:161 members; focused: 24)	substrate hit optimization (analogue synthesis)	phosphonate	transition-state analogue	Salisbury et al.[2], 2006
metallo-peptidase	aminopeptidase N (APN); human, pig, rat ortologs	*N*-acyl ACs (61 members)	-	*α*-amino-phosphonate	ground-state analogue	Drag et al.[9], 2010
protein tyrosine phosphatase (PTP)	PtpB	*O*-aryl phosphates (initial:140 members; focused: 45)	substrate hit optimization (analogue synthesis)	isoxazole carboxylic acid (phosphate isostere)	ground-state analogue	Soellner et al.[3], 2007

	PtpA	*O*-aryl phosphates (developed for PtpB)[3]	inhibitor optimization (analogue synthesis)	difluoromethyl-phosphonate (DFMP)	ground-state analogue	Rawls et al.[10], 2009
	STEP	*O*-aryl phosphates (developed for PtpB, PtpA)[3,10]	inhibitor optimization (analogue synthesis)	DFMP	ground-state analogue	Baguley et al.[11], 2013
protein tyrosine kinases	receptor tyrosine kinase	focused peptide library of phenols	optimization of a known peptidic substrate (tetrapeptide)	hydroxymethyl-tyrosine phosphate	transition-state mimetic	Chapelat et al.[13], 2012
	c-Src	phenols (88 members)	inhibitor optimization	tetrafluorophenol	ground-state analogues	Breen et al.[15], 2014
protein arginine deiminase (PAD)	PAD3	guanidines (>200 members, then focused libraries)	substrate hit optimization	chloroacetamidine	transition-state; ground-state analogues	Jamali et al.[16], 2015

6.3. Design of the substrate library

Apart from the most recent example by Jamali et al.[16], all initial SAS libraries reported so far counted less than 200 members (**Table 6.2**). In addition, most libraries were significantly biased by focusing largely on chemical functionalities that are known recognition elements for the target enzymes. Although details on the rationale behind the library design were in most cases not provided, it can be assumed that even for fragment-sized sets, libraries of < 200 members cover only a relatively limited part of chemical space; the chances for identifying structurally original fragments are therefore relatively small. Our own experiences with urokinase, caspase-4 and autophagin-1 inhibitor discovery indeed illustrate that identifying substrate "hits" among the non-biased (i.e. purely diversity-oriented) members of a SAS library of this size, is challenging.[17-19] In addition, a word of caution is required with respect to the repeated screening of the same substrate libraries on different targets within identical enzyme families. Although this feature, as mentioned, is interesting from a time/cost

efficiency perspective, it can also be expected that related or homologous enzymes may return identical substrate "hits".[6,10,11] Partially addressing these issues, more recent studies have used hierarchical, 2D extended connectivity analysis to guide library design, and this has been shown to have potential for the domain.[3,15,16] On the other hand, systematically implementing structure-based design during the substrate or inhibitor optimization process can not only facilitate the optimization process, but also resolve selectivity issues.[4-6,10]

6.4. Design of an efficient screening assay

Design of an efficient and sensitive screening assay is another crucial element of the SAS approach. Once established, the same screening methodology can be applied to every target within the same enzyme family. An optimal screening assay should preferably have a high throughput and be straightforward to perform, detect even very weak binders, avoid false positive and false negative results, and be cost- and time- efficient.

We have previously reported on MSAS (modified substrate activity screening) that combines optimal efficiency and maximum extraction of useful structural information during screening of SAS libraries (**Scheme 6.2**). Initially, we applied the classical SAS protocol to inhibitor discovery for urokinase plasminogen activator (uPA), a trypsin-like serine protease that is overexpressed in metastasizing solid tumours.[20,21] During our investigation, several shortcomings of the classical protocol were identified, the most important of which was the possibility of overlooking interesting fragments in the library. Using the established SAS approach, library fragments that possess affinity for the target's active center will only be identified if the processable unit to which they are linked, is positioned exactly in a way that allows interaction with the catalytic residues of the enzyme. Even small structural deviations from the ideal situation lead to a loss of substrate properties. This implies both a low hit rate during screening and the necessity to cover larger parts of chemical space around each structure type present in the library.[17]

In response, we devised an alternative experimental setup for library evaluation. In MSAS, the library is first screened for competitive, inhibitory fragments (**step 1, Scheme 6.2**). This step provides SAR data for all fragment types with target affinity that are present within the library. Step 1 also consumes significantly less enzyme and runs with higher time efficiency than the traditional SAS protocol. The latter is therefore performed in the second phase of MSAS (**step 2, Scheme 6.2**) and only on the library subset of fragments that were found to possess target affinity.

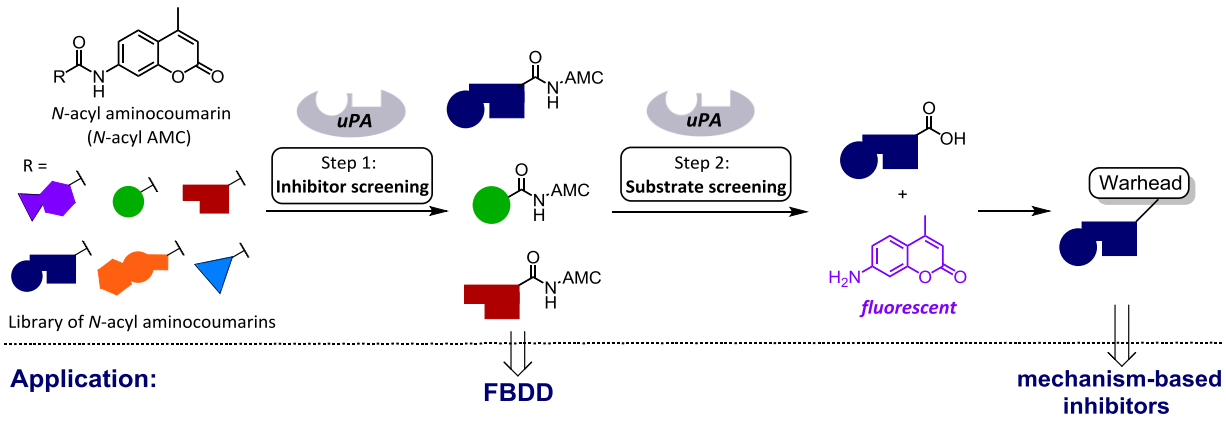

Scheme 6.2. Outline of the MSAS approach (adapted from Gladysz et al.[17]).

Application of MSAS to our library identified, among others, the guanidinophenyl derivative **6.9** and its homologue **6.10** as interesting fragments for uPA inhibitor design, of which only **6.10** was found to be a substrate of uPA (**Scheme 6.3**). Valorization of the affinity data obtained during the inhibitor screen (step 1, MSAS) was based on preparation of imidazopyridine scaffold-based inhibitors of uPA (compounds **6.11, 6.12**). Optimization of the initial inhibitor (compound **6.11**) was extensively guided by molecular docking, and afforded a potent imidazo[1,2-*a*]pyridine uPA inhibitor (compound **6.13**, IC_{50} = 97 ± 10 nM) with more than 1000-fold selectivity for a panel of closely related enzymes (tissue-type plasminogen activator, thrombin, factor Xa, plasmin, plasma kallikrein, trypsin, factor VIIa).[4] Using the hit valorization strategy of the original SAS approach, substrate **6.10** was transformed into an inhibitor by grafting the 4-guanidinopenethyl moiety on the potentially irreversible diphenyl phosphonate warhead to afford a selective, low-nanomolar inhibitor of uPA (compound **6.15**, IC_{50} = 9.7 ± 0.3 nM).[17]

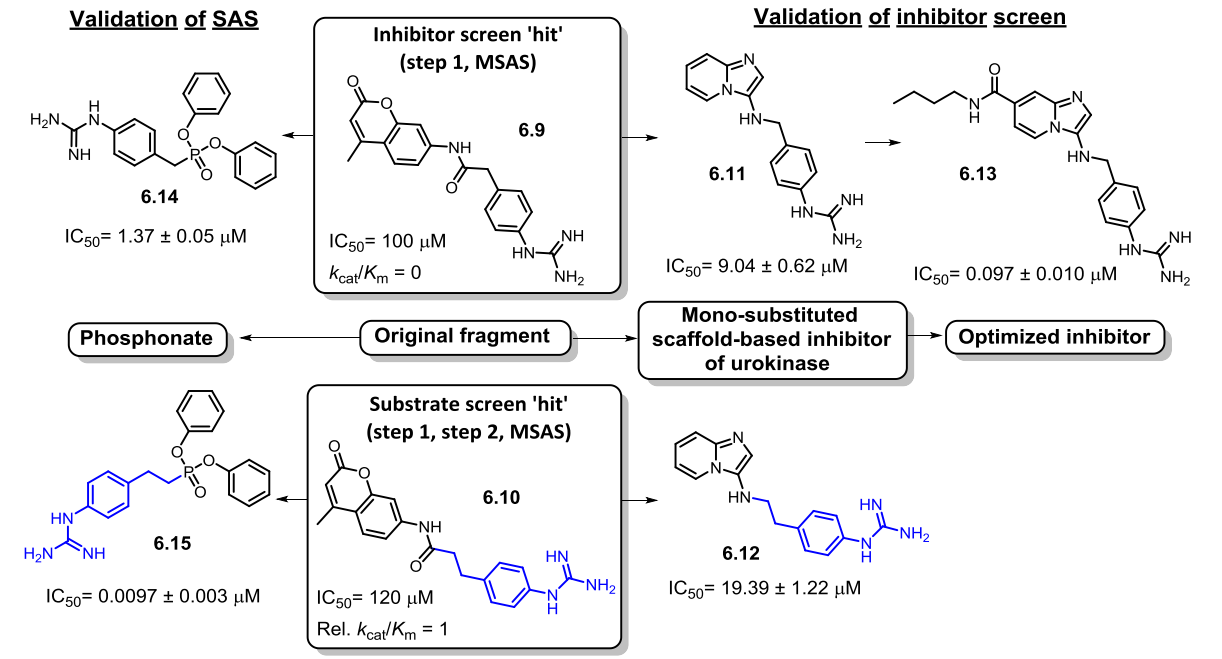

Rel. k_{cat}/K_m is defined as the "relative cleavage efficiency", so the cleavage rate of a given compound relative to the "best" substrate in the library (compound **6.10**). The substrates were assayed under sub-saturating substrate concentrations ([S] < K_m). Under these conditions the initial substrate conversion rate ("V_i") is proportional to k_{cat}/K_m. The exact k_{cat}/K_m-values were not determined.

Scheme 6.3. Two-fold validation of the MSAS approach.

We have also applied MSAS to inhibitor design for cysteine proteases: caspase 4 and the autophagy target Atg4B.[22-24] In both cases, application of the first step of MSAS allowed to identify fragments with target affinity, while the second step returned no hits. Results of the caspase 4 work have so far not been published.[18] In the Atg4B study, a novel screening method relying on in-gel densitometric quantification of Atg4B activity was used during the inhibitor screen of a 182-member SAS library. As a result, a 2-methylaminopyrazine fragment was identified as a competitive Atg4B inhibitor (IC_{50} in the high micromolar range) suitable for fragment-based Atg4B inhibitor discovery.[19]

Also a number of relevant literature examples show that target affinity and enzyme processing do not always go hand in hand for molecules with typical substrate architectures. The best-known case is that of methotrexate, an inhibitor of dihydrofolate reductase (K_i = 0.58 pM).[25] In spite of the high structural analogy of methotrexate and dihydrofolate, the pterin rings of these two ligands bind in opposite orientations in the enzyme active site. As a result, methotrexate does not act as a substrate but rather as a slow, tight-binding inhibitor of the enzyme.[26] In a recent study, a series of peptides were found to be inhibitors of β-secretase (BACE1), despite their structural similarity to the substrate of the enzyme (IC_{50} range: 82 - 169 μM). Interestingly, the reason for the inhibitory properties of these compounds is most probably the σ-π interaction occurring between the P2 region of the

peptides and BACE1-Arg235, leading to a vastly reduced k_{cat} value.[27] In another example, substitution of five residues of mupain-1, a 10-mer peptidic inhibitor of murine uPA (K_i = 0.55 μM), afforded a potent and selective inhibitor (K_i = 0.014 μM) of human plasma kallikrein (hPK). Interestingly, this inhibitor of hPK has several structural features of its natural substrates, and it binds to the enzyme in a substrate-like conformation.[28]

These examples re-confirm that the identification of potent fragments in a given library can be more efficient by investigating the inhibitory properties of the library members rather than their substrate characteristics. Furthermore, it is important to stipulate that the MSAS experimental setup, like that of the parent methodology, is not limited to protease inhibitor discovery. The same strategy can directly be applied to any other type of enzyme target, provided that the members of the library each contain a suitable enzyme-processable functionality.

6.5. Transforming substrates into inhibitors

The successful outcome of a SAS-campaign depends to a large extent on (1) being able to select the most promising "hits" from a library screen, and (2) applying an adequate strategy for transforming these "hits" into inhibitors. Critical for this ability is a thorough understanding of the kinetic and thermodynamic principles underlying both the enzymatic processing of substrates and the binding of inhibitors. By specifically binding the transition state (TS) with high affinity compared to the ground state, an enzyme lowers the free energy barrier that separates reactants from reaction products, allowing chemistry to proceed on a biologically relevant time scale. Enzymes typically bind the ground state of their substrates and then facilitate the formation of the transition state that is associated with the reaction they catalyze. A generalized interpretation of the thermodynamic relationship between ground state, transition state and formed products for both enzyme- and non-enzyme catalyzed reactions, is depicted in **Figure 6.2a**. This process, *via* a series of chemical equilibria, ultimately leads to formation of products. Relevant (kinetic) rate constants and (thermodynamic) dissociation constants that are associated with these equilibria are shown in **Figure 6.2b**.[29,30]

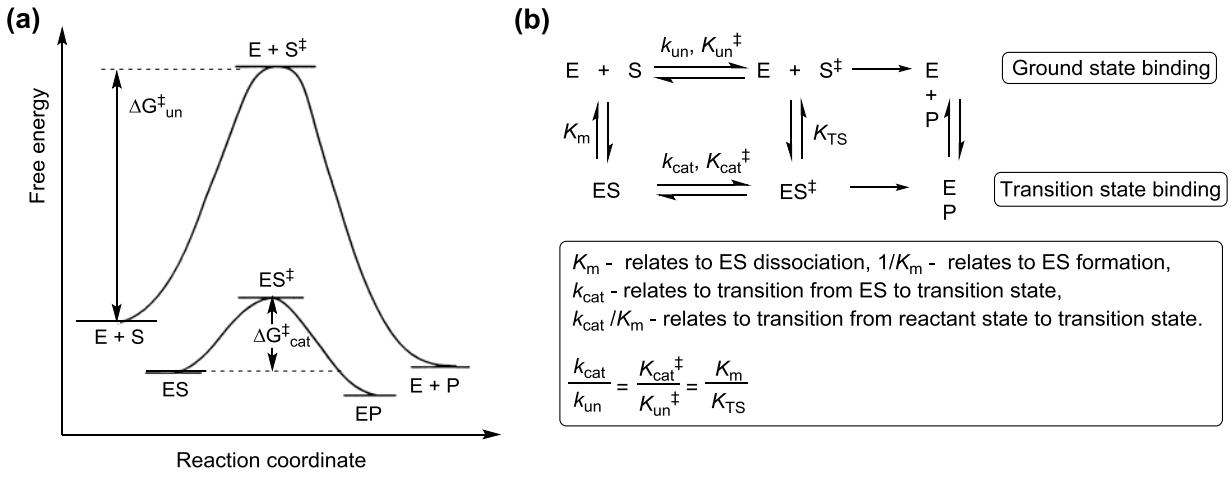

Figure 6.2. Thermodynamic and kinetic aspects of enzyme activity: (a) Free energy profile of a standard enzyme-catalyzed reaction. E, S, and P refer to enzyme, substrate and product, respectively. "$S^{‡}$" refers to the transition state form of a substrate. $\Delta G^{‡}_{cat}$ and $\Delta G^{‡}_{un}$ refer to the free energy of activation for enzyme catalyzed and noncatalyzed reaction, respectively. (b) Overview of chemical equilibria involved in enzyme and non-enzyme catalyzed substrate turnover. K_m (the Michaelis constant) and K_{TS} are dissociation constants for the ground and transition states of the enzyme-substrate complex, respectively. $K_{un}^{‡}$ and $K_{cat}^{‡}$ are pseudoequilibrium constants for the noncatalyzed and the enzyme-catalyzed reactions. k_{cat} is the first-order rate constant reflecting the catalytic turnover rate and k_{un} is the rate constant of the non-catalyzed reaction (adapted from Mader et al.[29] and Wolfenden et al.[30]).

Two of these parameters (k_{cat} and K_m) are crucial for successfully transforming an enzyme substrate in a corresponding, substrate-derived inhibitor. Such inhibitors ("Substrate analogs") are by definition competitive and can be divided into two primary categories, depending on the mechanism of binding: (1) transition state analogues and (2) ground state-based inhibitors (**Figure 6.3**).[9] Both types require different (k_{cat} and/or K_m-based) substrate ranking approaches during the design phase. They will be discussed separately below. The theoretical basis for these approaches had already been firmly established during the decades before the advent of SAS, as part of older strategies for substrate-based inhibitor discovery.[29]

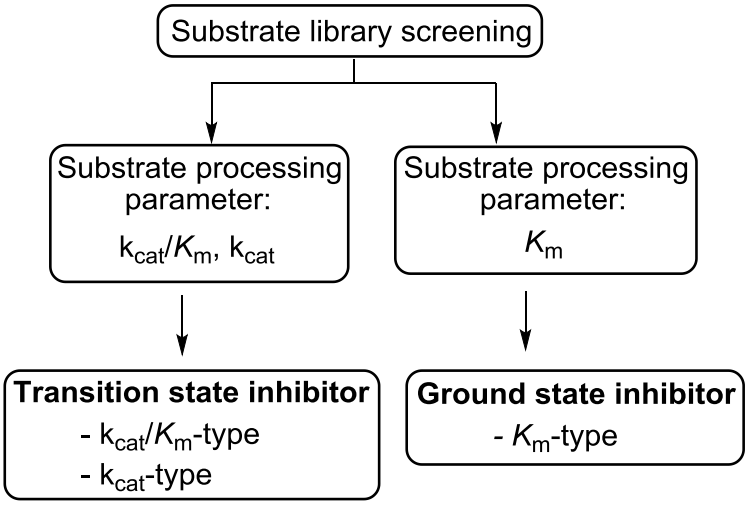

Figure 6.3. Overview of substrate processing parameters used in inhibitor design (adapted from Drag et al.[9]).

According to the transition state theory, the substrate in a transition state complex ($ES^{‡}$) will be considerably better stabilized by the enzyme than the ground state form in the Michaelis complex (ES) from which it is formed.[31] In general, if an enzyme catalyzed reaction proceeds faster than the uncatalyzed reaction ($k_{cat} > k_{un}$), the enzyme binds the transition state structure ($S^{‡}$) with an affinity enhanced over the substrate's ground state (S) by the same factor.[29,30,32] Therefore, inhibitors mimicking features of the transition state can be expected to form a much stronger complex with the enzyme than ground state-derived structures. The term "transition state analogue" is in most cases however not used very rigorously and applied to a wide range of enzyme inhibitors types that contain a substructure that mimics one or more features of the substrate's transition state. Well known examples include iminoribitol inhibitors of nucleoside hydrolases and phosphonamidate inhibitors of thermolysin.[33-35] Typically, the log(K_i)-values in a series of structurally related transition state analogues correlate linearly with the log(K_m/k_{cat})-values of the corresponding substrates from which they were derived (**Figure 6.4a**). Such inhibitors are classified as k_{cat}/K_m-type, as this parameter dominates the relationship between a substrate and the derived inhibitor. Additionally, many inhibitor types are known to adopt transition state features after an initial reaction with the catalytic machinery of the targeted enzyme. Relevant examples include inhibitor types equipped with reversible "warhead" functions, such as aldehyde and ketone inhibitors of serine and cysteine proteases.[1,36] Such molecules are also often referred to as transition state analogues and, noteworthy, also behave as k_{cat}/K_m-type inhibitors.

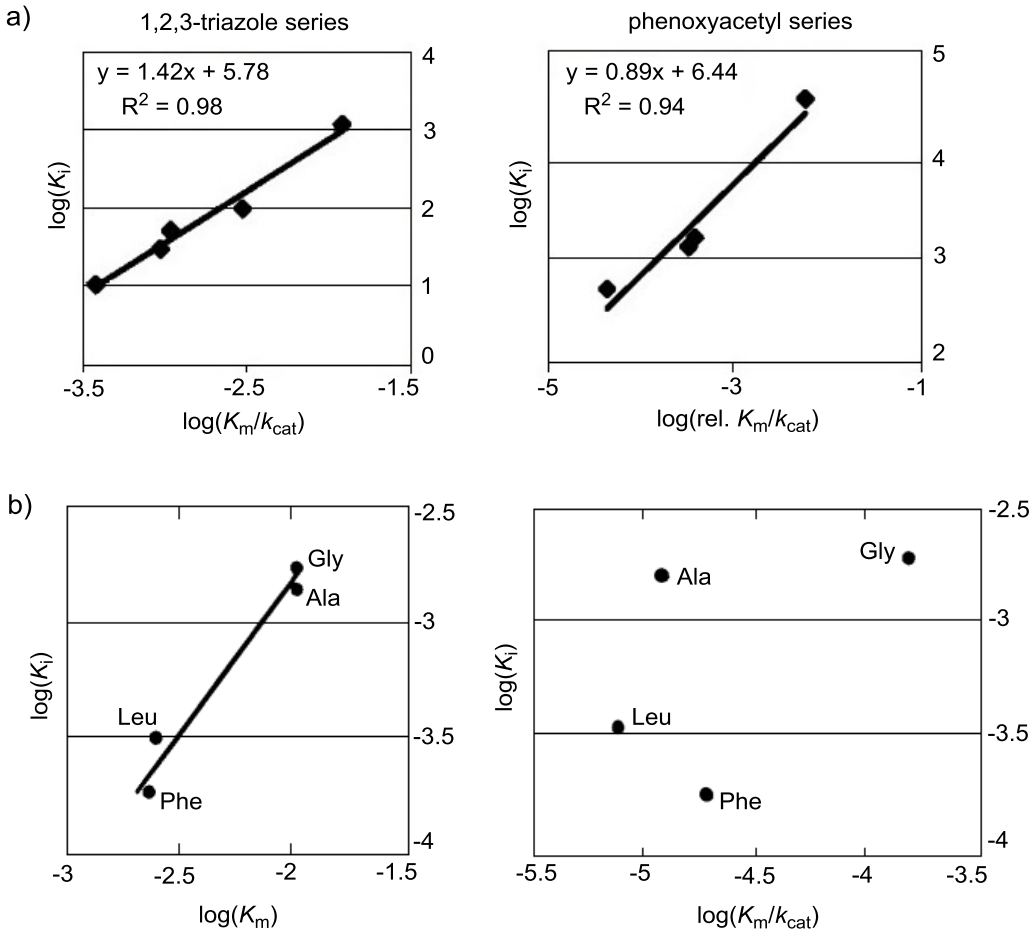

Figure 6.4. Plots showing a linear correlation between inhibitor log(K_i) values and log(K_m) or log(K_m/k_{cat}) values of the corresponding substrates expressed logarithmically for (a) triazole and phenoxyacetyl series of substrates and the corresponding aldehyde inhibitors of cathepsin S (reproduced with permission from Ref. 1: Wood et al., 2005); (b) peptide substrates and the corresponding fluoroalkene inhibitors of thermolysin (reproduced with permission from Ref. 39: Bartlett et al., 1995).

Finally, a third inhibitor subgroup is often, albeit more awkwardly, counted with the translation state analogues: inhibitors with an irreversible, mechanism-based "warhead" group. Examples include haloketone and acyloxymethylketone inhibitors of proteases.[37,38] Compounds of this type generally inactivate enzymes in a two-step process that bears similarity to the enzymatic processing of substrates. The first step consists of (non-covalent), affinity-based binding of the inhibitor to the target enzyme. It is characterized by an equilibrium constant (K_i) that can be envisaged as analogous to the K_m of a substrate. During the second and in most cases rate-limiting step, the inhibitor reacts irreversibly with the enzyme in a mechanism-based manner. The rate constant associated with this step (k_{inact}) can be regarded as analogous to the k_{cat}-value of a corresponding substrate.[29] Experimentally, the potency distribution in a series of irreversible inhibitors of this type is mostly

found to be correlated with the k_{cat} value of the substrates from which they are derived. Irreversible, mechanism-based inhibitors are therefore often referred to as of the k_{cat}-type.[38] Nonetheless, the potency of inhibitors of this kind is mostly expressed *via* a k_{inact}/K_i-value, as this parameter offers a balanced representation of a compound's affinity (K_i) and reactivity (k_{inact}). For the same reason, ranking of SAS-hits in publications reporting irreversible inhibitors has been carried out based on k_{cat}/K_m values.

Determining exact values for k_{cat} and K_m for individual substrates identified in a SAS experiment is often laborious and sometimes even impossible, for example, due to solubility problems.[16] In practice, approximations and simplifications are possible by carefully choosing experimental conditions. Illustrations thereof can be found in SAS manuscripts reporting aldehyde and nitrile inhibitors of cathepsin S, 2,3,5,6-tetrafluorophenoxymethyl ketone inhibitors of cruzain and pan-caspase, phosphonate inhibitors of chymotrypsin and uPA, or chloroacetamidine inhibitors of PAD3.[1,2,5-7,16,17]

In these studies, assays are performed at subsaturating substrate concentrations ([S] < K_m), but respecting steady-state conditions (where [ES] can be considered constant, i.e. the amount of substrate converted during the measurement is negligibly small). The latter can be obtained by using a sufficiently large molar excess of substrate over enzyme concentration. Under conditions where both requirements are fulfilled, the initial substrate conversion rate ("V_i", the read-out during a substrate screening experiment) is proportional to the catalytic efficiency (k_{cat}/K_m). This is shown in Equations 1 (the Michaelis-Menten equation) and 2.[29,32]

Equation 1: $V = (k_{cat}[E][S])/([S]+K_m)$

Equation 2: For $[S] << K_m$, $V = (k_{cat}/K_m)[E][S]$

where [E] is the total enzyme concentration and [S] is the substrate concentration at time 0. To avoid the need for determining K_m values for all obtained hits, one can choose to determine only the K_m value of the substrate with the highest cleavage efficiency. Subsequently, all obtained hits are investigated again at a concentration below the K_m value of the best substrate, with the latter serving as a reference, relative to which cleavage efficiencies are reported. Performing substrate assays under these conditions allows to use the following equations.[29]

Equation 3: $K_i = dK_{TS} = dK_m\ (k_{un}/k_{cat})$

Equation 4: $\log(K_i) = \log(K_m/k_{cat}) + \log(dk_{un})$

In Equations 3 and 4, *d* reflects the proportionality factor between K_i and $K_m(k_{un}/k_{cat})$, and it provides a measure for the effectiveness of a mechanism-based inhibitor as a transition state analogue.

A "perfect transition state mimic" would bind more tightly than the substrate with the same factor as the rate enhancement achieved by the enzyme (**Figure 6.2**). In that case *d* would be equal to 1. Within related series of substrates, *d* similar as k_{un} should remain constant, implying a linear correlation between log(K_i) and log(K_m/k_{cat}). This relationship has been used in reports on SAS for the cathepsin S inhibitor discovery (**Figure 6.4a**).[1,5]

So far, most SAS-publications have reported substrate-derived inhibitors with reversible or irreversible warhead types, relying on the approaches described above for transition-state analogues. Nonetheless, a different ranking strategy is required for reversible, non-covalent binders lacking "warhead" functionalities. Such compounds are typically ground state inhibitors with potencies that generally correlate with the K_m of the substrate from which they are derived. This is illustrated by a classical literature example of K_m-type fluoroalkene inhibitors of thermolysin (**Figure 6.4b**).[39] In the framework of SAS, this principle has been applied to the discovery of isoxazole carboxylate inhibitors of PtpB, DFMP inhibitors of PtpA and STEP, or tetrafluorophenol inhibitors of c-Src.[3,10,11,15,40]

It is worth mentioning that apparent deviations from these guidelines have been reported, also in the framework of SAS. With respect to the latter, the K_m parameter was found to govern the relationship between substrate and *α*-aminophosphonate inhibitors of APN, in spite of the fact that aminophosphonates are known to be transition state analogues of peptide bond hydrolysis.[9,41,42] In the case of the SAS-based identification of chloroacetamidine inhibitors of PAD3, substrates characterized by the highest relative k_{cat}/K_m values provided correspondingly potent inhibitors. However, the most efficiently cleaved substrate, did not yield the most potent inhibitor, which can indicate that the ground-state binding (K_m) dominated the substrate-inhibitor relationship.[16]

Although the approaches described above have proven their merit, one must keep in mind that they rely on a very simple model of a catalytic cycle and a number of assumptions that are likely shortcoming. Indeed, most enzymes have several intermediates in their catalytic cycle and each conversion step has its own transition state. When the free energy barriers between the different intermediates are similar, it appears plausible that SAS-substrates vary according to which step in the cycle is represented in the expression of k_{cat} or k_{cat}/K_m. A classical example is the hydrolysis of amides and ester bonds by chymotrypsin, where in some cases the acylation is rate determining and in others the deacylation.[43,44] The rational design of a good TS analogue presumes knowledge of the structure of the TS of the enzyme catalyzed reaction, which is not trivial. As SAS-libraries are frequently used to screen enzymes from the same family, it is noteworthy that highly homologous enzymes often have remarkably different TS structures.[45] For instance, the bovine, human and *Plasmodium falciparum* adenosine deaminase homologues catalyse the same reaction but have

different TS structures that are located at different positions of the reaction coordinate with different free energy barriers.[46] The variability of the TS must originate from fairly subtle differences between the three iso-enzymes since the residues of the catalytic site are completely conserved and the overall homology between the human and bovine enzyme is 91%.

Finally, most reported SAS-cases rely on the introduction of an appropriate warhead or a surrogate for the enzyme processed functional group as a key element in the transformation of substrates into inhibitors. Evaluation of different warheads can be crucial to obtain potent and selective inhibitors. In the work on cathepsin S inhibitors, replacing the aldehyde warhead by a nitrile led to significantly increased selectivity of the derived triazole-based inhibitor.[1,5] The report on application of SAS to cruzain inhibitors involved the evaluation of five different, mechanism-based warheads: up to 180-fold inhibitory potency (expressed *via* a k_{inact}/K_i-value) differences were observed between inhibitors that only differed in the warhead portion.[6] Analogously, the design of substrate-competitive c-Src inhibitors involved evaluation of three nonphosphorylatable phenol surrogates, including pyridine *N*-oxide, hydroxypyridine, and tetrafluorophenol, to identify the latter as the most potent one.[15] Except for these examples, other SAS-publications so far have not reported side-by-side comparison of different warheads or surrogates. While selecting a warhead type that has already been reported for a given target (e.g. in "classical" substrate-derived compounds) can be a good starting point, the possibility for further compound optimization by variation of this substructure is definitely worth exploring during a SAS-based approach. So far, however, no theoretical or experimental framework has been reported to identify optimal warheads or surrogates in an anticipative manner, making this mainly a trial-and-error task.

6.6. Conclusions

Since the first report a decade ago, SAS has been applied successfully to inhibitor discovery for a number of relevant pharmaceutical targets. The methodology is straightforward, conceptually simple and relatively accessible compared to other fragment-based approaches in drug discovery. For optimal results, several aspects require specific monitoring: (1) substrate library design, (2) screening assay design, (3) characterization of adequate kinetic and thermodynamic substrate parameters, and (4) selection of an appropriate warhead or isostere. Further research on these crucial elements of SAS-based methodologies will guide the further development of the domain and maximize its efficiency and reliability.

References

(1) Wood, W. J. L.; Patterson, A. W.; Tsuruoka, H.; Jain, R. K.; Ellman, J. A. Substrate Activity Screening: A Fragment-Based Method for the Rapid Identification of Nonpeptidic Protease Inhibitors. *J. Am. Chem. Soc.* **2005**, *127*, 15521–15527.

(2) Salisbury, C. M.; Ellman, J. A. Rapid Identification of Potent Nonpeptidic Serine Protease Inhibitors. *ChemBioChem* **2006**, *7*, 1034–1037.

(3) Soellner, M. B.; Rawls, K. A.; Grundner, C.; Alber, T.; Ellman, J. A. Fragment-Based Substrate Activity Screening Method for the Identification of Potent Inhibitors of the *Mycobacterium tuberculosis* Phosphatase PtpB. *J. Am. Chem. Soc.* **2007**, *129*, 9613–9615.

(4) Gladysz, R.; Adriaenssens, Y.; De Winter, H.; Joossens, J.; Lambeir, A.-M.; Augustyns, K.; Van der Veken, P. Discovery and SAR of Novel and Selective Inhibitors of Urokinase Plasminogen Activator (uPA) with an Imidazo[1,2-*a*]pyridine Scaffold. *J. Med. Chem.* **2015**, *58*, 9238–9257.

(5) Patterson, A. W.; Wood, W. J. L.; Hornsby, M.; Lesley, S.; Spraggon, G.; Ellman, J. A. Identification of Selective, Nonpeptidic Nitrile Inhibitors of Cathepsin S Using the Substrate Activity Screening Method. *J. Med. Chem.* **2006**, *49*, 6298–6307.

(6) Brak, K.; Doyle, P. S.; McKerrow, J. H.; Ellman, J. A. Identification of a New Class of Nonpeptidic Inhibitors of Cruzain. *J. Am. Chem. Soc.* **2008**, *130*, 6404–6410.

(7) Leyva, M. J.; Degiacomo, F.; Kaltenbach, L. S.; Holcomb, J.; Zhang, N.; Gafni, J.; Park, H.; Lo, D. C.; Salvesen, G. S.; Ellerby, L. M.; Ellman, J. A. Identification and Evaluation of Small Molecule Pan-Caspase Inhibitors in Huntington's Disease Models. *Chem. Biol.* **2010**, *17*, 1189–1200.

(8) Wickström, M.; Larsson, R.; Nygren, P.; Gullbo, J. Aminopeptidase N (CD13) as a Target for Cancer Chemotherapy. *Cancer Sci.* **2011**, *102*, 501–508.

(9) Drag, M.; Bogyo, M.; Ellman, J. A.; Salvesen, G. S. Aminopeptidase Fingerprints, an Integrated Approach for Identification of Good Substrates and Optimal Inhibitors. *J. Biol. Chem.* **2010**, *285*, 3310–3318.

(10) Rawls, K. A.; Lang, P. T.; Takeuchi, J.; Imamura, S.; Baguley, T. D.; Grundner, C.; Alber, T.; Ellman, J. A. Fragment-Based Discovery of Selective Inhibitors of the *Mycobacterium tuberculosis* Protein Tyrosine Phosphatase PtpA. *Bioorg. Med. Chem. Lett.* **2009**, *19*, 6851-6854.

(11) Baguley, T. D.; Xu, H.-C.; Chatterjee, M.; Nairn, A. C.; Lombroso, P. J.; Ellman, J. A. Substrate-Based Fragment Identification for the Development of Selective, Nonpeptidic Inhibitors of Striatal-Enriched Protein Tyrosine Phosphatase. *J. Med. Chem.* **2013**, *56*, 7636–7650.

(12) Hubbard, S. R.; Till, J. H. Protein Tyrosine Kinase Structure and Function. *Annu. Rev. Biochem.* **2000**, *69*, 373–398.

(13) Chapelat, J.; Berst, F.; Marzinzik, A. L.; Moebitz, H.; Drueckes, P.; Trappe, J.; Fabbro, D.; Seebach, D. The Substrate-Activity-Screening Methodology Applied to Receptor Tyrosine Kinases: A Proof-of-Concept Study. *Eur. J. Med. Chem.* **2012**, *57*, 1–9.

(14) Martin, G. S. The Hunting of the Src. *Nat. Rev. Mol. Cell Biol.* **2001**, *2*, 467–475.

(15) Breen, M. E.; Steffey, M. E.; Lachacz, E. J.; Kwarcinski, F. E.; Fox, C. C.; Soellner, M. B. Substrate Activity Screening with Kinases: Discovery of Small-Molecule Substrate-Competitive c-Src Inhibitors. *Angew. Chemie Int. Ed.* **2014**, *53*, 7010–7013.

(16) Jamali, H.; Khan, H. A.; Stringer, J. R.; Chowdhury, S.; Ellman, J. A. Identification of Multiple Structurally Distinct, Nonpeptidic Small Molecule Inhibitors of Protein Arginine Deiminase 3 Using a Substrate-Based Fragment Method. *J. Am. Chem. Soc.* **2015**, *137*, 3616–3621.

(17) Gladysz, R.; Cleenewerck, M.; Joossens, J.; Lambeir, A.-M.; Augustyns, K.; Van der Veken, P. Repositioning the Substrate Activity Screening (SAS) Approach as a Fragment-Based Method for Identification of Weak Binders. *ChemBioChem* **2014**, *15*, 2238–2247.

(18) Adriaennssens, Y., unpublished results.

(19) Cleenewerck, M.; Grootaert, M.; Gladysz, R.; Adriaenssens, Y.; Roelandt, R.; Joossens, J.; Lambeir, A.-M.; De Meyer, G.; Declercq, W.; Augustyns, K.; Martinet, W.; Van der Veken, P. Development and Validation of a Gel Electrophoresis-Based Assay for Atg4B Activity Determination and Inhibitor Screening, unpublished results.

(20) Mekkawy, A. H.; Pourgholami, M. H.; Morris, D. L. Involvement of Urokinase-Type Plasminogen Activator System in Cancer : An Overview. *Med. Res. Rev.* **2014**, *34*, 918–956.

(21) Dass, K.; Ahmad, A.; Azmi, A. S.; Sarkar, S. H.; Sarkar, F. H. Evolving Role of uPA/uPAR System in Human Cancers. *Cancer Treat. Rev.* **2008**, *34*, 122–136.

(22) Winkler, S.; Rösen-Wolff, A. Caspase-1: An Integral Regulator of Innate Immunity. *Semin. Immunopathol.* **2015**, *37*, 419–427.

(23) Jiménez Fernández, D.; Lamkanfi, M. Inflammatory Caspases: Key Regulators of Inflammation and Cell Death. *Biol. Chem.* **2015**, *396*, 193–203.

(24) Yorimitsu, T.; Klionsky, D. J. Autophagy: Molecular Machinery for Self-Eating. *Cell Death Differ.* **2005**, *12*, 1542–1552.

(25) Williams, J. W.; Morrison, J. F.; Duggleby, R. G. Methotrexate, a High-Affinity Pseudosubstrate of Dihydrofolate Reductase. *Biochemistry* **1979**, *18*, 2567–2573.

(26) Oefner, C.; D'Arcy, A.; Winkler, F. K. Crystal Structure of Human Dihydrofolate Reductase Complexed with Folate. *Eur. J. Biochem.* **1988**, *174*, 377–385.

(27) Hamada, Y.; Ishiura, S.; Kiso, Y. BACE1 Inhibitor Peptides: Can an Infinitely Small k_{cat} Value Turn the Substrate of an Enzyme into Its Inhibitor? *ACS Med. Chem. Lett.* **2012**, *3*, 193–197.

(28) Xu, P.; Xu, M.; Jiang, L.; Yang, Q.; Luo, Z.; Dauter, Z.; Huang, M.; Andreasen, P. A. Design of Specific Serine Protease Inhibitors Based on a Versatile Peptide Scaffold: Conversion of a Urokinase Inhibitor to a Plasma Kallikrein Inhibitor. *J. Med. Chem.* **2015**, *58*, 8868–8876.

(29) Mader, M. M.; Bartlett, P. A. Binding Energy and Catalysis: The Implications for Transition-State Analogs and Catalytic Antibodies. *Chem. Rev.* **1997**, *97*, 1281–1302.

(30) Wolfenden, R. Conformational Aspects of Inhibitor Design: Enzyme-Substrate Interactions in the Transition State. *Bioorg. Med. Chem.* **1999**, *7*, 647–652.

(31) Lienhard, G. E. Enzymatic Catalysis and Transition-State Theory. *Science* **1973**, *180*, 149–154.

(32) Copeland, R. A. *Evaluation of Enzyme Inhibitors in Drug Discovery*; Wiley: New Jersey, 2013.

(33) Schramm, V. L. Enzymatic Transition States and Transition State Analog Design. *Annu. Rev. Biochem.* **1998**, *67*, 693–720.

(34) Bartlett, P. A.; Marlowe, C. K. Phosphonamidates as Transition-State Analogue Inhibitors of Thermolysin. *Biochemistry* **1983**, *22*, 4618–4624.

(35) Schramm, V. L. Enzymatic Transition States, Transition-State Analogs, Dynamics, Thermodynamics, and Lifetimes. *Annu. Rev. Bochem.* **2011**, *80*, 703–732.

(36) Thompson, R. C. Use of Peptide Aldehydes to Generate Transition-State Analogs of Elastase. *Biochemistry* **1973**, *12*, 47–51.

(37) Powers, J. C.; Asgian, J. L.; Ekici, O. D.; James, K. E. Irreversible Inhibitors of Serine, Cysteine, and Threonine Proteases. *Chem. Rev.* **2002**, *102*, 4639–4750.

(38) Rando, R. R. Chemistry and Enzymology of k_{cat} Inhibitors. *Science* **1974**, *185*, 320–324.

(39) Bartlett, P. A.; Otake, A. Fluoroalkenes as Peptide Isosteres: Ground State Analog Inhibitors of Thermolysin. *J. Org. Chem.* **1995**, *60*, 3107–3111.

(40) Taylor, S. D.; Kotoris, C. C.; Dinaut, A. N.; Wang, Q.; Ramachandran, C.; Huang, Z. Potent Non-Peptidyl Inhibitors of Protein Tyrosine Phosphatase 1B. *Bioorg. Med. Chem.* **1998**, *6*, 1457-1468.

(41) Oleksyszyn, J. in *Aminophosphonic and Aminophosphinic Acids. Chemistry and Biological Activity* (Eds.: Kukhar, V. P.; Hudson, H. R.), Wiley, Chichester, **2000**, 537–557.

(42) Mucha, A.; Kafarski, P.; Berlicki, Ł. Remarkable Potential of the α-Aminophosphonate/ Phosphinate Structural Motif in Medicinal Chemistry. *J. Med. Chem.* **2011**, *54*, 5955–5980.

(43) Zerner, B.; Bender, M. The Kinetic Consequences of the Acyl-Enzyme Mechanism for the Reactions of Specific Substrates with Chymotrypsin. *J. Am. Chem. Soc.* **1964**, *86*, 3669–3674.

(44) Epand, R. M.; Wilson, I. B. Evidence for the Formation of Hippuryl Chymotrypsin during the Hydrolysis of Hippuric Acid Esters. **1963**, *238*, 1718–1723.

(45) Lewandowicz, A.; Ringia, E. A.; Ting, L. M.; Kim, K.; Tyler, P. C.; Evans, G. B.; Zubkova, O. V.; Mee, S.; Painter, G. F.; Lenz, D. H.; Furneaux, R. H.; Schramm, V. L. Energetic Mapping of Transition State Analogue Interactions with Human and *Plasmodium falciparum* Purine Nucleoside Phosphorylases. *J. Biol. Chem.* **2005**, *280*, 30320–30328.

(46) Luo, M.; Singh, V.; Taylor, E. A.; Schramm, V. L. Transition-State Variation in Human, Bovine, and *Plasmodium falciparum* Adenosine Deaminases. *J. Am. Chem. Soc.* **2007**, *129*, 8008–8017.

Chapter 7

“On-target” approaches to inhibitors of urokinase

7. "On-target" approaches to inhibitors of urokinase

7.1. Introduction

Target-guided strategies (TGS) have emerged as a powerful tool to identify ligands for various biological targets. In a number of relevant literature examples, the "on-target" research has been successfully applied to medicinal chemistry projects, demonstrating its potential to facilitate the identification of enzyme inhibitors. "On-target" strategies rely on direct assistance of a target enzyme, which functions as a physical template that selects fragments with affinity to the target, and subsequently assemblies them to form a finalized ligand molecule. In consequence, this approach allows combining several aspects of the drug design process, including synthesis and potency determination, in a single, time- and cost-efficient step. The main methods which emerged in the field of template-assisted organic synthesis include: (1) dynamic combinatorial chemistry (DCC) and (2) kinetic ligand amplification. Dynamic combinatorial chemistry uses mixtures of molecular building blocks, which can react with each other in a reversible manner by forming covalent or non-covalent bonds to afford dynamic combinatorial libraries (DCLs).[1,2] Reaction between these building blocks is an "equilibrium-driven" and "thermodynamically-controlled" process, therefore the reaction products are in theory formed and degraded in a reversible manner, and the product distribution depends on the stability of the formed compounds.[3] To this mixture of reacting building blocks a target is added, which functions as a physical template that can "select" a specific combination of building blocks, which is known as "ligand amplification". This in consequence leads to library re-equilibration, and the driving force behind ligand amplification is the binding of products which demonstrate the strongest target affinity. Several types of reversible reactions have been used in enzyme-templated DCC. However, these exchange reactions often result in metabolically unstable, reversible bond types (e.g. imines, hydrazones, hemithioacetals, thioethers, disulfide bridges, boronate esters, oximes). This feature is highly undesirable in inhibitor development, and requires a synthetic replacement of the unstable bonds by stable, isosteric replacements during separate optimization cycles. Nonetheless, since its discovery in the late 1990's the protein-templated DCC has been several times applied to inhibitor discovery, providing a number of potent molecules.[2] Especially, DCC exploiting imine formation has proven to be a powerful tool for enzyme inhibitor design. For instance, a study performed by the group of Barboiu and Supuran[4] allowed for the identification of inhibitors of human carbonic anhydrase (hCA II) from the imine-based DCL. Reducing the amplified imine compounds with $NaBH_3CN$ afforded a number of amines characterized by high inhibitory potencies, with the best inhibitor in low-nanomolar range (K_i = 21.4 nM). In another example, a hydrazone-based DCL was used for the identification of inhibitors of GABA transporter 1 protein mGAT1, which is involved in several neuronal diseases, such as epilepsy, Parkinson's disease,

and sleeping disorders. In this study, hydrazone compounds displaying the highest inhibitory potency of mGAT1 (pK_i values of 6.186 and 8.094), were converted into lead compounds for drug development by preparation of stable carba-analogues (**Figure 7.1**). The most potent carba-analogue displayed slightly reduced inhibition of the target protein, probably due to its decreased polarity compared to the original hydrazine derivative (pK_i = 6.930 ± 0.021).[2,5]

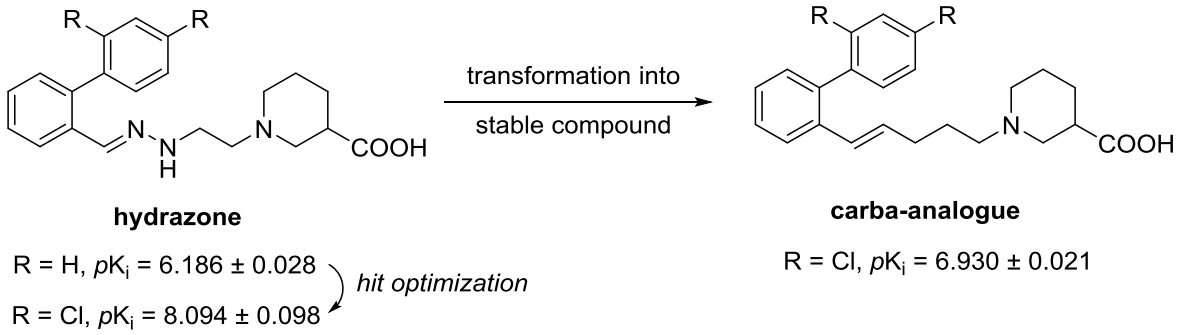

Figure 7.1. Transformation of hydrazone-based inhibitors of mGAT1 into stable analogues.

Application of reversible disulfide-bond formation in DCC was demonstrated by Schofield and co-workers[6] for the discovery of inhibitors of BcII metallo-β-lactamase (BcII MBL), an enzyme playing an important role in the development of resistance against β-lactam antibiotics. In this study, a template-assisted identification of the "hit" compounds from the generated disulfide-based DCLs was followed by replacement of the labile disulfide bond by a stable linker affording a series of cysteine-based analogues, with the most potent inhibitor displaying a K_i-value of 740 nM. Additionally, one of the most recent reports by Hirsch and co-workers[7] shows that combination of *de novo* structure-based design and DCC is a powerful technique for hit identification and optimization. This study used as model target endothiapepsin, a pepsin-like aspartic protease implicated in e.g. hypertension and malaria. Guided by the crystal structure of endothiapepsin, a library of acylhydrazones was first designed and subsequently generated in the presence of the target enzyme. The use of saturation-transfer difference NMR (^{1}H-STD-NMR) spectroscopy allowed to identify library members which were bound to the enzyme, and the most potent acylhydrazone-based inhibitor of endothiapepsin identified from this DCL displayed a K_i-value of 6 μM.

In kinetic ligand amplification, an approach proposed during the last decade by Sharpless and Fokin[8,9], a template is added to a mixture of building blocks, and as a result building blocks with affinity for the given template couple irreversibly on-target to create a new, tight-binding compound. This leads to "ligand amplification", and "close proximity" of the building blocks is used to explain why the reaction takes place on the template and is not occurring or is less efficient in solution (**Figure 7.2**).[10]

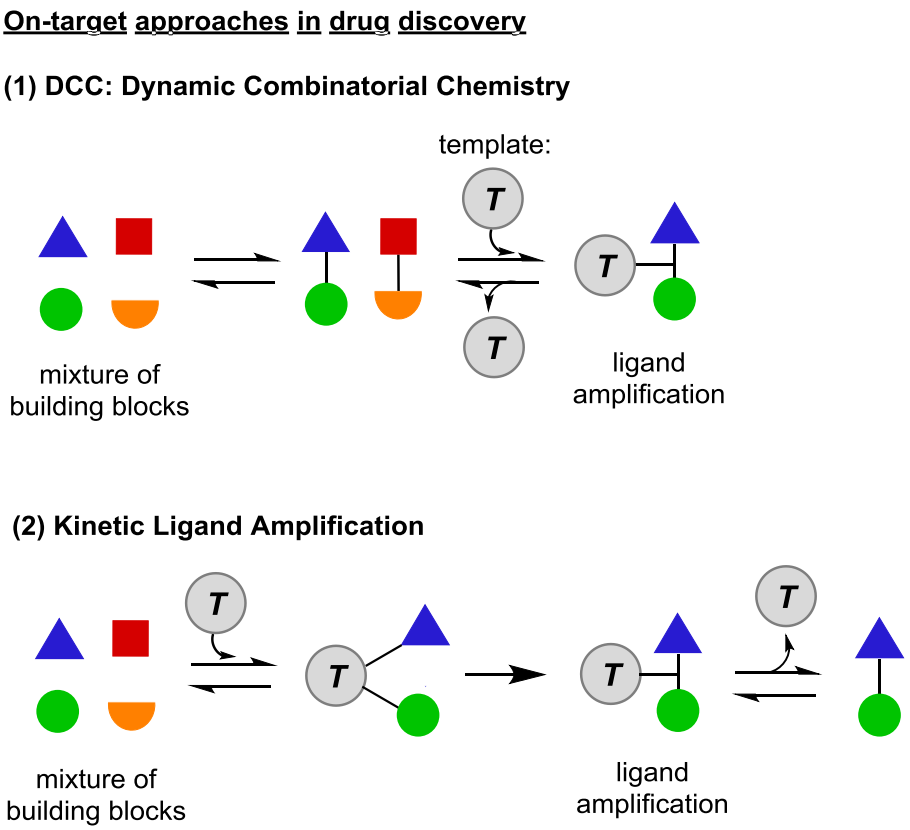

Figure 7.2. Simplified representation of on-target approaches in drug discovery.

Contrary to DCC this is a kinetic process, as the binding of building blocks to the template and their resulting proximity accelerate the synthesis of the best inhibitors.[3] To date, only a limited number of applications of this methodology have been reported, relying mainly on Huisgen 1,3-dipolar cycloaddition or on alkylation leading to coupling between two building blocks (**Table 7.1**).

The variant of bio-templated kinetic ligand amplification relying on Huisgen-1,3-dipolar cycloaddition of azides and alkynes to give the corresponding 1,2,3-triazoles, was first demonstrated by Sharpless and co-workers in 2002.[11] Since then, "*in situ* click chemistry" based on the Huisgen reaction has proven to be well-suited for the discovery of ligands and diverse biomolecules including enzymes,[12] protein-protein interactions,[13] RNA and DNA,[14] antibody-like protein capture agents,[15] as well as protein targeted drug delivery mechanisms.[16,9] In the initial report, the azide-alkyne cycloaddition was applied to the discovery of inhibitors of acetylcholinesterase (AChE), an enzyme playing a key role in neurotransmitter hydrolysis in the central and peripheral nervous system and implied in for e.g. Alzheimer's disease (AD). In this report, AChE was used as a template to select and assemble known, site-specific building blocks into a triazole-linked bivalent inhibitor of femtomolar potency and high selectivity for AChE.[11] This study was further elaborated and resulted in noncovalent inhibitors of AChE with three-fold improved binding affinity (K_d = 33 fM).[12,17] Besides, kinetic target-

guided synthesis (KTGS) based on the Huisgen cycloaddition was used in the discovery of inhibitors of carbonic anhydrase II (CA II),[18] HIV-1 protease[8], and chitinases[19]. Additionally, Iterative Peptide *In Situ* Click Chemistry (IPISC) has emerged as a methodology for the development of highly selective ligands, which bind to proteins with antibody-like affinity.[15] In a recent report by Deprez-Poulain and co-workers[20], KTGS has been used in the discovery of inhibitors of insulin-degrading enzyme (IDE), a metalloprotease cleaving insulin as well as other bioactive peptides (e.g. amyloid-β), and therefore implicated in Alzheimer's disease and type-2 diabetes. In this study, *in situ* click experiments allowed to identify the first catalytic site inhibitor of IDE (BDM44768, IC_{50} (*h*IDE) = 60 nM) of high selectivity for IDE with respect to a panel of related metalloproteases.

Also KTGS based on an alkylation reaction was proven to be a useful tool for the enzyme inhibitor discovery. In 2001, Nguyen and co-workers[21] demonstrated a target-assisted alkylation for the discovery of carbonic anhydrase II (CA II) inhibitors. In this report, a thiol molecule based on a known *p*-benzenesulfonamide fragment with affinity to CA II (α-mercaptotosylamide) was reacted with a series of alkyl chlorides in both the presence of the enzymatic template and without. This experiment revealed that addition of the CA II template strongly favored formation of the best thioether inhibitors of this enzyme (K_i values range: 59-770 nM). The most recent example of enzyme-templated alkylation was reported by Soellner and co-workers[22] for the discovery of inhibitors of c-Src, a nonreceptor tyrosine kinase implicated in metastasis of many cancer types. In this study, a library of 110 acrylamide fragments (MW ~ 235) was incubated with c-Src and in the presence of a thiol molecule, which was based on the structure of a known small-molecule inhibitor of c-Src (**Figure 7.3**). Subsequently, a continuous activity assay was performed, allowing for the identification of four hits: acrylamides that assemble into bivalent inhibitors of c-Src kinase. Since thioethers can easily undergo retro-Michael reactions in the assay buffer, their analogues with an all-carbon linker between the two fragments were prepared, to afford potent and selective inhibitors of c-Src kinase (K_i = 70 nM for the most potent analogue).

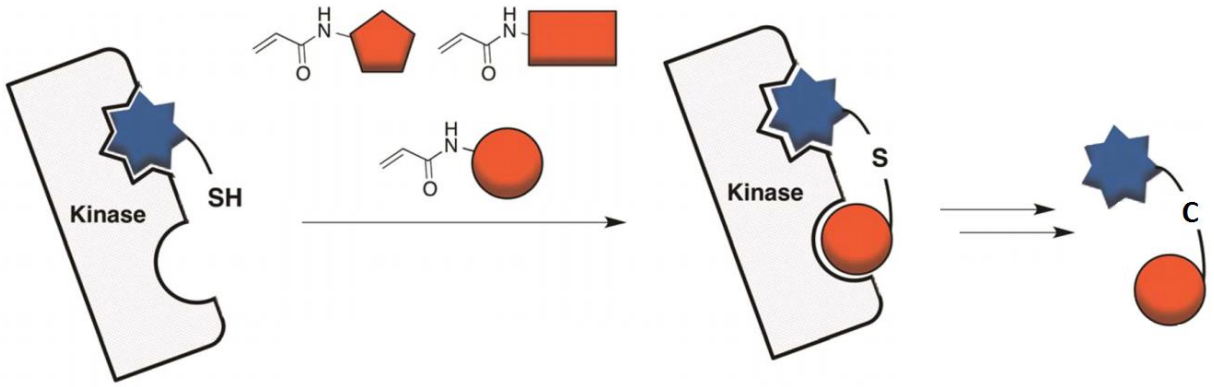

Figure 7.3. Outline of the enzyme-templated identification of c-Src kinase inhibitors using thiol-acrylamide chemistry (adapted from Kwarcinski et al.[22]).

Table 7.1. Reported examples of kinetic target-guided synthesis (KTGS).

Formed bond	Reaction scheme	Protein	Ref.
N-C	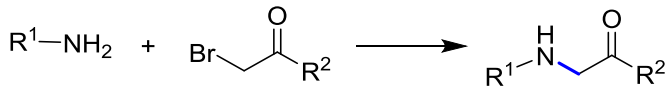	GAR TFase	Inglese et al.[23], 1991
	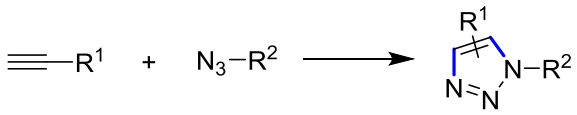	AChE	Lewis et al.[11], 2002; Manetsch et al.[12], 2004; Krasiński et al.[17], 2005
		CA II	Mocharla et al.[18], 2004
		HIV-1 protease	Whiting et al.[8], 2006
		chitinase	Hirose et al.[19,24], 2009, 2013
		IDE	Deprez-Poulain et al.[20], 2015
	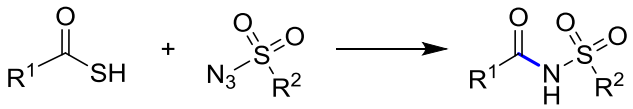	Bcl-XL	Hu et al.[25], 2008
	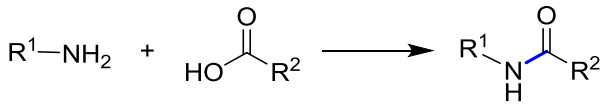	NAD kinase	Gelin et al.[26], 2012
S-C	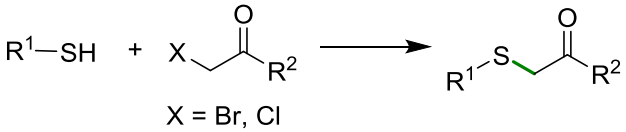 X = Br, Cl	CA II	Huc et al.[21], 2001
S-C	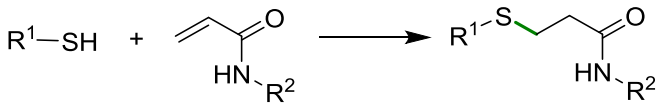	AChE	Oueis et al.[27], 2014
		c-Src kinase	Kwarcinski et al.[22], 2015
	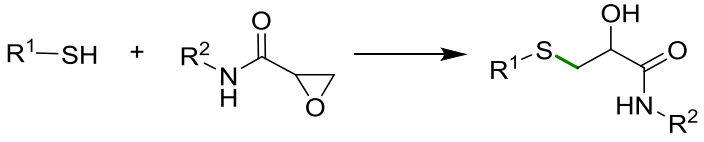	14-3-3 protein	Maki et al.[28], 2013
C-C	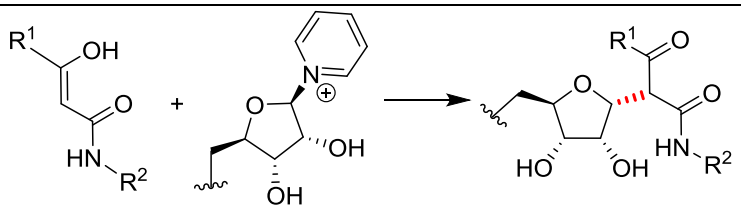	sirtuin	Asaba et al.[29], 2009
C-C & C-N	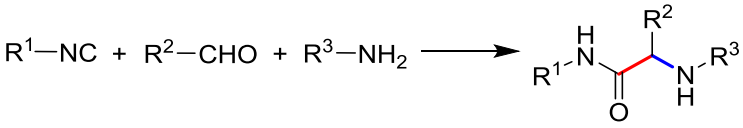	thrombin	Weber[30], 2004

7.1.1. "On-target" version of multicomponent reactions for drug discovery

A number of literature examples show that TGS can play a significant role in the drug discovery process. However, the application of this methodology remains limited so far. In order to increase the value of on-target approaches for drug discovery a number of factors are still required, and among them: (1) expansion of the range of (bio-orthogonal) chemistry types amenable to on-target methods, (2) improvement of the "druglikeness" of the obtained compound types, and finally (3) support for on-target experiments in molecular modeling studies, providing an insight into the fundamental kinetic and thermodynamic drivers of "on-target" reactions.

Isocyanide-based multicomponent reactions (IMCRs), including the Ugi and the Passerini reactions, and a number of related reactions, belong to the most widely used transformations in combinatorial drug discovery.[31] Different variants of these reactions yield molecules consisting of a central, heterocyclic scaffold decorated with substituents.[32] Due to the druglike architecture of such compounds, on-target versions of IMCRs can represent an important value for drug discovery. One variant of the Ugi reaction is the so-called Groebke-Blackburn-Bienaymé three-component reaction (GBB-3CR), in which an aminopyridine, an aldehyde and an isocyanide condense to afford an imidazopyridine scaffold decorated with substituents.[33] Noteworthy, imidazopyridines and related heterobicyclic scaffolds are harbored by several drug targets, which direct their substituents to the target's binding pockets, hence the high druglikeness of these classes of compounds.

In this work, the on-target version of the Groebke-Blackburn-Bienaymé (GBB) reaction was applied to inhibitor discovery using urokinase plasminogen activator as model target.

7.2. "On-target" version of the GBB reaction

7.2.1. Validation set of imidazopyridine inhibitors of uPA

Since no examples of the on-target Groebke-Blackburn-Bienaymé (GBB) reaction have been reported, the approach required validation. During earlier stages of this work, application of the MSAS strategy for fragment screening allowed to identify a set of ligands of the uPA S1 pocket.[34] Subsequently, the identified S1-binding fragments were converted into the corresponding isocyanide derivatives, and reacted with 2-aminopyridine and glyoxylic acid as a formaldehyde equivalent, using a classical GBB reaction protocol. The affinity data of the prepared compounds allowed to identify imidazo[1,2-*a*]pyridine as a potentially useful scaffold for the construction of uPA inhibitors. In order to optimize the most potent mono-substituted inhibitor, a set of imidazo[1,2-*a*]pyridines decorated with an S1-binding fragment at the 3-position, and one or two additional substituents has been prepared *via* classical organic synthesis. These molecules were characterized by a target affinity

ranging from nanomolar to high micromolar values.[35] Subsequently, the prepared inhibitors can be used as reference compounds to evaluate the outcome of the on-target GBB-reaction (**Figure 7.4**).

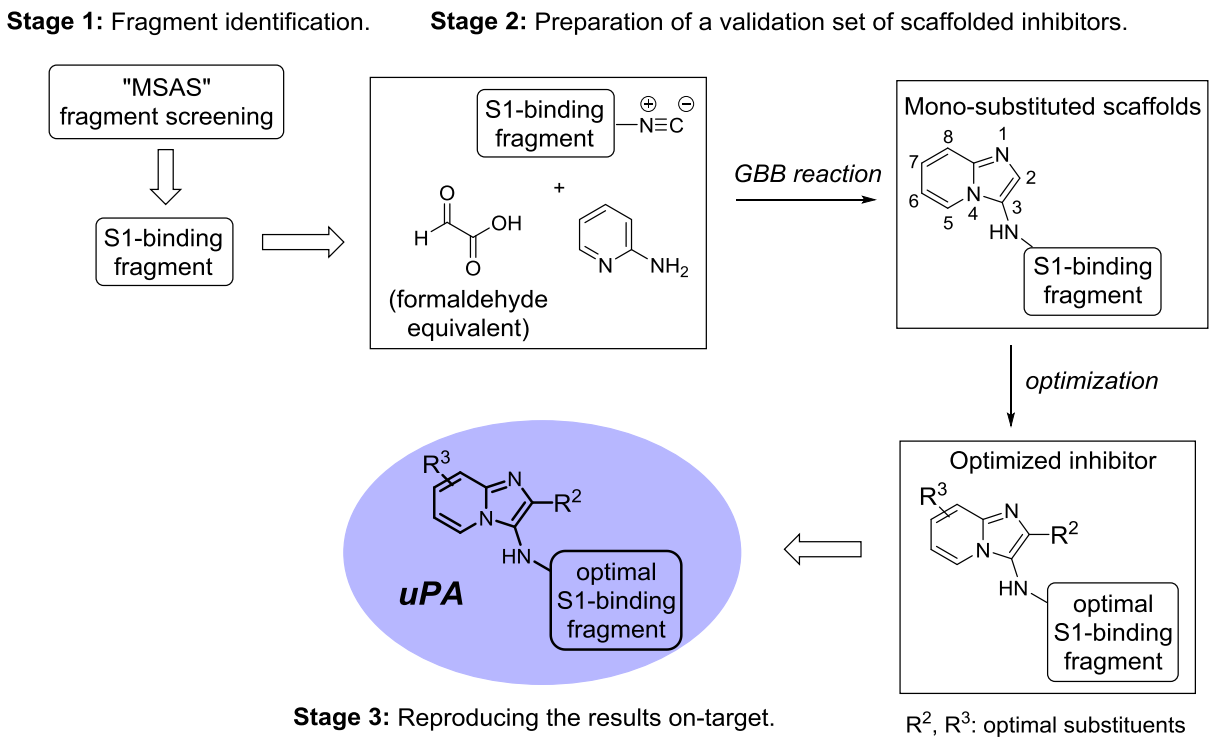

Figure 7.4. Stages followed during preparation of on-target version of the GBB-reaction.

7.2.2. Developing a general on-target protocol for the GBB reaction

Application of the on-target version of the GBB reaction to uPA inhibitor discovery required developing a general on-target protocol for this 3CR. A number of important challenges concerning the careful fine-tuning of experimental variables appeared in this context. Open questions with regards to e.g. (1) reaction medium, (2) pre-equilibration strategies, (3) appropriate method for analysis of the reaction mixtures and (4) (non-) stoichiometric enzyme *vs.* reactant concentration needed to be addressed here. Additionally, in order to permit minimal consumption of the costly target enzyme, the (5) lower limits for downscaling of the reaction had to be investigated.

The GBB reaction under classical organic synthesis conditions is performed in methanol, at room temperature, and in the presence of a (Lewis-)acid catalyst, without which the reaction proceeds at very low rates. The on-target version of this reaction relies on the hypothesis of “selective ligand amplification”. Once appropriately positioned by the target, the building blocks are reacting due to their close proximity, forming the desired imidazopyridines at considerable rates. According to the devised experimental protocol for the on-target GBB reaction, initially water (buffer) was selected as

reaction medium. In view of literature examples in which the Ugi-type transformations are performed in water, there are in theory no objections of running the GBB reaction in aqueous media.[31,36] However, due to occurrence of a side reaction in water (*vide infra*), the solvent from the original protocol was replaced by a water (HEPES buffer)/methanol mixture in 3:1-ratio, in which uPA retains its enzymatic activity (**Table 7.2a**). In addition, since aqueous conditions can hamper the initial imine formation step, pre-condensation of the aminopyridine and the aldehyde reaction components was also evaluated. Since some on-target experiments may require a longer reaction time, the activity of uPA in time was investigated under the on-target reaction conditions. The results show that urokinase retains its activity for 24 h, indicating that on-target experiments can be performed for at least 24 h (**Table 7.2b**).

Table 7.2. Influence of methanol on the catalytic activity of uPA.

(a) Catalytic activity of uPA in HEPES buffer/methanol mixture at 37 °C		**(b) Catalytic activity of uPA in function of time in HEPES buffer/methanol (3:1) at 37 °C**	
methanol [%]	**uPA activity [%][a]**	**time [h]**	**uPA activity [%][a]**
0	100	0	100
10	89	1	91
20	74	4	85
25	72	20	76
50	30	24	75

[a]Determined using the standard kinetic assay by monitoring processing of uPA chromogenic substrate (Biophen CS-61(44), c=800 μM), in HEPES buffer, pH 8.1, during 5 min, and at 37 °C. The control experiment used water instead of methanol.

Analysis of the reaction mixtures during on-target experiments was performed using UPLC and mass spectrometry in a multiple reaction monitoring (MRM) mode, which was earlier demonstrated to be a sensitive method for the detection of the desired product.[8,37] In addition, lower detection limits were determined using previously prepared inhibitor **5.18a** (*vide supra*, Chapter 5) at different concentrations. The results suggest that the selected MRM method allows the detection of the compound at 50 nM concentration or lower (**Figure 7.5**). Nonetheless, under such concentration range of building blocks, no reaction was observed, and for on-target experiments higher concentrations of the reaction components were required.

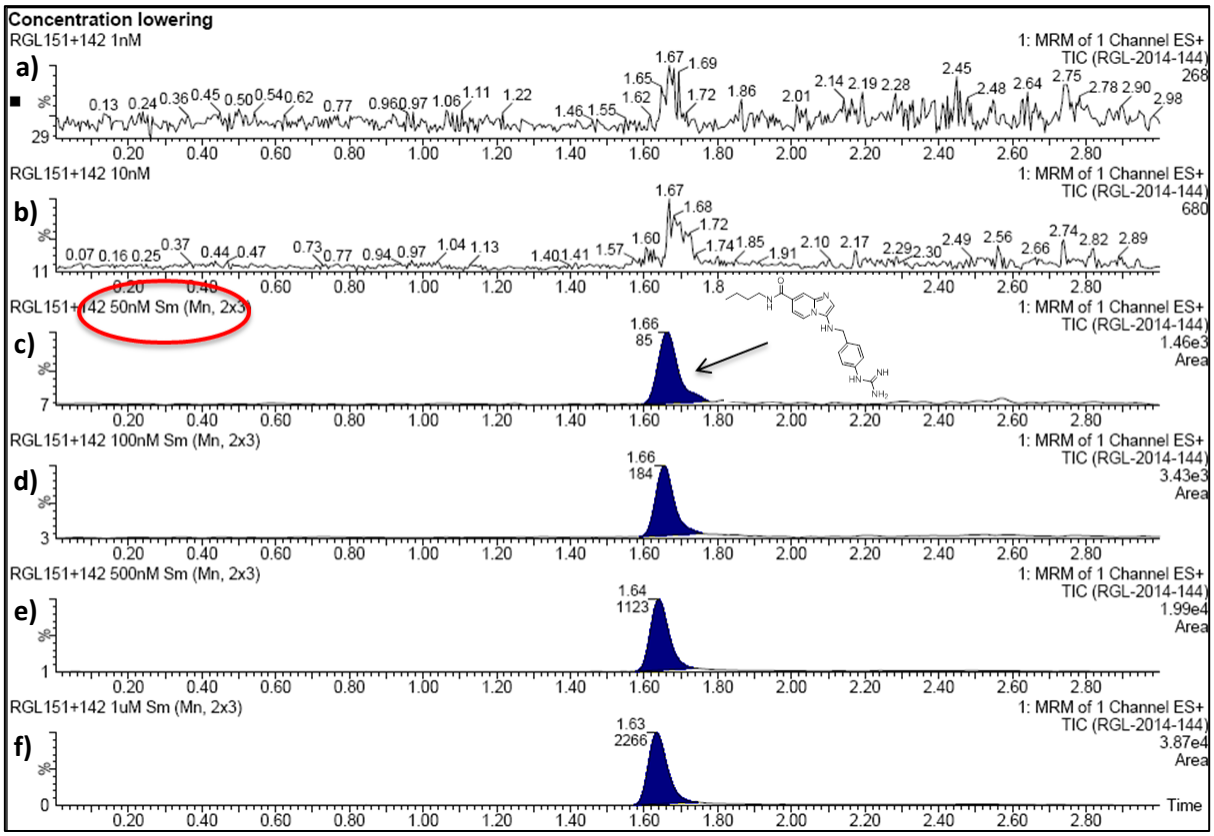

Figure 7.5. Determination of lower detection limits using compound 5.18a at concentrations: (a) 1 nM; (b) 10 nM; (c) 50 nM; (d) 100 nM; (e) 500 nM, and (f) 1 µM.

7.3. Chemistry

In order to reproduce the most potent imidazopyridine inhibitors of uPA on-target, the appropriate starting material had to be obtained first. For the classical organic synthesis variant of the GBB reaction the aminopyridine, the aldehyde and the 1-(4-(isocyanomethyl)phenyl)-2,3-di-Boc-guanidine (**5.6a**) components were reacted to form a compound, in which the basic guanidine group was protected with Boc groups. The desired product was then obtained by a simple Boc deprotection step (*vide supra*, Chapter 5). In order to ensure molecular recognition of the S1-binder-derived isocyanide in the uPA's active site, the isocyanide with free guanidine function was required. The standard procedure for removal of Boc groups uses acidic conditions, usually a TFA or HCl solution. However, isocyanides are sensitive to these conditions. Instead, refluxing 1(4-(isocyanomethyl)-phenyl)-2,3-di-Boc-guanidine (**5.6a**) or 1-(4-(2-isocyanoethyl)phenyl)-2,3-di-Boc-guanidine (**5.6b**) in water allowed to obtain the desired Boc-deprotected molecules (**Scheme 7.1**). To date, no other examples of isocyanides carrying a free guanidine function have been reported.

Scheme 7.1. Synthesis of starting material isocyanides 7.1a and 7.1b for the on-target GBB reaction.[a]

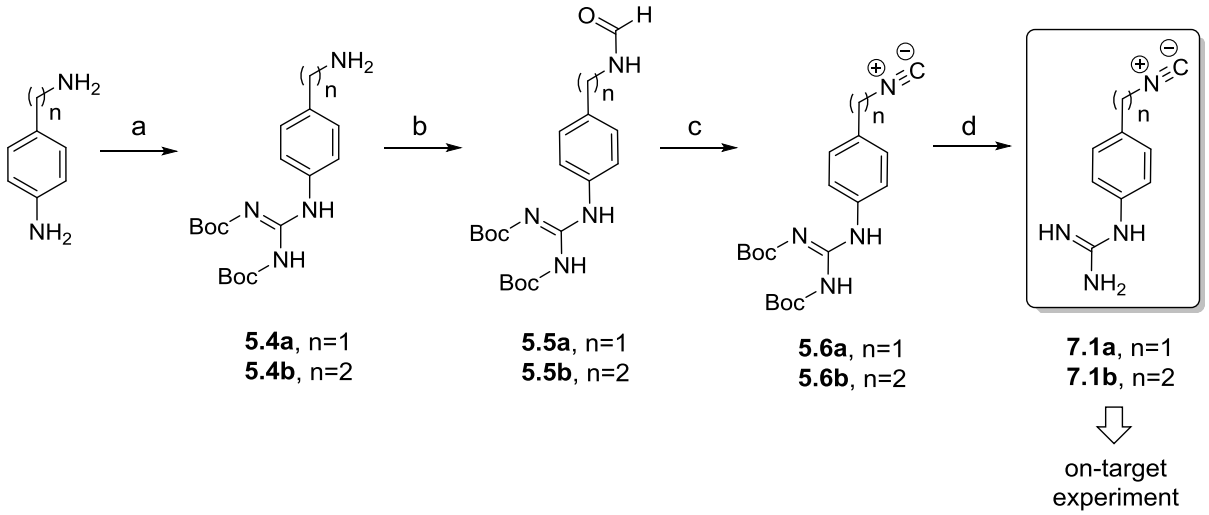

[a]Reagents and conditions: (a) *N,N'*-di-Boc-1*H*-pyrazole-1-carboxamidine, 1,4-dioxane, 10 % aq acetic acid; (b) ethyl formate, TEA, 55 °C, 24 h; (c) $POCl_3$, DIPA, DCM; (d) H_2O, reflux, 15 h.

Before proceeding with the on-target GBB reaction, a number of experiments using classical organic synthesis were performed to verify whether an isocyanide with a free guanidine function can easily participate in this 3CR (**Scheme 7.2**). All these experiments involved pre-condensation of the aminopyridine and glyoxylic acid components for 1 h at room temperature to form the corresponding imine. When the reaction was performed in methanol, the desired product **7.2** was formed within 5 h. Surprisingly, when water was used as the reaction medium, formation of the Passerini reaction product **7.3** was observed instead of the target compound **7.2** (**Scheme 7.2**). Performing the reaction in a 3:1 water/methanol mixture resulted in a mixture of compound **7.2** and the undesired Passerini product **7.3**. The same was observed when formaldehyde solution was used instead of glyoxylic acid. It can be therefore expected that in case of the on-target experiments a similar scenario takes place.

Scheme 7.2. Experiment using isocyanide 7.1b in the classical variant of the GBB reaction.[a]

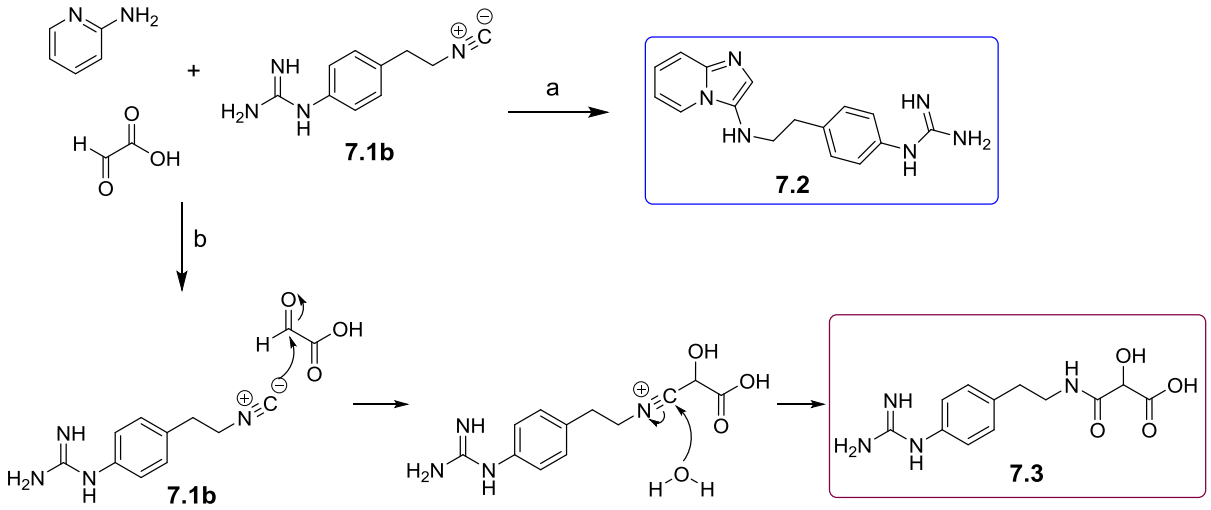

[a]Reagents and conditions: (a) MeOH, rt, 5 h; (b) H_2O, rt, 24 h.

7.4. Results and discussion

For obtaining a proof-of-concept for the target-mediated synthesis of uPA inhibitors using the GBB reaction a number of experiments were performed. Initially, the on-target reaction was carried out at 1 µM concentration of each of the building blocks and 3 µM of urokinase, making the total concentration of building blocks equal to the enzyme concentration. Similar conditions were reported by Ludlow and co-workers[38] in a work concerning the identification of ephedrine receptors. The low-micromolar concentration range was chosen as a compromise between the consumption of costly target enzyme and conditions for the reaction to occur. However, under these conditions no formation of the target compound was observed. Only increasing the concentration of the reaction components to low-millimolar range (1 mM) allowed for the desired product formation (**Scheme 7.3**). Under these conditions, only catalytic amount of urokinase could be used (5 µM). Although the rate of the GBB reaction was higher in the presence of uPA, a control experiment (without enzyme) also revealed formation of the target compound (**Figure 7.6**).

Scheme 7.3. On-target variant of the GBB reaction for the formation of uPA inhibitor 7.4.[a]

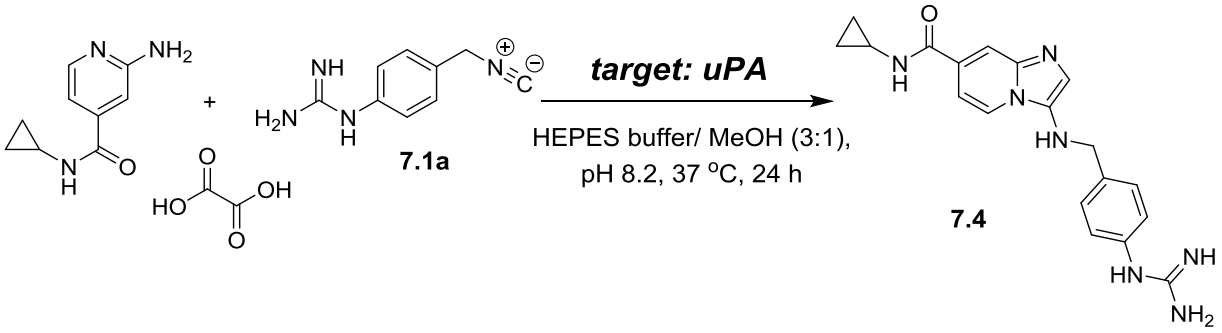

[a]Each of the building blocks at 1 mM concentration, uPA at 5 µM concentration. Inhibitor **7.4** was also previously prepared *via* classicial organic synthesis (compound **5.18b**, Chapter 5).

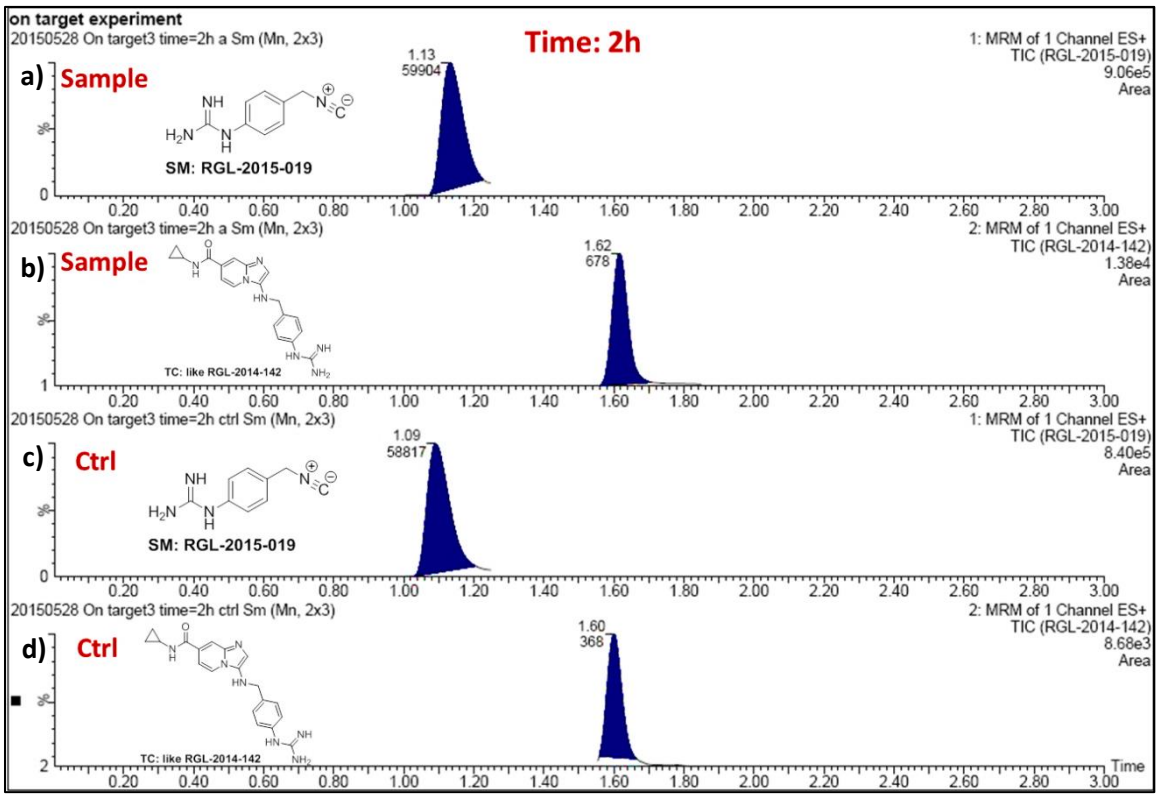

Figure 7.6. On-target experiment for the formation of inhibitor 7.4 monitored using a Waters Acquity UPLC instrument in the multiple reaction monitoring (MRM) mode: (a) isocyanide 7.1a after 2 h of on-target reaction; (b) inhibitor 7.4 formed after 2 h of on-target reaction; (c) isocyanide 7.1a after 2 h of the background reaction; (d) Inhibitor 7.4 formed after 2 h of the background reaction (solvent: water (HEPES buffer)/methanol in 3:1 ratio, total concentration of building blocks: 3 mM, concentration of uPA ~5 µM).

Further attempts for performing the GBB reaction on-target involved: (1) lowering the concentration of reagents to reach the level at which the spontaneous reaction would stop but the enzyme catalyzed variant would keep on proceeding; (2) using several other combinations of building blocks (giving rise to one single product); (3) replacing glyoxylic acid with a formaldehyde solution; (4) longer pre-condensation of the aminopyridine and the (form-)aldehyde solution (up to 3 h); (5) changing the ratio of the building blocks, e.g. using the isocyanide as limiting reagent and preincubating with uPA at the same concentration (10 μM), while adding the other reaction partners at a few-fold higher concentration; and (6) changing the reaction medium (water, buffer, or mixtures of methanol and aqueous medium at different ratio). These attempts yielded a preliminary proof-of-concept for the target-mediated variant of the GBB reaction. Nonetheless, this work is still at the preliminary stage, and more experiments would have to be performed before making a clear conclusion.

7.5. Conclusions

The performed study yielded a general experimental protocol as well as a preliminary proof-of-concept for the target-mediated synthesis of uPA inhibitors *via* the GBB reaction. The developed protocol can then be adapted and used in target-guided synthesis involving different enzymatic targets or/and reaction types. Because this research is still at the initial stage, it would be interesting to continue it further to obtain a full proof-of-concept for the "on-target" version of the GBB reaction.

7.6. Experimental section

7.6.1. Chemistry

All commercially available starting materials, solvents and other research consumables were obtained as described in the Experimental sections of Chapters 4 and 5, as well as information with regard to the analytical techniques and equipment used for the synthesis, purification, and characterization of synthesized compounds.

1-(4-(Isocyanomethyl)phenyl)guanidine (7.1a). The title compound was obtained by refluxing 1-(4-(isocyanomethyl)phenyl)-2,3-di-Boc-guanidine (**5.6a**) (0.5 g, 1.335 mmol) in water (25 mL) during 24 h. After this time, removal of the Boc groups was complete. The aqueous phase was washed with diethyl ether (3 x 25 mL), and evaporated under reduced pressure to afford pure target compound as a white solid (0.21 g, 91 %). ^{1}H NMR (400 MHz, DMSO) δ 7.27 (d, J = 7.6 Hz, 2H), 6.98 (m, 2H), 4.76 (s, 2H). ^{13}C NMR (101 MHz, DMSO) δ 156.07, 128.04, 123.52, 44.61. UPLC/MS: t_r 0.20 min, *m/z* 175.2 $[M+ H]^+$.

1-(4-(2-Isocyanoethyl)phenyl)guanidine (7.1b). The title compound was obtained by refluxing 1-(4-(isocyanoethyl)phenyl)-2,3-di-Boc-guanidine (**5.6b**) (0.4 g, 1.030 mmol) in water (30 mL) during 24 h. After this time, removal of the Boc groups was complete. The aqueous phase was washed with diethyl ether (3 x 30 mL), and evaporated under reduced pressure to afford pure target compound as a white solid (0.18 g, 94 %). ^{1}H NMR (400 MHz, DMSO) δ 7.19 (d, J = 8.3 Hz, 2H), 6.92 (d, J = 8.1 Hz, 2H), 3.75−3.68 (m, 2H), 2.89−2.80 (m, 2H). ^{13}C NMR (101 MHz, DMSO) δ 155.67, 129.52, 123.17, 42.58, 34.12. UPLC/MS: t_r 0.32 min, *m/z* 189.3 $[M + H]^+$.

7.6.2. "On-target" experiments

All commercially available starting materials and other research consumables were obtained as described in the Experimental sections of Chapters 4 and 5, as well as information with regard to the analytical techniques and equipment used for the "on-target" experiments.

The "on-target" experiments were performed using a ThermoMixer® C from Eppendorf (Hamburg, Germany). Data acquisition was performed using a Waters Acquity UPLC® system. Especially for compounds containing a guanidine group an appropriate UPLC method was developed. A Waters Acquity UPLC® BEH C18 1.7 µm, 2.1 mm × 50 mm column was used as a stationary phase. The mobile phase was consisting of solvent A: 5 mM ammonium acetate buffer (pH 4.0 adjusted with formic acid), and solvent B: acetonitrile.[39]

Gradient of the mobile phase: 0-0.15 min: 98% solvent A, 2% solvent B (isocratic); 0.15-1.5 min: linear gradient from 98% to 80% solvent A; 1.5-1.8 min: linear gradient from 80% to 50% solvent A; 1.8-2.1 min: linear gradient from 50% to 0% solvent A; 2.1-2.2 min: 0% solvent A, 100% solvent B (isocratic); 2.2-3.0 min: further system equilibration. The flow rate of the mobile phase was 0.65 mL/min. The wavelength for UV detection was 254 nm. The developed method allowed for a good chromatographic separation of different guanidylated compounds giving t_r values between 1-1.6 min, while with the normally used UPLC method (solvent A, water with 0.1% formic acid; solvent B, acetonitrile with 0.1% formic acid), all compounds containing a guanidine group were characterized by almost identical retention times (t_r ~ 0.2 min), hence hampering data analysis. Analysis of the on-target reaction mixtures was carried out using the in-house Waters Acquity UPLC-MS/MS instrument (ESI ionization/TQD-detection) in the MRM (multiple reaction monitoring) mode based on a tuning file, prepared using a reference compound (potent imidazopyridine inhibitors of uPA: **5.8a**, **5.8b**, **5.18a**, **5.18b**, *vide supra*, Chapter 5). The MRM method allowed for monitoring of multiple product ions from the precursor ion.[37]

Human enzyme, the urokinase plasminogen activator (uPA) from HYPHEN BioMed was used in "on-target" experiments. The on-target experiments were conducted in duplicate at 37 ^{o}C and using as solvent a 50 mM HEPES buffer solution at pH 8.2 or a mixture of methanol/HEPES buffer. Additionally, control experiments were always included (without uPA) for comparison of enzyme-promoted reactions with background reactions. The experiments were performed in 0.5 mL PCR tubes (Eppendorf), and the total reaction volume was 400 µL or 250 µL. Stock solutions (10 mM) of the aminopyridine, formaldehyde (or glyoxylic acid) and isocyanide building blocks were prepared in Milli-Q water, and then further re-diluted with Milli-Q water to the concentration required for the on-target experiment. The uPA solution was prepared using HEPES buffer (50 mM, pH 8.2). Each experiment involved preformation of the imine reaction component by mixing an aminopyridine and a formaldehyde equivalent for at least 1 h at 37 ^{o}C, and then adding the solution of uPA and the isocyanide component. In one series of experiments the total concentration of building blocks used at stoichiometric amounts was equal to the enzyme concentration (3 µM building blocks and ~3 µM urokinase). Besides, a number of experiments involved a catalytic amount of enzyme (~5 µM), and the building blocks at higher concentration (total concentration: 3 mM). Also experiments involving the isocyanide as limiting reaction partner (10 µM), each of the remaining other building blocks at 100 µM concentration and urokinase at ~5 µM were performed.

Analysis of the on-target reaction mixtures took place at times 0 min, 2h, 4h, and after 24 h.

In addition, the loss of urokinase activity over time or in an alternative water/methanol mixture was determined by performing the standard kinetic assay using a BioTek microplate reader, as previously described (*vide supra*, Chapter 5).

References

(1) Li, J.; Nowak, P.; Otto, S. Dynamic Combinatorial Libraries: From Exploring Molecular Recognition to Systems Chemistry. *J. Am. Chem. Soc.* **2013**, *135*, 9222–9239.

(2) Mondal, M.; Hirsch, A. K. H. Dynamic Combinatorial Chemistry: A Tool to Facilitate the Identification of Inhibitors for Protein Targets. *Chem. Soc. Rev.* **2015**, *44*, 2455–2488.

(3) Cheeseman, J. D.; Corbett, A. D.; Gleason, J. L.; Kazlauskas, R. J. Receptor-Assisted Combinatorial Chemistry: Thermodynamics and Kinetics in Drug Discovery. *Chem. Eur. J.* **2005**, *11*, 1708–1716.

(4) Nasr, G.; Petit, E.; Supuran, C. T.; Winum, J. Y.; Barboiu, M. Carbonic Anhydrase II-Induced Selection of Inhibitors from a Dynamic Combinatorial Library of Schiff's Bases. *Bioorg. Med. Chem. Lett.* **2009**, *19*, 6014–6017.

(5) Sindelar, M.; Wanner, K. T. Library Screening by Means of Mass Spectrometry (MS) Binding Assays-Exemplarily Demonstrated for a Pseudostatic Library Addressing γ-Aminobutyric Acid (GABA) Transporter 1 (GAT1). *ChemMedChem* **2012**, *7*, 1678–1690.

(6) Liénard, B. M.; Hüting, R.; Lassaux, P.; Galleni, M.; Frère, J. M.; Schofield, C. J. Dynamic Combinatorial Mass Spectrometry Leads to Metallo-Beta-Lactamase Inhibitors. *J. Med. Chem.* **2008**, *51*, 684–688.

(7) Mondal, M.; Radeva, N.; Köster, H.; Park, A.; Potamitis, C.; Zervou, M.; Klebe, G.; Hirsch, A. K. H. Structure-Based Design of Inhibitors of the Aspartic Protease Endothiapepsin by Exploiting Dynamic Combinatorial Chemistry. *Angew. Chem. Int. Ed.* **2014**, *53*, 3259–3263.

(8) Whiting, M.; Muldoon, J.; Lin, Y.-C.; Silverman, S. M.; Lindstrom, W.; Olson, A. J.; Kolb, H. C.; Finn, M. G.; Sharpless, K. B.; Elder, J. H.; Fokin, V. V. Inhibitors of HIV-1 Protease by Using In Situ Click Chemistry. *Angew. Chem. Int. Ed.* **2006**, *45*, 1435–1439.

(9) Sharpless, K. B.; Manetsch, R. Click Chemistry: A Powerful Means for Lead Discovery. *Expert Opin. Drug Discov.* **2006**, *1*, 525–538.

(10) Oueis, E.; Sabot, C.; Renard, P.-Y. New Insights into the Kinetic Target-Guided Synthesis of Protein Ligands. *Chem. Commun.* **2015**, *51*, 12158–12169.

(11) Lewis, W. G.; Green, L. G.; Grynszpan, F.; Radić, Z.; Carlier, P. R.; Taylor, P.; Finn, M. G.; Sharpless, K. B. Click Chemistry In Situ: Acetylcholinesterase as a Reaction Vessel for the Selective Assembly of a Femtomolar Inhibitor from an Array of Building Blocks. *Angew. Chem. Int. Ed.* **2002**, *41*, 1053–1057.

(12) Manetsch, R.; Krasiński, A.; Radić, Z.; Raushel, J.; Taylor, P.; Sharpless, K. B.; Kolb, H. C. In Situ Click Chemistry: Enzyme Inhibitors Made to Their Own Specifications. *J. Am. Chem. Soc.* **2004**, *126*, 12809–12818.

(13) Ohkanda, J. Module Assembly for Designing Multivalent Mid-Sized Inhibitors of Protein-Protein Interactions. *Chem. Rec.* **2013**, *13*, 561–575.

(14) Di Antonio, M.; Biffi, G.; Mariani, A.; Raiber, E. A.; Rodriguez, R.; Balasubramanian, S. Selective RNA versus DNA G-Quadruplex Targeting by In Situ Click Chemistry. *Angew. Chem. Int. Ed.* **2012**, *51*, 11073–11078.

(15) Millward, S. W.; Agnew, H. D.; Lai, B.; Lee, S. S.; Lim, J.; Nag, A.; Pitram, S.; Rohde, R.; Heath, J. R. In Situ Click Chemistry: From Small Molecule Discovery to Synthetic Antibodies. *Integr. Biol.* **2013**, *5*, 87–95.

(16) Ogasawara, D.; Itoh, Y.; Tsumoto, H.; Kakizawa, T.; Mino, K.; Fukuhara, K.; Nakagawa, H.; Hasegawa, M.; Sasaki, R.; Mizukami, T.; Miyata, N.; Suzuki, T. Lysine-Specific Demethylase 1-Selective Inactivators: Protein-Targeted Drug Delivery Mechanism. *Angew. Chem. Int. Ed.* **2013**, *52*, 8620–8624.

(17) Krasiński, A.; Radić, Z.; Manetsch, R.; Raushel, J.; Taylor, P.; Sharpless, K. B.; Kolb, H. C. In Situ Selection of Lead Compounds by Click Chemistry: Target-Guided Optimization of Acetylcholinesterase Inhibitors. *J. Am. Chem. Soc.* **2005**, *127*, 6686–6692.

(18) Mocharla, V. P.; Colasson, B.; Lee, L. V.; Röper, S.; Sharpless, K. B.; Wong, C. H.; Kolb, H. C. In Situ Click Chemistry: Enzyme-Generated Inhibitors of Carbonic Anhydrase II. *Angew. Chem. Int. Ed.* **2004**, *44*, 116–120.

(19) Hirose, T.; Maita, N.; Gouda, H.; Koseki, J.; Yamamoto, T.; Sugawara, A.; Nakano, H.; Hirono, S.; Shiomi, K.; Watanabe, T.; Taniguchi, H.; Sharpless, K. B.; Omura, S.; Sunazuka, T. Observation of the Controlled Assembly of Preclick Components in the In Situ Click Chemistry Generation of a Chitinase Inhibitor. *Proc. Natl. Acad. Sci. U. S. A.* **2013**, *110*, 15892–15897.

(20) Deprez-Poulain, R.; Hennuyer, N.; Bosc, D.; Liang, W. G.; Enée, E.; Marechal, X.; Charton, J.; Totobenazara, J.; Berte, G.; Jahklal, J.; Verdelet, T.; Dumont, J.; Dassonneville, S.; Woitrain, E.; Gauriot, M.; Paquet, C.; Duplan, I.; Hermant, P.; Cantrelle, F.-X.; Sevin, E.; Culot, M.; Landry, V.; Herledan, A.; Piveteau, C.; Lippens, G.; Leroux, F.; Tang, W.-J.; van Endert, P.; Staels, B.; Deprez, B. Catalytic Site Inhibition of Insulin-Degrading Enzyme by a Small Molecule Induces Glucose Intolerance in Mice. *Nat. Commun.* **2015**, *6*, 8250.

(21) Nguyen, R.; Huc, I. Using an Enzyme's Active Site to Template Inhibitors. *Angew. Chem. Int. Ed.* **2001**, *40*, 1774–1776.

(22) Kwarcinski, F. E.; Steffey, M. E.; Fox, C. C.; Soellner, M. B. Discovery of Bivalent Kinase Inhibitors via Enzyme-Templated Fragment Elaboration. *ACS Med. Chem. Lett.* **2015**, *6*, 898-901.

(23) Inglese, J.; Benkovic, S. J. Multisubstrate Adduct Inhibitors of Glycinamide Ribonucleotide Transformylase: Synthetic and Enzyme-Assembled. *Tetrahedron* **1991**, *47*, 2351–2364.

(24) Hirose, T.; Sunazuka, T.; Sugawara, A.; Endo, A.; Iguchi, K.; Yamamoto, T.; Ui, H.; Shiomi, K.; Watanabe, T.; Sharpless, K. B.; Omura, S. Chitinase Inhibitors: Extraction of the Active Framework from Natural Argifin and Use of In Situ Click Chemistry. *J. Antibiot. (Tokyo).* **2009**, *62*, 277–282.

(25) Hu, X.; Sun, J.; Wang, H.; Manetsch, R. Bcl-X_L-Templated Assembly of Its Own Protein-Protein Interaction Modulator from Fragments Decorated with Thio Acids and Sulfonyl Azides. *J. Am. Chem. Soc.* **2008**, *130*, 13820–13821.

(26) Gelin, M.; Poncet-Montange, G.; Assairi, L.; Morellato, L.; Huteau, V.; Dugué, L.; Dussurget, O.; Pochet, S.; Labesse, G. Screening and In Situ Synthesis Using Crystals of a NAD Kinase Lead to a Potent Antistaphylococcal Compound. *Structure* **2012**, *20*, 1107–1117.

(27) Oueis, E.; Nachon, F.; Sabot, C.; Renard, P.-Y. First Enzymatic Hydrolysis/Thio-Michael Addition Cascade Route to Synthesis of AChE Inhibitors. *Chem. Commun.* **2014**, *50*, 2043–2045.

(28) Maki, T.; Kawamura, A.; Kato, N.; Ohkanda, J. Chemical Ligation of Epoxide-Containing Fusicoccins and Peptide Fragments Guided by 14-3-3 Protein. *Mol. BioSyst.* **2013**, *9*, 940–943.

(29) Asaba, T.; Suzuki, T.; Ueda, R.; Tsumoto, H.; Nakagawa, H.; Miyata, N. Inhibition of Human Sirtuins by in Situ Generation of an Acetylated Lysine-ADP-Ribose Conjugate. *J. Am. Chem. Soc.* **2009**, *131*, 6989–6996.

(30) Weber, L. In Vitro Combinatorial Chemistry to Create Drug Candidates. *Drug Discov. Today Technol.* **2004**, *1*, 261–267.

(31) Dömling, A.; Ugi, I. Multicomponent Reactions with Isocyanides. *Angew. Chem. Int. Ed.* **2000**, *39*, 3168–3210.

(32) Dömling, A.; Wang, W.; Wang, K. Chemistry and Biology Of Multicomponent Reactions. *Chem. Rev.* **2012**, *112*, 3083–3135.

(33) Groebke, K.; Weber, L.; Mehlin, F. Synthesis of Imidazo[1,2-*a*] Annulated Pyridines, Pyrazines and Pyrimidines by a Novel Three Component Condensation. *Synlett* **1998**, 661–663.

(34) Gladysz, R.; Cleenewerck, M.; Joossens, J.; Lambeir, A.-M.; Augustyns, K.; Van der Veken, P. Repositioning the Substrate Activity Screening (SAS) Approach as a Fragment-Based Method for Identification of Weak Binders. *ChemBioChem* **2014**, *15*, 2238–2247.

(35) Gladysz, R.; Adriaenssens, Y.; De Winter, H.; Joossens, J.; Lambeir, A.-M.; Augustyns, K.; Van der Veken, P. Discovery and SAR of Novel and Selective Inhibitors of Urokinase Plasminogen Activator (uPA) with an Imidazo[1,2-*a*]pyridine Scaffold. *J. Med. Chem.* **2015**, *58*, 9238–9257.

(36) Pirrung, M. C.; Das Sarma, K. Multicomponent Reactions Are Accelerated in Water. *J. Am. Chem. Soc.* **2004**, *126*, 444–445.

(37) Murray, K. K.; Boyd, R. K.; Eberlin, M. N.; Langley, G. J.; Li, L.; Naito, Y. Definitions of Terms Relating to Mass Spectrometry (IUPAC Recommendations 2013). *Pure Appl. Chem.* **2013**, *85*, 1515–1609.

(38) Ludlow, R. F.; Otto, S. Two-Vial, LC-MS Identification of Ephedrine Receptors from a Solution-Phase Dynamic Combinatorial Library of over 9000 Components. *J. Am. Chem. Soc.* **2008**, *130*, 12218–12219.

(39) Lakshmi Narasimham, Y. S.; Barhate, V. D. Development and Validation of Stability Indicating UPLC Method for the Simultaneous Determination of Beta-Blockers and Diuretic Drugs in Pharmaceutical Dosage Forms. *J. Chem. Metrol.* **2010**, *4*, 1–20.

Chapter 8

Conclusions and outlook

8. Conclusions and outlook

The primary goal of this PhD research was the application of the substrate activity screening (SAS) approach and its modified variant (MSAS) to the discovery of potent and selective inhibitors of urokinase plasminogen activator (uPA). As a result we have developed a straightforward synthetic strategy for transforming low-affinity fragments into potent, druglike compounds with a decorated scaffold architecture. A series of imidazopyridine inhibitors of uPA with nanomolar potency and high selectivity with respect to the related proteases (tPA, thrombin, FXa, plasmin, plasma kallikrein, trypsin, and FVIIa) was obtained. To the best of our knowledge, this is the first reported application of an imidazo[1,2-*a*]pyridine scaffold to uPA inhibitor discovery. Also inhibitors with a diaryl phosphonate warhead function were prepared. Here, the fragment identified during the substrate screening was converted into a mechanism-based phosphonate inhibitor of low nanomolar potency and high selectivity for uPA, on the contrary to a homologous non-substrate fragment. In this way, our study provided a proof-of-concept for the SAS-based identification of uPA inhibitors.

Additionally, during this PhD research attempts have been made to elaborate the “on-target” version of the Groebke-Blackburn-Bienaymé (GBB) reaction for the construction of uPA inhibitors. Our study provided a general experimental protocol as well as an early proof-of-concept for the on-target GBB reaction.

8.1. Outlook

8.1.1. Screening the prepared fragment library against other enzymatic targets

It would be interesting to screen the constructed library of *N*-acyl aminocoumarins (*N*-acyl AMC) against other enzymatic targets. Apart from uPA, we have applied MSAS to a number of other ongoing projects dealing with inhibitor design for cysteine proteases: caspase 4 and the autophagy target Atg4B. In the meantime, the initial library has been enriched in several subsets (in total ~ 200 compounds). In the future, this library could be further screened against other proteases (serine, cysteine, metallo-, and aspartate proteases) to identify useful fragments for inhibitor design and hence expand the existing SAR knowledge on the active site of these enzymes. However, as pointed out in Chapter 6, the repeated screening of the same substrate libraries against different targets within closely related enzyme families may also create a risk of returning identical fragment “hits”.

8.1.2. Further modifications of the obtained imidazopyridine inhibitors of uPA

Although our study resulted in potent and selective imidazopyridine inhibitors of urokinase, further modification of the obtained molecules would be interesting. During the course of this PhD we observed that amide substituents at the 7-position of the imidazo[1,2-*a*]pyridine scaffold had a

favorable effect on the affinity as well as the selectivity of the formed inhibitors. The molecular modeling study explained this increase in binding affinity by formation of an additional bond between the C7-amide nitrogen and the hydroxyl group of Tyr-151 in the active site of uPA. In order to limit the risk of compound degradation *in vivo*, mediated by unspecific peptidase activity, it would be interesting to replace the amide bond by its isostere (e.g. trifluoroethylamine, thioamide).[1] Besides, replacing the C7-amide substituent by its retroamide analogue could be also evaluated.

Another issue which could be addressed is the presence of a guanidine group in the obtained imidazopyridine inhibitors of uPA. This feature might hamper further development of these inhibitors. A solution to overcome this issue could be a prodrug strategy involving the use of a hydroxyguanidine precursor in order to improve bioavailability of derived molecules. The same strategy has been used in the discovery of Mesupron® (Upamostat, WX-671), an orally bioavailable prodrug (amidoxime) of WX-UK1 - Wilex's amidine-based inhibitor of uPA.[2,3]

Also an interesting modification would be so-called "scaffold hopping" approach to novel scaffold-based uPA inhibitors. Applying two GBB-related isocyanide-based reaction types could expand the scope of our strategy for transforming fragments into scaffolded uPA inhibitors (*vide supra*, Chapter 5) to two additional scaffold types (**Scheme 8.1**).[4] In comparison to the initial inhibitors obtained *via* the GBB reaction, the compounds produced by these additional transformations are decorated with identical substituents (R, R' and R''-groups) but contain a modified central scaffold.

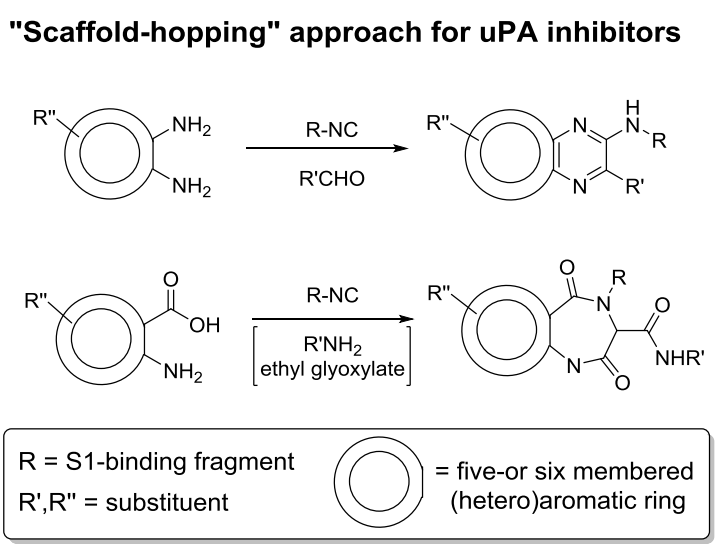

Scheme 8.1. The alternative isocyanide-based multicomponent reactions proposed for the "scaffold-hopping" approach for uPA inhibitors.

8.1.3. Further elaboration of the "on-target" approach for uPA inhibitors

The final part of this PhD research yielded a general experimental protocol as well as an early proof-of-concept for the "on-target" version of the GBB reaction. Although our preliminary results suggest that a full proof-of-concept can reasonably be expected to be within reach, still more experiments need to be performed here. First of all a reliable on-target version of the GBB reaction has to be elaborated. Once the on-target GBB reaction allows reproducing a potent imidazopyridine uPA inhibitor from a mixture of three building blocks (substituted aminopyridine, formaldehyde equivalent, and S1 binder-derived isocyanide), the on-target experiments can be continued by at a time keeping two building blocks unaltered while including a mixture of different possible third building blocks. Selection of the latter will be done either based on potencies of the reference compounds (*vide supra*, Chapter 5) or using computational design. The final goal of these experiments would be the selective formation of high-affinity inhibitors over less potent congeners. Besides, once successful, the on-target GBB experiments could be followed by a "scaffold-hopping" approach to expand the scope of this target-assisted methodology to related isocyanide-based reaction types.

Additionally, it is important to highlight the relevance of computational approaches which can be used to model on-target reactions and rationalize their outcome and rate, including molecular docking techniques, and hybrid quantum and molecular mechanics (QM/MM) implementations. These approaches may provide an insight at the molecular level on whether the developed on-target variant of GBB reaction can promote the "selective ligand amplification". To date, there is just one published report on a computational study of an on-target reaction, which deals with the on-target version of the Huisgen 1,3-dipolar ("*in situ* click") cycloaddition.[5]

References

(1) Choudhary, A.; Raines, R. T. An Evaluation of Peptide-Bond Isosteres. *ChemBioChem* **2011**, *12*, 1801–1807.

(2) *Therapeutic Target Mesupron*; Wilex Ag: Munich; http://www.wilex.de/portfolio-English/mesupron/therapeutic-Target/ (accessed january 19, 2015).

(3) Heinemann, V.; Ebert, M. P.; Laubender, R. P.; Bevan, P.; Mala, C.; Boeck, S. Phase II Randomised Proof-of-Concept Study of the Urokinase Inhibitor Upamostat (WX-671) in Combination with Gemcitabine Compared with Gemcitabine Alone in Patients with Non-Resectable, Locally Advanced Pancreatic Cancer. *Br. J. Cancer* **2013**, *108*, 766–770.

(4) Dömling, A.; Wang, W.; Wang, K. Chemistry and Biology Of Multicomponent Reactions. *Chem. Rev.* **2012**, *112*, 3083–3135.

(5) Hirose, T.; Maita, N.; Gouda, H.; Koseki, J.; Yamamoto, T.; Sugawara, A.; Nakano, H.; Hirono, S.; Shiomi, K.; Watanabe, T.; Taniguchi, H.; Sharpless, K. B.; Omura, S.; Sunazuka, T. Observation of the Controlled Assembly of Preclick Components in the in Situ Click Chemistry Generation of a Chitinase Inhibitor. *Proc. Natl. Acad. Sci. U. S. A.* **2013**, *110*, 15892–15897.

Chapter 9

Summary

9. Summary

9.1. Target protein: urokinase plasminogen activator (uPA)

Urokinase plasminogen activator (urokinase, uPA) was selected as target protein for the research performed during my PhD project.

Urokinase is a trypsin-like serine protease and a therapeutical target for several cancer types, including breast, ovarian, and pancreatic cancer. It is part of an extracellular multicomponent enzyme system involved in many physiological and pathological processes.[1] In the case of cancer, it triggers a proteolytic cascade through which cancer cells degrade the surrounding tissue (extracellular matrix, ECM), invade the healthy tissues and blood vessels, and finally migrate to target metastatic tissues. The ECM degradation and activation of growth factors associated with cancer cells promote tumor cell proliferation, migration, invasion, angiogenesis, and metastasis.[2,3] Since the components of the uPA system are differently expressed in cancer tissues than in healthy tissues, they can be used as prognostic and/or therapeutic anticancer targets.[4]

Although uPA is a relevant oncology target, clinical investigations of uPA inhibitors have been often disappointing due to a poor biopharmaceutical profile and insufficient selectivity of the compounds being developed. However, the field of urokinase inhibitor discovery still produces valuable compounds, mostly small molecules with a competitive, reversible inhibition profile. Wilex's amidine-based inhibitor WX-UK1 and its orally bioavailable prodrug WX-671 (Mesupron®) are currently the most advanced products, and the first uPA inhibitors in oncology clinical trials worldwide.[5]

Except cancer, the uPA system has been associated with the pathogenesis of several other diseases, such as for instance chronic ulcers, rheumatoid arthritis, and atherosclerosis.

9.2. Modification of the substrate activity screening (SAS) approach as an efficient method for fragment identification

Fragment-based drug discovery (FBDD) has evolved into an established approach for "hit" identification. However, most applications of FBDD depend heavily on specialized cost- and time-intensive biophysical techniques.[6] The substrate activity screening (SAS) approach has been proposed as a relatively cheap and straightforward alternative for the identification of fragments for enzyme inhibitors.[7] In this PhD research we decided to apply SAS to the discovery of inhibitors of urokinase.

We started our investigations with the synthesis of a SAS library of fluorogenic molecules as potential substrates of uPA. The library members contained various fragment-sized acyl residues, which were selected either in a non-target- or target-biased manner. In the next step the library was screened for substrates of urokinase using a simple fluorescence-based assay. During our investigation, a number

of unreported limitations of the SAS approach were uncovered. In response, we proposed an efficient modified methodology: "MSAS" (modified substrate activity screening). In MSAS, the library is first screened for inhibitory fragments (step 1), and the identified "hits" are next assayed using a traditional SAS experiment (step 2). This allows (1) reducing the consumption of costly target protein and screening time, and (2) avoiding the occurrence of "false positives" and "false negatives".

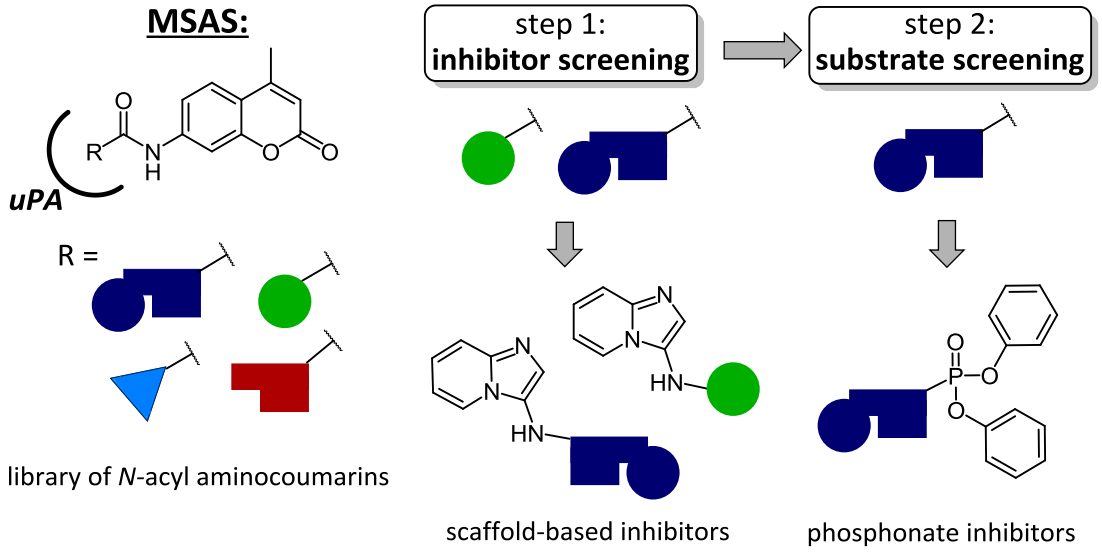

Scheme 9.1. Outline of the MSAS approach followed during this study.

As a result, MSAS circumvents the limitations of SAS and broadens its scope by providing additional fragments and more coherent SAR data. The validation of the MSAS approach was based on the construction of scaffold-based inhibitors of uPA (**Scheme 9.1**). It allowed identifying imidazopyridine as an interesting scaffold for uPA inhibitor design. Also inhibitors with a diaryl phosphonate warhead function were prepared (**Scheme 9.1**), providing a proof-of-concept for the SAS-based identification of uPA inhibitors (**Figure 9.1**).[8]

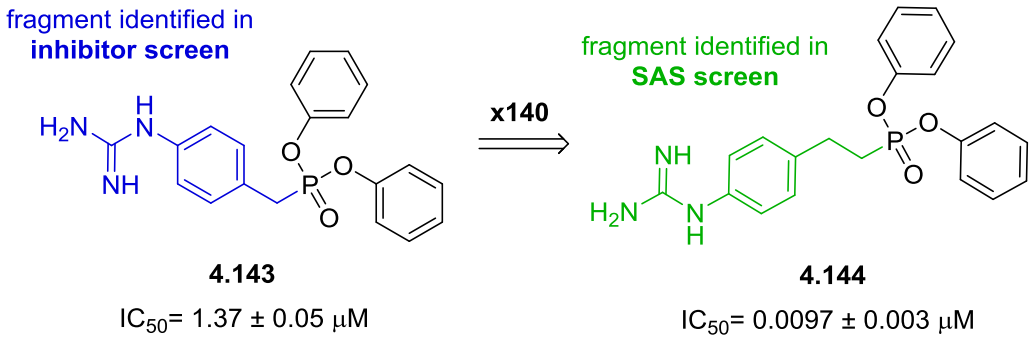

Figure 9.1. Proof-of concept for the SAS-based identification of uPA inhibitors. Fragment hit of a SAS screen (marked in green) can be converted into a potent phosphonate inhibitor, on the contrary to a non-SAS fragment (marked in blue).

9.3. Discovery and SAR of novel and selective inhibitors of uPA with an imidazo[1,2-*a*]pyridine scaffold

In the next part of this PhD project, the fragments identified using the MSAS approach were transformed into a novel class of uPA inhibitors with an imidazo[1,2-*a*]pyridine scaffold. Based on our preliminary results (*vide supra*, Part 9.2), we hypothesized that a fragment with affinity for uPA can be transformed into a druglike inhibitor of by grafting it onto an imidazopyridine scaffold. To this end, we followed a general strategy consisting of two steps: (1) preparation of a set of monosubstituted scaffolds for selection of an optimal fragment, and (2) further structural optimization by introducing additional affinity-conferring substituents. Evaluation of the uPA inhibitory potency of the monosubstituted imidazo[1,2-*a*]pyridines identified the guanidinophenyl derivatives as the most potent analogues. The optimization of the initial hit compound **5.8a** was based on investigating the influence of additional substituents on the imidazo[1,2-*a*]pyridine scaffold, which extensively relied on the molecular modeling studies (**Figure 9.2**).

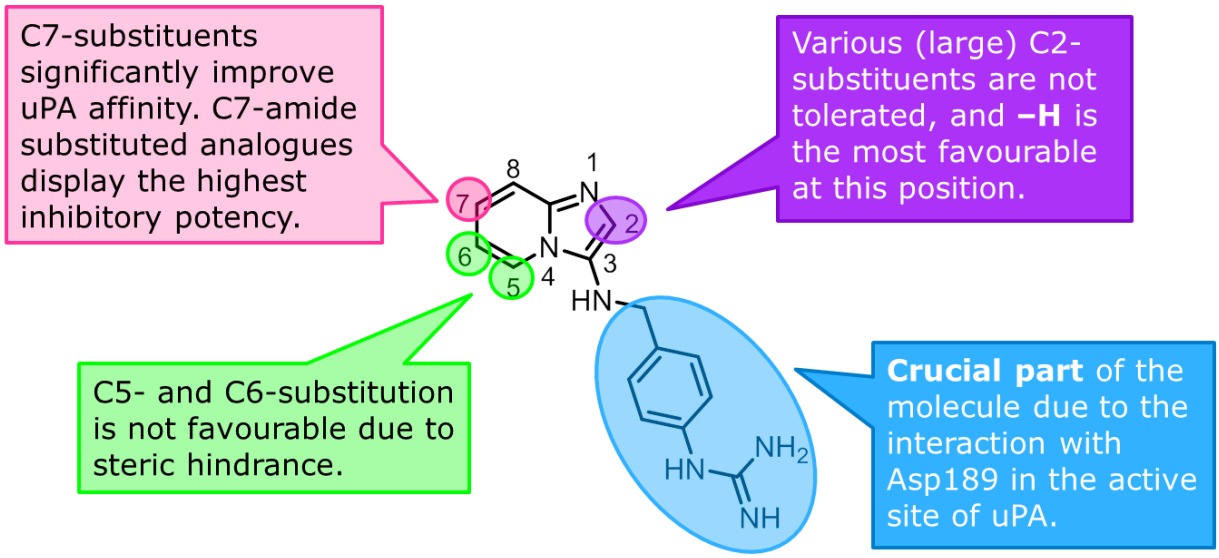

Figure 9.2. SAR summary of the imidazopyridine inhibitors of uPA.

The exploration of the SAR for uPA inhibition around the imidazopyridine scaffold identified the C7-amide substituted analogues as the best compounds in the series. The most potent inhibitor **5.18a** is characterized by nanomolar uPA potency and remarkable selectivity with respect to the related trypsin-like serine proteases (**Figure 9.3**).

Importantly, the approach followed for translating fragments into small molecules with a decorated scaffold architecture is conceptually straightforward and can be expected to be broadly applicable in fragment-based drug design.[9]

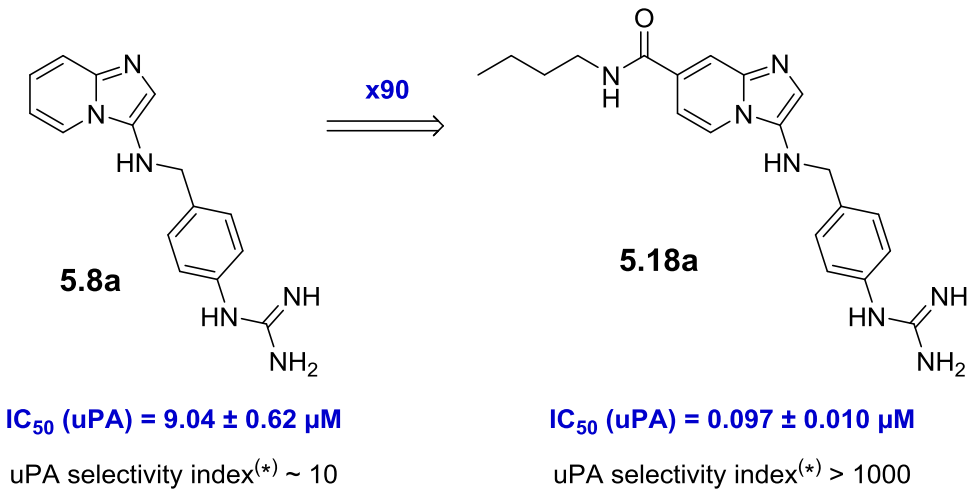

Figure 9.3. Optimization of the initial hit compound (* - determined with respect to related proteases: thrombin, tPA, factor Xa, plasmin, plasma kallikrein, trypsin, and factor VIIa).

9.4. Discussion on SAS and related approaches in medicinal chemistry: strategic advances and lessons learned

The results obtained during the parts of this PhD thesis dealing with the exploration of SAS, MSAS, and the validation of these fragment-based strategies, allowed to draw a number of relevant conclusions (**Scheme 9.2**).

SAS is a straightforward fragment-based method with a great potential for the design of enzyme inhibitors. Since its discovery a decade ago, SAS and derived variants, including the MSAS approach, have been applied successfully to inhibitor discovery for different families of enzymatically active drug targets.

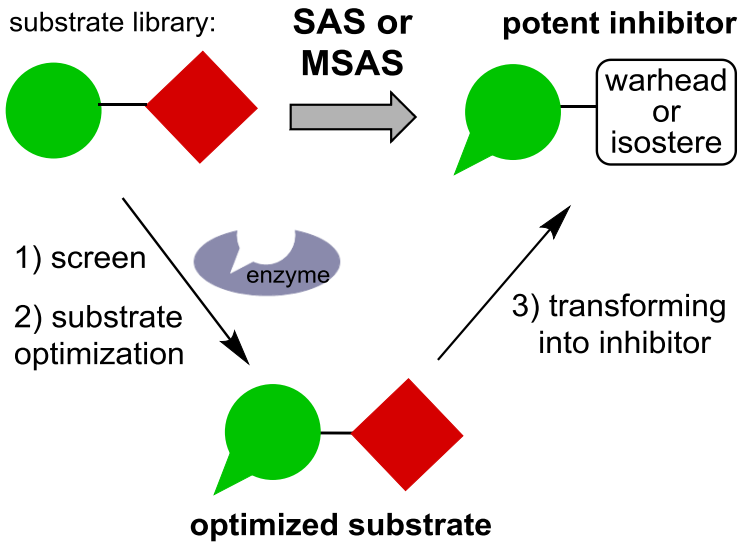

Scheme 9.2. Application of the SAS and MSAS approaches in drug discovery.

Nonetheless, in order to maximize the efficiency and reliability of these fragment-based approaches, a number of aspects require special attention. These include (1) a proper design of the substrate library and (2) screening assay, (3) determination of adequate kinetic and thermodynamic substrate parameters, and selection of an (4) appropriate warhead or isostere. A thorough understanding of these parameters is crucial for successfully transforming the identified fragments into potent inhibitors.[10]

9.5. "On-target" approaches to inhibitors of urokinase

In the last part of this PhD project the "on-target" approach to inhibitors of uPA has been explored.

On-target strategies in drug discovery rely on the direct assistance of the drug target, which serves as a physical template that selects useful drug fragments and assembles them into finalized molecules. It allows merging the synthesis and potency determination, as well as several other aspects of drug design into a single, time-efficient step. Multicomponent reactions (MCRs) are the most widely used transformations in combinatorial drug discovery.[11] Different variants of these reactions yield molecules characterized by a druglike architecture, therefore the on-target versions of MCRs can have a great potential for drug discovery. In this PhD research we studied the on-target version of the so-called Groebke-Blackburn-Bienaymé (GBB) reaction, in which three components - an aminopyridine, an aldehyde and an isocyanide - condense to form an imidazopyridine scaffold decorated with substituents (**Scheme 9.3**).[12] As reference for the on-target work, we used the previously prepared uPA inhibitors (*vide supra*, Part 9.3). This investigation yielded a general experimental protocol as well as an early proof-of-concept for the on-target version of the GBB reaction.

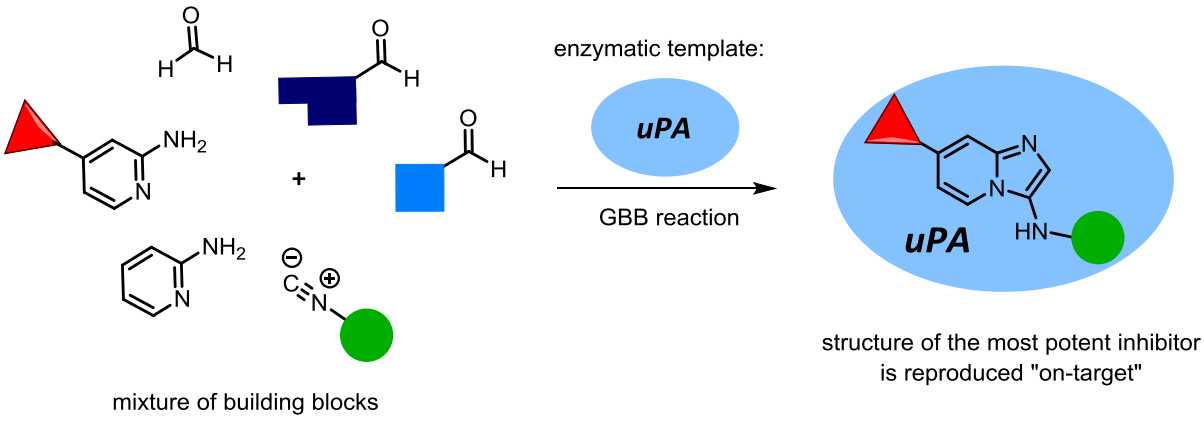

Scheme 9.3. Outline of the on-target version of the GBB reaction for uPA inhibitor discovery.

References

(1) Dass, K.; Ahmad, A.; Azmi, A. S.; Sarkar, S. H.; Sarkar, F. H. Evolving Role of uPA/uPAR System in Human Cancers. *Cancer Treat. Rev.* **2008**, *34*, 122–136.

(2) Mekkawy, A. H.; Pourgholami, M. H.; Morris, D. L. Involvement of Urokinase-Type Plasminogen Activator System in Cancer : An Overview. *Med. Res. Rev.* **2014**, *34*, 918–956.

(3) Ulisse, S.; Baldini, E.; Sorrenti, S.; D'Armiento, M. The Urokinase Plasminogen Activator System: A Target for Anti-Cancer Therapy. *Curr. Cancer Drug Targets* **2009**, *9*, 32–71.

(4) Duffy, M. J.; McGowan, P. M.; Harbeck, N.; Thomssen, C.; Schmitt, M. uPA and PAI-1 as Biomarkers in Breast Cancer: Validated for Clinical Use in Level-of-Evidence-1 Studies. *Breast Cancer Res.* **2014**, *16*, 428: 1-10.

(5) Heinemann, V.; Ebert, M. P.; Laubender, R. P.; Bevan, P.; Mala, C.; Boeck, S. Phase II Randomised Proof-of-Concept Study of the Urokinase Inhibitor Upamostat (WX-671) in Combination with Gemcitabine Compared with Gemcitabine Alone in Patients with Non-Resectable, Locally Advanced Pancreatic Cancer. *Br. J. Cancer* **2013**, *108*, 766–770.

(6) Congreve, M.; Chessari, G.; Tisi, D.; Woodhead, A. J. Recent Developments in Fragment-Based Drug Discovery. *J. Med. Chem.* **2008**, *51*, 3661–3680.

(7) Wood, W. J. L.; Patterson, A. W.; Tsuruoka, H.; Jain, R. K.; Ellman, J. A. Substrate Activity Screening: A Fragment-Based Method for the Rapid Identification of Nonpeptidic Protease Inhibitors. *J. Am. Chem. Soc.* **2005**, *127*, 15521–15527.

(8) Gladysz, R.; Cleenewerck, M.; Joossens, J.; Lambeir, A.-M.; Augustyns, K.; Van der Veken, P. Repositioning the Substrate Activity Screening (SAS) Approach as a Fragment-Based Method for Identification of Weak Binders. *ChemBioChem* **2014**, *15*, 2238–2247.

(9) Gladysz, R.; Adriaenssens, Y.; De Winter, H.; Joossens, J.; Lambeir, A.-M.; Augustyns, K.; Van der Veken, P. Discovery and SAR of Novel and Selective Inhibitors of Urokinase Plasminogen Activator (uPA) with an Imidazo[1,2-*a*]pyridine Scaffold. *J. Med. Chem.* **2015**, *58*, 9238–9257.

(10) Gladysz, R.; Lambeir, A.-M.; Joossens, J.; Augustyns, K.; Van der Veken, P. Substrate Activity Screening (SAS) and Related Approaches in Medicinal Chemistry. *ChemMedChem* **2016**, *11*, 467–476.

(11) Dömling, A.; Wang, W.; Wang, K. Chemistry and Biology Of Multicomponent Reactions. *Chem. Rev.* **2012**, *112*, 3083–3135.

(12) Bienaymé, H.; Bouzid, K. A New Heterocyclic Multicomponent Reaction For the Combinatorial Synthesis of Fused 3-Aminoimidazoles. *Angew. Chem. Int. Ed.* **1998**, *37*, 2234–2237.

Chapter 10

Samenvatting

10. Samenvatting

10.1. Het doelwit-proteïne: urokinase plasminogeen activator (uPA)

Urokinase plasminogeen activator (urokinase, uPA) werd geselecteerd als doelwit-proteïne voor mijn doctoraatsonderzoek.

Urokinase is een trypsine-achtig serine-protease en een therapeutisch doelwit voor verschillende kankertypes, waaronder borst-, eierstok-, en pancreaskanker. Het is onderdeel van een extracellulair multi-component enzymesysteem dat betrokken is in vele fysiologische en pathologische processen.[1] In het geval van kanker zet het een proteolytische cascade in werking, waardoor kankercellen het omringende weefsel (de extracellulaire matrix, ECM) afbreken, gezonde weefsels en bloedvaten binnendringen, en uiteindelijk migreren naar metastatische doelwitweefsels. De ECM-degradatie en de activatie van groeifactoren geassocieerd met kankercellen bevorderen de proliferatie, migratie, invasie, angiogenese en metastase van tumorcellen.[2,3] Vermits de componenten van het uPA-systeem een verschillende expressie kennen in kankerweefsels en gezonde weefsels, zijn ze zowel prognostisch als therapeutisch bruikbaar in de strijd tegen kanker.[4]

Hoewel uPA een relevant oncologisch doelwit is, waren klinische onderzoeken naar uPA-inhibitoren vaak teleurstellend vanwege hun onaantrekkelijk biofarmaceutisch profiel alsook vanwege de beperkte selectiviteit van de ontwikkelde moleculen. Desalniettemin levert het onderzoeksdomein van uPA-inhibitoren nog steeds waardevolle structuren op, veelal kleine moleculen met een competitief reversibel inhibitieprofiel. Wilex' amidine-gebaseerde inhibitor WX-UK1 en zijn oraal biobeschikbare prodrug WX-671 (Mesupron®) zijn momenteel de meest geavanceerde producten, en tevens wereldwijd de eerste uPA-inhibitoren in oncologische klinische testen.[5]

Het uPA-systeem wordt naast kanker ook geassocieerd met de pathogenese van verschillende andere ziekten, waaronder chronische zweren, reumatoïde artritis en arteriosclerose.

10.2. Modificatie van de substraat-activiteitsscreening (SAS)-benadering als een efficiënte methode voor fragment-identificatie

Fragment-gebaseerde geneesmiddelontdekking (fragment-based drug discovery, FBDD) is uitgegroeid tot een gevestigde waarde als benadering voor 'hit'-identificatie. De meeste toepassingen van FBDD zijn echter in grote mate afhankelijk van kosten- en tijdsintensieve biofysische technieken.[6] De substraat-activiteitsscreening (substrate activity screening, SAS)-benadering werd reeds voorgesteld als een relatief goedkoop en waardevol alternatief voor de identificatie van fragmenten voor enzyme-inhibitoren.[7] In dit doctoraatsonderzoek werd SAS aangewend voor de ontdekking van urokinase-inhibitoren.

Het onderzoek werd aangevat met de synthese van een SAS-bibliotheek van fluorogene moleculen als potentiële substraten voor uPA. De structuren in de bibliotheek omvatten uiteenlopende acylresidu's van fragmentformaat, die hetzij op een doelwit-gerichte hetzij op een niet-gerichte wijze geselecteerd waren. In een volgende stap werd de bibliotheek gescreend voor substraten van urokinase door middel van een eenvoudig fluorescentie-gebaseerd experiment. Tijdens ons onderzoek kwamen er echter verschillende ongerapporteerde beperkingen van de SAS-benadering aan het licht. Naar aanleiding hiervan stelden wij een efficiënte aangepaste methodologie voor: "MSAS" (modified substrate activity screening – aangepaste substraat-activiteitsscreening). In MSAS wordt de bibliotheek eerst gescreend voor inhiberende fragmenten (stap 1), en de geïdentificeerde 'hits' worden vervolgens onderworpen aan een traditioneel SAS-experiment (stap 2). Dit laat toe om (1) zowel het verbruik van kostbaar doelwit-proteïne als de screeningstijd te verminderen, en (2) om het voorvallen van "valse positieven" en "valse negatieven" te vermijden.

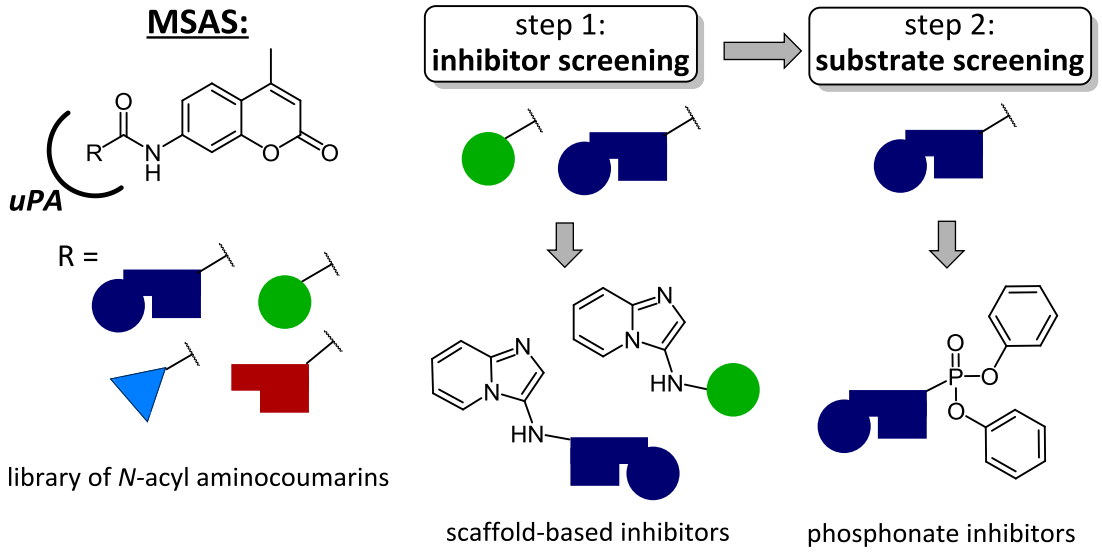

Schema 10.1. Schematisch overzicht van de MSAS-benadering gevolgd tijdens deze studie.

Hierdoor omzeilt MSAS de beperkingen van SAS, en breidt het de toepassing van SAS uit door extra fragmenten en meer coherente SAR-gegevens aan te reiken. De validering van de MSAS-benadering was gebaseerd op de constructie van motief-gebaseerde uPA-inhibitoren (**Schema 10.1**). Het liet ons toe om imidazopyridine te identificeren als een interessant motief voor het ontwerp van uPA-inhibitoren. Tevens werden inhibitoren met een diarylfosfonaat-'warhead' bereid (**Schema 10.1**), die als proef op de som dienden om de SAS-gebaseerde identificatie van uPA-inhibitoren aan te tonen (**Figuur 10.1**).[8]

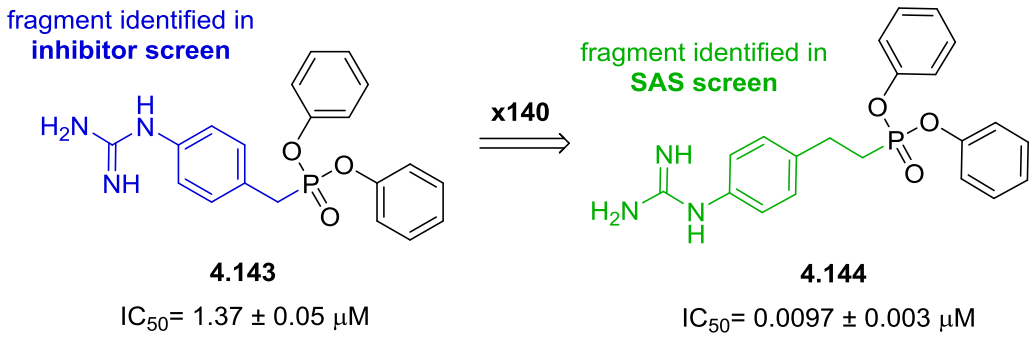

Figuur 9.1. Proef op de som voor de SAS-gebaseerde identificatie van uPA-inhibitoren.

10.3. Ontdekking en SAR van nieuwe en selectieve uPA-inhibitoren gebaseerd op het imidazo[1,2-*a*]pyridine-motief

In het volgende gedeelte van dit doctoraatsonderzoek werden de fragmenten, die eerder geïdentificeerd werden met behulp van de MSAS-benadering, getransformeerd tot een nieuwe klasse uPA-inhibitoren gebaseerd op het imidazo[1,2-*a*]pyridine-motief. Gebaseerd op onze preliminaire resultaten (*vide supra*, Hoofdstuk 10.2) veronderstelden we dat een fragment met affiniteit voor uPA getransformeerd kan worden tot een geneesmiddelachtige inhibitor door het vast te hechten aan een imidazopyridine-motief. Hiertoe werd een algemene procedure gevolgd bestaande uit twee stappen: (1) de bereiding van een groep monogesubstitueerde motieven ter selectie van een optimaal fragment, en (2) de verdere structurele optimalisatie van dit fragment door de introductie van additionele affiniteitsverhogende substituenten. Tijdens de evaluatie van de uPA-inhibitiepotentiaal van de monogesubstitueerde imidazo[1,2-*a*]pyridines werden derivaten van guanidinofenyl geïdentificeerd als de meest potente analogen. De optimalisatie van het oorspronkelijke 'hit'-molecule **5.8a** was gebaseerd op het onderzoeken van de invloed van additionele substituenten op het imidazo[1,2-*a*]pyridine-motief, waarvan de selectie in grote mate berustte op moleculaire modelleringsstudies (**Figuur 10.2**).

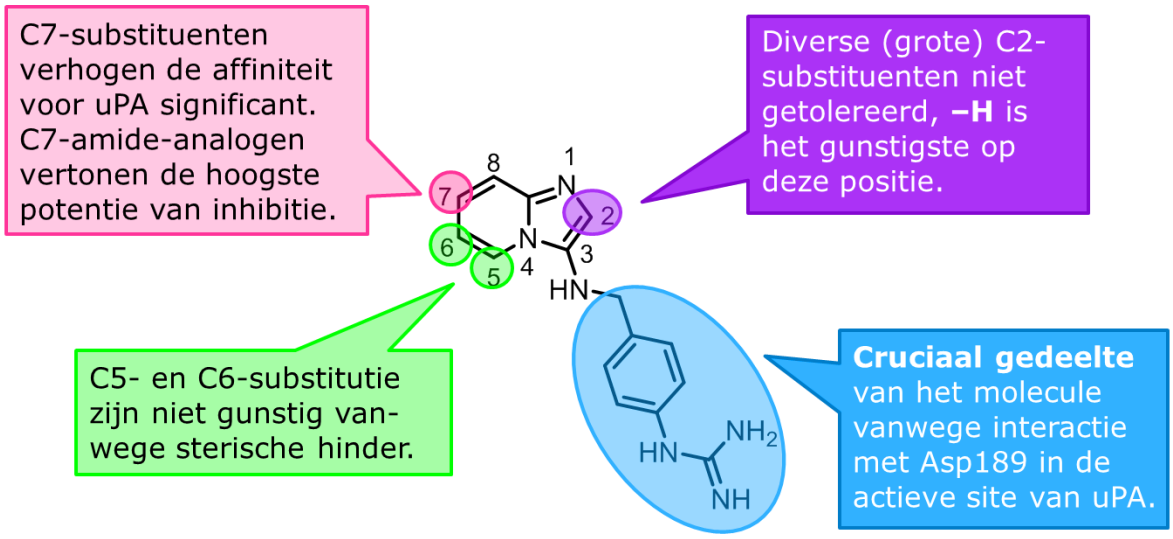

Figuur 10.2. SAR-overzicht van de imidazopyridine uPA-inhibitoren.

Tijdens de SAR-verkenning voor uPA-inhibitie rond het imidazopyridine-motief werden analogen met een C7-amidesubstituent geïdentificeerd als de beste moleculen van de groep. De meest potente inhibitor **5.18a** wordt gekenmerkt door een nanomolaire uPA-inhibitiepotentiaal en tegelijk een frappante selectiviteit ten opzichte van de verwante trypsine-achtige serine-proteasen (**Figuur 10.3**). Het is belangrijk om op te merken dat de gevolgde benadering voor het vertalen van fragmenten naar kleine moleculen met een gedecoreerd basismotief conceptueel eenvoudig is alsook wellicht breed toepasbaar is in fragment-gebaseerde geneesmiddelontdekking.[9]

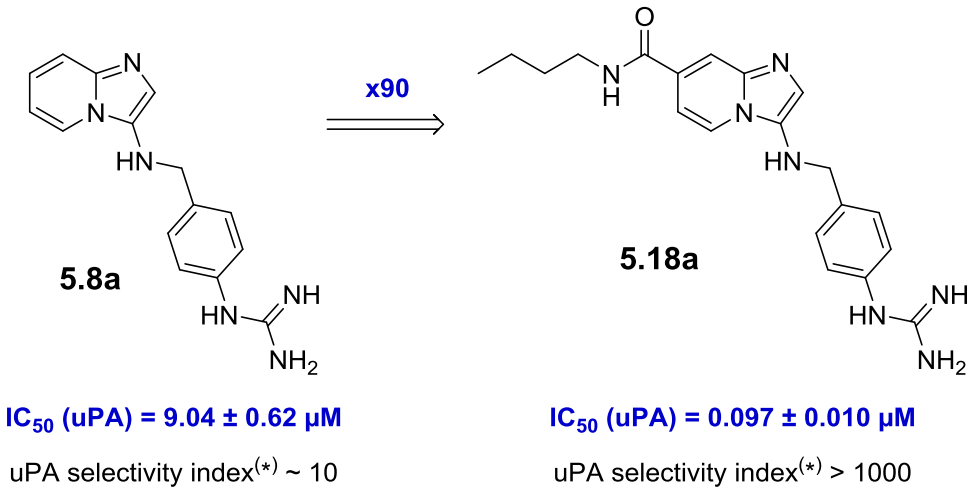

Figuur 10.3. Optimalisatie van de oorspronkelijk 'hit'-structuur (* - bepaald ten opzichte van verwante proteasen: trombine, tPA, factor Xa, plasmine, plasma kallikreïne, trypsine, en factor VIIa).

10.4. Bespreking van SAS en verwante benaderingen in de medicinale chemie: strategische vooruitgangen en geleerde lessen

De resultaten verkregen doorheen de delen van dit doctoraatsonderzoek rond de verkenning van SAS, MSAS en de validering van deze fragment-gebaseerde benaderingen laten ons toe een aantal relevante conclusies te trekken (**Schema 10.2**).

SAS is een eenvoudige fragment-gebaseerde methode met een groot potentieel voor het ontwerp van enzyme-inhibitoren. Sinds hun ontdekking een decennium geleden werden SAS en afgeleide varianten zoals de MSAS-benadering succesvol toegepast bij de ontdekking van inhibitoren voor verschillende families van enzymatische geneesmiddeldoelwitten. Niettegenstaande verdienen een aantal aspecten speciale aandacht om de doelmatigheid en de betrouwbaarheid van deze fragment-gebaseerde benaderingen te maximaliseren. Hieronder vallen (1) een adequaat ontwerp van de bibliotheek van substraten en (2) het screeningsexperiment, (3) bepaling van de passende kinetische en thermodynamische parameters van het substraat en (4) selectie van een geschikt 'warhead' of isosteer. Een diepgaand inzicht in deze parameters is onontbeerlijk bij de succesvolle omzetting van de geïdentificeerde fragmenten naar potente inhibitoren.[10]

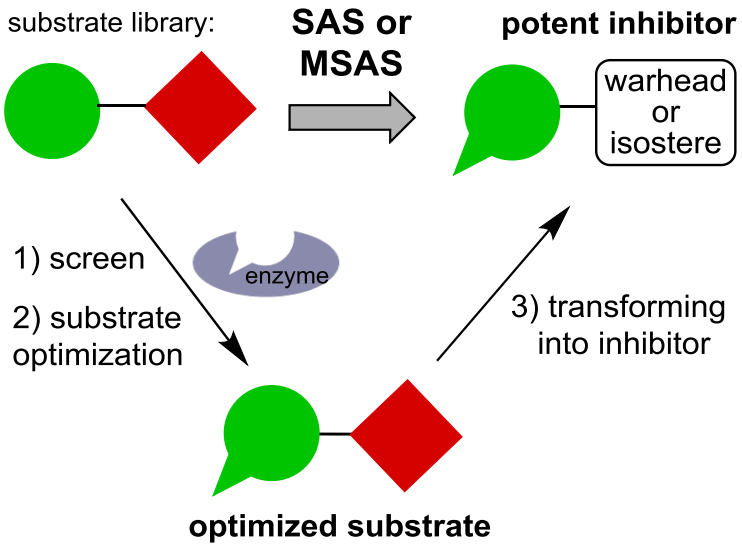

Schema 10.2. Toepassing van de SAS- en MSAS-benaderingen in geneesmiddelontwikkeling.

10.5. "On-target"-benaderingen voor uPA-inhibitoren

In het laatste gedeelte van dit doctoraatsonderzoek werd de 'on-target'-benadering voor uPA-inhibitoren onderzocht. "On-target"-strategiën in geneesmiddelontdekking berusten op de directe assistentie van het geneesmiddeldoelwit, dat dienst doet als fysiek sjabloon ter selectie van nuttige geneesmiddelfragmenten om deze vervolgens te assembleren tot gefinaliseerde moleculen. Hierdoor kunnen zowel de synthese als de potentiebepaling, alsook verschillende andere aspecten van het geneesmiddelontwerp gecombineerd worden tot één enkele tijdsefficiënte stap. Multicomponentreacties (MCR's) zijn de meest wijdverbreide transformaties in combinatoriële geneesmiddelontdekking.[11] Verschillende varianten van deze reacties leveren moleculen op die gekenmerkt worden door hun geneesmiddelachtige structuur, vandaar dat de "on-target"-versies van MCR's een groot potentieel kunnen betekenen voor geneesmiddelontdekking. In dit doctoraatsonderzoek werd de "on-target"-versie van de zogenoemde Groebke-Blackburn-Bienaymé (GBB)-reactie bestudeerd, een reactie waarin drie componenten (een aminopyrdine, een aldehyde, en een isocyanide) condenseren ter vorming van een imidazopyridine-motief gedecoreerd met substituenten (**Schema 10.3**).[12] Als referentie voor het "on-target"-onderzoek, maakten we gebruik van de uPA-inhibitoren die eerder bereid werden (*vide supra*, Hoofdstuk 10.3). Dit onderzoek leidde tot een algemeen experimenteel protocol en leverde tevens een vroegtijdige proof-of-concept op van de "on-target"-versie van de GBB-reactie.

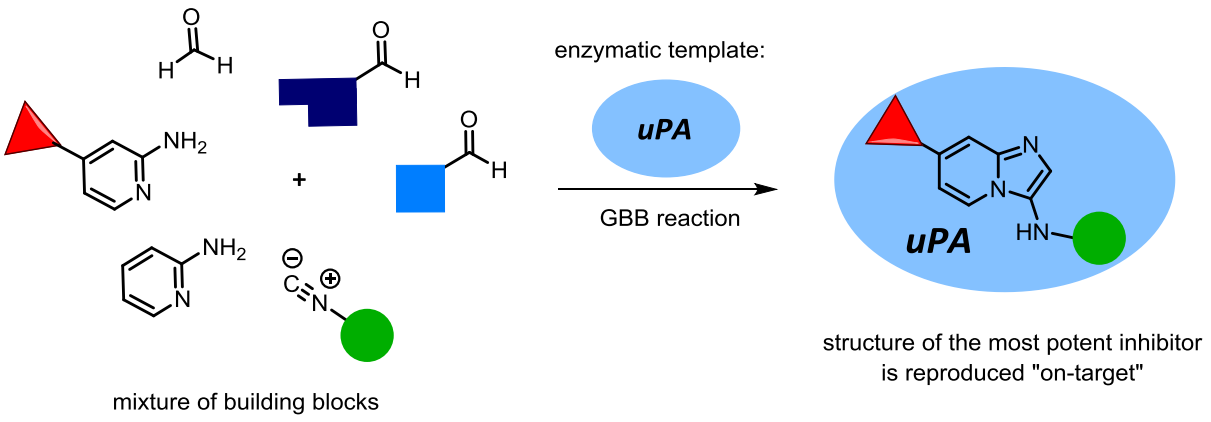

Schema 10.3. Schematisch overzicht van de "on-target"-versie van de GBB-reactie voor de ontdekking van uPA-inhibitoren.

Referenties

(zie hoofdstuk 9)

Curriculum vitae

Curriculum vitae

Personal information

First name	Rafaela
Surname	Gladysz
Date and place of birth	March 24th 1986, Prudnik (Poland)
E-mail	rafaela.gladysz@gmail.com
Nationality	Polish

Education

2012-2016 PhD in Pharmaceutical Sciences, Laboratory of Medicinal Chemistry (UAMC), University of Antwerp

2010-2012 Internship in the Laboratory of Medicinal Chemistry (UAMC), University of Antwerp

2005-2010 Master of Science in Biotechnology in the specialization Medicinal Chemistry, with the grade excellent. Wroclaw University of Technology (Poland)

2002-2005 Secondary education: Mathematics-Physics, Adam Mickiewicz 1st General Secondary School, Prudnik

Scientific research

Publications

1) **Gladysz, R.**; Lambeir, A.-M.; Joossens, J.; Augustyns, K.; Van der Veken, P. Substrate Activity Screening (SAS) and Related Approaches in Medicinal Chemistry, *ChemMedChem*, **2016**, *11*, 467-476.
2) **Gladysz, R.**; Adriaenssens, Y.; De Winter, H., Joossens, J.; Lambeir, A.-M.; Augustyns, K.; Van der Veken, P. Discovery and SAR of novel and selective inhibitors of urokinase plasminogen activator (uPA) with an imidazo[1,2-*a*]pyridine scaffold, *Journal of Medicinal Chemistry*, **2015**, *58*, 9238-9257.
3) Van Soom, J.; Cuzzucoli Crucitti, G.; **Gladysz, R.**; Van der Veken, P.; Di Santo, R.; Stuyver, I.; Buck, V.; Lambeir, A.-M.; Magdolen, V.; Joossens, J.; Augustyns, K. The first potent diphenyl phosphonate KLK4 inhibitors with unexpected binding kinetics. *MedChemComm* **2015**, *6*, 1954-1958.

4) **Gladysz, R.**; Cleenewerck, M.; Joossens, J.; Lambeir, A.-M.; Augustyns, K.; Van der Veken, P. Repositioning the Substrate Activity Screening (SAS) Approach as a Fragment-Based Method for Identification of Weak Binders. *ChemBioChem* **2014**, *15*, 2238-2247.

5) Cleenewerck, M.; Grootaert, M.; **Gladysz, R.**; Adriaenssens, Y.; Roelandt, R.; Joossens, J.; Lambeir, A.-M.; De Meyer, G.; Declercq, W.; Augustyns, K.; Martinet, W.; Van der Veken, P. Development and Validation of a Gel Electrophoresis-Based Assay for Atg4B Activity Determination and Inhibitor Screening. Submitted to *Bioorg. Med. Chem.* **2015**.

Oral Presentations

- Oral presentation: *Fragment-based approaches to inhibitors of urokinase plasminogen activator (uPA)*, presented during Departmental Research Day of Pharmaceutical Sciences, University of Antwerp, **2015.**
- Oral presentation: *Application of the Modified Substrate Activity Screening (MSAS) approach in the discovery of non-peptidic protease inhibitors*, presented during the 12th Chemistry Conference for Young Scientists (ChemCYS 2014), **2014.**

Poster Presentations

- Poster presentation: *Application of the MSAS approach in the discovery of potent and selective inhibitors of urokinase*, presented during The 51st International Conference on Medicinal Chemistry – 51e RICT, Avignon, France, **2015.**
- Poster presentation: *Application of the modified substrate activity screening (MSAS) approach in the discovery of non-peptidic protease inhibitors*, presented during The 18th Sigma-Aldrich Organic Synthesis Meeting, Duinse Polders, Blankenberge, **2014.**
- Poster presentation: *Application of the modified substrate activity screening (MSAS) approach in the discovery of non-peptidic protease inhibitors*, presented during Annual One-Day Meeting on Medicinal Chemistry of SRC & KVCV, Janssen Pharmaceutica, Beerse, **2013.**
- Poster presentation: *The modified substrate sctivity screening (MSAS) approach and its validation in the discovery of scaffold-based inhibitors of urokinase*, presented during the 16th Sigma-Aldrich Organic Synthesis Meeting, Sol Cress Spa, **2012.**
- Poster presentation: *Repositioning the substrate activity screening approach for identification of weak binders in fragment-based drug discovery*, presented during Annual One-Day Meeting on Medicinal Chemistry of SRC & KVCV, Château de Colonster, Liège, **2012.**

Other activities

- Co-authorship of a patent application-Sołoducho J., Cabaj J., Nowakowska-Oleksy A., **Gładysz R.**, *Biosensor warstwowy do wykrywania związków fenolowych (Hybrid biosensor for the detection of phenolic compounds)*, P 389041, **2009.**

Scientific archievements

2010	Award in the competition for the best graduate of the Chemistry Department of the Wroclaw University of Technology (7th place among 341 students) in the academic year 2009/2010
2010	Scholarschip of president of Wrocław for outstanding students pursuing international research in science
2006-2010	Scholarschip for exceptional study results granted by the Wroclaw University of Technology

Supervision of Bachelor/Erasmus exchange students

10/2011-02/2012	Janusz Wisniewski, Erasmus exchange student, Faculty of Biotechnology, University of Wroclaw, Poland
02/2013-06/2013	Philip Pedraza, Bachelor thesis student, Artesis-Plantijn Hogeschool, Antwerpen

Acknowledgments

Acknowledgments

My adventure with Belgium started from an Erasmus project on the last year of my master studies at the Wroclaw University of Technology. Although I really enjoyed this short research stay I would never guess that during the following few years I would have an opportunity to continue my research during PhD studies at the University of Antwerp. But life can sometimes bring us surprises, and here I am at the end of my PhD project, ready to close an important chapter in my life, a chapter full of colorful chemistry, new inspirations, predictable but also unexpected results, achievements and disappointments, nostalgia and new friendships. During this time I learnt a lot, and not only about organic chemistry but also about life. I was very lucky to be surrounded by kind, helpful and intelligent people, what made the past five years even more enjoyable. With these acknowledgments I would like to say thank you to people, with which I had the pleasure to work as well as share my daily life during my doctoral studies.

First of all, I would like to thank my promoters, **Prof. Dr. Pieter Van der Veken** and **Prof. Dr. Koen Augustyns**, for giving me the possibility of performing this doctoral research. I greatly appreciated their guidance, kindness and hints obtained in the course of this study. **Pieter**, thank you for your support, understanding and useful advices while struggling with various chemistry- and biochemistry-related problems. I really appreciated your constructive comments and corrections of my scientific articles. Also thank you for help during preparations to my IWT exam as well as to several other presentations. I have learnt from you a lot. Moreover, I would like to thank my promoters for reading the draft version of this thesis and providing useful remarks.

I would like to thank a member of my doctoral committee, and jury chair, **Prof. Dr. Magda Claeys-Maenhaut**, for reading the draft version of this thesis as well as for providing language corrections and advice during the final stages of my PhD. I greatly appreciated her helpfulness and kindness.

I would like to thank a member of my doctoral committee, **Prof. Dr. Kourosch Abbaspour Tehrani**, for reading the draft version of this thesis as well as for providing constructive remarks.

I would also like to thank the external members of my doctoral jury, **Prof. Dr. Arthur Van Aerschot** (KU Leuven) and **Prof. Dr. Annemieke Madder** (UGent), for having accepted the jury task as well as for reading the draft version of this thesis, and providing constructive remarks.

I would like to thank **Prof. Dr. Anne-Marie Lambeir** for help with the design and interpretation of the biochemical screening assays performed in course of this doctoral study. **Prof. Lambeir** was always ready to share with me her excellent knowledge in the field of enzyme kinetics, which I greatly appreciated. Moreover, I am grateful for providing valuable remarks and suggestions during work on my scientific articles.

I would like to thank **Prof. Dr. Hans De Winter** for performing the molecular docking studies of the prepared imidazopyridine inhibitors of uPA as well as for useful remarks, and corrections of my scientific article.

I would like to thank **Em. Prof. Dr. Achiel Haemers** for help with the preparations to my IWT exam.

Besides, I am thankful to the **IWT-Vlaanderen** (Institute for Innovation by Science and Technology-Flanders) for financing my doctoral research.

Dr. Jurgen Joossens, thank you for useful hints and advice obtained from you during my PhD. I have always appreciated your positive attitude towards research, combined with common sense, and friendliness.

Dr. Oxana Ryabtsova, who used to work in our group as a postdoc. First months in Belgium were not easy, far away from family, friends, and approaching the IWT exam. I was happy to find a friend among my colleagues from work. In the lab you were always ready to share your knowledge in practical and theoretical organic chemistry, and outside the university you managed to find time to meet in the city center or go for a bike ride. I greatly appreciate your helpfulness and friendship.

Sophie Lyssens and **Ingmar Stuyver**, thanks for excellent technical assistance and nice atmosphere in the lab.

My labmates from laboratory A2.22, **Yves Adriaenssens** and **Dr. David Thomae**, thanks for the great atmosphere at work during last few years, I really enjoyed sharing the lab with you guys. **Yves**, thanks for useful tips and all the help with UPLC ☺!

All other researchers who have worked in our group during the whole period of my PhD studies, **Dr. Jonas Messagie, Dr. Koen Jansen, Dr. Matthias Breugelmans, Dr. Leen Heirbaut, Dr. Kurt Lebeau, Dr. Muthusamy Venkatraj (Venkat), Yves Adriaenssens, Jens Fissers, Filipe Elvas, Matthias Cleenewerck, Sam Hofmans, Jeroen Van Soom, Dr. David Thomae, Dr. Marion Toussaint, Dr. Agnese Maggi, Dr. Naiara Vazquez, Dr. Thomas Verbrugghen, Eleni Pitta, Maciej Rogacki, Olga Balabon, Dr. Irene Garcìa Salado, Dr. Giuliana Cuzzucoli Crucitti, Dr. Artem Kulago, Dries Van Rompaey, Lars Devisscher, An De Decker, Antonella Messore, Lara Zonnekein, Carlos Moreno, Eduardo Ruivo**; I would like to thank you all for many cheerful moments and pleasant atmosphere both in the UAMC lab, and outside the university walls during conferences, meetings, and lab events. I shall long remember them. Thanks guys ☺!

I would like to express my deep gratitude to my family and friends, especially to my mother, **Jadwiga Gładysz**, my sister **Diana**, and my brother **Rajmund**, for their infinite love, support, and faith in me. In loving memory of my father, **Edward Gładysz**. Serdecznie Wam dziękuję za Wasze wsparcie i pomoc.

And finally, I would like to express special thanks to my partner, **Johannes Vrijdag**, for filling my life with dreams, love and happiness. **Johannes**, meeting you was for sure one of the most valuable accomplishments during my doctoral studies. And circumstances were indeed academic; the 16th Sigma-Aldrich Organic Synthesis Meeting, 6-7 December 2012, Spa, Belgium. The first day of the symposium was followed by a walking dinner in medieval style, when in particular one of the organic chemists from KU Leuven, dressed as a monk, was very interested in my research topic (FBDD!). Several discussions, bike trips, and sightseeings later, he has become an integral part of my life. **Johannes**, thanks for all your support, care, and faith in me. I also owe you many thanks for the proofreading of my manuscript as well as revising organic chemistry with me, it was real fun ☺! Hartelijk bedankt voor je liefde, steun en wijze adviezen.

Thank you – Dank u wel – Dziękuję bardzo!

Rafaela

Antwerp, April 2016